Probabilistic Assessment of Unbalance in Distribution Networks Based on Limited Monitoring

A thesis submitted to The University of Manchester for the Degree of

Doctor of Philosophy

in the Faculty of Engineering and Physical Sciences

2014

Miss Zhixuan Liu

TABLE OF CONTENTS

Final word count: 59,159

LIST OF FIGURES

LIST OF TABLES

ABSTRACT

Probabilistic Assessment of Unbalance in Distribution Networks Based On Limited Monitoring

Miss Zhixuan Liu, the University of Manchester, May 2014

This thesis assesses the voltage unbalance in distribution networks due to load asymmetry or line asymmetry, based on measurement data from a limited number of monitors. The main outcomes of this research are a probabilistic methodology for estimating both momentary and long term unbalance and an optimal monitor placement providing the highest accuracy for the monitored level of unbalance.

With increasing numbers of large single-phase loads and distributed generation integrated into the power system, the future distribution network is expected to be more flexible, robust and "smart". This results in the requirement for high quality of electricity supply to be delivered to customers and is a challenge for the operation of the system. As the unbalance results in excessive heating, accelerated thermal ageing, reduction of efficiency and financial losses, the unbalance should be regulated to be below the statutory limit. Given the fact that unbalance is a long term phenomenon that may not cause any triggering of protection or faulty response of equipment, it can be only determined from available data such as loading levels of a network and the incomplete monitored voltage of a network. Due to limited monitoring in the network and therefore insufficient data, unbalance may be unobservable. This thesis therefore aims to develop a methodology to increase the observability of unbalance in the network in spite of limited monitoring.

This research uses Voltage Unbalance Factor (VUF) to quantify the level of unbalance. The first major part investigates the unbalance caused by asymmetrical loadings. By properly identifying the source of unbalance, the basic patterns of propagation of unbalance under possible scenarios are revealed and a methodology of probabilistic estimation of unbalance can be developed accordingly. Seen from the MV level of distribution networks, the loads are usually in the constant power form. Therefore, the variation in the load can be modelled by changing either active power or reactive power or both of them, depending on the data availability. The combinations of daily loading curve at buses and the normally distributed power factors in three phases of loads are used to create an unbalanced condition at the sources. Realistic assumptions of power factors and reasonable categories of types of loads result in realistic modelling of the unbalanced load. The probabilistic VUFs at different buses in the network are calculated and the weak areas in the network are identified using heat maps. The simulation results match the real VUF levels measured in the distribution network. The second part of the thesis explores the influence of asymmetrical lines in addition to the asymmetrical loading on propagation of unbalance. The last part provides a guideline for optimal monitor placement for unbalance. Two methods, manual ranking of buses and automatic optimization using Genetic Algorithm, are proposed. The two methods indicate the same optimal locations for monitor placement in the network. The developed methodologies enable the assessment of unbalance in the network when monitoring is limited and can be applied to real networks to assess the level of unbalance at non-monitored buses.

DECLARATION

No portion of the work referred to in this thesis has been submitted in support of an application for another degree or qualification of this or any other university or institute of learning.

COPYRIGHT STATEMENT

[1] See http://www.campus.manchester.ac.uk/medialibrary/policies/intellectual-property.pdf
[2] See http://www.manchester.ac.uk/library/aboutus/regulations

ACKNOWLEDGEMENTS

I must express my deepest gratitude to my supervisor Prof. Jovica V. Milanović for the guidance, kind encouragement and hearty support throughout this research. Without his invaluable technical advice and professional industrial vision, this project would not have been completed. The outstanding patience and exceptional effort he applied to review this thesis and the publications which have arisen from it has been impressive and appreciative. The suggestions for the life are extremely motivating.

Acknowledgement goes to Western Power Distribution (previously E.ON Central Networks) who has sponsored this project. Special thanks go to Mr Robert Ferris, Mr Nigel Johnson, Mrs Rachel Stanley and Mr Jonathan Berry for their help and guidance.

Last but not least, I would like to express my appreciation to all my friends and colleagues in the Power Quality and Power Systems Dynamics Group at the University of Manchester. Special thanks must go to Dr Nick Woolley and Dr Huilian Liao for their extraordinary help and suggestion regarding the research. I also wish to thank Dr José Manuel Avendaño Mora, Miss Yizheng Xu, Mrs Atia Adrees and Mr Sami Abdelrahman for their selfless advices and support during the years.

To my beloved parents,

for their endless love, resolute inspiration and unconditional support

1 INTRODUCTION

1.1 POWER QUALITY

Power quality describes the extent at which voltage or current waveform deviates from the ideal three-phase sinusoidal wave. A power quality problem is any unexpected deviations in magnitude, angle or frequency in voltage or current, causing failure or misoperation of any power system component or customer device [1][2]. The power quality phenomena include short term interruptions and long term disturbances.

Power quality also represents the compatibility between the power system supply and the connected equipments at the point of connection. If the power is supplied with poor quality, the asset may suffer excessive heating, accelerated thermal ageing and reduced efficiency. This would result in additional financial costs for both end-users and the network operator [3][4]. Therefore, the problem is concerned with two aspects: how the power system affects the load and how the load affects the power system in return. From the customer's perspective, the power system is expected to supply steady state high performance voltage that can continually feed applications. Otherwise, poor power quality may cause a loss of temporary work, process delay, equipment damage and possible penalties due to late delivery [3]. From the utility's perspective, the load is

expected to be of good design that has sufficient immunity to small disturbances in the power supply and would not harm the electrical power system and other loads [5][6]. By improving its service for customers, the utility can reduce maintenance costs and penalties which arise when the power quality contract is breached.

The problems can be categorized for both customer side and utility side. The issues relating to power quality at the customer side are: voltage sag and surges, short term outages, transients, voltage unbalance, harmonics, electrical system design and construction and grounding. For the utility side, the issues are: voltage stability, voltage sag, voltage transients, voltage unbalance, frequency, phase shifts, harmonics and flicker [6]-[8]. By addressing the issues above, good power quality allows electrical power system to function normally and ensure the lifetime of all equipments along the line [2].

In the European Union, it is estimated that the total annual cost caused by power quality problems is €150 billion [9]. In the UK, the economic cost incurred due to power quality issues is about £3.7 billion per year [10], with inflation adjusted.

This thesis covers one of the power quality problems: voltage unbalance.

1.2 VOLTAGE UNBALANCE

For end users, overheating of equipment is the main effect of unbalance that can be observed. The effect can also be a sign of possible device deration and breakdown. For utilities, it is essential to know the degree of unbalance that exists in the network against the regulatory requirements. By obtaining the database with voltages at different buses in the network, the utility can assess the aspects of influence of unbalance, such as losses, heating and operation choices. To achieve this, it is necessary to quantify the

level of voltage unbalance, the causes of unbalance, the damage caused by unbalance, and the standard limitations for unbalance.

1.2.1 IMPORTANCE OF UNBALANCE ASSESSMENT

The increasing flexibility of power networks, due to improving operational practices and automation, emphasizes the requirement for high power quality of delivered electricity to end users. There are increased uncertainties, such as the integration of new types of intermittent and stochastic distributed generation (single-phase or three-phase, connected through power electronic interface to the grid), and changing types of end user devices (both more sensitive to network disturbances on the one hand and a source of those on the other). In spite of these uncertainties, the network is still expected to provide power conforming to the standard limitations. The changes in generation and demand types and profiles, in particular single-phase generation and load, call for robust assessment of propagation of voltage unbalance in distribution networks by both utilities and academia.

Unbalance was, in the past, a severe problem for high voltage transmission systems, caused by the asymmetrical line impedance in the transmission network [11]-[14]. In such a way, the electrical power system suffers upstream inherited voltage unbalance from high voltage to low voltage without regulation and so unbalance propagates to the downstream infrastructure. By fully transposing the transmission lines, it was generally successfully eliminated by the 1990s [13].

However, over the last ten years, changes in distribution network structures have aggravated the unbalance problem again. Due to the increasing installations of small distributed generations (DGs), especially single-phase renewable energy resources, which are connected to distribution networks, outstanding fluctuation of power is

injected to the point of connection and hence causes voltage unbalance. DGs may either mitigate unbalance or even aggravate unbalance. For instance, some domestic photovoltaics, employed by residential users, reduce the single-phase loading seen from the transformer. They might ease the burden of heavily loaded feeders in order to alleviate unbalance or they might be the cause of different loadings between phases that aggravate unbalance. As for the customer side, the growing usage of large single-phase or dual phase loads, such as electric vehicles, increases the unbalance from downstream and this negatively influences other buses and lines in the network [15]. In addition, depending on the customer wiring plan, the asymmetrical distribution of loads among three phases amplifies the unpredictability of unbalance in the network. Therefore, the initial network construction plan may not provide a balanced working condition for customers with the temporal and spatial variation in distribution of customer loads.

There are no actual research surveys on the financial cost of unbalance. In [3], an estimate is calculated under the regulatory limit of unbalance. It is reported that induction motors rated over 100kW have additional losses of 2.4%, synchronous generators rated over 100kW have additional losses of 4.2% and transformers have additional losses between 1% and 4%, when exposed to the regulatory limit level of unbalance. The losses on transformers represent one third of the network losses in the UK [16] and therefore the extra cost for the additional losses on the transformers is between 63GWh and 252GWh with the total annual loss being 18895GWh [17]. Using a loss incentive of £50/MWh [18] which is valid from 1 April 2010 until 31 March 2015, the additional cost that is incurred by transformers alone is between £3.15 million and £12.6 million.

As unbalance yields extra costs on operation, maintenance or replacement for both Distribution Network Operators (DNOs) and end customers, it is a very timely topic for the future designs of smart grids where the presence of single-phase generators (such as

photovoltaics) and loads (such as electric vehicles) in particular will noticeably increase [19]-[21].

1.2.2 DEFINITION

If the three-phase voltages of a bus in a power system are not equal in magnitude or do not phase shift by 120 degrees to each other, the system is considered as unbalanced or asymmetrical [15]. Fig. 1.1 shows the normal condition of balanced three-phase voltages and in comparison an arbitrary unbalanced condition. Under a balanced condition, all of three-phase voltages have the same magnitude with fixed phase shift 120 degrees to each other whereas the unbalanced voltages behave differently.

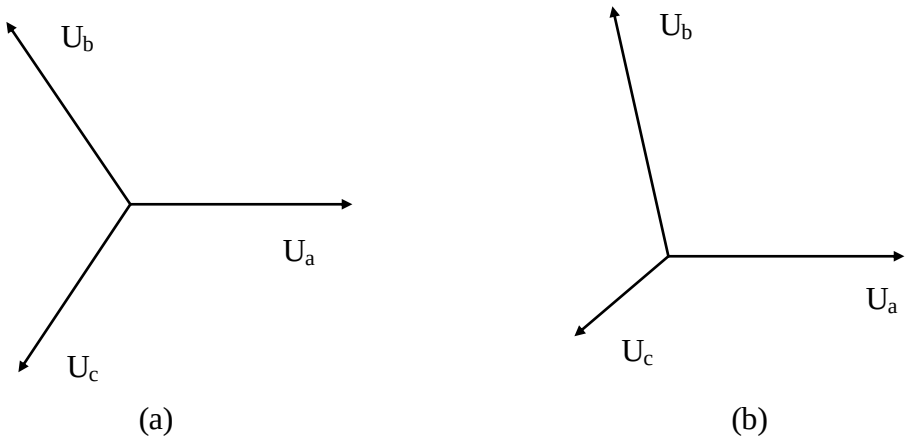

Fig. 1.1 Examples of balanced and unbalanced three-phase voltages. (a) Balanced three-phase voltages; (b) Unbalanced three-phase voltages.

1.2.3 CAUSE OF UNBALANCE

The main cause of unbalance is asymmetrical loading. At the distribution level, there are uneven distributions of single-phase and line-to-line connected loads which are frequently switched [19] by commercial and domestic users. For example, unknown numbers of single-phase loads such as PCs and lights at home are continually connected and disconnected from the distribution network. In LV network operations, unbalanced

three-phase loads may be integrated into the system as well as large single-phase loads such as railway traction [22][23]. In addition, one of the future large single-phase loads is electric vehicles (EV). It is expected to have an extremely noticeable effect in the evening in particular, varying in time and space and contributing to the unequal distribution of load per phase [20]. At the generation side, large power plants such as synchronous machine and induction machine are designed to be highly balanced. Due to the symmetrical construction and operation, central generation does not introduce any unbalance into the power system. Because the loads are distributed among three phases according to a previous construction plan, the changes in demand are unpredictable and there can hardly be an equilibrium among the three phases internally [15]. As there is always the probability of connecting unbalanced loads, the balanced condition of the whole system is very difficult to guarantee.

The most influential and sensitive loads in the network are typically those connected through adjustable speed drives (ASDs). They are time-varying three-phase or single-phase loads, and can be a source of unbalance themselves [19]. The large hourly variation of this load contributes to the fluctuations of flows in the network, leads to harmonic distortion, and makes the balance condition more unattainable.

Recently, small-scale distributed generators are increasingly employed by customers. They can be single-phase generators, such as photovoltaics and small wind turbines, or three-phase generators, such as large wind farms [21]. These applications may be connected to the distribution network via single-phase or three-phase power electronic inverters. With high impedance, low short-circuit current and time-varying generation, they also add to the source of unbalance within distribution networks [15].

In contrast to the fully transposed lines of transmission systems, overhead lines in distribution networks are often partially transposed or non-transposed, providing a

potential source of unbalance [24][25]. Under asymmetrical line conditions, the unequal mutual coupling impedances between phases lead to uneven voltage drops in phases and cause unbalance. Due to the distances between two adjoining buses, asymmetrical power loss along the line may have a noticeable effect on the network and needs to be specified [11][26]-[28].

Lastly, abnormal system conditions like equipment malfunction, incorrect human operation, and especially unbalanced faults (line to ground, phase to phase, and open conductor faults) also produce unbalance [15] in the network. However, this thesis is related to steady state conditions and these abnormal conditions are not considered.

1.2.4 EFFECT OF UNBALANCE

Unbalance causes negative sequence power flow and sometimes overvoltage in some of the phases. These effects contribute to thermal ageing and furthermore the reduction of an equipment's lifetime. Owing to the unexpected negative sequence power that flows in the same path with normal power, the capacities of equipments along the line are decreased. For generators and motors, the efficiency is also physically reduced.

For three-phase loads, voltage unbalance from supplied power usually signifies overvoltage in one or two phases and under-voltage in the other one or two phases. Considering the structure of a three-phase application or domestic wiring, the abnormal voltage in one phase can lead to irregular operation of the phase and furthermore the malfunction of the equipment.

Except for the negative impacts on equipment construction and utilization, the damage caused by unbalance will finally result in additional economic costs, such as replacing

the equipment and higher maintenance costs, which are unanticipated by both DNOs and customers.

Due to different application tolerances to unbalance, equipments are discussed separately below.

1.2.4.1 INDUCTION MACHINE

When working normally, a three-phase induction machine creates an internal magnetic field and produces a positive torque as a result. The magnetic field and torque are proportional to the positive sequence voltage of the induction machine. Once exposed to unbalance, the existence of negative sequence component generates an inverse rotating magnetic field, which changes the circular trajectory into elliptical [15] and produces an inverse torque, forcing the machine to decelerate [29]. Fig. 1.2 shows the sequence torques (T) against the slip (s). Positive sequence torque (T_1) is known as the normal working condition torque, and negative sequence torque (T_2) acts against the rotation (Note that the figure is for demonstration purposes only. In reality, the negative sequence torque is in smaller scale than the positive sequence torque). In other words, under unbalanced conditions, the negative torque is added to the working torque so that the total torque is reduced compared to the initial working torque. With the presence of the negative sequence torque, the machine cannot rotate at full torque and full speed. At the same time, because of the induced torque components at twice the system frequency, the pulsating torques may appear and the shaft bearings are exposed to higher mechanical stress. Because of the negative sequence impedance, the negative sequence component causes large negative sequence current [19]. This in turn could amplify the input unbalance by 6-10 times [30]. As a result, both the stator and rotor of the machine experience overheating [31]-[33] and loss as well as fast thermal ageing.

In terms of the automatic slowing down, there are also American National Electricity Manufacturer's Association (NEMA) [30] and International Electrotechnical Commission (IEC) [34] standards defining the derating requirements for safety consideration for induction motors (Voltage Unbalance Factor VUF is the ratio of negative sequence voltage to positive sequence voltage), shown in Table 1.1:

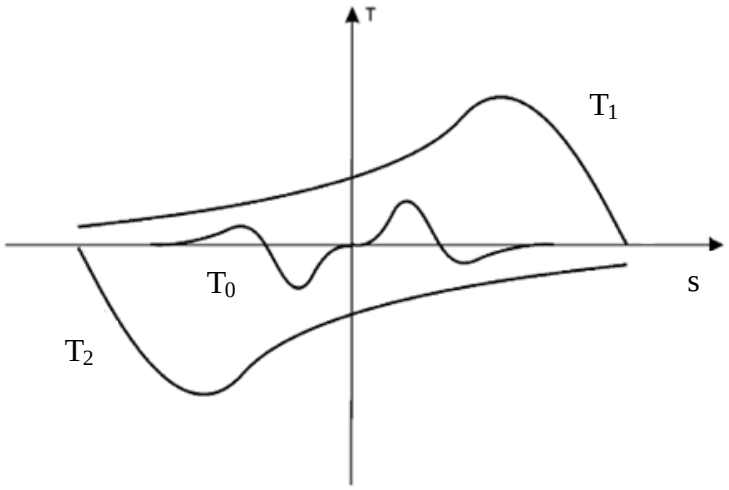

Fig. 1.2 Sequence Component Torques of Induction Machine (adopted from [15]).

Table 1.1 Derating Requirements for Induction Motors [30][34].

VUF	NEMA	IEC
1%	None	None
2%	95%	96%
3%	88%	90%
4%	82%	83.5%
5%	75%	76%

More detail about the effect on induction machine is available in [31][32][35].

1.2.4.2 SYNCHRONOUS GENERATOR

The effects on synchronous generators are similar to those of induction motors. However, for a synchronous machine, overheating is the most hazardous event, as it may cause damage to the inner construction, such as damper windings, where negative sequence and zero sequence currents are induced [33]. When exposed to unbalance, there is the possibility of a severer transient stability problem [36][37].

1.2.4.3 TRANSFORMERS

Regarding transformers, two effects can be discovered. Firstly, depending on the transformer winding connection type, zero sequence power flow may become possible if zero sequence current exists. Although it does not cause a large problem for the network, it may circulate within the delta winding and contributes to the increment of winding temperature, leading to additional loss and damage. Secondly, by flowing in the same path as positive sequence power flow, negative sequence flux and current can cause parasitic losses in the transformer structure [15]. It is estimated that there are 2.4 GWh and $134,000 additional annual losses due to the presence of unbalance based on 17600 transformers in Brazil [38].

1.2.4.4 POWER ELECTRONIC CONVERTERS

Power electronics interfaces, e.g. the ASDs, are sensitive to the input current. The ASDs are typically composed of diode rectifier front-ends [19][39] or Pulse Width Modulated (PMW) rectifier front-ends [19][40]. The uncontrolled diode rectifier front-ends [39] lead to irregular harmonics and resonance. When a PMW rectifier is exposed to unbalanced input voltage, the current distortion is increased as well as the reactive power and double frequency voltage ripple appears in the dc-link capacitor [19][40]. The double-pulse input current waveform can become single-pulse, and three-phase operation can become single-phase [41]. With unbalanced voltage injection, the ASD input current may increase to twice the rated value [41]. It is reported in [1] that ASDs can show 50% overcurrent under unbalanced conditions and the maximum magnitude of voltage within three phases is 3.6% higher than that of the minimum. The excessive currents appear in one or two phases, enabling the aggravation of the unbalance phenomenon and the potential triggering of the protection [19][39].

1.2.4.5 CAPACITY

The load capacities of transformers, cables and overhead lines are established by rated power. In order to carry the useless and loss-causing negative sequence current, the amount of positive sequence current must be downgraded. Consequently, the capacity for carrying normal current is reduced [42]-[44]. Therefore, when confronting unbalanced operating conditions, the system elements require larger capacities while suffering excessive losses [15].

1.2.4.6 GENERAL PROBLEMS

The negative sequence current induced by unbalanced sequence coupling affects all the apparent powers and power factors along the line.

To sum up, the common damage to all applications is overheating. For that reason, machine efficiency is immediately reduced and degration may need to be applied; furthermore it raises economic cost issues. Heating also accelerates ageing, which means the asset lifetime is decreased. Additionally, extra noise and vibration are likely to occur during unbalance [45].

1.2.5 MEASUREMENT AND QUANTIFICATION OF UNBALANCE

1.2.5.1 SYMMETRICAL COMPONENTS

Using Fortescue transformation [41][46][47], symmetrical components enable the transformation from the phase domain to the sequence domain for three-phase voltages and currents. In this way, a three-phase system is decomposed into three symmetrical components: positive sequence component (V_1 or I_1), negative sequence component (V_2 or I_2) and zero sequence component (V_0 or I_0). Transformation from the phase domain to the sequence domain is achieved using the transform (1.1)[46].

$$\begin{bmatrix} V_0 \\ V_1 \\ V_2 \end{bmatrix} = \frac{1}{3} \times \begin{bmatrix} 1 & 1 & 1 \\ 1 & a & a^2 \\ 1 & a^2 & a \end{bmatrix} \times \begin{bmatrix} V_a \\ V_b \\ V_c \end{bmatrix} \quad (1.1)$$

where $a=e^{j120°}$.

In the transformation matrices, all the voltage symbols "*V*" can be directly replaced by the current symbols "*I*".

In balanced conditions, both the negative sequence and the zero sequence components should be zero. However, in unbalanced conditions, if there is a path for zero sequence power flow such as a grounded-neutral system on both sides, zero sequence power flow becomes a problem especially inside the transformer windings. Because it does not have an impact on an ungrounded-neutral system, zero sequence flow is of little concern [48]. Even when the zero sequence power flow exists, the zero sequence voltage is about 10 to 100 times smaller than the negative sequence voltage, has a negligible effect and can be controlled by maintenance [49]. With all the powers having the ability to flow through the same path as the positive sequence component, the negative sequence is of main concern.

1.2.5.2 VOLTAGE UNBALANCE FACTOR

Widely accepted by standards and international working groups [48][50]-[56] including EN50160 [48], the Voltage Unbalance Factor (VUF), the ratio of negative sequence voltage (V_2) and positive sequence voltage (V_1), is the most widely used measure of unbalance. It is calculated using (1.2) [48]. This factor expresses the proportion of negative sequence power flow to the normal working condition [22]. Zero sequence power flow has a much smaller effect than negative sequence power flow, reflected by its absence in this factor.

$$\text{VUF} = \frac{V_2}{V_1} \times 100\% \quad (1.2)$$

In the thesis, VUF, which takes angular information into account, is used to achieve an accurate estimation of unbalance. There are also other factors, as introduced below.

1.2.5.3 LINE VOLTAGE UNBALANCE RATE

NEMA uses the average voltage of three-phase line voltages. The definition named "Line Voltage Unbalance Rate (LVUR)" uses only three-phase line voltage magnitudes and ignores voltage angles [30], shown in (1.3).

$$\text{LVUR} = \frac{\text{maximum voltage deviation from average line voltage}}{\text{average line voltage}} \times 100\% \tag{1.3}$$

LVUR enhances the significance of average value, and takes the maximum deviation into account. By ignoring the behaviour of the other two voltages, it theoretically cannot result in high accuracy. However, LVUR is reported to have the ability to achieve close results with "true value" of voltage unbalance VUF in realistic networks [57].

1.2.5.4 PHASE VOLTAGE UNBALANCE RATE

Similar to NEMA, the Institute of Electrical and Electronics Engineers (IEEE) defines a factor "Phase Voltage Unbalance Rate (PVUR)" using phase voltage magnitude information [57][58], shown in (1.4).

$$\text{PVUR}_1 = \frac{\text{maximum voltage deviation from average phase voltage}}{\text{average phase voltage}} \times 100\% \tag{1.4}$$

Alternatively, another form of PVUR is also presented in IEEE standards, shown in (1.5).

$$\text{PVUR}_2 = \frac{\text{difference between maximum and minimum phase voltage}}{\text{average phase voltage}} \times 100\% \tag{1.5}$$

Because both LVUR and PVUR ignore voltage angle information, under extreme working conditions, the result may show an error of up to 13% [59]. When zero sequence power flow is present, PVUR deviates from true value significantly [60].

In the recent IEEE standard IEEE 1159 [61], both $PVUR_1$ and VUF are presented.

1.2.5.5 PRACTICAL APPROXIMATION FOR VUF

IEC/TR 61000-3-13 [62] extends a practical algebraic approximation from IEC 61000-4-30 [63] for VUFs, shown in (1.6) and (1.7). This approximation employs only line magnitude values. It is reported to have a good agreement with the VUF value [64]-[67].

$$VUF = \sqrt{\frac{1-\sqrt{3-6\epsilon}}{1+\sqrt{3-6\epsilon}}} \tag{1.6}$$

$$\epsilon = \frac{|V_{ab}|^4 + |V_{bc}|^4 + |V_{ca}|^4}{(|V_{ab}|^2 + |V_{bc}|^2 + |V_{ca}|^2)^2} \tag{1.7}$$

where V_{ab}, V_{bc} and V_{ca} are fundamental line-to-line RMS voltages.

1.2.6 MITIGATION OF UNBALANCE

Corresponding to the main cause of unbalance, the most basic mitigation method for unbalance is to rearrange the loads to an evenly distributed condition among three phases [68]-[70]. This can be achieved by manual or automatic reconfiguration of the network [71][72]. Loads can be either connected to a higher voltage level or to a more balanced point [71].

Transposition of overhead lines certainly reduces the effects of unbalance due to line asymmetry during the propagation process. But for economic considerations, this approach is rarely taken in distribution networks. Instead, a better tower design at the transposition point is recommended [14][71][73][74]. With lines of small impedances, it is an effective approach to moderate the effect of unbalance due to load asymmetry. By using special transformers, zero sequence power flow is avoided and furthermore contributes to the balanced conditions of the system [15]. Overall, low internal network impedance reduces the phase coupling and sequence coupling, resulting in a smaller

negative sequence voltage, current and power [15], which contributes to the mitigation of unbalance.

The use of special power electronic circuits effectively controls the connected source of unbalance as power electronics respond swiftly to compensate for the changes in each phase when exposed to an unbalanced load or generation [15]. The shunt connected static compensators, such as passive static VAR compensators [75][76], static synchronous compensators [75]-[78] and distribution static compensators [79], injecting or absorbing reactive power to or from the power system, help regulating the voltage unbalance in the network. In a similar way, the series connected static compensators, such as static synchronous series compensators [76][80]-[82] and dynamic voltage restorers [83], inject active compensating voltages to the network in series with the supply to perform a correction of unbalanced voltages. Some Flexible AC transmission system (FACTS) devices, such as active power filters [84]-[86] and unified power quality conditioners [84][87][88], have the ability to regulate voltage amplitude and shift powers between phases to mitigate unbalance. In addition, energy storage systems can help mitigate the unbalance caused by the randomly located DGs [89].

1.2.7 STANDARD LIMITATION

All applications are expected to have intrinsic tolerance for small levels of unbalance. With devices partially immune to the unbalanced power supply, there is often no necessity to change the system design to save costs. However, due to the different sensitivities to the unbalance of various equipment, common limitations of unbalance are required for safety reasons. The most relevant standards in Europe are reviewed here.

Widely applied in Europe, EN 50160 [48] defines that 95% of the 10-minute average VUFs over a one week period should not exceed 2% for LV and MV networks, and 1%

for HV networks. The limitation for any instantaneous value of unbalance is set to 4% by this standard. DNOs do not usually carry out mitigation until VUF rises beyond 2%. Due to insufficient monitoring data, the VUFs of buses are not always available. However, it is necessary to predict the possible VUF ranges as they may exceed 2% and lead to the increased possibility of failure in the network.

IEC 61000-2-2 [90] and IEC 61000-2-12 [91] allow 2% VUF in LV and MV system and it can be up to 3% where most loads are single-phase. But they do not give the allowance for HV system. CIGRE working group 36.05 [92] defines that, for 95% of the daily 3 second intervals, the compatibility of unbalance for HV is 1% VUF, and for LV and MV is 2%. CIGRE/CIRED Joint Working Group C4.07 [3] uses EN50160 and especially defines 2% limitation for HV network and 1.5% for EHV network.

In the UK, according to Engineering Recommendation P29 [93], a 2% VUF tolerance for the short term (no more than 1 minute) is applied for all voltage levels. For the long term, the unbalance should never exceed 1%. Specifically, for nominal voltages under 33kV, the tolerance is 1.3%; for nominal voltages no greater than 132kV, the tolerance is 1% and should not last more than 5 minutes in any half an hour period.

1.3 VOLTAGE UNBALANCE MONITORING

To assess the real-time level of unbalance, monitoring the power flows in the network is the best and easiest way to derive the database for the whole network. There are developed methodologies for the optimal monitor placement for voltage sag and the fault locations. It is shown in [94] that the results of those methodologies can also achieve certain accuracy for estimating unbalance. However, no methodology for monitoring unbalance has been developed. In addition, the monitors are installed for

other purposes, other than deriving the best accuracy of unbalance. As reported by the DNO, they are usually alerted to the existence of unbalance by customer feedback or if there are significant problems in the monitoring device reports.

1.4 Overview of Past Research

Even though it increased in volume in the last ten years, most research related to voltage unbalance analyzes the influence of unbalance on individual equipment or specified phenomenon, such as the effect on induction motors [31][32][35]. There is only a little research that deals with unbalance itself.

The term "assessment of unbalance" specified here is not about the assessment of the effect of unbalance on power system equipment discussed in the previous section. It refers to the estimation of the level of unbalance in the network, including the sources of unbalance, contributions of each source, propagation of unbalance and the impact of power system equipments on overall unbalance in the network.

Although the causes and effects of unbalance are stated [15], the characters of unbalance that lead to the consequence have not been fully investigated. There are suggestions [45][94][95] for the identification of the unbalance source but there is no other application of the proposed methodologies or any verification based on actual data. There is also a lack of real-time simulation, which would be practical and would benefit both distribution operators and customers. All these topics need to be carefully considered for future accurate assessment of economic costs.

1.4.1 Assessment of Unbalance

With their own sensitivities to diverse unbalances, buses in a network have different VUFs when exposed to unbalance originating from the same location. To discover if

any patterns exist, how unbalance propagates through the network and what influences the propagation are key areas of interest for this study.

Papers [96][97] study the combined impact of line asymmetry and load asymmetry where [97] particularly represents the dominant factor for the overall unbalance and the cancellation of different types of unbalance. In [98], the lines are stated to be negligible sources of unbalance compared to the loads in real distribution networks. A one-day estimation of unbalance and the losses of unbalance are also presented in [98]. Although the unbalance in distribution networks is mainly caused by loads as described in the previous section of the causes of unbalance, there are estimations of the unbalance caused by lines for distribution networks. Research has been carried out for 66kV HV networks and claimed that the line can cause unbalance up to a similar level of unbalance caused by loads under specified assumptions [71][99]-[101]. In fact, when inspecting the VUF vectors caused by lines and loads respectively, it can be found that the line asymmetry compensates the load asymmetry to a certain extent although the modulus of the VUFs are comparable [100][101]. To investigate how the line injects and aggravates unbalance in distribution networks, the fundamental manufacturing structure for lines elaborated and formulated in [46] is extended to examine all possible cases in [96].

The investigations of DGs cover two aspects: their positive effect and negative effect on the systematic unbalance. For three-phase constant power generation, reference [102] shows the impact is relevant to DGs' penetration and their ability to change the load seen from the feeder. For single-phase DGs, [89][103] verify the positive and negative influences on the system depending on the connection point. Without the influence of load asymmetry, DGs, such as small wind turbines and photovoltaics, can inject unbalanced power into the power system [104]-[106]. DGs do not violate voltage constraints [103] but the presence of large penetration is a problem, because it is likely

that more single-phase DGs result in the increase in an overall negative sequence current [107]. To compensate for heavy loading, DGs can be connected to the critical point to mitigate the effect on the network [108][109].

1.4.1.1 PROPAGATION OF UNBALANCE

The transfer coefficient, or the transfer function, defines the relationship between two buses in time domain voltages, sequence voltages or VUFs. In the study of unbalance, it is usually referred to as the VUF transfer coefficient which is composed of the sequence domain values and therefore time domain values.

Reference [71] reveals transfer coefficients for networks of the same voltage level and for networks with a higher voltage power delivering to lower voltage levels. It starts from IEC 61000-3-13 [62] and aims for a global emission level of unbalance. The transfer coefficient from a higher voltage to a lower voltage is calculated using comprehensive parameters, including the load composition, power factors of different types of loads, detailed induction motor parameters and power system rating [110][111]. For the same voltage level, the transfer coefficient can be calculated using negative sequence voltages at both ends, the sequence line impedance, voltage drops across the line and power system ratings [71]. Different from the complicated and detailed methodologies, [112] defines a simplified transfer coefficient over transformers using the voltage at the sending end, the current in the line, the transformer connection type and the turns ratio.

1.4.1.2 IDENTIFICATION OF SOURCE OF UNBALANCE

It is essential to know the source of unbalance so that the mitigation and measurement can be carried out properly. Once unbalance appears, it is likely to flow into the whole network and the source may not be obvious. Because at distribution voltage levels, the

main cause of unbalance is the asymmetrical loading, most methodologies used to identify the source are based on an unbalanced load assumption, with a few exceptions.

Reference [45] suggests that the angle of negative sequence power of the source is usually bigger than +90° or smaller than -90° as concluded from observations. If a load has an angle within the specified range, it is on the side of the source of unbalance seen from a transformer. The importance of the ability to generate the negative sequence power of the source is again emphasized by [95], indicated by a significant amount of negative sequence active power present at the source, compared to little injections of balanced loads. To allow the source to stand out, [94] uses the ratio of negative sequence apparent power to positive sequence apparent power and declares that only the source will have a significant value of this factor.

Apart from these general approaches which require easily accessible values, based on [71][110][111] for the transfer functions between different voltage levels or the same voltage level, [100][101] make clear the individual contributions of a load (including induction motors), a line and upstream unbalance for both radial and meshed networks.

1.4.2 DISTRIBUTION NETWORK STATE ESTIMATION (DNSE)

Traditional state estimation is calculated using single-phase models, and it is assumed that the network is entirely balanced. If the voltage magnitudes and angles at every bus are available for all operating conditions, the network is considered as fully observable [113].

However, the assessment of unbalance requires three-phase state estimation, because unbalance is between phases and the assessment focuses on the evaluation of the difference between phases. By using three-phase state estimation, the voltage and

current vectors of all three phases are approachable, as demonstrated in [94][114]-[116]. Similar to the single-phase state estimation [46][113], Weighted Least Square method [46] is applied to the three-phase state estimation whereas the state variable equations and Jacobian matrix should cover all three phases and their correlations.

Unlike traditional state estimation which assumes enough measurements from monitors in the power system [113][117][118], Distribution Network State Estimation (DNSE) is designed for the situation in distribution networks where the measurements are less available due to the limited number of monitors. Due to a lack of operating data, DNSE is needed in order to provide full observability of the network aiming at real-time estimation. To achieve this goal, pseudo measurement [114][115][119][120] is employed to estimate the parameters in the unobservable area. In this way, the estimated values developed from historical data enable the full observability of the power system [115][120]-[123]. DNSE is usually executed under a balanced condition in which the network is again considered as single-phase [121][124], but it can be extended to three phases.

DNSE uses the same power flow equations with Newton-Raphson power flow method. The probabilistic three-phase load flow structure is developed in [120][125] and detailed flow equations are discussed in [115][116]. The probabilistic nature of the methodology enables both real-time and long term studies of voltage variations in power systems.

1.4.3 Optimal Monitor Placement Technique

So far there is no optimal monitor placement for measuring unbalance. There are methodologies of optimal monitor placement including the employment of artificial intelligence techniques [94], developed for state estimation [125]-[128], load estimation

[129], dynamic performance of power systems [130] or other power quality problems [131][132] such as voltage sag [131][133][134] and harmonics [132][135]. Although they are all designed for other purposes such as voltage sag, it is verified that the placement is functioning properly for monitoring unbalance [94]. Most methodologies focus on the placement for Phasor Measurement Units (PMUs) which are not typically used in distribution networks. But the methodologies can be used as instructions for the placement of monitors for distribution networks.

The monitoring of unbalance requires full observability of the network, in order to avoid errors in operational judgement and the malfunction of equipment. Based on this, it is expected that the selected monitor set can achieve the best accuracy with a fixed number of monitors and that there is a balance between the given optimum and computational time. The following methodologies aim at a solution to the problem.

Monitor Reach Area Method is developed based on the observability of fault locations with the size proportional to the voltage drop [133] and has been developed as an integer linear problem in programming [131]. By setting a threshold for the voltage drop, the method can be applied to detect the voltage sags in the network [133].

Monitor Location Area Method, another monitor placement method for the fault location, starts from the coverage for each location of monitor, aiming at the minimum number and optimal locations of monitors [136]. This method can also take the installation costs of monitors into account.

In [137], an optimal monitor placement for state estimation is defined, which is similar to the Monitor Reach Area Method. It is assumed that monitors are installed in the network to record three-phase incoming and outgoing active power, reactive power, voltage and current so that the parameters of interconnected buses can be computed. In other words, when the parameters at a bus are monitored, the adjacent bus or buses are

also considered as observable. By defining the valid locations of monitors to make a bus observable and the actual placement, the full observability of the whole network can be checked.

In [4][138]-[140], genetic algorithm (GA) is applied to derive the optimal monitor placement for various objectives including power system monitoring. As an optimization tool, GA implements inheritance, selection, crossover and mutation to automatically search for the best solution for a defined objective function [141]. At the beginning of the optimization, a random test set (called "population") is selected and will be repeatedly modified to produce the next generation through the aforementioned procedures. The improvement of population stops at the pre-set maximum number of iterations. For DNSE, the objective function can be set to achieve the highest accuracy of the estimated level of unbalance with a fixed number of monitors.

1.5 PROBLEM STATEMENT

The developed transfer coefficients in literature are based on known load flow values and detailed individual power system equipment parameters, and are not valid for conditions where the data is incomplete. Therefore, the methodology is obviously not suitable for real networks, particularly large networks.

The unbalance in a network is rarely considered under a probabilistic condition. As the uncertainty in the load is time-varying and unpredictable, the estimation, especially long term estimation, should be carried out on a probabilistic basis. A methodology for close-to-realistic modelling of the variation of the loads has not been addressed. Therefore, a clear and easy-to-use methodology with sufficient accuracy needs to be defined.

There are controversial conclusions on the impact of an asymmetrical line so that a critical condition needs to be established to define the influence of lines to be ignored or not.

As for the optimal monitor placement, Monitor Reach Area Method is objectively designed to detect the fault location and cannot provide sufficient accuracy for monitoring unbalance. Monitor Location Area Method tests numerous combinations and may not converge because it could exceed memory capacity for applications in large networks. The optimal monitor placement for state estimation, defined in [137], aiming at full observability, can provide various solutions but cannot define the accuracy of solutions and show an optimum.

1.6 AIMS OF RESEARCH

This research aims at providing solutions to the identified problems stated in the last section. Starting with the identification of the source of unbalance, a methodology is expected to be developed to trace the propagation of unbalance in existing networks and provide the optimal solution for the monitor placement with a minimum number of monitors. Therefore, the main objectives of the research are:

- To verify the existing methodologies of identification of the source of unbalance in the network;
- To develop a probabilistic framework for estimations of unbalance in both real-time detection and long term prediction;
- To develop a distribution network state estimator to trace unbalance in the distribution network including identification of the source of unbalance, as well

as achieving full network observability with respect to steady state voltage variation including the unbalance at non-monitored buses;

- To investigate the influence of line configurations on unbalance and establish the criterion when line conditions are necessary to be accounted for;
- To apply optimization algorithm to derive optimal monitor placement. This includes minimum error using a limited number of monitors and the location of monitors, taking into account existing monitors;
- To develop a user friendly interface to the developed software for the assessment of network performance clearly indicating areas of the network affected by the unbalanced voltages.

1.7 MAJOR CONTRIBUTIONS OF THIS RESEARCH

This research uses the developed distribution network state estimator to contribute to both the methodologies of probabilistic estimation of unbalance and the optimal placement for monitors. The contributions are summarized below. Note that parts of the related results are submitted for publication or published in international journals or proceedings of conferences and are indicated in the parentheses. A full list of publications can be found in Appendix F.

- Appropriate load model is derived by considering the types and proportions of different classes of customers (industrial, commercial, domestic). The integration of daily loading curves for each type of load closely simulates the daily change in the loads. This overcomes the problem when only a maximum loading at a bus is known. In this way, loads, the main cause of unbalance in distribution networks, can be modelled robustly to form the potential sources of unbalance [F1][F4][F5].

- Induction motors, wind turbine generators which represent three-phase distributed generation and photovoltaics which represent single-phase distributed generation are modelled in detail and an appropriate simplified version is applied in distribution network state estimation. Their impact on the attenuation of unbalance is investigated [F1].
- Existing methodologies for identification of source of unbalance are presented and examined.
- A distribution network state estimator and a methodology for probabilistic unbalance estimation are developed. They use the available power system parameters to calculate the health status of the network, considering the uncertainties in the network. The probabilistic results suit both real-time indication and long term estimation [F1][F3][F4][F5].
- The impact of lines is investigated, including the impact of the size of impedance and the asymmetry between three phases. The boundary for lines whose impact can be neglected, is established [F1].
- Two methods for optimal monitor placement for unbalance are demonstrated, enabling the unbalance and identification of the source to be traced. Both the manual ranking and the employment of genetic algorithm provide the same results for the locations of a minimum number of monitors, through different working processes and workloads. The methodologies provide the best solution with the highest accuracy for monitoring, using a limited number of monitors. Another optimal monitor placement method using particle swam optimization is also developed based on these methodologies [F2].
- By considering the already installed monitors in the network and encompassing their monitoring data, the suggested monitor set leads to the identification of the area affected by the unbalance. This is valid for the close-to-real-time estimation

or the update of unbalance in the network at all relevant network buses (monitored and non-monitored buses). A varying range for non-monitored buses for a prolonged period of time is suggested.

- Graphical presentation is developed to enable the on-screen presentation of results of unbalance propagation. Graphical user interface is developed to facilitate the use of the developed DNSE software using the network single line diagram as background [F1][F4]. The user manual for the developed software is given in Appendix E.

1.8 THESIS OVERVIEW

This thesis is organized into seven chapters.

Chapter 1 Introduction

This chapter introduces the background information of voltage unbalance and motivation of the research. It summarizes previous work in this area and discusses the unsolved problems. This is followed by the aims and major contributions of the thesis.

Chapter 2 Modelling of Power System

This chapter describes the basic models and possible computational tools for the study of unbalance. The power system components and the simulation and calculation methods presented in this chapter are used throughout the thesis. For the assessment of unbalance, three-phase models for equipments are a basis and any calculation should be carried out under three-phase conditions. Both the commercial accessible software package and customer-made program are introduced as well as all the test power systems used for demonstration of developed methodologies.

Chapter 3 Unbalance due to Asymmetrical Load

This chapter provides an overview of existing methodologies for the identification of source of unbalance in the network. By using the test network, the methodologies are commented with corrections and shortcomings. Based on the sources, the propagation of unbalance due to asymmetrical load is demonstrated by using different case studies to illustrate the behaviour of the network under different conditions of unbalance. This is a prerequisite for the probabilistic estimation in the next chapter.

Chapter 4 Probabilistic Estimation of Load Unbalance

This chapter develops a heuristic methodology for a one-day estimation of unbalance, illustrated in a section of a real distribution network in the UK. The methodology includes the consideration of the changing demands during a day in the network and the composition of the load seen at each site. By employing the variation in the power factors of three phases of a load, the unpredictable time-varying load is modelled with uncertainties to make it close to realistic. With reasonable assumptions of the changing loads and the operating conditions, the simulation results are compared and have good agreements with the real data in the network. The attenuations of induction motor, wind turbine generator and photovoltaic sources are respectively demonstrated.

Chapter 5 Unbalance Due to Asymmetrical Line

This chapter focuses on the impact of the line on the resultant level of unbalance. Starting from the detailed modelling of a line in the power system, the difference between balanced lines and unbalanced lines is introduced through both physical explanation and the mathematical modelling. The research of the line includes two aspects of its impact: the size of the impedance and the degree of its asymmetry. For both radial and meshed networks, the influences of an asymmetrical line are discussed. The margin for ignoring the asymmetry in the line is also suggested.

Chapter 6 Optimal Monitor Placement for Unbalance Monitoring

This chapter firstly introduces the background of unbalance monitoring and the motivation for optimal monitor placement for unbalance. Secondly, by using DNSE and the developed methods for ranking the importance of buses or optimization of monitor locations, the accuracy of different monitor sets is discussed and the optimal monitor placement is recommended. Finally, the DNSE results are compared to the data resulting from simulations of real loading data or real monitoring data. A long-run estimation based on the DNSE results is also illustrated using a heat map. The simulations are performed using a 24-bus section of the UK distribution network and a generic 295-bus distribution network.

Chapter 7 Conclusion

This chapter outlines the major conclusions of this thesis. Suggestions about further work and potential improvements of the presented work in the future are also indicated.

2 MODELLING OF POWER SYSTEM

2.1 INTRODUCTION

In simulations, a power system is represented as an equivalent mathematical model aiming at a close-to-realistic agreement with the true values of the system. Therefore, by studying the response of the modelled network, the status of the real network can be approximately estimated. With limited input data and available analytical tools, the simulated output is expected to be sufficient and accurate.

This chapter describes the tools selected and designed to assess unbalance, for which the three-phase basis is crucial, including three-phase power system models, calculation methods and software. The power systems used for the calculation are also presented. This framework is applied throughout the thesis.

2.2 MODELLING OF POWER SYSTEM EQUIPMENT

The most important characteristics in the assessment of unbalance are the three-phase voltages, as they can be converted into sequence domain to derive the quantified level

of unbalance. Three-phase models for power system equipments are necessary so that three-phase voltages and related parameters can be achieved within a distribution network. The models used in this thesis are all designed for steady state calculations without taking into account dynamic responses. The steady state models, i.e., models of three-phase load, line and transformer, are introduced in this section.

2.2.1 LOAD

There are linear and non-linear loads connected to the mains grid. Because the unbalance only focuses on the steady state loads at fundamental frequency and the study is based on distribution level (predominantly 11kV feeders), the loads are aggregated and can be represented using simple models.

2.2.1.1 CONSTANT POWER LOAD

As seen from 11kV substations, the loads are in the power form: $\boldsymbol{S} = P+\mathrm{j}Q$, where P and Q are the power demands aggregated at the substations and $\boldsymbol{S}$ stands for the apparent powers. For a three-phase assessment, loads are required to be distributed in three phases; each one represents individual values that are correlated or non-correlated. In other words, there are six typical values for a three-phase load: P_a, P_b, P_c, Q_a, Q_b and Q_c. Only in this way, the unbalance caused by loads can be separately quantified and the effects can be observed and classified.

With peak values provided by DNOs, the total loading will be distributed evenly among three phases for a balanced condition. The loads may be adjusted to an unbalanced condition or varied according to the daily loading curve, depending on the dedicated simulations.

2.2.1.2 INDUCTION MOTOR

Induction motors are only used here when their attenuation of unbalance is studied. They are always three-phase and operated according to the industrial load's schedule.

An induction motor is physically represented as an asynchronous machine with fixed impedance, inertia and efficiency. The input of the induction motor is governed by *P* and *Q* cannot be guaranteed.

2.2.2 LINE AND CABLE

The lines (both overhead line and cable) in this research are all modelled as an equivalent π model including one part of line impedance and two identical parts of shunt capacitance, shown in Fig. 2.1. In the calculation, they are transformed into the admittance forms. Both the line admittance matrix ($\boldsymbol{Y_L}$) and the shunt admittance matrices ($\boldsymbol{Y_S}$) are 3×3 matrices. $\boldsymbol{Y_S}$ should be added to "FROM end" and "TO end" of the line model after completing $\boldsymbol{Y_L}$. That is the last stage of calculating the overall matrix for a line. Therefore, when the construction of the detailed model of line impedance matrix ($\boldsymbol{Z_L}$) is discussed, as the detailed calculation will be demonstrated in Chapter 5, the shunt capacitances are ignored. The admittance matrix can be derived using (2.1).

$$\boldsymbol{Y_L} = \boldsymbol{Z_L}^{-1} = \boldsymbol{G} + \mathrm{j}\boldsymbol{B} \tag{2.1}$$

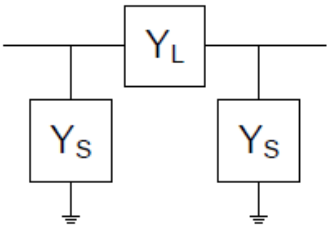

Fig. 2.1 π Equivalent Circuit Model of a Line.

In a balanced condition, the impedance matrix contains equal diagonal elements and equal off-diagonal elements respectively, and is assumed to be constant under all circumstances, ignoring changes of temperature, on-load transformer tap change, etc. Therefore, the admittance matrix for the line has equal diagonal elements and identical

off-diagonal elements respectively. For asymmetrical lines, the admittance matrix is 3×3 with non-zero and different values of off-diagonal elements.

2.2.3 TRANSFORMER

There are three different types of transformer windings: delta, star and earthed-star. The equivalent circuit for an ideal transformer (regarded as single-phase) can be represented by using a primary side leakage impedance, a secondary side leakage impedance, turns ratio and a magnetizing impedance. Because the magnetizing admittance is usually small (μS), its excitation can be ignored and it is always neglected in simulations [46]. For the assessment of unbalance, where three-phase modelling is a necessity, robust models should be developed for three-phase load flow or three-phase state estimation.

For the simulations in this thesis, transformers are modelled using the equivalent sequence circuits and sequence impedances in p.u. The positive sequence circuit has the same topology with the presented network and the negative sequence powers flow through the same paths with positive sequence power. The zero sequence equivalent circuit is determined by the winding connection type, neutral grounding and the core construction [46], and may be blocked by the disconnection of zero sequence power flow path. Zero sequence circuits for five connection types are shown in Fig. 2.2 [46]. The absence of the arrows that indicate the flow direction of zero sequence power means the zero sequence flow is halted.

Taps are designed on windings so that their position can be changed to fulfil the voltage demand of the secondary side. The on-load tap-changers automatically change taps when the transformers are energizing [46]. With nominal per unit turns ratio (n), transformers can be represented by a π equivalent model using the positive sequence impedance matrix ($\boldsymbol{Z}$) [73], which is similar to the line model, shown in Fig. 2.3.

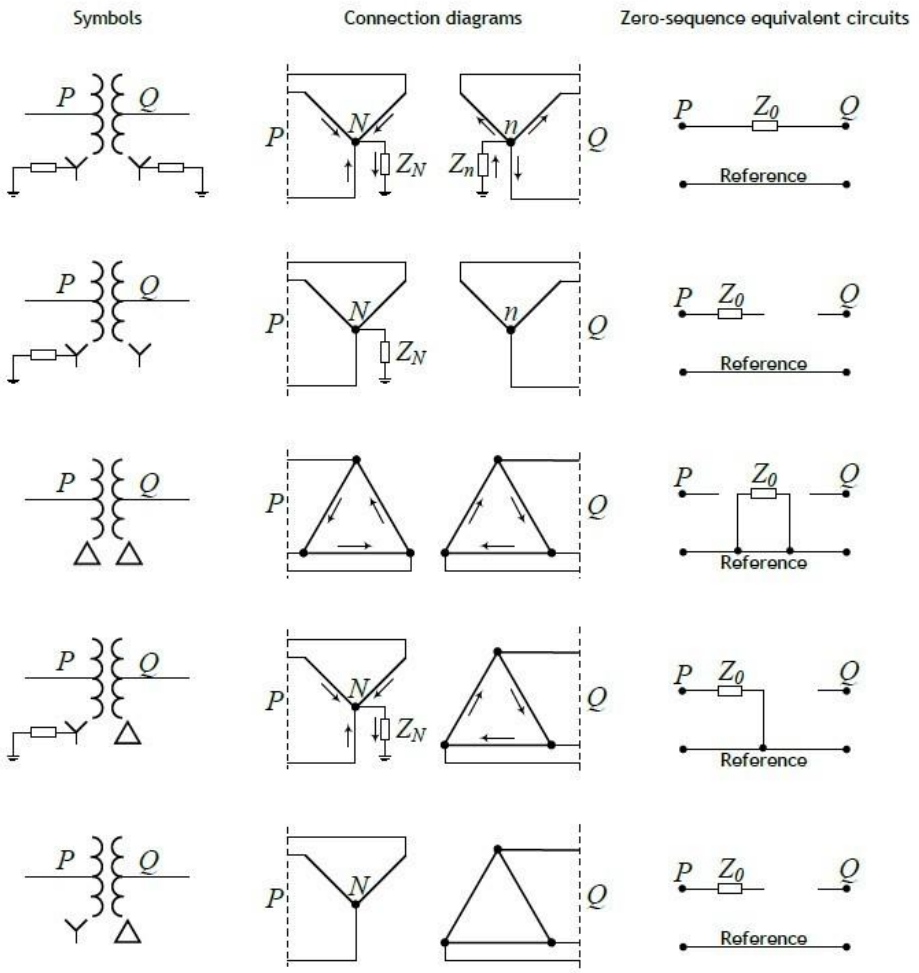

Fig. 2.2 Zero sequence equivalent circuits of five three-phase transformer banks (adopted from [46]).

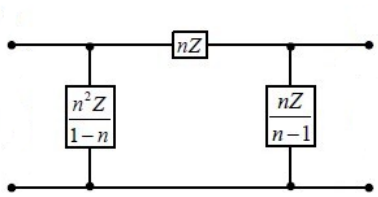

Fig. 2.3 Equivalent circuit for tap changing transformer (adopted from [73]).

Depending on the transformer connection type, phase shifts may occur between primary side voltages and secondary side voltages. In mathematical modelling, that can be achieved by advancing or retarding the positive sequence voltage and current of the unknown side by a certain degree. The connection of windings determines both the zero sequence circuit and phase shift.

The transformer type used in the study is delta-earthed-star, which blocks zero sequence components. The transformers are assumed to be on-load tap changing transformers with secondary side taps [94][142]. The transformer admittance matrix is formed involving sequence domain components. In total, the input characters for transformers in p.u. are: connection type, tap information, positive sequence impedance and zero sequence impedance.

2.2.4 GENERATOR

2.2.4.1 EXTERNAL GRID

The power supply is not specifically modelled in this research. Instead of a model of a synchronous machine, it is always represented as an "External Grid"; in other words, a slack bus with fixed unity output voltage as the reference voltage for the network. It is an ideal voltage source that can be regarded as an infinite bus. The slack bus, with an intrinsic short circuit inverse impedance that flexibly varies according to the output power, is expected to meet the power demand for the whole power system. In addition, the power supply is always assumed to be perfectly balanced, providing a source for mitigating unbalance.

2.2.4.2 WIND TURBINE

A wind turbine generator, as a three-phase distributed generator, physically consists of a wind turbine, a drive train and generation system [143]. It captures the kinetic energy of the wind by its blades, converts the energy to electric power and transports the controlled power to the mains grid through a transformer and power electronics [144]. The output power (P) of a wind turbine generator is determined by the power coefficient (C_p), air density (ρ), wind velocity (V) and the swept area of rotor blade (A), as given in (2.2). Because the power coefficient and rotor blade are fixed for a specific design and

the air density around an area usually stays constant, the output of the generator is varied in terms of the wind speed.

$$P = 0.5 C_p \rho V^3 A \tag{2.2}$$

2.2.4.3 PHOTOVOLTAIC SOURCE

A photovoltaic (PV) system is physically composed of p-n junctions that can convert the solar energy into electricity through photovoltaic effect. Its equivalent circuit is composed of a photocurrent source, a diode, a parallel resistor that stands for a leakage current and an internal series resistor [144]. The formulations of PV consider the factors such as the photocurrent, induced due to solar insolation, and the ambient temperature, influenced by solar energy. For the assessment of unbalance, PV stands for single-phase generators whose detail parameters are not required. Therefore, in the study, a PV is controlled by the output active power, which varies according to solar insolation.

2.3 DISTRIBUTION NETWORK STATE ESTIMATION

State estimation aims to derive the current state of the power flow in the network by using incomplete data. Due to a lack of necessary data, conventional load flow may not be performed. State estimation can then be employed to eliminate this limitation [46]. On the other hand, when there is little available data, the state estimation may not converge. Under this circumstance, some values from the three-phase load flow can be employed, which can provide the likely values for the three-phase state estimation with certain errors. By using the load flow results, the three-phase state estimation has an increased possibility of converging towards the true value.

2.3.1 THREE-PHASE LOAD FLOW

Three-phase load flow is fundamental to the unbalance analysis and provides the flow equations to describe the topology of the network. By employing the appropriate software tools, the whole network can be represented by proper models that are ready for a load flow. After running a load flow, all the voltages, currents and powers can be derived, i.e., the network profiles can be achieved.

In order to solve the unbalance problem, three-phase load flow is required rather than single-phase load flow, because only three-phase load flow can specify the results for each phase separately and distinguish the differences between arbitrary phases. In single-phase simulations, all the phase elements are considered to be the same and only a total result for three phases is provided.

When only the loading data are available without any actual monitoring data, three-phase load flow can provide the likely range of level of unbalance, as demonstrated in the following chapters.

2.3.1.1 FULL NEWTON-RAPHSON METHOD EQUATIONS

Instead of single-phase load flow, three-phase load flow is required to detect a real-time level of unbalance. Based on generator terminal voltages, loads, line impedances and transformer impedances, three-phase full Newton-Raphson load flow gives the expected results including phase voltages that are crucial in calculating the level of unbalance.

The single-phase load flow equations for powers injected in bus i from bus k (k=1, 2, 3 …) are (2.3)(2.4)[46]:

$$P_i = V_i \sum_{k=1}^{n} V_k [G_{ik} \cos(\theta_{ik}) + B_{ik} \sin(\theta_{ik})] \tag{2.3}$$

$$Q_i = V_i \sum_{k=1}^{n} V_k [G_{ik} \sin(\theta_{ik}) - B_{ik} \cos(\theta_{ik})] \quad (2.4)$$

where $\boldsymbol{Y}$=G+jB denotes the line admittance matrix (including shunt elements) between any two buses, and θ denotes the voltage angle between two buses.

Similar to single-phase load flow, there are five types of measurements in three-phase load flow: net injections of active power (P_i^p) and reactive power (Q_i^p) at bus i of phase p, line impedances matrix ($\boldsymbol{Y}$=G+jB), voltage magnitudes at bus i of phase p (V_i^p) and voltage angles between two buses and two phases (θ_{ik}^{pm}). By considering the values of each phase separately, three-phase load flow from bus k to bus i can be calculated using (2.5)(2.6) [46]:

$$P_i^p = V_i^p \sum_{k=1}^{n} \sum_{m=1}^{3} V_k^m \left[G_{ik}^{pm} \cos\left(\theta_{ik}^{pm}\right) + B_{ik}^{pm} \sin\left(\theta_{ik}^{pm}\right) \right] \quad (2.5)$$

$$Q_i^p = V_i^p \sum_{k=1}^{n} \sum_{m=1}^{3} V_k^m \left[G_{ik}^{pm} \sin\left(\theta_{ik}^{pm}\right) - B_{ik}^{pm} \cos\left(\theta_{ik}^{pm}\right) \right] \quad (2.6)$$

where p and m can be either A, B or C phase.

In addition, three-phase line flow equations can be deducted from (2.7)(2.8) [116]:

$$P_{ik}^p = V_i^p \sum_{m=1}^{3} V_k^m \left[G_{ik}^{pm} \cos\left(\theta_{ik}^{pm}\right) + B_{ik}^{pm} \sin\left(\theta_{ik}^{pm}\right) \right] \quad (2.7)$$

$$Q_{ik}^p = V_i^p \sum_{m=1}^{3} V_k^m \left[G_{ik}^{pm} \sin\left(\theta_{ik}^{pm}\right) - B_{ik}^{pm} \cos\left(\theta_{ik}^{pm}\right) \right] \quad (2.8)$$

The load flow needs to be computed on a p.u. basis to eliminate voltage level transformation. Therefore, every character used in the equations must be converted to p.u. value before being calculated.

By using the Jacobian matrix ($\boldsymbol{H}_x$) [46] shown in (2.9), the derivatives of load flow equations are calculated through sequential differentiation of (2.5) and (2.6).

$$\mathbf{H_x} = \frac{\partial \mathbf{H}(\mathbf{x}_\mathrm{k})}{\partial \mathbf{x}} \tag{2.9}$$

where $\boldsymbol{x_k}$ denotes the estimation of desired value ($\boldsymbol{V}$ or θ) at the k^{th} iteration, $\boldsymbol{H(x)}$ is the equation defining P in (2.5) or Q in (2.6).

The final converged values can be derived by iterating the computing process, shown by (2.10), until the deviations are small enough to satisfy the set error ε, shown by (2.11).

$$\mathbf{x}_{\mathrm{k+1}} = \mathbf{x}_\mathrm{k} + \Delta\mathbf{x} = \mathbf{x}_\mathrm{k} - [\mathbf{H_x}(\mathbf{x}_\mathrm{k})]^{-1} \times \mathbf{H}(\mathbf{x}_\mathrm{k}) \tag{2.10}$$

$$|\Delta\mathbf{x}| \leq \varepsilon \tag{2.11}$$

The three-phase voltages derived by the load flow results can then be transformed to three sequence voltages [47] for the assessment of unbalance.

A slack bus for the three-phase load flow is necessary to be defined, with voltage of 1.0 p.u. in magnitude and 0° angle in phase *A*. The voltages in phase *B* and *C* are of the same magnitude and have -120° or 120° phase shift with respect to phase *A*.

2.3.1.2 INPUTS AND OUTPUTS OF THREE-PHASE LOAD FLOW

In addition to $\boldsymbol{Y}$ admittance matrix for the lines and a reference voltage at the slack bus, six parameters of each load are required:

- Active power load for phase *A*, *B* and *C*: P_a, P_b, P_c
- Reactive power load for phase *A*, *B* and *C*: Q_a, Q_b, Q_c

The following results can be derived from the load flow analysis for all buses:

- Active power for phase *A*, *B* and *C*
- Reactive power for phase *A*, *B* and *C*
- Three-phase p.u. voltage magnitudes at each bus
- Three-phase voltage angles at each bus

- Three-phase powers at sending end and receiving end of a line
- Three-phase powers at primary side and secondary side of a transformer

For three-phase load flow, as well as the state estimation discussed in the following section, the power system is assumed to be operating under a steady state condition, without any dynamic issues or additional disturbances. All loads are considered as constant power loads. The power system parameters, such as the transformer impedance and the line impedance, are accurate and remain unchanged with respect to thermal ageing.

2.3.2 THREE-PHASE STATE ESTIMATION

In the real world, all operating parameters of power systems are recorded via monitors. Due to the influence of the precision and accuracy of a monitor introduced by the structural materials, measurement gross errors (whose distributions typically fit normal distributions) always exist. On the other hand, monitors are designed to record specified character parameters within certain coverage areas. Because they are not installed at every bus in the network, the observability of some buses may be lost. The full observability of the whole network can only be achieved by selective placement of monitors across the network if the number of monitors is limited. Depending on the type, different monitors have different coverage, recording characteristics and accuracy. To cope with these two problems, three-phase state estimation is useful to provide reliable results. Using incomplete data from the monitors, related missing quantities can be assessed by calculation.

2.3.2.1 WEIGHTED LEAST SQUARES

State estimation is a powerful tool which uses incomplete datasets to estimate full power flow data in the network. In addition, it can be used to avoid measurement errors and assist in the detection of fault data.

In three-phase state estimation, the number of equations may be more than the number of state variables. The limited parameters derived from monitoring data or from the load flow are a prerequisite for state estimation and are represented as the state variables **x**. State estimation aims at the smallest error of the estimated variable to its true value, as defined in (2.12).

$$\mathbf{e} = \mathbf{z} - \mathbf{z}_{\text{true}} = \mathbf{z} - \mathbf{H}(\mathbf{x}) \tag{2.12}$$

where $\boldsymbol{z}$ is the vector of measurements, $\boldsymbol{H(x)}$ is a non-linear set of equations formulating the relation between the true state of the power system with state variable $\boldsymbol{x}$, and $\boldsymbol{e}$ is the vector between the true state values and the observed state variable values [46]. $\boldsymbol{e}$~$N(0, \boldsymbol{R})$, where $\boldsymbol{R}$ is the covariance matrix of the measurement errors (**e**).

In the Weighted Least Squares method, the objective function of state estimation is shown in (2.13).

$$\min_{x} [\mathbf{z} - \mathbf{H}(\mathbf{x})]^{\mathrm{T}} \mathbf{R}^{-1} [\mathbf{z} - \mathbf{H}(\mathbf{x})] \tag{2.13}$$

By using the Newton-Raphson load flow equations, the state estimation can be solved by using updating equations iteratively, as shown in (2.14) and (2.9):

$$\mathbf{x}_{\mathrm{k+1}} = \mathbf{x}_{\mathbf{k}} + (\mathbf{H}_{\mathrm{x}} \mathbf{R}^{-1} \mathbf{H}_{\mathrm{x}})^{-1} \mathbf{H}_{\mathrm{x}}^{\mathrm{T}} \mathbf{R}^{-1} [\mathbf{z} - \mathbf{H}(\mathbf{x}_{\mathrm{k}})] \tag{2.14}$$

where $\boldsymbol{x_k}$ is the estimation of the state variables at the k^{th} iteration and $\boldsymbol{H_x}$ is the Jacobian matrix.

In this study, $\boldsymbol{x}$ is defined as the three-phase voltage magnitudes and angles of each bus [46].

2.3.2.2 GENERALIZED LEAST SQUARES

The generalized least squares (GLS) [145] method, rather than the weighted least square method [46][113], emphasizes the importance of the correlation of measurements in a covariance matrix, by presenting non-zero off diagonal elements in $\boldsymbol{R}$. GLS is suitable

for three-phase distribution network state estimation because it accounts for the correlation of measurement errors between any two of the three phases [114]. The off-diagonal elements are the reciprocal of the measurement error variances, like the diagonal elements. The measurement error correlation in a three-phase network can be derived by inspecting the historical measurement data as described in more detail in [146]-[148].

The elements of the covariance matrix of two measurements $\boldsymbol{x}_i$ and $\boldsymbol{x}_j$ are defined by (2.15):

$$\mathrm{cov}(\mathrm{X_i}, \mathrm{X_j}) = \sigma_{\mathrm{ij}}^2 \tag{2.15}$$

where i and j denote the bus number, σ denotes the standard deviation of measurements.

The standard deviations for diagonal elements and off-diagonal elements are different and require detail specifications for each case, with considerations of a particular kind of monitor and special measurement assumptions.

2.3.3 Assumptions of Modelling Unbalance in DNSE

There are three types of measurements in the network: real measurement, virtual measurement and pseudo measurement.

Real measurements are from the buses where monitors are installed. The measurements may cover three-phase active and reactive power consumptions at a bus, the voltage and current of a bus, including both magnitudes and angles. The measurements of monitoring data are considered as independent and do not have any correlation with one another. The accuracy of real measurements depends on the error of monitors and is assumed to be modelled using normal distribution with a standard deviation of 0.2% [94][149].

Virtual measurements are assumed for the buses with zero net power injections, i.e., unloaded buses, because it is certain that there is no power consumption at the bus. They are assumed to have a standard deviation of 2×10^{-7} [123] and are independent from each other as well.

Pseudo measurements are used in the non-monitored load buses. The value is assumed according to historical data, including loading data and customer billing data. The measurements are assumed to be correlated between phases and are affected by many factors such as ambient weather, season, types of customers, and time point of the day [94].

There are five important values for three-phase state estimation, defined by [94]:

- Variance of errors in each phase: $\sigma_{X_i^a}$, $\sigma_{X_i^b}$, $\sigma_{X_i^c}$
- Real power error correlation, all phases, at bus *i*: $corr\,(e_{P_i^p}, e_{P_i^m})$
- Reactive power error correlation, all phases, at bus *i*: $corr\,(e_{Q_i^p}, e_{Q_i^m})$
- Real and reactive power error correlation, all phases, at bus *i*: $corr\,(e_{P_i^p}, e_{Q_i^m})$
- Real-real, reactive-real, reactive-reactive error correlation, at bus *i*, *j*: $corr(e_{X_i^p}, e_{X_j^m})$

X corresponds to an arbitrary measurement of active or reactive power, *p* and *m* can be any phases of *A*, *B* and *C*, and *i* and *j* are arbitrary buses.

The values for three types of measurements are listed in Table 2.1. The pseudo measurements are calculated from two monitoring sites with three-phase measurements every 30 minutes for 10 days and with mixtures of domestic (80% and 88%), commercial (18% and 11%) and industrial loads (2% and 1%) [94].

Table 2.1 Measurement Error Variances and Correlations of the Different Types of Measurement Models

Measurement Type	Real Measurements	Virtual Measurements	Pseudo Measurements
$\sigma_{X_i^a}$	0.2%	2×10^{-7}	7%
$\sigma_{X_i^b}$	0.2%	2×10^{-7}	7%
$\sigma_{X_i^c}$	0.2%	2×10^{-7}	7%
$corr(e_{P_i^p}, e_{P_i^m})$	0	0	0.99
$corr(e_{Q_i^p}, e_{Q_i^m})$	0	0	0.97
$corr(e_{P_i^p}, e_{Q_i^m})$	0	0	0.90
$corr(e_{X_i^p}, e_{X_j^m})$	0	0	0.52

2.3.4 THE WHOLE DNSE PROCESS

Fig. 2.4 shows the flow chart of the whole state estimation process. In simulations, parameters are set in detail for three-phase load flow such that it can provide all required values prepared for three-phase state estimation. In this way, an arbitrary monitor set can be assumed and tested. By calculating the state estimation, the status of the whole network can be observed with varying degrees of accuracy. When regarding the existing monitors in the real network, data are far more incomplete and only a few values can be read from the monitors. Therefore, the load flow results may be used to assist the state estimation.

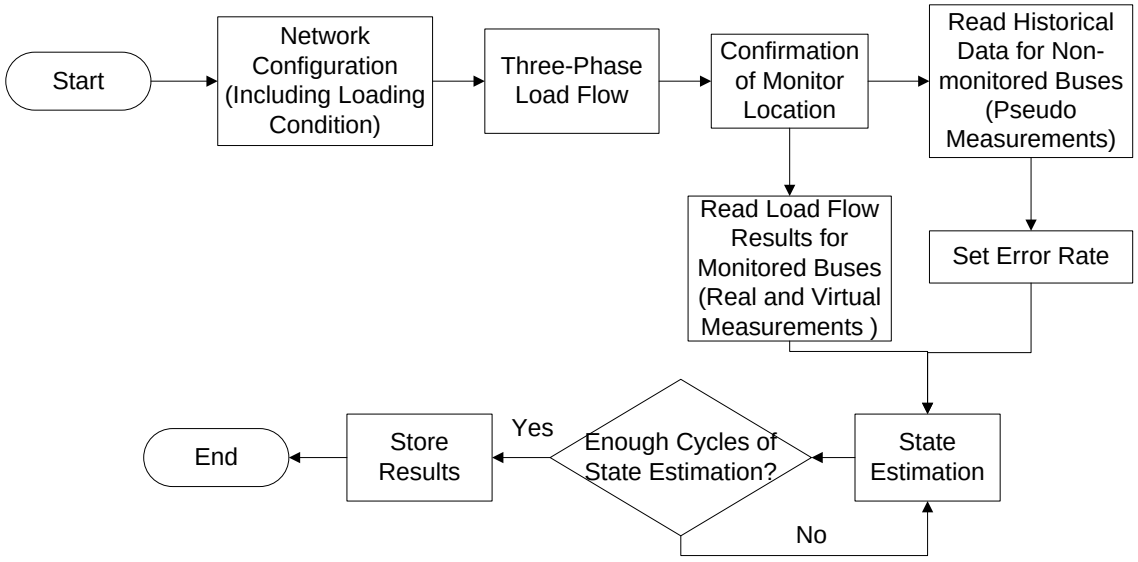

Fig. 2.4 Process of distribution network state estimation.

2.4 VOLTAGE UNBALANCE ASSESSMENT SOFTWARE

All simulations that merely use three-phase load flow are calculated by the network model developed in both DIgSILENT PowerFactory and the developed Matlab dedicated software, and validated against each other under all conditions and against IPSA+ results under a balanced condition. The results presented in this thesis are obtained in DIgSILENT PowerFactory. The three-phase unbalanced load flow results of DIgSILENT PowerFactory and Matlab models showed an average relative error between VUFs of about 4.5%, considering the different requirements and accuracies of these modelling environments. Comparison of results obtained in different modelling environments is given in Appendix A.

Because DIgSILENT PowerFactory can only perform single-phase state estimation, the simulations related to three-phase state estimation are all calculated in the dedicated software in Matlab, providing greater capacity and more flexibility for the computation. The full listing of Matlab code is given in the Appendix B.

2.5 TEST NETWORK

2.5.1 4-BUS TEST RADIAL NETWORK

A 4-bus radial network is developed for the study of the impact of line impedance. It is composed of 1 generator, 4 11kV buses, 3 identical overhead lines and 3 loads, shown in Fig. 2.5. Power flow from the synchronous machine is considered as entirely balanced, producing 1.0 per unit voltage with a reference angle of 0° in phase *A*. An unbalanced load is located at bus 3 (the middle loaded bus), while the loads connected to bus 2 and bus 4 are both balanced. Under a balanced condition, the three loads are all 0.03+j0.03 p.u. (each phase takes 0.01+j0.01 p.u.) for three phases based on a 100MVA

system power base. The lines between buses have identical impedances and are fully transposed, i.e., they do not present sources of unbalance. It is assumed that the positive sequence impedances and negative sequence impedances of the lines are equivalent, with a value of 0.2+j0.4 p.u.

Because the network is radial, by varying one or two variables each time, these single-variable experiments will indicate the influence of line impedance on the overall system unbalance.

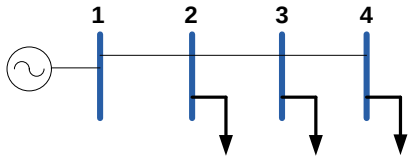

Fig. 2.5 4-bus test radial network.

2.5.2 5-Bus Test Meshed Network

A 5-bus meshed network, which is used to test the propagation of unbalance and illustrate the methodology, is shown in Fig. 2.6. It consists of 1 generator, 5 11kV buses, 5 overhead lines and 4 loads. It is assumed to have an entirely balanced power supply from the upstream network. All the lines are symmetrical, with an impedance of 0.1+j0.2 p.u. Initially the four loads are all balanced, with 0.02+j0.005 p.u. loading per phase per load. In later simulations, the load at bus 5 will always be balanced while the loads at three upstream buses will be modified to represent an unbalanced condition.

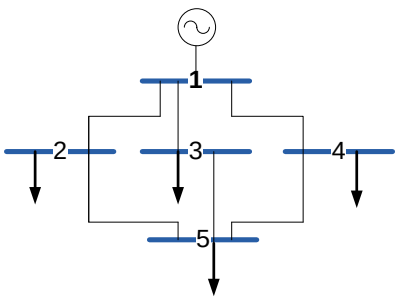

Fig. 2.6 5-bus test meshed network.

2.5.3 24-Bus Section of Real UK Distribution Network

Fig. 2.7 shows a meshed 24-bus network that contains 14 33kV buses (labelled green) and 10 11kV buses (labelled red), with all the topology and parameters taken from a real distribution network in UK. This section receives perfectly balanced power flow from an external grid through bus 1, which is the only power supply for this area. The 12 transformers have delta earthed-star (Dyn11) winding connection, which blocks zero sequence flows. Every 11kV bus serves a local load whilst 33kV buses have no direct loads. In theory, there are 10 loads and 17 lines in the network that can be considered as unbalance sources. In the simulations, they will be adjusted to unbalanced condition depending on different aims of research. The network is used for most simulations presented in this thesis. The developed methodologies for probabilistic estimation of unbalance due to loads and for optimal monitor placement will be illustrated on this network as well as the boundaries of influence of line impedance.

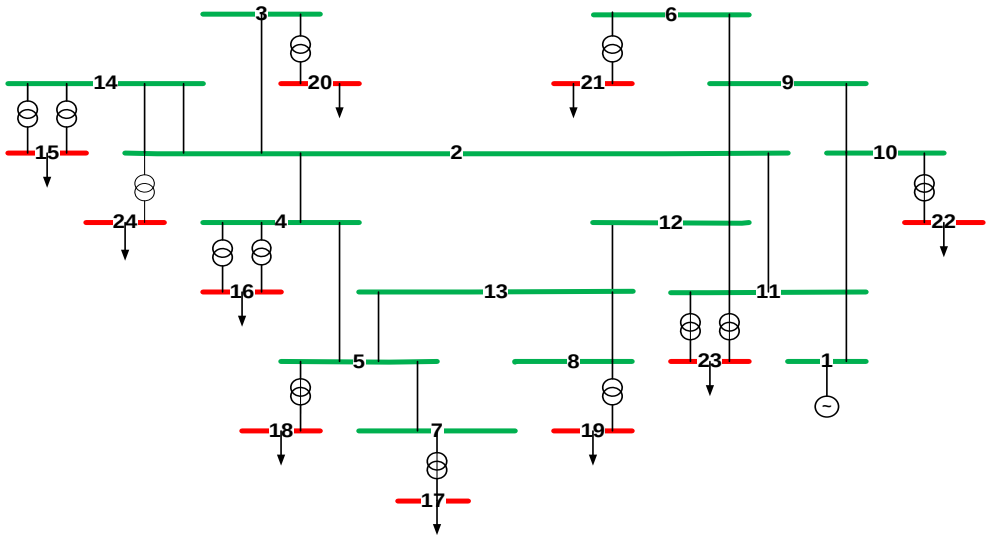

Fig. 2.7 24-Bus UK distribution network.

Due to the proximity to bus 1, buses 11 and 23 are considered to be located in the "power supply area". Other buses are further from the power supply compared to buses 11 and 23. The loads at buses 15 and 23 are the largest while the load at bus 18 is the smallest.

Detailed parameters are given in Appendix C.1. The actual names of substations in the network are not presented due to commercial restrictions.

2.5.4 295-BUS GENERIC DISTRIBUTION NETWORK

The 295-bus generic distribution network is shown in Fig. 2.8. It is designed to represent a generic UK distribution network for academic study [150]. The network derives power from 400kV/275kV transmission in-feeds. The 132kV and 33kV networks are predominantly meshed while the 11kV and 3.3kV networks are predominantly radial. It comprises 295 buses, 276 overhead lines and underground cables, 39 transformers and 148 loads. The developed methodology for optimal monitor placement will be illustrated by using this network, particularly the 11kV section of the network. Detailed parameters are given in Appendix C.2.

2.6 SUMMARY

The assessment of unbalance necessitates three-phase modelling of the power system. The chapter introduces the equivalent models for power system equipments on a three-phase basis. To analytically quantify the level of unbalance, even when the network data are incomplete, the techniques of three-phase load flow and three-phase state estimation introduced in this chapter can be applied to derive the desired data. The measurement errors are also defined in order to have a realistic approximation of the true values in the real networks. Different networks used for various purposes are also described in this chapter. It is also stated that all the results presented in this thesis are obtained using DIgSILENT PowerFactory or the dedicated Matlab programme, developed during this research.

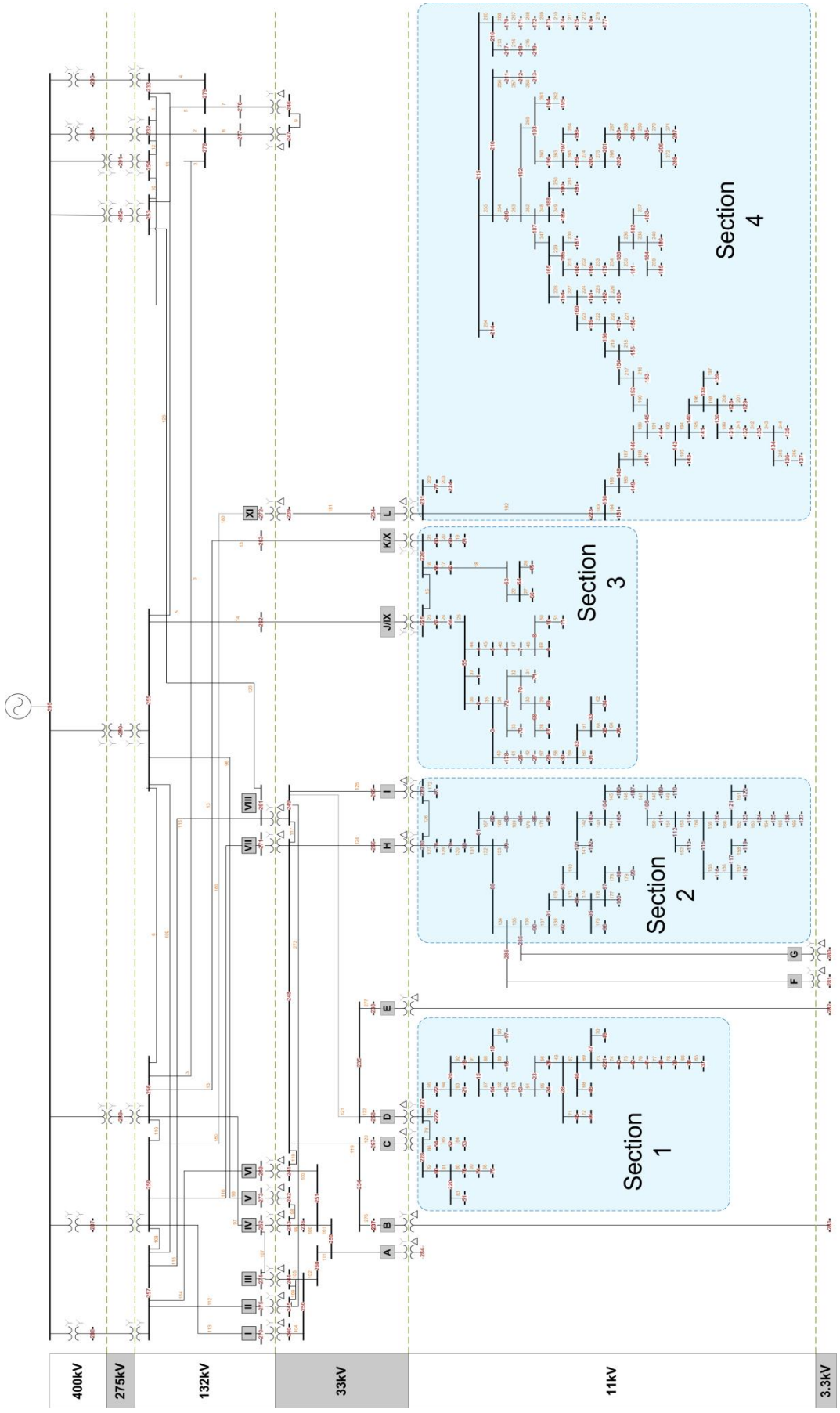

Fig. 2.8 295-bus generic distribution network.

3 UNBALANCE DUE TO ASYMMETRICAL LOAD

3.1 INTRODUCTION

If an unbalance phenomenon exists, system equipments and user applications are influenced by reduced power quality. Overheating, derating of machines and further problems may cause damage to electrical equipments and have negative effects on the efficiency and will accelerate the ageing of the apparatus. For both DNOs and end users, that is definitely unexpected because of the incurred economic costs. Because voltage unbalance is a long term phenomenon [15][151], it requires specific calculations and methodology to discover and detect the source.

Under normal conditions, there should not be any negative sequence power flow theoretically. But for abnormal conditions such as voltage unbalance, negative sequence power appears and affects the network states through flowing currents. When unbalance is observed, because it propagates to all buses in the network, the source may not be apparent. This problem raises the importance of identifying the origin of unbalance. If the source is discovered, measures can be taken accordingly.

As unbalance propagates to the whole network, its behavior and influence on the network are important to the observer. Starting from the source of unbalance, whether aggregation or cancellation occurs during the propagation determines the weak area of the network and indicates where the attention should be paid to.

This chapter examines methodologies to identify the unbalance source and studies the basic propagation of unbalance for the preparation of probabilistic estimations. The aim is to verify existing methodologies as well as to develop a reliable index indicating the source of unbalance. The knowledge of propagation is demonstrated on the 5-bus network to facilitate the understanding of relevant physical relationships and therefore further research on unbalance. The simulations in this chapter only focus on an unbalanced load which is the most likely cause of unbalance in a distribution network, disregarding any other types of source.

3.2 Identification of Source of Unbalance

3.2.1 Feasible Methodologies

The unbalance described in this section is quantified by VUF. A new factor called "Apparent Power Unbalance Factor" is also introduced in the sequel to identify the source of unbalance.

3.2.1.1 Negative Sequence Power Angle

Reference [45] suggests a methodology for identification of the source of unbalance at the load side by inspecting the negative sequence power angle. The angle of the origin of unbalance is reported to be usually bigger than +90° or smaller than -90°, located either in the second quadrant or third quadrant using the rectangular coordinate. When the result at the measuring point matches this range, the bus is on the side of the source

of unbalance seen from a transformer. As additionally stated, when only one unbalanced load exists, a negative sequence power angle within a specified range indicates that the load at that point is the source of unbalance.

The reliability of this rule however needs to be examined because of the unknown quantity of samples. Exclusion may exist when there is only one load in the system.

3.2.1.2 INJECTION OF NEGATIVE SEQUENCE

Reference [95] emphasizes the ability of the source to generate negative sequence active power at fundamental frequency and indicates that both the line unbalance and load unbalance should obey this rule. Buses other than the source of unbalance can only perform as negative sequence power sinks, not the generating unit. This statement actually is a further and simpler expression of the methodology of [45]. Using graphical representation, the methodology can be easily examined and verified.

3.2.1.3 RATIO OF NEGATIVE SEQUENCE POWER TO POSITIVE SEQUENCE POWER

To clearly identify the source of unbalance, [94] develops the factor "Complex Apparent Power Unbalance Factor (SUF)", shown in (3.1). It is declared that only the source of unbalance results in a significant value of this factor. Compared to the previous two methodologies, this definition takes both the power magnitude and angle into consideration.

$$SUF = \frac{Negative\ sequence\ apparent\ power}{Positive\ sequence\ apprant\ power} \tag{3.1}$$

3.2.2 ILLUSTRATIVE RESULTS OF DIFFERENT METHODOLOGIES

3.2.2.1 ASSUMPTION OF CASE STUDY

The methodologies are examined using the 24-bus network. In this test, the source of unbalance is set to be the load at bus 15. Twenty independent cases are considered. For an individual case, six random values of scaling coefficient ranging from 0.5 to 1.5 are

generated by Matlab. In total, there are 120 random values of scaling coefficient for the variation of the source of unbalance, shown in (3.2).

$$\text{Input Unbalance Scaling Coefficient} = \begin{bmatrix} x_{1,1} & \cdots & x_{1,6} \\ \vdots & \ddots & \vdots \\ x_{20,1} & \cdots & x_{20,6} \end{bmatrix} \tag{3.2}$$

where the scaling coefficient $x_{i,j}$ is $0.5 \leq x_{i,j} \leq 1.5$.

The random values of $x_{i,j}$ are multiplied by the active power and reactive power of the initial balanced load at bus 15 to create unbalanced input. For each case, the application of the random variables is shown in (3.3). The 20 groups of new loads at bus 15, instead of the balanced load, will be used to calculate 20 load flow cases separately.

$$\text{Input Unbalance Load at Bus 15} = \begin{bmatrix} P_a & Q_a \\ P_b & Q_b \\ P_c & Q_c \end{bmatrix} = \begin{bmatrix} x_{i,1} \times P & x_{i,4} \times Q \\ x_{i,2} \times P & x_{i,5} \times Q \\ x_{i,3} \times P & x_{i,6} \times Q \end{bmatrix} \tag{3.3}$$

where i denotes the i^{th} case.

Note that for all 20 cases, the unbalanced load is always connected to bus 15 with all other loads and lines remaining entirely balanced and unchanged. This means, for the whole network, the load at bus 15 is the only variable (the only source of unbalance) with no other interferences.

Three-phase load flow is employed to calculate all the desired parameters. Assuming there are no monitor placement issues or state estimation issues in the network, the network is considered as fully observable without uncertainty.

3.2.2.2 VUF PROBABILITY DISTRIBUTION

Fig. 3.1 illustrates the resultant probability density function (PDF) of the VUFs of bus 15 for the 20 cases. Because the input unbalance scaling coefficient is randomly distributed within 0.5 and 1.5 and because 20 cases is a relatively small number for a Monte Carlo (MC) calculation, the VUFs disperse across the achievable values and do

not fit any statistical distributions. If more random input values are taken into account, the PDF bars should be more average. The range from 0.5 to 1.5 results in bigger loading than the usual working loading condition and leads to possible severe conditions of unbalance among three phases of the source. Therefore, the average VUF for these 20 cases is high, around 2.0577%. There is also one case with the VUF around 4% which exceeds the instantaneous limitation. Compared to the 95% weekly restriction of 2%, 40% of resultant VUFs rise beyond 2% and are intolerable.

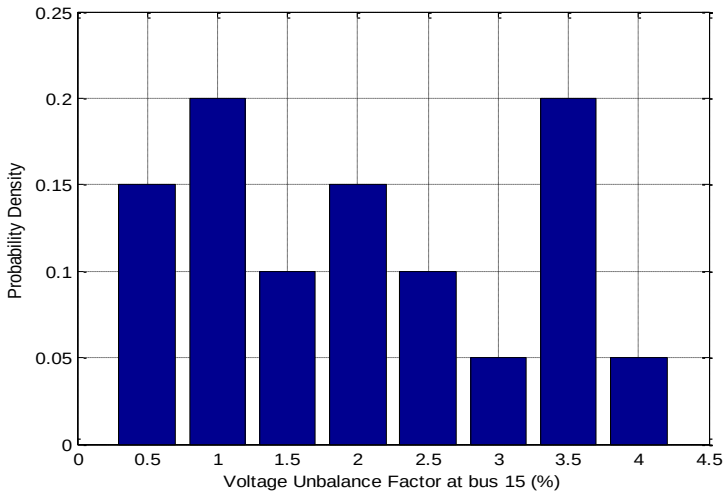

Fig. 3.1 Probability Density of VUF Distribution of 20 Cases.

Fig. 3.2 shows the VUFs for all loaded buses. Fig. 3.2 (a) is the box plot of statistical VUFs at the buses. By ordering the data for each bus in ascending sequence, the 25^{th} percentile (1^{st} quartile) and 75^{th} percentile (3^{rd} quartile) form the blue box in the box plot. Therefore, the box can be interpreted as the inter-quartile range which contains half of the total values. The red horizontal line inside the box denotes the mean value (50^{th} percentile) of the data. The black vertical lines at both ends of the blue box indicate the full scales of data distribution. However, the maximum length of the black lines is 1.5 times the height of the box, showing a reasonable distribution of the data. If there are any extreme values located outside the maximum range, they will be shown as red crosses (none in this figure). Fig. 3.2 (b) displays inter-quartile ranges of buses

separately. Generally, by disregarding extreme samples, an inter-quartile range can represent the possible severity of VUF.

It can be seen from Fig. 3.2 that, although only one source of unbalance exists and injects unbalanced power into the network, voltage unbalance propagates throughout the network and results in observable VUF values at other buses. All other buses though have much smaller VUFs than the source bus.

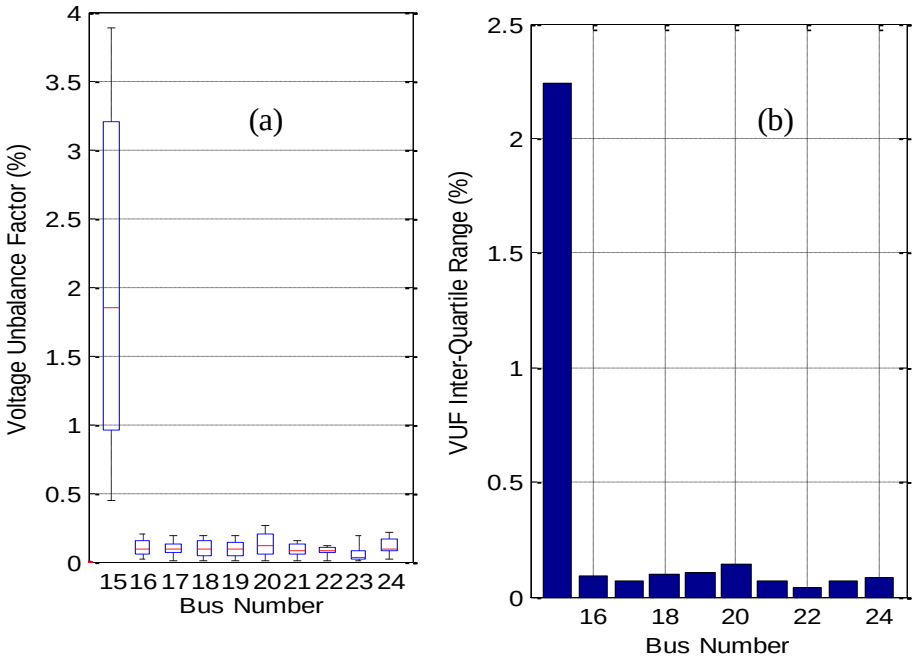

Fig. 3.2 VUF Ranges for Load Buses. (a) Boxplot of VUFs. (b) Inter-quartile Ranges of VUFs.

3.2.2.3 Apparent Power Probability Distribution

The ratio of negative sequence apparent power and positive sequence apparent power, named SUF for short, is a powerful tool used for identifying the sources. The SUFs of 20 cases are plotted in Fig. 3.3 using a similar representation with Fig. 3.2. As seen from Fig. 3.3 (a), the source of unbalance illustrates a large range of SUF while SUFs at other buses are nearly zero. In Fig. 3.3 (b), this effect is more evident because there is only one value for the inter-quartile range, at bus 15. By investigating the SUF, the source of unbalance is clearly identified.

Compared with other buses, only the source of unbalance exhibits a negative sequence power which takes a noticeable proportion to the positive sequence power. If there is no unbalance injected, no negative sequence power is generated by the local bus. But there are tiny negative sequence power fluctuations at other buses as a result of negative sequence power flow in the network and the floating accuracy of the software. In this simulation, SUFs of non-source buses are of 10^{-4} order of magnitude, which can be ignored.

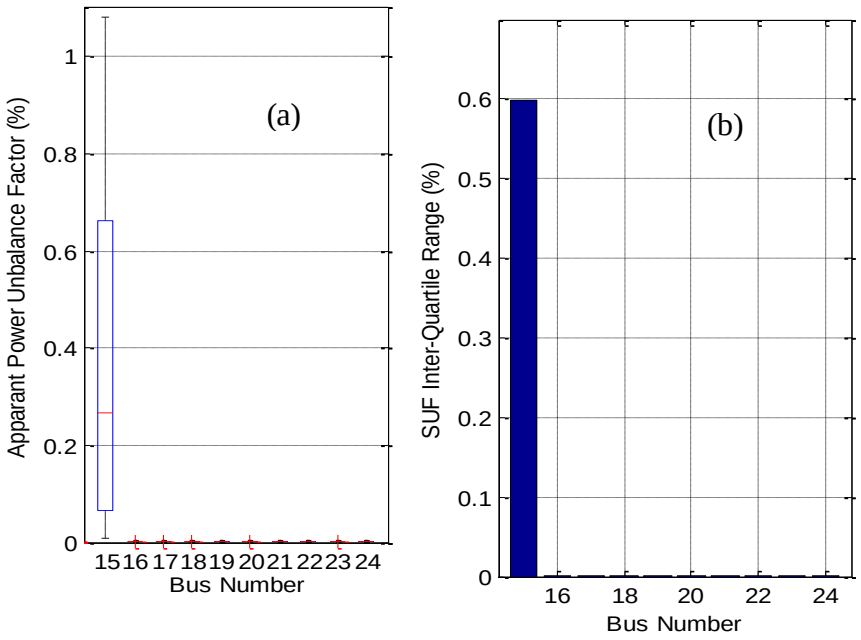

Fig. 3.3 SUF Ranges for Loaded Buses. (a) Box plot of SUFs; (b) Inter-quartile Ranges of SUFs.

3.2.2.4 NEGATIVE SEQUENCE POWER ANGLE

The distribution of 20 cases of negative sequence power angles of bus 15 is shown in Fig. 3.4. The angles appear to be similar. Except for five values, most of the angles are fixed between 265° and 267°, disregarding the level of unbalance. According to the theory [45] mentioned in Section 3.2.1.1 (i.e., negative sequence power angle of the source should lie in the second or third quadrant), the simulation results satisfy the specified scope.

However, although all the negative sequence power angles of the source in 20 cases are located in the third quadrant, it is possible that there are angles at other buses, located in different flow paths of transformers, in the second quadrant. This leads to misjudgement according to the observation in [45].

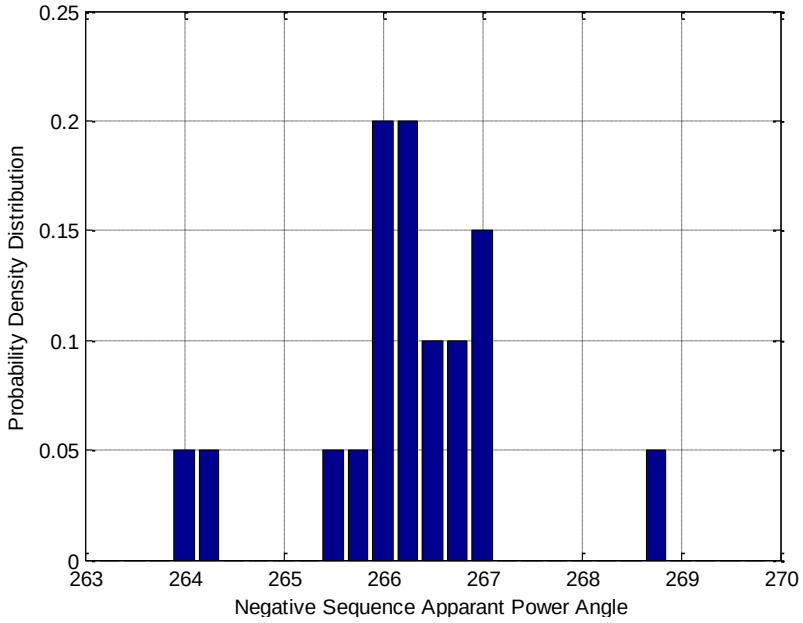

Fig. 3.4 Distribution of negative sequence power angle of the source of unbalance.

3.2.2.5 MULTI-SOURCE IDENTIFICATION

The 20 cases in the previous sections only contain one unbalanced source at a fixed location. Therefore, for more than one unbalanced source, the methodologies still need to be examined.

In this simulation, 4 buses (bus 15, 18, 21 and 23) are selected to be the sources of unbalance. They are located at least 3-bus adjacent to each other, i.e., in different parts of the network. Considering the loads of those four buses, buses 15 and 23 have much bigger loads than all other buses; buses 18 and 21 have much smaller loads than the other buses.

Those four loads are changed according to the following steps:

- Keep phase *B* unchanged. Multiply by the same factor f_a both active and reactive powers of phase *A*. Multiply by the factor $(2-f_a)$ active and reactive powers of phase *C*. The number "2" in $(2-f_a)$ represents the initial loadings in two phases in p.u.
- Run load flow and derive results.
- Adjust f_a to make VUF at the bus 1% (considering only the contribution of this local source).
- Repeat the above steps for all four individual sources of unbalance.
- Set all four sources to an unbalanced condition simultaneously and derive the final load flow results.

The resultant VUFs and SUFs are displayed in Fig. 3.5. VUFs at the source buses are significantly larger than the other buses. Different from the initial injection of 1% VUF locally, the final results of all four sources of unbalance exceed 1%, indicating a certain superposition, which will be discussed in the following sections. As for SUF, the four source buses also demonstrate high values against flat SUFs of the other buses.

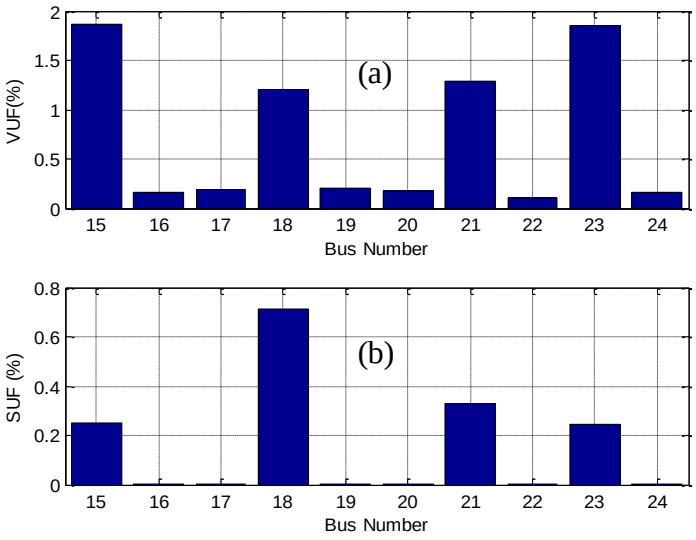

Fig. 3.5 Inter-quartile ranges of VUFs and SUFs for load buses of multi-source. (a) VUFs for load buses. (b) SUFs for load buses.

The negative sequence active power and reactive powers of all loaded buses are plotted in Fig. 3.6. The VUFs of buses 15 and 23 are larger than that of bus18, but the SUF of bus 18 is larger than those of buses 15 and 23. The reason is that the load at bus 18 is the smallest of all buses (the loads at buses 15 and 23 are about 15 times the load at bus

18), which means the positive sequence power at bus 18 is the smallest. With the smallest denominator of SUF, bus 18 shows a SUF of 0.71% while the SUF at bus 15 is 0.25%, although the negative sequence powers of bus 15 is about 5 times that of bus 18 at the same time.

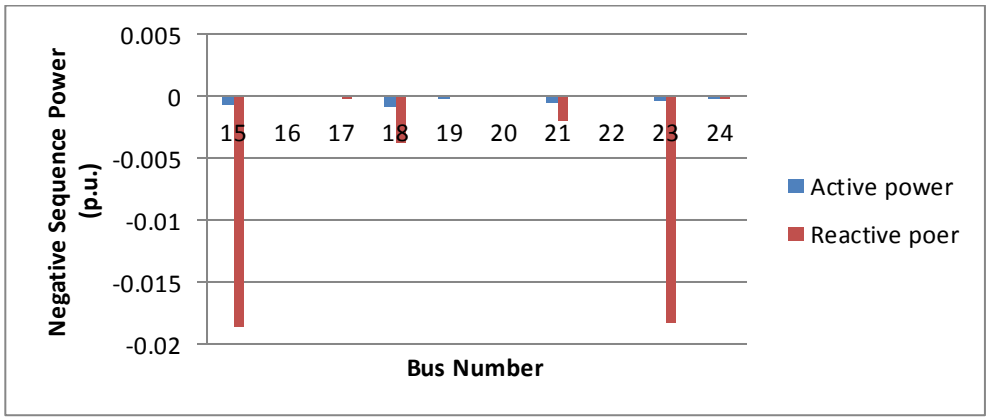

Fig. 3.6 Negative sequence active and reactive power consumptions of load buses of multi-source case.

The methodology using SUF to identify the source of unbalance is verified by a multi-source test.

As seen from these simulations, preliminary conclusions confirm that a large divergence in three-phase load can result in larger unbalance, whatever the unbalance type is.

However, with different unbalanced injections at the same bus, the affected bus shows various VUFs. For this reason, the propagation of unbalance needs to be investigated, which will be discussed in the following sections.

3.3 Propagation of Unbalance

3.3.1 Setting up 1% VUF

In this simulation, the VUF is set to 1% at the only source of unbalance, bus 15. This simulation aims at a snapshot of the propagation of voltage unbalance. The simulation process is similar with previous section, as follows: firstly, adjust the magnitude and

angle (by adjusting both active power and reactive power) of the asymmetrical load to achieve 1% VUF locally. Then, by recording voltage profiles of all buses, VUFs at other buses can be obtained. Moreover, factors that influence the propagation of unbalance can be analysed.

The VUFs for all buses with the location of the source at bus 15 are plotted in Fig. 3.7. Because bus 15 is already an end load, no downstream VUFs can be calculated. Compared to bus 15, all other buses are located upstream to it or in different power flow path. It is obvious that buses near balanced power source (bus 1, 11 and 23) have little voltage unbalance and bus 14 which is directly connected to bus 15 has the largest VUF compared to other buses (except bus 15).

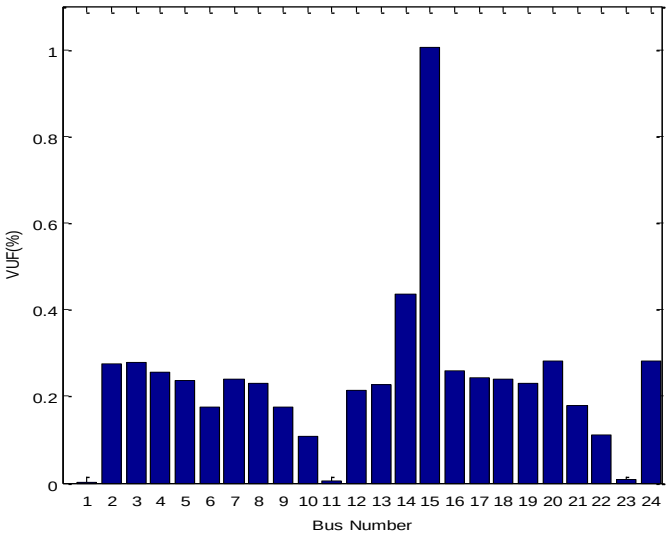

Fig. 3.7 VUFs of Individual buses in 24 bus network with 1% VUF source unbalance.

When the unbalance source is at the user end, upstream propagation is largely mitigated by the connecting transformer (almost half in this case). All other load buses in other parts of the network remain largely unaffected.

By using Dyn11 transformers, the zero sequence power flow component gets blocked and can be neglected. The negative sequence component, however, flows through the same path as the positive sequence component and therefore continues to contribute towards the voltage unbalance.

3.3.2 MAGNITUDE UNBALANCE AND ANGULAR UNBALANCE

The nature of the source of unbalance is modelled by two idealized models: "Magnitude Unbalance (MU)" and "All-in-One Unbalance (AU)". For this specific network and the illustration purposes, the unbalanced phase is assumed to have double apparent power of the initial apparent power. Starting from a balanced point, MU enlarges *P* and *Q* in one phase proportionally. Consequently the apparent power of this phase is larger than the other two, but the three-phase power factors are still the same. AU, on the other hand, varies either *P* or *Q* of one phase at different scales to preserve double apparent power in that phase; hence there is a difference between power factors of three phases. The types of unbalance and corresponding parameters are shown in Table 3.1. (The original values of powers are as follow: P_o=0.02p.u., Q_o=0.005 p.u. and S_o=0.0206 p.u.)

Table 3.1 Unbalanced Type (MU & AU) and Parameters

Type	P (p.u.)	Q (p.u.)	S (p.u.)
MU ($P=2P_o$; $Q=2Q_o$)	0.04	0.01	0.0412
AU1 ($S=2S_o$; $Q=Q_o$)	0.041	0.005	0.0412
AU2 ($P=P_o$; $S=2S_o$)	0.02	0.036	0.0412

The simulations are carried out using single-variable analysis. Powers at one or two or all of buses 2, 3 and 4 are adjusted to create unbalanced conditions and the impacts on bus 5 are analysed. In this way, the propagation of unbalance can be traced. Table 3.2 lists the detailed parameters of the tests, where *A, B* and *C* denote the phases. The test network used in this case is the network shown in Fig. 2.6.

3.3.3 CASE STUDY: RULES OF PROPAGATION

3.3.3.1 CASE 1: UNBALANCE AT 1 BUS

The three-phase voltages and VUFs of all buses with only one source of unbalance, at bus 2, are shown in Fig. 3.8. With the increase in the power in one phase, the

discrepancies between phases create a path for the sequence coupling; therefore negative power flow is induced. At the same time, the heavy loading in one phase also leads to the excessive decrease in the phase voltage (predominantly composed of positive sequence voltage) for all the buses, irrespectively of the type of unbalance. These two changes in negative and positive sequence voltages jointly contribute to unbalance at bus 2, represented using VUF in the figure. Different colours in left column figures are related to different phase voltages.

Table 3.2 Assumption of Propagation Test for Test Network

Case Number	Bus 2	Bus 3	Bus 4
Case 1: Unbalance at 1 bus			
Case 1.1	MU in A	-	-
Case 1.2	AU1 in A	-	-
Case 1.3	AU2 in A	-	-
Case 2: Unbalance at 2 buses			
Case 2.1	MU in A	MU in A	-
Case 2.2	MU in A	MU in B	-
Case 2.3	AU1 in A	AU1 in A	-
Case 2.4	AU1 in A	AU1 in B	-
Case 2.5	AU1 in A	AU2 in A	-
Case 2.6	AU1 in A	AU2 in B	-
Case 3: Unbalance in different phases at 3 buses			
Case 3.1	MU in A	MU in B	MU in C
Case 3.2	AU1 in A	AU2 in B	AU2 in C
Case 3.3	AU1 in A	AU2 in B	AU1 in C
Case 4: Unbalance in the same phase at 3 buses			
Case 4.1	MU in A	MU in A	MU in A
Case 4.2	AU1 in A	AU2 in A	AU1 in A

It can be seen from the figure that the induced negative sequence power (reflected in the negative sequence voltages) flows to the other buses, i.e., it spreads through the whole network. However, because the other buses have direct (buses 3 and 4) or indirect (bus 5) paths to the balanced power supply, their VUFs are smaller. Although the negative sequence current flows from bus 2 to bus 5, it has been reduced by the currents flowing through bus 3 and 4 from the source. If the branch flows from bus 3 to bus 5 and from bus 4 to bus 5 are regarded as two separate radial networks, the change of VUF along the transmission line is roughly proportional to the line impedance. Bus 5, located in the

downstream network, experiences larger negative sequence voltage and lower positive sequence voltage than bus 1, 3 and 4 due to the losses on the line. Since all line impedances are identical, the VUFs at bus 3 and 4 are almost half of the sum of VUFs of bus 1 and 5. The vicinity to the regulated balanced power supply, therefore, mitigates negative sequence flow.

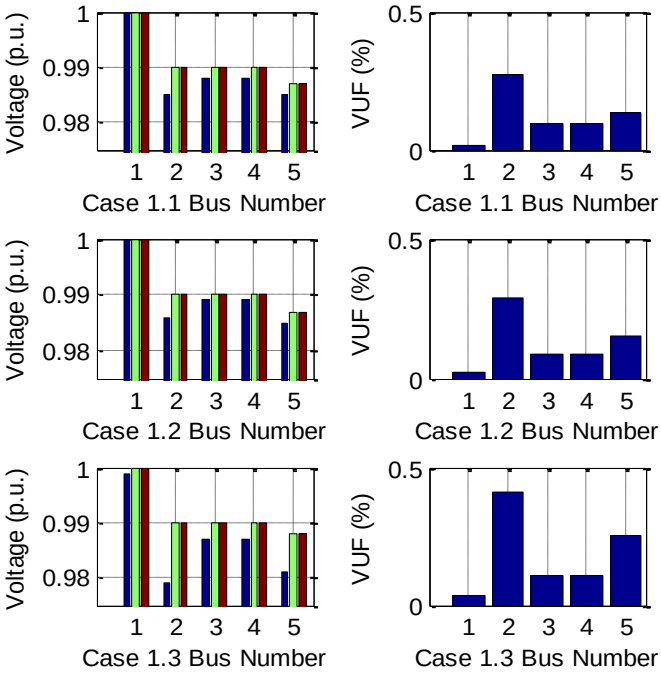

Fig. 3.8 Voltage magnitude and VUF for Case 1.

When comparing the results of Case 1.2 and 1.3, it can be seen that the resultant overall VUFs in Case 1.3 are relatively larger, since AU2 changes the initial loading condition more (both in magnitude of the power and power factor) than AU1.

3.3.3.2 CASE 2: UNBALANCE AT 2 BUSES

The three-phase voltage magnitudes and VUFs of Case 2 with two unbalanced buses are displayed in Fig. 3.9. As the unbalances originate from both phases *A* of two buses in Case 2.1 and 2.3, they contribute to the unbalance at bus 5 together. On the contrary, in Case 2.2 and 2.4, the unbalances created from phase *A* of bus 2 and phase *B* of bus 3 respectively cancel each other to a certain extent, reflecting the lower overall levels of VUFs than those of Case 2.1 and 2.3. The negative sequence voltages for all cases are

listed in Table 3.3 and it can be seen that the angular difference between them contributes to this cancellation of unbalance. The results of simulations also show that the cancellation only takes place when the type of unbalanced sources is the same. When it comes to Case 2.5 and Case 2.6 that have different types of unbalances originating from two buses (see Table 3.3), the angles of negative sequence voltages of bus 2 and 3 are closer, i.e., voltage phasors are closer to each other, so the unbalance magnifies.

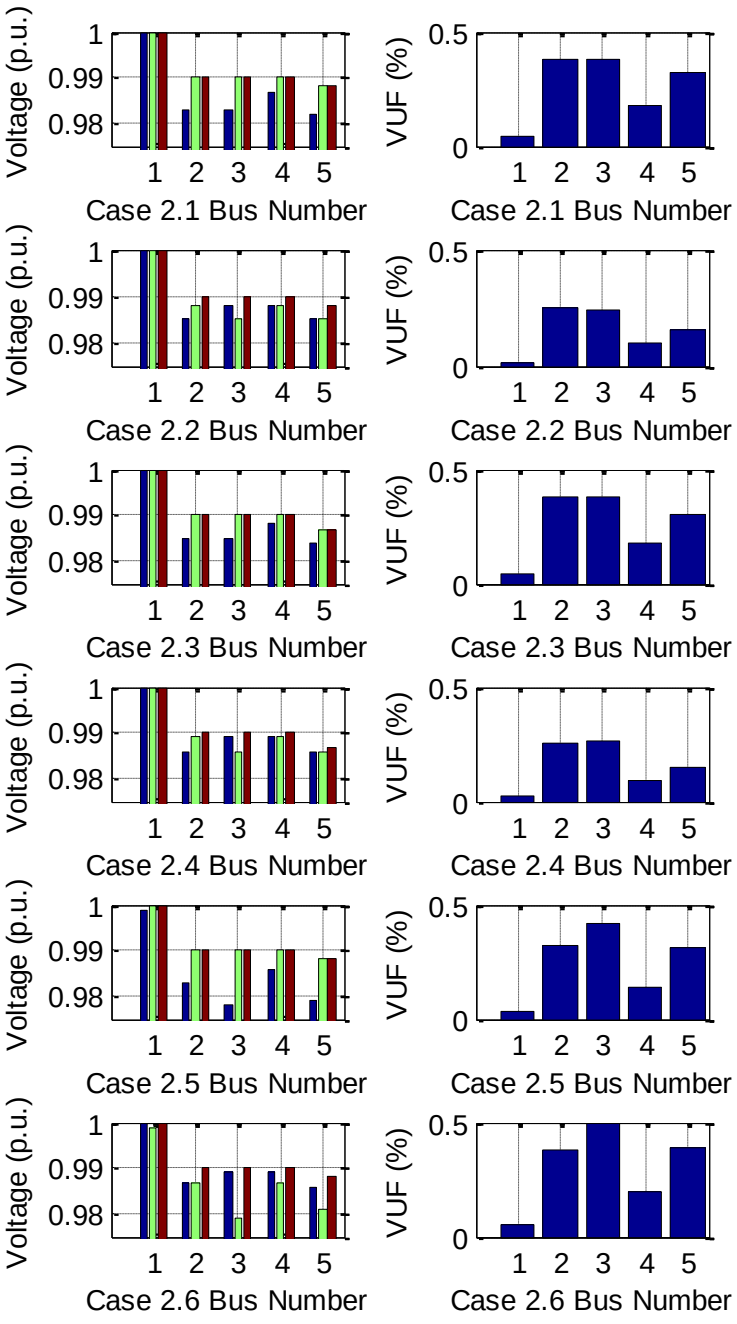

Fig. 3.9 Voltage magnitude and VUF for Case 2.

Table 3.3 Negative Sequence Voltages for Bus 2and 3 for Case 2

Case Number	Bus 2 Negative sequence Voltage (p.u.)		Bus 3 Negative sequence Voltage (p.u.)	
	Magnitude	Angle	Magnitude	Angle
2.1	0.0037	-129.46	0.0037	-129.46
2.2	0.0025	-106.86	0.0023	-28.97
2.3	0.0038	-117.12	0.0038	-117.12
2.4	0.0025	-101.62	0.0027	-15.41
2.5	0.0032	-138.54	0.0041	166.52
2.6	0.0037	-104.72	0.0048	-90.41

As mentioned in previous section, the AU2 type of unbalance (increase in *S* and constant *P*, effectively increase in *Q*) causes larger unbalance than AU1 (increase in *S* and constant *Q*, effectively increase in *P*). With two unbalanced sources in the network AU2 yields the higher overall level of unbalance than AU1.

3.3.3.3 CASE 3: UNBALANCE IN DIFFERENT PHASES AT 3 BUSES

Fig. 3.10 shows the results of Case 3. It is obvious that the same unbalances in different phases at three buses cancel each other when propagated to bus 5. The negative sequence voltages flowing from the three upstream buses in this case are of equal magnitudes and equally phase-shifted (see Table 3.4). The VUFs at bus 5 resulting from phase *A* of bus 2, phase *B* of bus 3 and phase *C* of bus 4 are $0.1345\angle -120.194°$, $0.1345\angle -0.194°$ and $0.1345\angle 119.806°$ respectively. By plotting the corresponding vectors together as shown in Fig. 3.11, it can be seen that the voltage rebalances at bus 5. Case 3.1 is also a clear example of the reduction in phase voltage due to heavy loading at that phase.

In Case 3.2, the unbalance does not cancel at bus 5 because of the asymmetrical upstream power flows (see Table 3.4). Regarding bus 2, the reduction of the voltage in phase A due to local load, as well as the reductions of voltages in phase *B* and *C* due to the unbalances from bus 3 and 4, makes the three-phase voltages the same. The unbalance at the bus, however, is not zero due to the different phase shifts between phases. The slight difference in VUFs of bus 3 and bus 4, in spite of similar deviations from the balanced condition (see Table 3.5), is the consequence of the transformation

from time domain to sequence domain (The different unbalance in different phase voltages results in different sequence component values and consequently in different VUFs). The results of Case 3.3 are similar to those of Case 3.2.

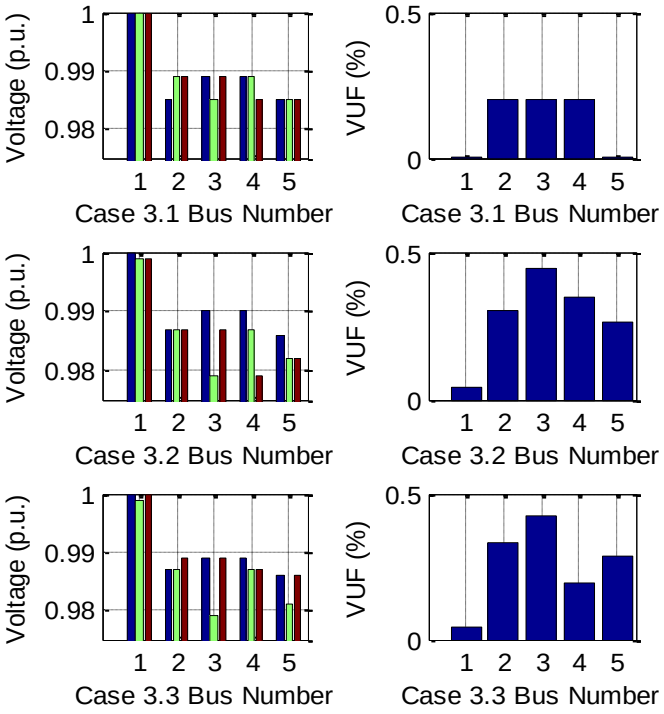

Fig. 3.10 Voltage magnitude and VUF for Case 3.

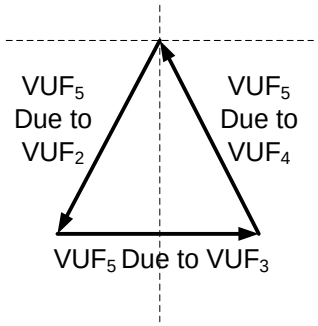

Fig. 3.11 The VUF vectors at bus 5 resulting from three upstream buses respectively.

Table 3.4 Negative Sequence Voltages for Case 3.1 and 3.2

Bus Number	**Negative Sequence Voltage (p.u.)**			
	Magnitude	**Angle**	**Magnitude**	**Angle**
	Case 3.1		**Case 3.2**	
2	0.0020	-132.65	0.0030	-90.84
3	0.0020	-12.65	0.0042	-74.06
4	0.0020	107.35	0.0034	6.39
5	1.17028E-16	161.57	0.0026	-60.03

Table 3.5 Three phase Voltages for Bus 3 and 4 for Case 3.2

Phase/ Sequence	Bus 3			Bus 4		
	Mag (p.u.)	Angle	Deviation (angle)	Mag (p.u.)	Angle	Deviation (angle)
A	0.99	-0.8	0	0.99	-0.8	0
B	0.979	-120.36	-0.44	0.987	-120.58	-0.22
C	0.987	119.42	-0.22	0.979	119.64	-0.44
Zero	0.0034	6.39	-	0.0044	-74.06	-
Positive	0.985	-0.58	-	0.985	-0.58	-
Negative	0.0044	-74.06	-	0.0034	6.39	-
VUF	0.445%			0.349%		

3.3.3.4 CASE 4: UNBALANCE IN THE SAME PHASE AT 3 BUSES

The resultant phase voltages and VUFs of Case 4 are shown in Fig. 3.12. In Case 4.1, the unbalances originate from the same phases of the loads at all three upstream buses causing the largest unbalance so far. With the same level of negative sequence current flowing into bus 5 and declining positive sequence voltage, the VUF at bus 5 exceeds those of upstream buses. In Case 4.2, AU2 causes the largest unbalance at bus 3 among five buses. But since there is no cancellation in this case, the VUF at bus 5 is similar to those of bus 2 and 4.

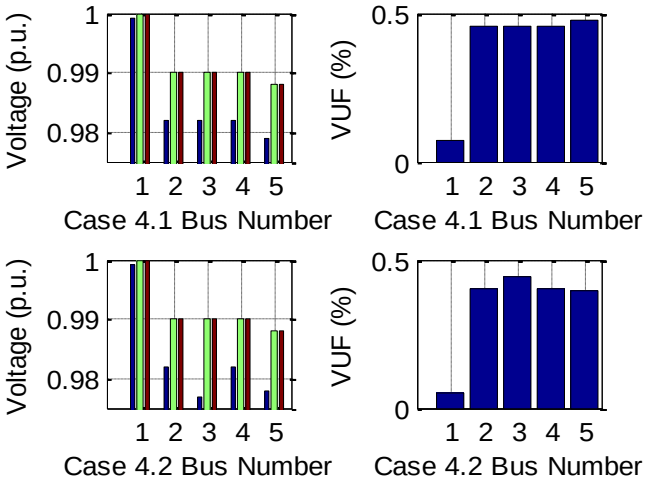

Fig. 3.12 Voltage magnitude and VUF for Case 4.

The network in Case 4.1 can be an example of a radial network by regarding bus 2, 3 and 4 which present the same voltages as a single bus. With unmitigated negative sequence voltage to bus 5, downstream bus experience the same level of unbalance with

upstream buses with a little increase due to the positive sequence voltage drop along the line.

Contrarily, Case 1.1 demonstrates the system behaviour of a meshed network. Despite obtaining power from bus 2 which is the unbalanced source, bus 5 has other paths to the balanced power supply through bus 3 and 4 and experiences reduced unbalance owing to the regulation from alternative paths. With respect to the paths from bus 3 to bus 5 or from bus 4 to bus 5, because the source of unbalance is the downstream bus, the decrease in VUF over the line is proportional to the line impedance. Since all line impedances are identical, the VUFs at bus 3 and 4 are half of the sum of VUFs of bus 1 and 5.

3.4 SUMMARY

In this chapter, existing methodologies for identification of unbalance source are investigated. By taking advantage of sequence power values, as well as the active power magnitudes, reactive power magnitudes and apparent power angles, the source of unbalance can be confirmed.

In the simulation results, all of the angles locate in the 3rdquadrant, which verifies Method 1 (the origin of unbalance usually has a negative sequence power angle lying in 2nd or 3rdquadrants). However, the angles of non-source buses, even though the buses are not on the same side seen from a transformer, would present angles in the specified range. This theory can possibly suggest the area of the location of the source, but not exactly the source bus. In addition, the simulations here demonstrate that, compared to active power, the negative sequence reactive power contributes more to unbalance injections. This partially verifies Method 2 (the source of unbalance injects negative

sequence active power to the rest of the network) on the negative sequence apparent injection and also corrects the statement on whether the active power or reactive power is the main contributor. Method 3 identifies the source of unbalance using SUF and shows clear evidence that the source of unbalance can be identified in this way.

Finally, the studies performed illustrate that without appropriate voltage regulation, once a source of unbalance (typically an asymmetrical load) appears in distribution network, the unbalance will propagate throughout the network. The propagation of unbalance, however, will be mitigated or constrained to a certain extent, by the proximity of the asymmetrical load to the balanced power supply and low impedance transmission lines. Additionally, it is demonstrated that there is a degree of cancellation of unbalance originating from various sources, i.e., the unbalance from different sources may not simply add up. The nature of cancellation is similar to harmonic cancellation, i.e., it depends to a large extent on the angle of negative sequence voltage at the source.

The conclusions about the patterns of propagation of unbalance facilitate the analysis in the following probabilistic estimation.

4 PROBABILISTIC ESTIMATION OF UNBALANCE

4.1 INTRODUCTION

The main cause of voltage unbalance in distribution networks is the asymmetrical loading of three phases, though this may change in the future with increased connection of single-phase generation and storage. As the power supplied from transmission level is regulated to be balanced, the unbalance in distribution networks is not emitted from upstream infrastructure. Although the transmission lines in distribution networks are either non-transposed or partially-transposed, they are short and have small line impedances [19][98], so they may not contribute significantly to unbalance in the network. To accurately assess the level of unbalance in the network, it is necessary to have full observability of three-phase voltages at all buses for a prolonged period of time. Since the monitors are not installed at every bus due to economic reasons, the shortage of monitoring data presents a significant challenge in estimating the unbalance of the whole network. In reality, DNOs are typically made aware of significant power

quality problems from monitoring device reports or customers' feedback. Being a "long term" phenomenon, i.e., the type of phenomenon that does not typically cause immediate disconnection of equipment from the supply, unbalance may be left unnoticed and be continuously present in the system. This, on the other hand, could ultimately yield noticeable financial losses to both utility and end users. Therefore, a methodology for the assessment of unbalance in the network, based on limited monitoring information, would be a useful tool for DNOs, allowing them to estimate the level of unbalance in the network and to take appropriate mitigating measures.

End user devices are unevenly distributed among three phases, with largely unpredictable switching on/off patterns both in time and space. Under this circumstance, the balanced condition of the system cannot be guaranteed and can be expected to further deteriorate in the future particularly due to connection of EVs and single-phase DGs. Due to existing and increasing uncertainties associated with network operation, the research into unbalance propagation and estimation should focus on probabilistic rather than the deterministic estimation. There are some past papers investigating the identification of unbalance sources [98] and the transfer function of unbalance between two buses [71][100][101]. These, however, are deterministic approaches assuming availability of significant amount of detail data about the network and load. A general approach that considers only typically available data and large amount of uncertainties associated with network operation and parameters is still missing. Furthermore, the stochastic methodology for assessment or prediction of unbalance over longer period of time, i.e., time variation or trend, of unbalance in the network is missing.

The previous chapter investigated the basic pattern of propagation of unbalance. Based on that, a probabilistic methodology for modelling sources of unbalance for large network studies can be proposed. This chapter firstly develops a probabilistic methodology on the 5-bus network and then illustrates the application of the

methodology to a real distribution network that can be extended to enable the estimation of unbalance in the network based on limited monitoring. The methodology facilitates both real-time estimation and long term prediction of unbalance in the network by highlighting the role of the asymmetrical load. Its probabilistic nature facilitates modelling of uncertainties in the asymmetrical load and daily load variation in the network. Finally, the superposition of unbalance originating from different sources in the network is examined to establish a framework for estimation of unbalance from statistical data when the monitoring of all buses of potential interest is not possible.

4.2 LOAD VARIATION

For LV system, there are detailed models for passive loads (constant impedance, constant current and constant power loads) and induction motors [71]. When constant resistance loads are connected to the feeder, they only contribute to the increment in the active power consumption of the network. For example, the large amount of lights adds up the active power observed at point of common coupling. But constant power loads and constant current loads will give rise to both the active and reactive powers. If new VAR compensations or shunt capacitors are installed, they cause the increasing or decreasing in *Q*. Therefore, observed from the point of common coupling, there can be increases in either *P* or both *P* and *Q*. In reality, it is likely to have *P* and *Q* growths at the same time. Therefore, for the MV network studied here, the generic loads are modelled as constant power loads and partially induction motors under certain condition. But the power factor of the loads cannot be guaranteed to stay constant. The variation in power factor of the load is hence the best option to simulate unbalanced load.

Industrial load works based on certain work plan and is typically, if not always, three-phase. According to the data provided by the DNO, its loading peak appears in the

afternoon. Similarly, the peak demand of commercial load is in the afternoon when business activity intensively takes place and building maintenance is carried out. There are typically two peaks in residential customers' loading curve: from 6 a.m. to 9 a.m. and from 18 a.m. to 21 a.m., when people get up or come back home from work. During those periods, constant impedance loads, like lighting and cooking, and constant power loads, such as PCs and TVs, lead to a significant increase in active power and also some increase in reactive power seen at the feeder.

Most commercial loads are single-phase while some are on-demand three-phase installations. Single-phase commercial load includes: pure resistive load that will only give rise to active power, such as cooking and conventional lighting; other load that contributes to the increments of both active and reactive powers including load categories such as refrigeration, power electronic and compact fluorescent lamps [152]-[155]. Three-phase commercial load includes heating, ventilation, and air conditioning (HVAC) systems. Other customers, such as transportation, education and health, have similar demand trends with commercial customers [156]-[158].

With the gradual increase in the number of electric vehicles (EV), it is expected that there will be a noticeable amount of EV charging throughout the day (at places of work) but mostly in the evening (at home). This additional single-phase load which is distributed in time and space will certainly add to unequal distribution of load per phase [20].

4.2.1 DAILY LOADING CURVE

In order to simulate the time-varying loads, statistical daily loading curves for domestic, commercial and industrial loads are used in this research. The three types of loads have different sizes, amounts, peaks and changing trends. Therefore, the loads in this network

are classified into three classes and treated separately, each having a different daily loading curve with different peaks and changing trends. Although the load at a single bus in the real network is typically a mixture of two or three load classes in reality, for simplicity, at the first stage for this demonstration, individual loads at buses are considered as purely single class loads.

According to the sizes and the locations of the loads, loading buses are categorized into three classes, as shown in Table 4.1. The test network shown in Fig. 2.7 is used for this study.

Table 4.1 Categories of Load Types for Buses in 24-bus Network

Load Class	Bus Number	Total Load (MW)
Domestic	18, 21	3.262
Commercial	16, 17, 19, 20, 22, 24	20.231
Industrial	15, 23	43.943

With time-varying demand for electrical energy, in order to avoid waste of energy, generators are adjusted to fulfil the power demand. Simultaneously, the inevitable losses are expected to be as low as possible. As a result of different agreements for supply and demand, at different time points of a day, the system presents different parameters for power flow, which affect the results of estimation of unbalance. When involving customer daily loading factors in the estimations, results are more accurate and realistic.

The three typical daily loading curves for winter weekdays for domestic, commercial and industrial loads (shown in Fig. 4.1) are derived from statistic data of California, America, 2010-2011. The peak of residential loads lies between 20 o'clock and 21 o'clock. Seen from statistic data, industrial loads operate according to a certain working plan and have the heaviest loading in the afternoon. The highest demand seen from commercial loads appears also in the afternoon.

For simulation purpose, the twenty-four hours of a day are divided into three-hour slots, namely, eight time zones. The loading factors for all time zones of three types of loads

are derived in the following way: firstly, in each time zone, take the average value as the loading of that zone. Secondly, for each of eight time zones, set the highest value as reference 1.0 per unit loading. Lastly, normalise the loadings of other time zones to the reference value.

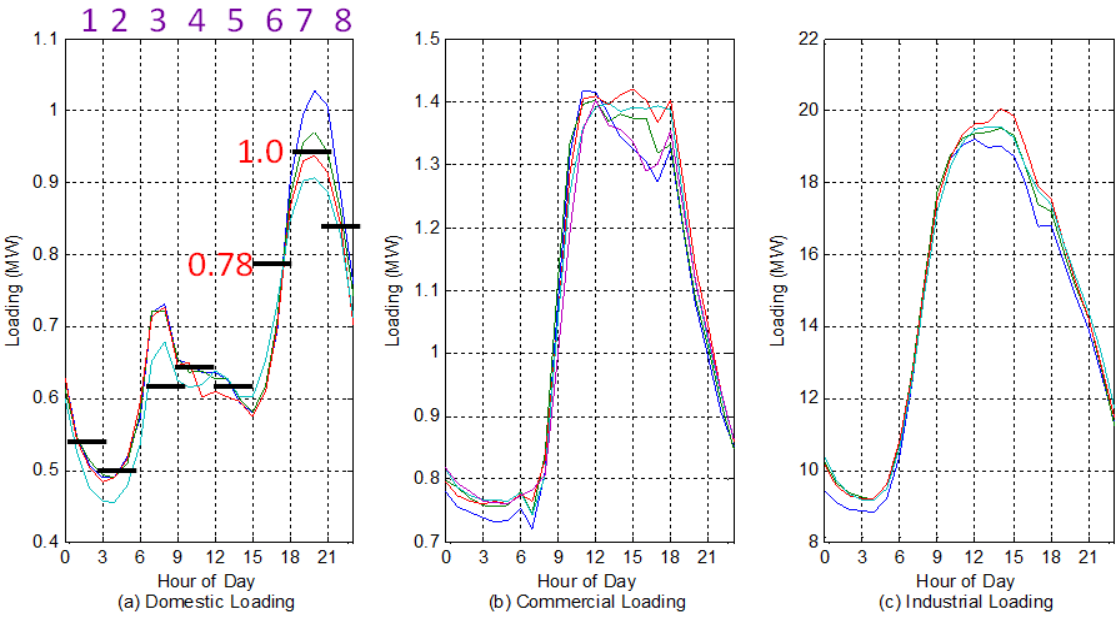

Fig. 4.1 Daily loading curves. (a) Domestic loading curve; (b) Commercial loading curve; (c) Industrial loading curve.

The total daily loading factors can then be obtained by summing up all three types of the loads, considering the actual sizes of loads in the network, shown in Fig. 4.2. All loadings factors are shown in Table 4.2. It can be seen from the table that the peak loading of total loads appears in Time Zone 5 while Time Zone 2 has the lightest loading during the day. Under this assumption, the dominant type of load for the whole network is the industrial load.

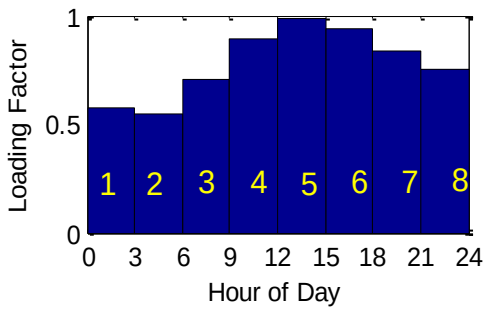

Fig. 4.2 Daily loading curve for the network.

Table 4.2 Daily Loading Factor for The Network

Time Zone	Total	Domestic	Commercial	Industrial
1	0.575	0.57	0.53	0.597
2	0.551	0.52	0.55	0.554
3	0.705	0.71	0.66	0.725
4	0.894	0.69	0.85	0.929
5	0.983	0.65	1	1.000
6	0.942	0.78	0.98	0.936
7	0.833	1	0.88	0.798
8	0.752	0.91	0.72	0.755

By multiplying the loading factors by the actual sizes of loads, the loading levels for each of the ten loads in each of the eight time zones are obtained and illustrated in Fig. 4.3. In the axis of the figure, per unit values apply to 100 MVA system base.

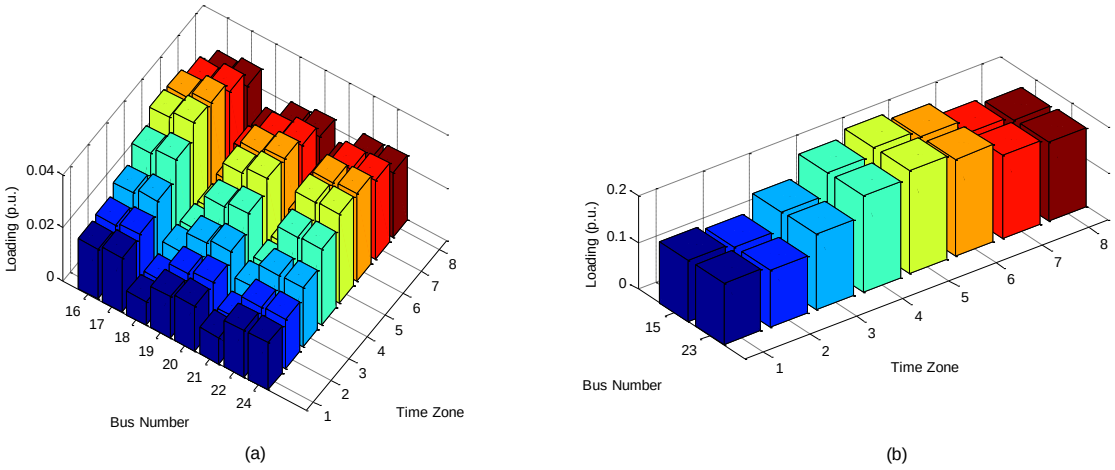

Fig. 4.3 Daily loading for ten loads. (a) Daily loading for domestic loads and commercial loads; (b) Daily loading for industrial loads.

4.2.2 Power Factor Variation

For voltage unbalance, asymmetrical loads are the main cause for unbalance and therefore the main concern of related studies. Corresponding to this fact, in the following simulations, loads are adjusted to be unbalanced within their own three phases to form the source of unbalance.

According to monitoring data received from the DNO, single-phase power factor angles are around 15° for general loads, 0° for lighting loads and 36.87° for induction motors, which equate to power factors of 0.966, 1 and 0.8 respectively. Therefore, derived from

historical data provided by local DNO, three base values of power factor, 1.0, 0.95 and 0.8, corresponding to lighting load, general load and induction motor load respectively, are selected as typical power factors. The large differences in power factors will present a relatively severe source of unbalance.

There are three ways to modify the source of unbalance in the network in order to simulate unbalanced load. The first one considers P as constant and adjusts Q according to the power factor. The second one keeps Q constant and changes P. The third one maintains the apparent power unchanged and adjusts both P and Q according to the power factor. All these three methods are discussed in the sequel. In reality the load per phase at distribution bus of interest may change according to any of the previous three ways. For simulation purpose, however, all the unbalanced loads are adjusted using the same way, chosen from the three ways described above.

4.2.3 Normally Distributed Unbalanced Load

The probabilistic assessment of unbalance in the network is carried out using Monte Carlo simulations. The random variation of power factors of individual single-phase loads is used for modelling the source of unbalance. By adjusting the three-phase powers of the source according to different power factors, unbalanced condition is achieved. In a real network, the changes in load are not fixed and therefore cannot be accurately predicted. For this consideration, a normal distribution is employed to model the uncertainty in load power factor and hence the uncertainty in the source of unbalance.

To create a large number of unbalanced loading scenarios, three normal distributions are used to model the possible variations of three-phase power factors at the sources. Setting the aforementioned 1, 0.95 and 0.8 as the mean values for the normal

distributions, random values are generated within ±20% (±3σ) of the mean values. All values of calculated power factors above 1.0 are discarded (see Fig. 4.4). As ±3σ covers 99.8% of the normal distribution values, the rest 0.2% can be regarded as extreme loading conditions. That is, for power factor 1.0, the values are varied between 0.8 and 1.0; for power factor 0.95, from 0.76 to 1.0; and for power factor 0.8, between 0.64 and 0.96. (If total loading for every bus is available, power factor 0.97, which stands for the general load, can be applied to simulate the uncertainty in general load.)

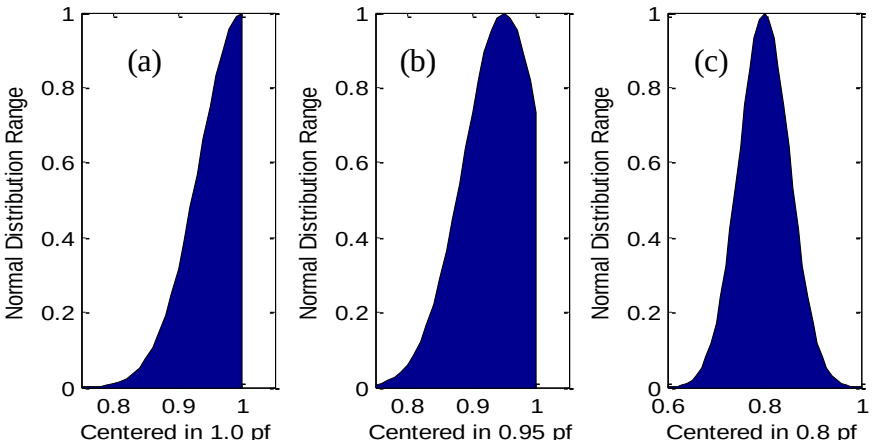

Fig. 4.4 Normally distributed power factor values.

For one load flow, the power factors for three phases of the source of unbalance are randomly selected from the three normal distributions, i.e., phase *A* from distribution (a) in Fig. 4.4, phase *B* from distribution (b), etc. Load flow is repeatedly performed for different random combinations of power factors. This ensures the loadings of each phase of the asymmetrical load and each single load flow are different.

Different ways of creating unbalance discussed above and the choice of power factor probability distributions per phase will result in different unbalances at the source. The large number of MC simulations performed guarantees to a large extent that the overall distribution of unbalance at the source will remain the same irrespectively how the unbalance in different phases was modelled.

Considering that transmission lines and transformers in real network have rated capacities, two limitations, given by (4.1) and (4.2), are set for variation of power in each phase:

- Three-phase total apparent power (S_{TOTAL}) should be no more than 110% of the equipment's MVA rating (S_{RATING});
- The active power in each phase (P_{PHASE}) should not exceed 110% of the per-phase active power rating (one third of the three-phase active power rating P_{RATING}).

$$S_{TOTAL} \leq 1.1 \times S_{RATING} \tag{4.1}$$

$$P_{PHASE} \leq 1.1 \times \frac{1}{3} \times P_{RATING} \tag{4.2}$$

In the probabilistic estimation, all three loads at bus 2, 3 and 4 are modelled as unbalanced simultaneously with the load at bus 5 kept balanced.

4.3 Case Studies

4.3.1 Clarification of Methodology

The proposed methodology is illustrated on the 5-bus distribution network of Fig. 2.6 in order to investigate the nature of propagation of unbalance and to select the best way of power factor modulation to produce appropriate range of unbalance at the bus of interest indicated by commonly used Voltage Unbalance Factor.

4.3.1.1 Constant P and Variable Q

Loads at bus 2, 3 and 4 of the 5-bus network are varied according to the aforementioned probabilistic methodology using random power factors, without the modification according to daily loading curves. First, the "constant *P* and variable *Q*" method is used

to generate random values for power factors in different phases. The results of 500 MC simulations are shown in Fig. 4.5 using box plots. Since *P* stays balanced and unchanged all the time in this case, the only restriction for the adjustment is (4.1).

The boxes in Fig. 4.5 denote the inter-quartile ranges of the VUFs at the buses and the middle lines represent the median values. The three phases of the unbalanced loads in this case have random power factors within the range specified in Fig. 4.4 so that the three loads are all asymmetrical on diverse scales.

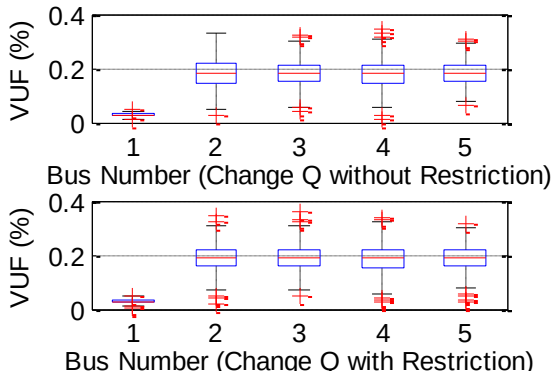

Fig. 4.5 Probabilistic VUFs for 5 buses obtained by varying reactive power.

The results illustrate the most likely range of VUFs at the buses and verify the results of propagation studies presented in previous chapter. Since the reactive powers at buses are relatively small, the total apparent powers are usually within the limits imposed originally by (4.1). The restriction does not have a significant impact on the results as demonstrated by very similar mean values given in Fig. 4.5. The relevant mean values are shown in Table 4.3.

Table 4.3 Mean Values of VUFs of 5 Buses Obtained by Varying Q

Bus Number	Without Restriction	With Restriction
1	0.027%	0.028%
2	0.182%	0.190%
3	0.184%	0.188%
4	0.183%	0.187%
5	0.179%	0.186%

4.3.1.2 CONSTANT Q AND VARIABLE P

The results of MC simulations obtained by keeping Q constant and changing P for power factor generation are displayed in Fig. 4.6. The relevant mean values are shown in Table 4.4.

With the restriction on P imposed by (4.2), the resulting VUFs are a bit smaller than the ones obtained using previous method. This is because the variation in P introduced to generate the required power factor may considerably reduce the amount of P at the bus; hence the lighter loading condition will lead to smaller unbalance in the network. Furthermore, some extreme values of VUF can be obtained as indicated in the top plot of Fig. 4.6. This is not likely to happen, as in this case (without restrictions) the real power can become infinitely large when varied to produce power factor close to 1 with constant Q.

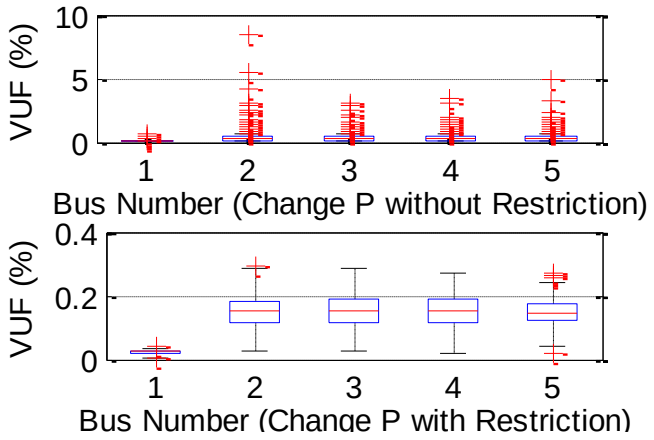

Fig. 4.6 Probabilistic VUFs for 5 buses obtained by varying real power.

Table 4.4 Mean Values of VUFs of 5 Buses Obtained by Varying P

Bus Number	Without Restriction	With Restriction
1	0.046%	0.022%
2	0.323%	0.149%
3	0.297%	0.152%
4	0.309%	0.153%
5	0.307%	0.149%

4.3.1.3 CONSTANT S AND VARIABLE P AND Q

In this case, with constant apparent powers at each bus, both *P* and *Q* are modified according to the randomly generated power factors. The results of MC simulations are shown in Fig. 4.7.

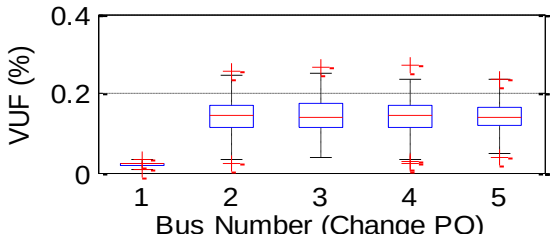

Fig. 4.7 Probabilistic VUFs for 5 buses obtained by varying P and Q.

Since the apparent power is fixed at rated value, both *P* and *Q* will always stay under the rated value, yielding similar results as with variation in *P* only, i.e., possible decrease in *P* to meet power factor variation which results in lighter loading condition and smaller unbalance in the network. The relevant mean values are shown in Table 4.5.

Table 4.5 Mean Values of VUFs of 5 Buses Obtained by Varying Both P and Q

Bus Number	Without Restriction
1	0.021%
2	0.142%
3	0.142%
4	0.143%
5	0.140%

Disregarding the non-restricted (impractical) variation in *P*, the parameters of probability density function (PDF, fitted by normal distribution) of VUF at the target bus (bus 5) for the three examined methods of simulating unbalance at the bus are presented in Table 4.6. It can be seen that random variation of power factor obtained by varying *Q* only yields the largest resultant VUF at the target bus. The variation of power factor obtained by varying both *P* and *Q* results in the lowest mean value and smallest standard deviation of the PDF of the VUFs.

In simulations involving realistic networks, all three methods for simulating unbalance at the bus can be applied. A selection of the most suitable method will depend on the

available information such as historical operating data of the network, capabilities of the simulation tool (software: DIgSILENT PowerFactory/PSCAD/OpenDSS) and user's preference.

Table 4.6 Normal Distribution Parameters for Restricted VUFs at Bus 5

Variable	Mean Value	Standard Deviation
Q	0.186	0.0433
P	0.149	0.0428
P&Q	0.141	0.035

The probabilistic nature of the methodology enables studies of unbalance over a specified period of time (day, week, or year) and in the absence of measurements in the network or accurate information about the source of unbalance. It is based on three-phase load flow and probabilistic modulation of power factor of each single-phase load at load buses. It is simple yet effective and can be easily applied to study unbalance using any commercial software capable of performing three-phase load flow.

4.3.2 Assumptions for 24 Bus Network

The developed daily loading curve closely models the changing demand for active power in the network. Therefore, for a particular time zone, the active power per phase is kept constant and the load unbalance is modelled by varying only the reactive power component per phase using the probabilistic methodology developed, considering specified limitations (4.1).

4.3.3 Simulation Procedure

The power factors of three phases of the source of unbalance are varied using MC simulation and assuming normal distributions of power factor values with means of 1.0, 0.95 and 0.8. In reality, instead of distributing the values of power factors around those selected values (ranging from 0.64 to 1), the reported power factors typically range from

about 0.7 to 1 [154][155]. In order to model the relatively severe unbalance source of the bus in simulation, different mean values of power factor for each of the three phases are used. The simulation procedure used in this study is described below:

- For a selected time zone, apply loading factors of the time zone to all loads according to individual classes of loads.
- Generate 500 random groups of normally distributed asymmetrical power factors for three phases of all ten loads respectively using the Monte Carlo simulation such that the groups of random variables for every load are independent and different.
- Run repeatedly (500 times) three-phase load flow with only one unbalance source in the network – bus 15, while keeping all other loads balanced. This results in 500 VUFs for each bus in the network.
- Select second unbalance source – bus 17 and repeat step 3 with two unbalance sources in the network.
- Repeat step 4 by adding one new source of unbalance every time until all 10 loads are modelled as unbalance sources. (In the tenth simulation, all ten loads are modelled as unbalanced.) The results of each simulation are stored separately.
- Repeat steps 1-5 for the remaining seven time zones.

The original sequence of adding the unbalance sources is: bus 15, 17, 21, 23, 18, 22, 16, 19, 20 and 24. Different sequences of adding unbalance sources yield different results. This will be discussed in the sequel.

4.4 Daily Loading Simulation for 24 Bus Network

4.4.1 Results for a Single Time Zone

The median values of VUFs from 500 simulations at all buses in the network for Time Zone 5 with the sequential addition of one unbalance source at a time are displayed in

Fig. 4.8. The bottom blue curve shows the VUFs when only one unbalance source, bus 15, is present in the network. Once a new unbalance source is added, a new curve is plotted. The top red curve presents the unbalance at each bus with all 10 unbalance sources in the network.

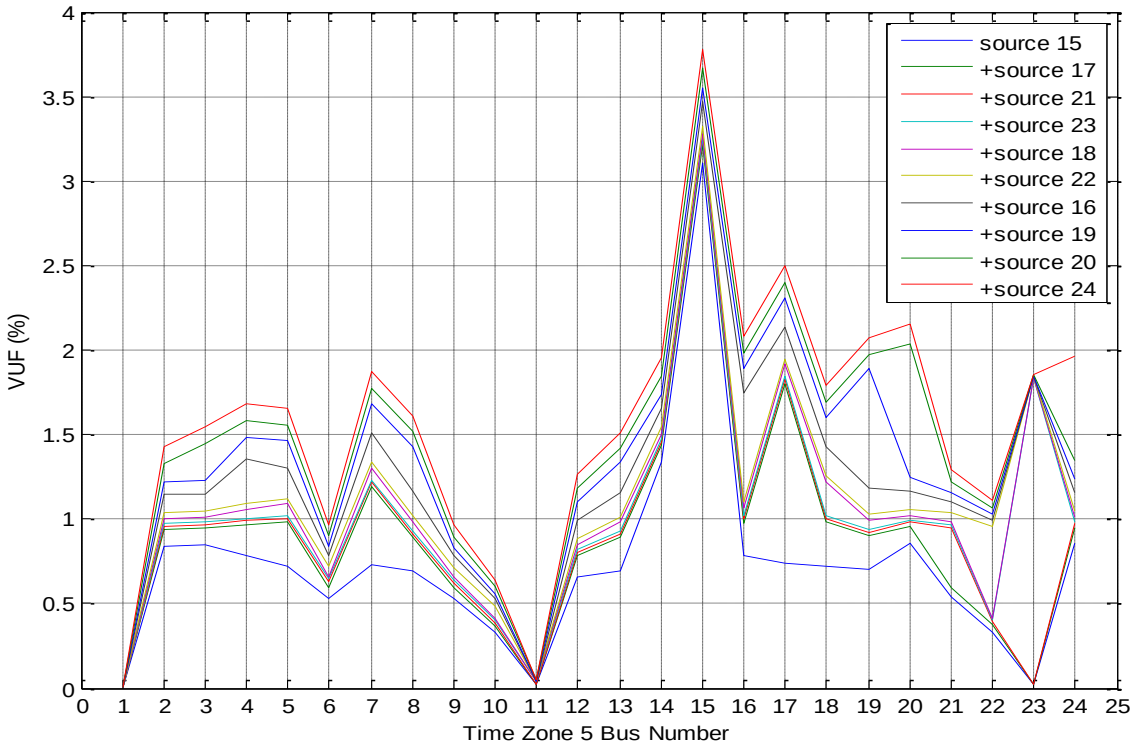

Fig. 4.8 VUFs of 24 buses in Time Zone 5.

Because Time Zone 5 has the heaviest loading during the day, the largest VUFs are observed at all buses compared to other time zones. It can be seen that VUFs of buses 15, 17, 19 and 20 exceed the 2% statutory limit and that the peak of VUF of bus 15 is 3.78%.

Due to the balanced power supply, the power supply area (power supply at bus 1 and buses 11 and 23 near the power supply) always stays balanced except when there is an asymmetrical load at bus 23. It can be observed that VUFs decrease from remote buses to the power supply area, which means the balanced power supply helps extinguish unbalance.

Among the ten loads in the network, the industrial loads at bus 15 and 23 are the largest, which should theoretically lead to the largest contributions to unbalance in the network. Due to the proximity to the balanced power supply, however, asymmetrical load at bus 23 does not have a significant effect on the rest of the network. On the other hand, the unbalanced load at bus 15 contributes the most to the unbalance in the network, by significantly increasing VUFs at all buses. The loads at bus 18 and 21 (domestic loads), being the smallest in the network, do not noticeably contribute to unbalance in the network. Moreover, in Time Zone 5, while both the loading factors of the commercial load and the industrial load are 1, the loading factor of the domestic load is 0.65, which further reduces contributions from buses 18 and 21. However, because of the big transformer impedance between bus 21 and bus 6, it magnifies the unbalance level at bus 21 but reduces the unbalance propagating to upstream buses.

Regardless of the noticeable influence of bus 15, every load bus is mostly affected by its local unbalanced load, and every 33kV bus that has a direct downstream load is also mostly affected by that load with a few exceptions. For instance, bus 2 is interconnected to seven buses including bus 11 (balanced power supply area), so its VUF is the result of the cumulative effect of the unbalanced loads at all other buses. The VUFs of 33kV buses that are not connected to a transformer are influenced by the adjacent buses and show a constant increase in VUF whenever a new unbalance source is added. The resultant VUF of a bus is therefore influenced by both its distance to the balanced power supply and its distance to the source of unbalance. For example, with the first source of unbalance, bus 15, although bus 4 is nearer to the power supply than bus 5, it locates closer to bus 15 and has a larger VUF than that of bus 5. After the appearance of a new source, bus 17, VUF at bus 5 becomes larger than VUF at bus 4.

The asymmetrical load at bus 17 considerably affects the increments of VUFs of bus 16, 18 and 19 as well as their corresponding upstream buses. The asymmetrical loads at bus

16, 18 and 19 have similar but smaller effects on other buses as they are smaller in size. This confirms that the influence of an asymmetrical load at the bus on overall unbalance in the network is determined by both its location and size.

The system behavior, reflecting in the increments of VUF, will change if the sequence of adding unbalance source is altered. Therefore, a further task is to look into the influence of adding sequence.

4.4.2 CHANGE OF ADDING SEQUENCE OF THE SOURCES

The previous sequence was bus 15, 17, 21, 23, 18, 22, 16, 19, 20, 24 and was selected to account for different unbalanced load types and the geographical distribution of loads in the network. To investigate the impact of load size, two more sequences are examined, namely, the descending sequence (adding asymmetrical loads from the largest to the smallest) and the ascending sequence (adding asymmetrical loads from the smallest to the largest). The summary of three sequences is shown in Table 4.7.

Table 4.7 Three Sequences of Adding Unbalance Source.

Sequence	Bus Number
Initial	15, 17, 21, 23, 18, 22, 16, 19, 20, 24
Descending	23, 15, 17, 16, 24, 22, 20, 19, 21, 18
Ascending	18, 21, 19, 20, 22, 24, 16, 17, 15, 23

The VUF curves for the three sequences are shown in Fig. 4.9. It can be seen from Fig. 4.9 that there is an overall increase of unbalance in the network with each new unbalanced load added. The impact of a source is proportional to its size (except bus 23).

From Fig. 4.9 (b), due to the proximity of the power supply, the unbalanced load at bus 23 does not cause any big problem to the network except to itself. The VUF of bus 23 is dominantly determined by the asymmetry of local load. Clearly, after the unbalanced load at bus 15 is injected into the network, VUF at bus 15 exceeds 2% and most other

buses in the network exhibit higher unbalance. No other unbalanced load in the network has such strong effects as the load at bus 15.

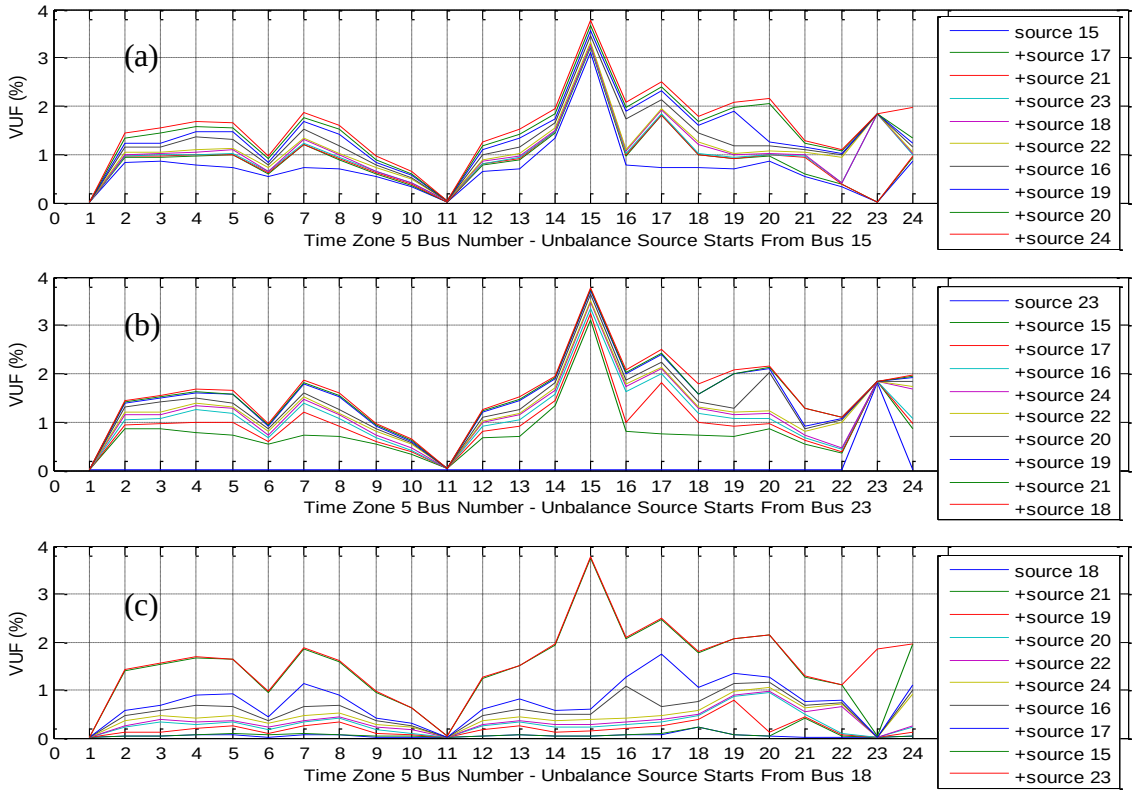

Fig. 4.9 VUFs of 24 buses of three sequences of Time Zone 5. (a)Initial order; (b) Descending order; (c) Ascending order.

Fig. 4.9 (c) verifies the previous observation. When the asymmetrical loads are small such as the load at bus 18, their effects can be neglected. With the increasing of the size of load, its influence on unbalance propagation gets enlarged. The critical factor is the load at bus 15. It is clear that only when the load at bus 15 is set to unbalanced, VUFs at other buses in the network may exceed the 2% threshold. Therefore, by ensuring the symmetry of the load at bus 15, the unbalance in the whole network can be maintained below the statutory limit.

By observing the increments of each source, it can be seen that the contribution of a source to the unbalance at other buses seems to be constant. The superposition of VUFs due to individual sources will be discussed in later section.

4.4.3 Comparison of Unbalance at Different Time Zones

As described above, Time Zone 2 has the lightest loading and Time Zone 5 has the heaviest loading. These two time zones are clear examples of the correlation between the loading level and the unbalance level. With ten unbalance sources in the network, the distributions of VUFs across the network of two time zones are illustrated in Fig. 4.10.

With fixed unbalance source location, the statistic influences of unbalance to the other buses are alike. Therefore, the two distributions have the similar shape but different scales. The maximum VUF of Time Zone 5 reaches nearly 9% while that of Time Zone 2 is about 4.5%. Focusing on the inter-quartile ranges, in Time Zone 2, only VUFs at bus 15 exceed the 2% limitation. When it comes to Time Zone 5, there are ten buses (7, 14, 15, 16, 17, 18, 19, 20, 23, 24) where VUFs rise beyond 2% and six other buses (2, 3, 4, 5, 8, 13) are at risk. There are also four buses (14, 15, 17, 23) that have instantaneous VUF larger than 4%. Therefore, during the peak loading period of the day, the network is exposed to a higher level of unbalance than at any other time.

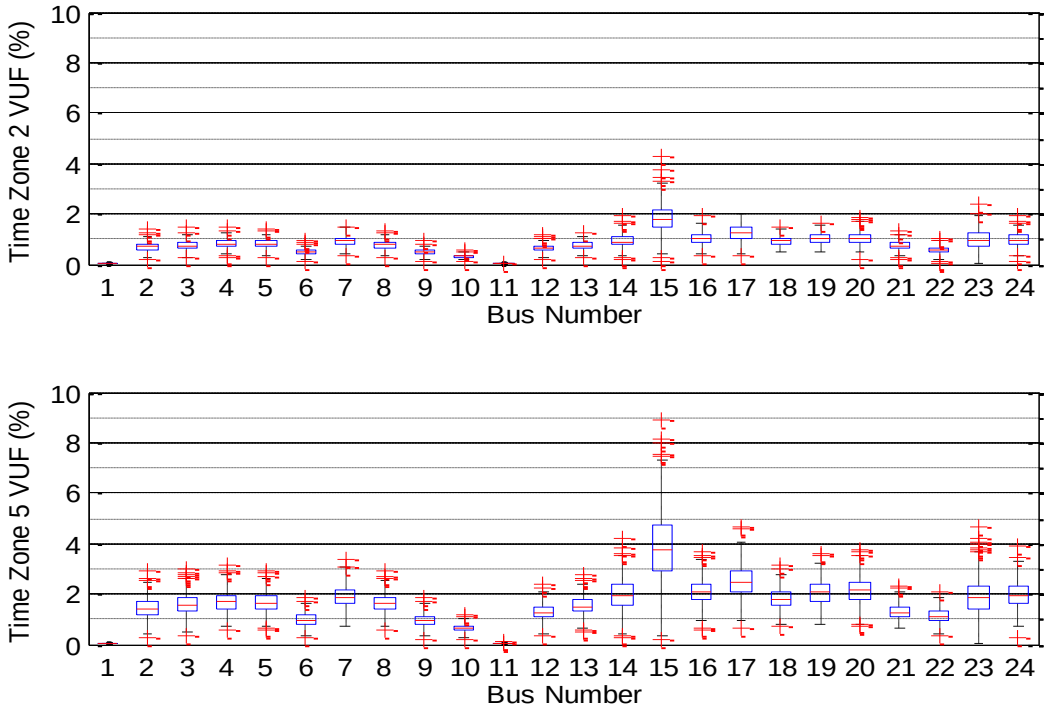

Fig. 4.10 Distributions of VUFs of Time Zone 2 and Time Zone 5.

When VUF stays below 2%, DNO would not take any measures. But seen from the results, in the simulation with such assumption, with the peak loading during the day, the network is always hazardous and requires attention and mitigation. Even when considering the average VUF over a long period of time according to EN50160, the unbalance of bus 15 is always larger than the 2% VUF weekly limitation and necessitates treatment.

It is a human nature that people can quickly understand the happening circumstance by seeing it. In power system analysis, a visual presentation of the current network in terms of disturbances is a powerful assistance for viewer's awareness. Heat maps (Fig. 4.11) for all time zones are plotted using the mean values of 500 VUFs of all buses. Median values with ten unbalance sources are employed. After adjusting to the same scale, the eight heat maps clearly demonstrate the diverse degrees of unbalance existing in individual time zones.

Heat Map provides a visual understanding of the degree of unbalance in the network and the correlation between VUFs and the locations of buses. The heat map clearly indicates propagation and severity of unbalance in the network. It identifies the areas with high VUF and points out to network operator where mitigation measures should be applied. Seen from the heat maps, buses 15, 20 and 17, for example, in Time Zone 5 are more "orange" than in Time Zone 2.

Being consistently orange during four time zones out of eight, bus 15 can be defined as the most vulnerable part of the network to unbalance. The yellow colour indicates the area where VUF exceeds the weekly 2% limit and where there might be some noticeable negative effects on customers' devices. Therefore, additional attention needs to be paid to the weak areas to ensure the power quality. The power supply area usually remains blue, which stands for nearly no unbalance.

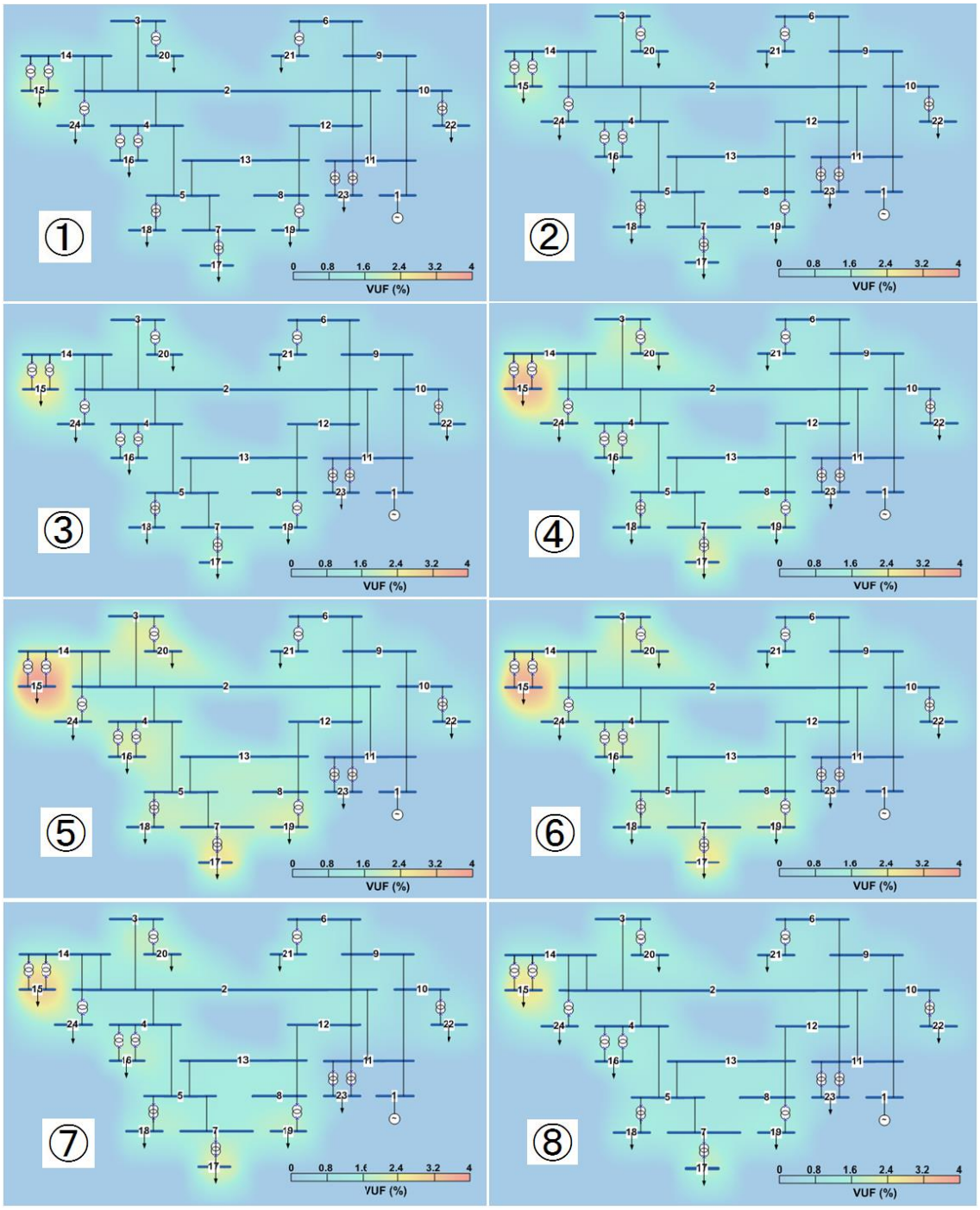

Fig. 4.11 Heat maps of eight time zones.

4.4.4 Unbalance at Individual Buses

The curves for the changing trends for all buses in different time zones with different numbers of sources of unbalance are shown in Fig. 4.12. The adding sequence of sources is the original sequence. The line colours stands for the same unbalance sources with those in Fig. 4.8.

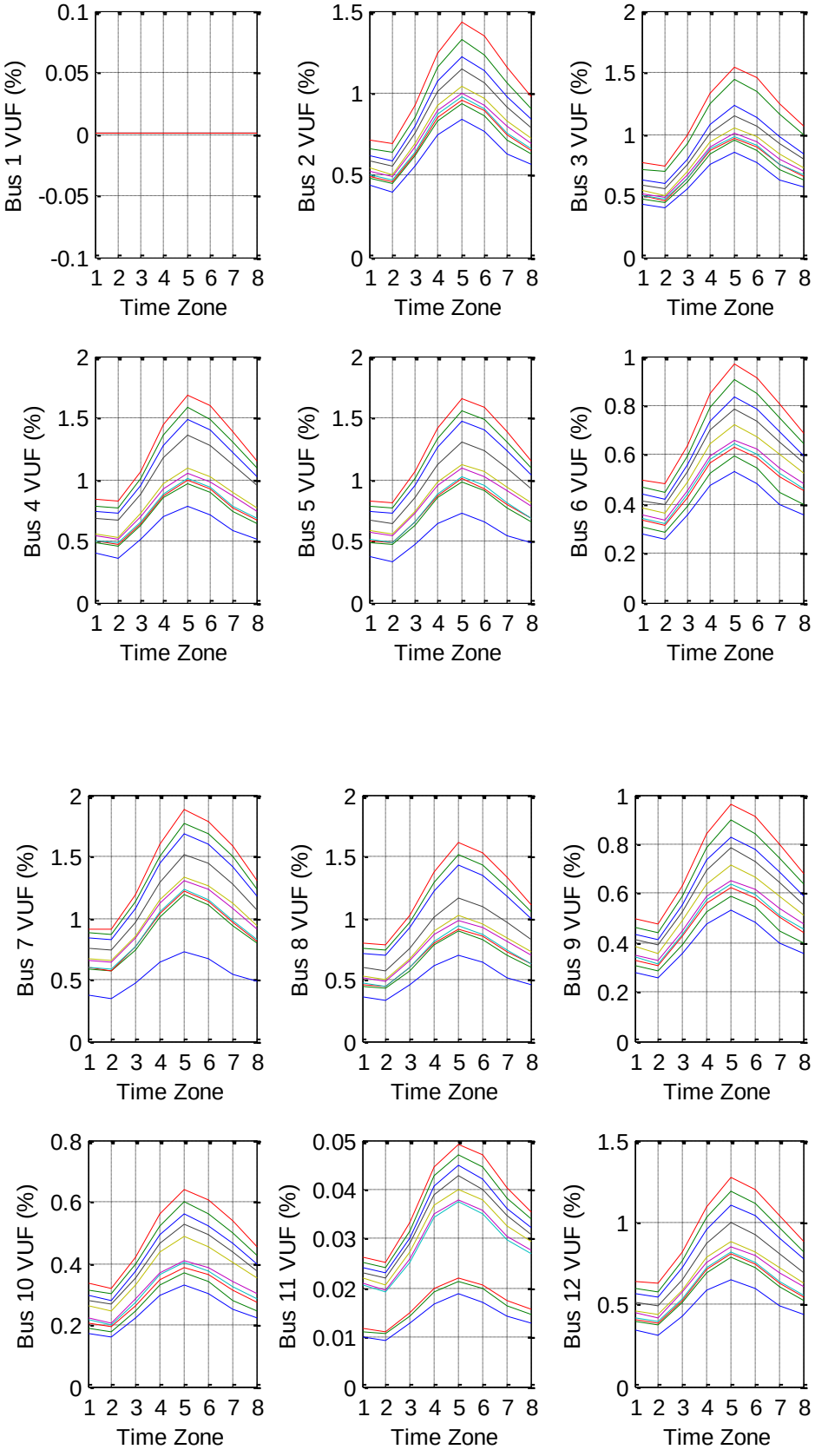
Bus 1 VUF (%)
Bus 2 VUF (%)
Bus 3 VUF (%)
Bus 4 VUF (%)
Bus 5 VUF (%)
Bus 6 VUF (%)
Bus 7 VUF (%)
Bus 8 VUF (%)
Bus 9 VUF (%)
Bus 10 VUF (%)
Bus 11 VUF (%)
Bus 12 VUF (%)
Time Zone

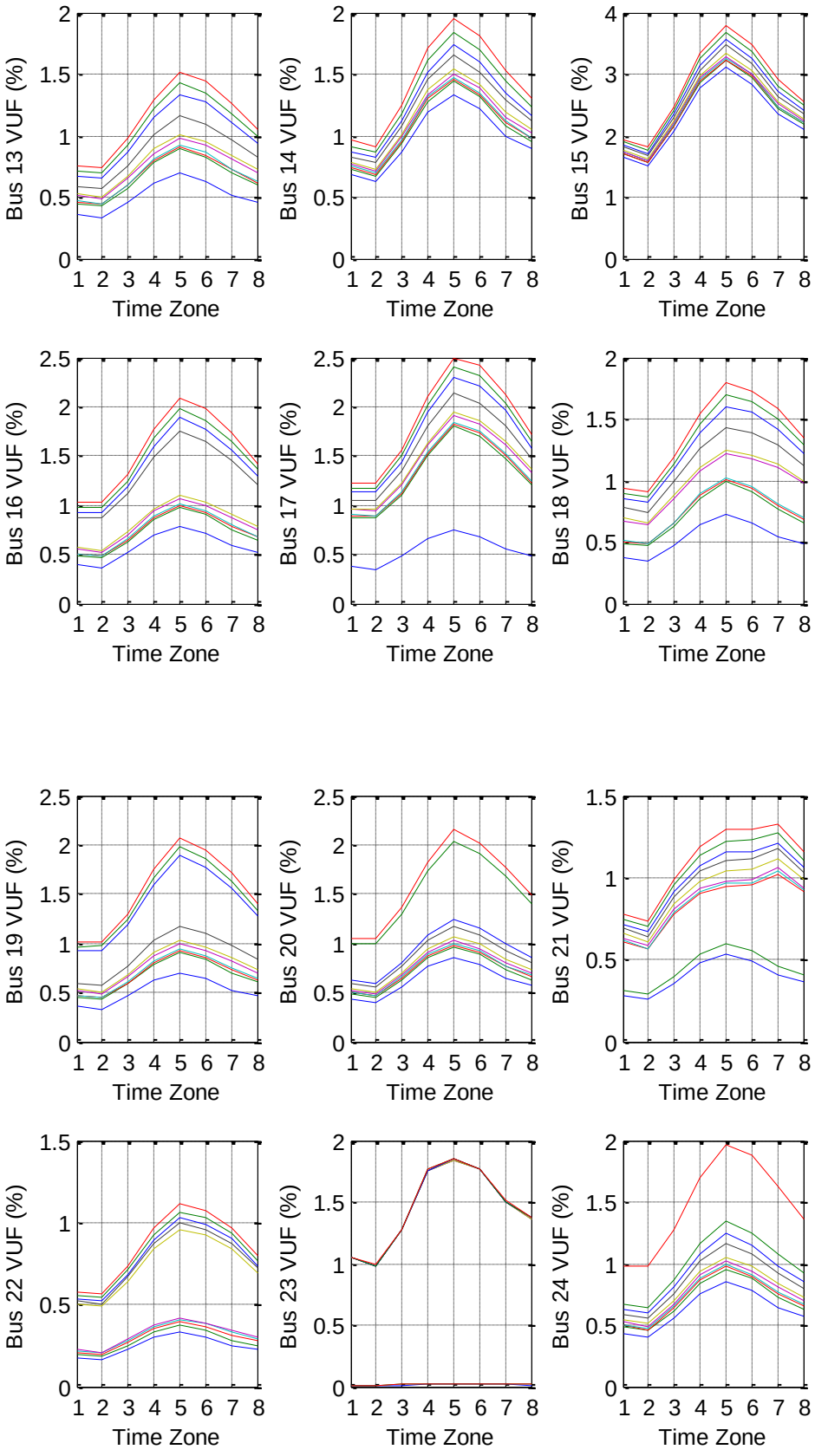

Fig. 4.12 VUFs of individual buses in 8 time zones.

Bus 1 is set to be the reference bus and will not be affected by any unbalance. It can be seen that VUF at bus 1 stays zero all the time. The power supply area, including bus 1, 11 and 23, remains relatively balanced. If concentrating on loads, the only influential element to this area is the load at bus 23.

As discussed in previous sections, corresponding to the relationship between size of load and the resultant VUF, VUFs of all buses achieve the largest values in Time Zone 5 except bus 21. When concerning a single bus, i.e., bus 2, the shapes of curves for every added unbalance source are alike. That means the changing trend of the curves is dominated by the loading level. For example, although buses 16, 17, 18 and 19 are all commercial loads, the shapes of their curves are still established by the total loading of the time zone, in other words, the industrial load, without the interference of any extremely large transformer impedance. Therefore, even though the loading factor of commercial load of Time Zone 2 is bigger than the one of Time Zone 1, VUFs of these buses of Time Zone 2 are smaller than VUFs of Time Zone 1.

Bus 21 reaches its loading peak in Time Zone 7, where the peak demand of domestic load appears. Compared to the two lowest curves which behave the same as the curves of other buses, the changing point of the curves of bus 21 is the asymmetrical local load. The reason why the local VUF is accentuated is the remarkable large impedance of the transformer connecting it. However, as a result of the small size of load at bus 21, the upstream bus is not strongly affected and obeys the pattern of load size and VUF.

From individual bus plots, it is more obvious that the VUFs of load buses (except bus 18 whose load is too small to have effect on itself and the network) are largely scaled up when the local load is adjusted to asymmetrical condition. The shifts in VUFs in the pairing upstream buses caused by direct downstream buses are also more apparent than those caused by any other buses. The VUF increments at interconnecting buses such as

bus 2 and 12 are almost constant because they are not strongly influenced by any single unbalanced source and their resulting unbalance is the combination of unbalance coming from different buses.

Because bus 10, 9 and 6 locate near the power supply area, the unbalances in these buses are mitigated by the balanced power propagating from bus 11. Hence, the resulting VUFs stay below 1%, constructing the second lowest VUF area in the network.

By studying the effects of individual unbalance source in the network, geographical location becomes a significant concern. It is noticed that the neighbouring buses to the source of unbalance have similar behaviour, i.e., similar VUF, as the source bus (if they were not regulated by balancing source). In addition, there are districts of the network with similar level of unbalance depending on the location of the source of unbalance. For example, once a source of unbalance appears in one district, it leads to bigger increase in the VUFs of buses in the same area, rather than buses in any other areas. In terms of the different responses to unbalance, along with the consideration of the geographical locations of buses, the network can be divided into six areas:

1) Power supply: 1, 11, 23;
2) Cluster: 2, 24;
3) Independent group A: 3, 20;
4) Independent group B: 14, 15;
5) Independent group C: 6, 9, 10, 21, 22 (bus 21 can also be classified as a individual group);
6) Large independent group: 4, 5, 7, 8, 12, 13, 16, 17, 18, 19.

The sub-division of the network into different areas of influence is shown in Fig. 4.13.

4.4.5 GROUPING OF BUSES

By studying the behaviour of individual buses, it is recognized that there are certain unbalance levels that buses can achieve. Regardless of bus 1, the grouping of the buses

into five groups, according to the mean values of their VUFs with ten sources of unbalance in the network, is shown in Table 4.8. If specific features of different buses are considered, Group 1 only contains 33kV buses while the buses in Group 4 and Group 5 are all 11kV load buses. The interconnecting buses 2, 12 and 13, are all classified in Group 2, maintaining a relatively low level of unbalance. Group 3 contains the rest of the buses.

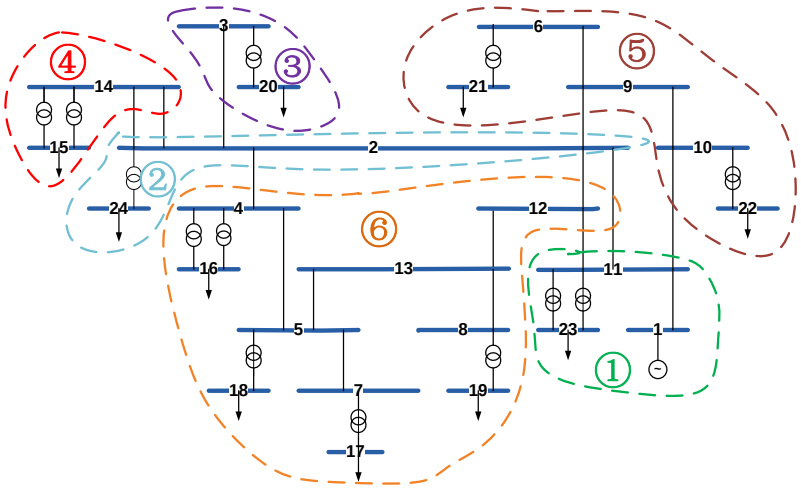

Fig. 4.13 Area sub-division according to individual performance of the buses of the network.

Table 4.8 Grouping of Buses According to the Mean Level of Unbalance

Group	VUF Range	Bus Number
1	<1%	6, 9, 10, 11
2	1% ~ 1.5%	2, 12, 13, 21, 22
3	1.5% ~ 2%	3,4, 5, 7, 8, 14, 18, 23, 24
4	2% ~ 2.5%	16, 17, 19, 20
5	>2.5%	15

In Table 4.8, the upper limits of the ranges are not strictly conformed. For example, if the maximum value of the VUFs of a bus is less than 1.55%, this bus will be sorted into the 1% ~ 1.5% group instead of 1.5% ~ 2% group.

The grouping result has similarities with the area division in previous section. Buses of Group 1 (except bus 11) are all located in Area 5, and three buses out of four of Group 4 are situated in Area 6. Group 5 only has one bus. Group 2 and Group 3 are mixtures of buses of different locations and different types.

In the previous study, only the mean values of VUFs were used which did not provide an adequate analysis of the level of unbalance that can be achieved. However, in Fig. 4.14 below, all the results from 500 MC simulations, instead of only the mean values, are shown. It shows the VUF variations of typical buses, one from each of the five groups, in eight time zones with ten unbalance sources. The loading curves of the buses are also shown in this figure, plotted by using magenta lines against the mean values of VUFs inside the boxes.

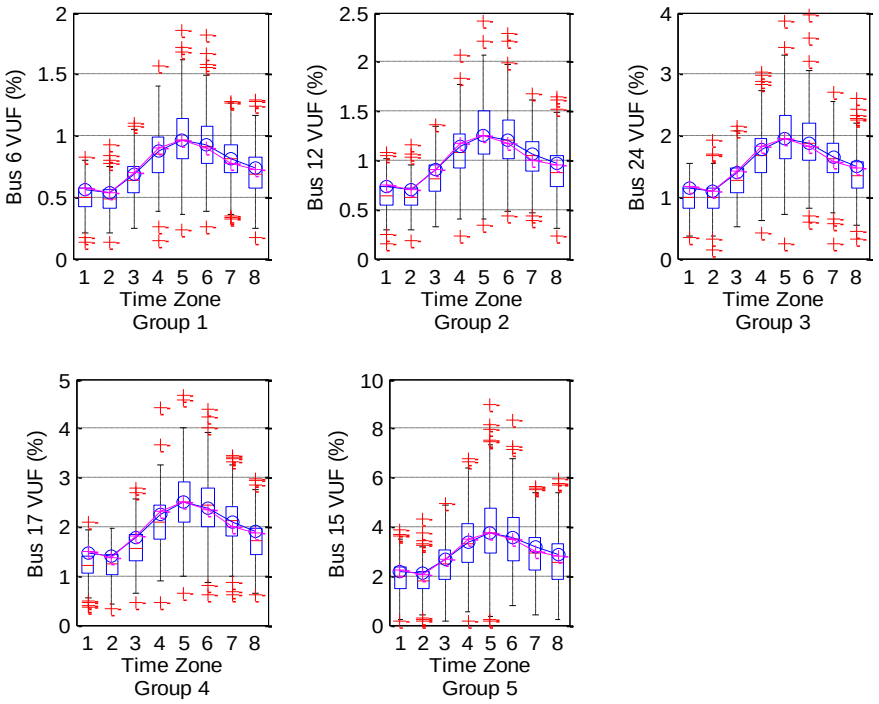

Fig. 4.14 VUF distributions for typical buses of five groups, with loading curve plotted.

It can be seen that the peak VUF (from 500 MC simulations) values under certain conditions can be as high as double the median values. The instantaneous VUFs may exceed the standard specified threshold of 4% while the mean value stays below 4% (e.g. bus 17 in Time Zone 4, 5 and 6). The peak values of VUFs within each range (from 500 MC simulations) still comply with the groups catalogued, i.e., from Group 1 to Group 5, the peak values increase gradually, but not linearly. By overlapping the curves of the loading level in Fig. 4.14 and corresponding curves connecting resultant

mean VUFs from each box in individual plots of Fig. 4.14, they show a close match, i.e., correspondence between loading level and mean VUF.

The maximum values (referred to median value) of Group 2 and 3 are less than 2% VUF. However, the peak values (from 500 simulations) exceed 2%. Regarding Group 5, the peak value reaches about 9%. This high unbalance may trigger protection devices and lead to further losses. That is a reason why unbalance in certain area should be dealt with carefully.

Fig. 4.15 shows the probability density functions of the same five typical buses from five groups for Time Zone 5 with ten sources of unbalance in the network.

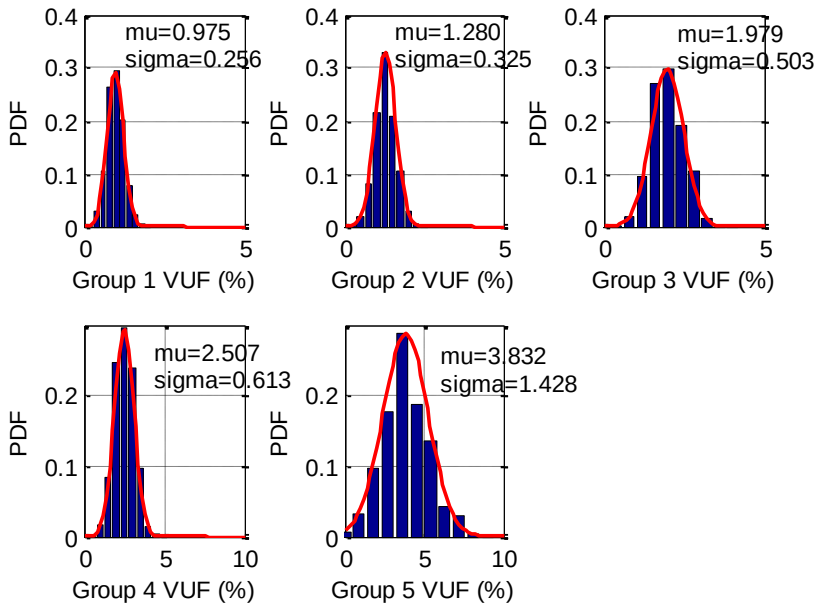

Fig. 4.15 PDFs of VUF distributions of typical buses in five groups.

The PDFs of these five buses correspond to normal distribution. The mean value (μ) of these PDFs moves towards higher values gradually from Group 1 to Group 5 and the standard deviations (σ) also increase, indicating bigger ranges of possible VUF and wider propagation of unbalance.

4.4.6 SUMMARY OF PROBABILISTIC ESTIMATION

As the power supply is assumed to be entirely balanced, the proximity of a bus to the power source helps diminish unbalance. Without considering the power regulation from the supply end, the resultant overall level of unbalance in the network is proportional to the size of the source. That is to say, large unbalanced load facilitates severer unbalance and wider propagation of unbalance throughout the network. This conclusion also relates to the changing demand in customer load. During the peak demand period, VUFs of all buses are higher than at any other time, i.e., there is a higher risk of exceeding unbalance limit of 2% or 4%. It is clear that in Time Zone 2 (lightest loading), only bus 15 and to certain extent bus 23 are at risk of exceeding unbalance limit while there are four buses exceeding 4% instantaneous limit in Time Zone 5 (heaviest loading) and many more potentially exceeding 2% limit.

The variation in power factors of individual loads and the utilisation of daily loading curves help to generate close-to-realistic probabilistic loading of the network for voltage unbalance studies. After Monte Carlo simulations using the proposed methodology, the degree and propagation of unbalance in the network can be estimated and weak area in the network (with respect to voltage unbalance) can be identified. Developed heat map presentation of the results facilitates easy tracking of unbalance through the network and identification of areas where mitigating solutions should be applied.

4.5 SUPERPOSITION OF UNBALANCE

The aim of this section is to discover whether there is a pattern for the superposition of unbalance. In that way, once unbalance appears, the contribution of a single source of unbalance can be established from statistical data. After determining the locations of

individual sources of unbalance, the overall performance of the network can be estimated by combining contributions from individual sources appropriately.

4.5.1 Comparison of Impacts of One Source and Ten Sources

Whenever a new unbalance source appears in the network, typically, the unbalance level of the certain area rises (Although small-size unbalance source does not have significant impact on other buses, it still contributes to the increments in global VUFs. The cancellation of unbalance may not be obvious, which will be discussed in the sequel.). Therefore, with increasing number in unbalance sources, the results can be scaled up.

Fig. 4.16 shows that, during the day, if the most serious unbalance source bus 15 exists (lower sub-figure), the maximum median VUF can reach about 3% and the peak value (from 500 simulations) is a little larger than 8% VUF. However, if ten unbalance sources exist, the maximum median value goes up to near 4% and the peak value rises to around 9%. Both of the mean values and peak values for eight time zones with ten sources are greater than those with a single unbalance source.

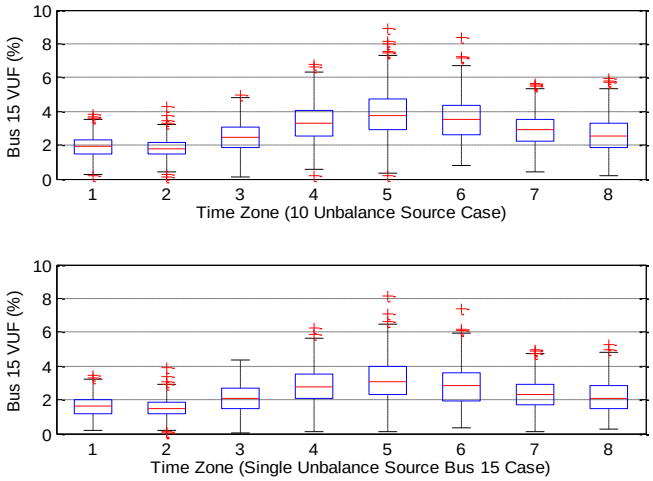

Fig. 4.16 Comparison of VUFs of bus 15 with 10 unbalance source and with one unbalance source during the day.

4.5.2 PROPOSED METHOD FOR SUPERPOSITION

4.5.2.1 GROUPING OF DATA

In each individual time zone, all ten loads are set to be unbalanced. The load flow results (referred to VUF, marked as VUF_{ref}) with ten sources of unbalance are regarded as the reference group that will be used for comparison later.

For every time zone, initially there is only one source of unbalance in the network. The cumulative result of superposition is derived by the following steps:

- Run 500 load flows for the current location of the source of unbalance.
- Store the results for these 500 load flows (the results of the whole group are marked as VUF_1) and return this unbalanced load back to a balanced condition.
- Repeat the previous two steps for the other nine locations of sources of unbalance and collect all the data (marked as VUF_2, $VUF_3 \ldots VUF_{10}$). Note that in all load flows, there is always only one source of unbalance.
- The cumulative VUF (VUF_{cum}) of any bus in a specific time zone is the total sum of the VUFs read from the previous ten individual simulations with different locations of sources, as formulated in (4.3).

$$VUF_{cum}=VUF_1+VUF_2+\ldots+VUF_{10} \tag{4.3}$$

Note that the varying factors used for every individual asymmetrical load are the same as the corresponding ones used in the reference group, when the time zone numbers matched. This ensures that the unbalanced conditions resulting from one source of unbalance should theoretically be the same.

The calculation procedure is shown in Fig. 4.17 using a flow chart.

4.5.2.2 METHOD OF COMPARISON

The discrepancy between the reference result and the cumulative result is compared using Relative Error (RE), as calculated in (4.4).

$$RE = \frac{VUF_{ref} - VUF_{cum}}{VUF_{ref}} \times 100\% \tag{4.4}$$

There are three methods for comparison. In one time zone, method 1 calculates the relative errors between cumulative VUFs and reference VUFs for 500 loops individually and then averages them. Method 2 averages the 500 results of both reference group and cumulative group separately and then computes the relative error. The focus of method 1 is on the discrepancy between individual VUFs while the second one concentrates on the mean VUFs. The third method compares the 95th percentiles of VUFs of both groups based on the standard requirement as well as the maximum VUFs. In the following analysis, all these three methods will be applied.

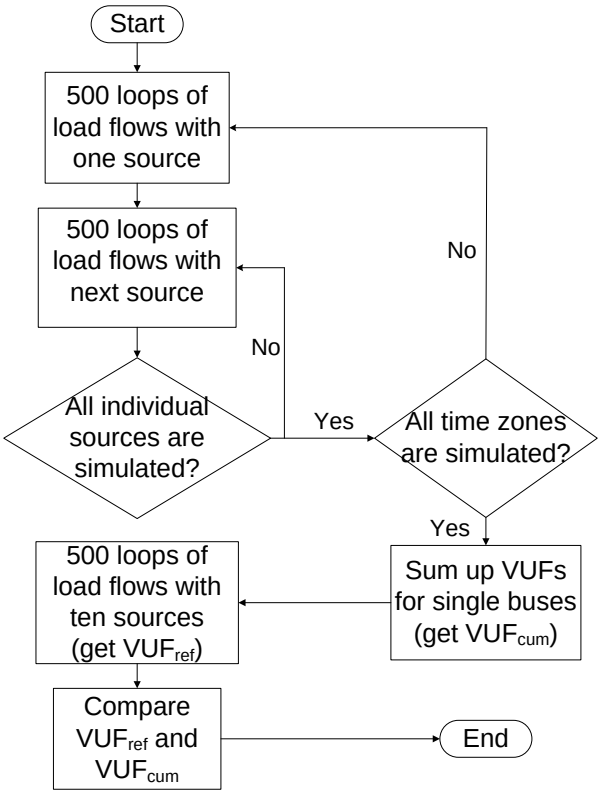

Fig. 4.17 Flow chart of superposition process.

In the VUF superposition, the difference between algebraic summation and vectorial summation will be discussed. In addition to the sum of VUFs due to individual sources, the sequence voltages in the network with individual sources are also analysed, as they are a direct reflection of the propagation of unbalance. In the cumulative voltage

superposition, for a selected bus, its negative sequence voltage is calculated as the sum of the negative sequence voltages derived from ten simulations (with one unbalance source in the network at a time) and its positive sequence voltage is calculated as the average of the corresponding ten voltages from ten individual cases. Its VUF is then calculated by dividing the cumulative negative sequence voltage by the cumulative positive sequence voltage and finally it is compared to the results calculated by superposing the VUFs directly.

4.5.3 Result and Accuracy of Superposition

The VUF of Bus 1 is always zero and will not be included in the following analysis.

4.5.3.1 Results for Algebraic Summation

The discrepancy of cumulative VUF and reference VUF is calculated according to method 1, as shown in Table 4.9 and Fig. 4.18. The thick black lines in the figure are the average discrepancies of individual buses or different time zones. The negative sign in the vertical axis denotes that the calculated VUF is larger than the reference VUF in general.

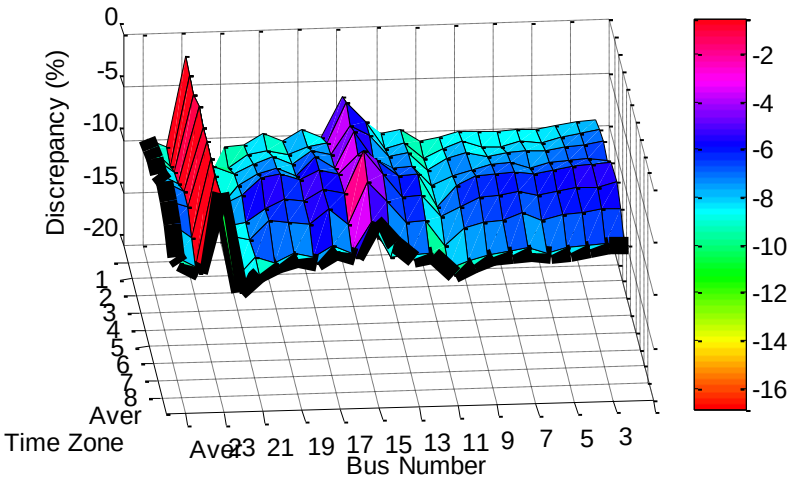

Fig. 4.18 Discrepancy between cumulative VUF and reference VUF using method 1.

The overall difference is -7.13%, which means the absolute value of the difference is less than 10%. For example, if VUF_{ref} is 1.0%, the VUF_{cum} derives 1.0713%. Because most of the mean values of VUFs of eight time zones (except those in heavy loading time zones) are below or around 2%, the absolute errors are usually less than 0.14% VUF.

Table 4.9 Relative Errors of Two Groups According to Method 1

Bus Number	**Relative Error (%)**								
	Time Zone								**Average**
	1	2	3	4	5	6	7	8	
2	7.85	7.07	6.57	6.76	5.49	5.70	6.51	8.57	6.81
3	8.00	7.37	6.86	6.50	5.45	6.05	6.63	8.32	6.90
4	8.26	7.82	7.05	6.69	5.65	6.01	6.86	8.41	7.09
5	8.48	8.23	7.43	6.82	6.01	6.33	6.99	8.55	7.35
6	8.54	7.92	7.32	7.34	6.36	6.74	7.43	8.94	7.57
7	8.55	8.42	7.52	6.82	6.05	6.27	6.74	8.43	7.35
8	8.49	8.50	7.67	6.89	6.16	6.50	7.30	8.77	7.54
9	8.51	7.87	7.29	7.35	6.36	6.72	7.41	8.97	7.56
10	9.00	8.43	7.80	7.93	7.08	7.52	8.03	9.53	8.16
11	9.33	9.32	8.89	8.76	9.11	8.37	9.58	10.24	9.20
12	8.22	7.77	7.16	6.87	6.00	6.29	7.05	8.63	7.25
13	8.46	8.25	7.49	6.91	6.12	6.45	7.17	8.69	7.44
14	7.70	5.74	5.44	6.01	4.46	4.26	5.16	8.94	5.96
15	4.84	3.76	4.37	3.39	3.99	1.91	3.35	5.46	3.88
16	8.63	7.65	7.18	6.77	5.74	5.96	7.29	8.50	7.21
17	7.84	7.98	6.76	5.71	5.30	5.48	5.70	7.64	6.55
18	8.98	8.52	7.92	7.43	6.18	6.60	7.21	8.63	7.68
19	8.20	8.21	7.21	6.54	5.47	6.31	6.91	8.22	7.13
20	9.23	8.41	7.87	7.18	5.85	7.25	6.73	9.03	7.69
21	9.40	9.74	8.69	8.13	7.45	8.43	8.49	8.53	8.61
22	16.89	10.61	7.95	10.37	8.32	8.71	8.12	10.58	10.20
23	0.54	0.72	1.01	0.47	0.87	0.56	0.65	0.58	0.68
24	9.05	9.43	8.25	7.89	6.97	6.83	8.08	9.26	8.22
Average	8.39	7.73	7.03	6.76	5.93	6.14	6.76	8.32	7.13

The discrepancy of the two result sets at bus 23 is mostly less than 1% (only one exception), meaning the computing result is fairly accurate at this bus. But for bus 11, because the VUF is always smaller than 0.05%, a tiny difference in VUF can result in big discrepancy and this is the reason why the discrepancy at bus 11 is relatively large. The biggest difference appears at bus 22, where the cumulative result is on average 10.2%

larger than true value. Among all buses, the cumulative results are always bigger than reference results. This indicates that, in the case of ten simultaneous sources of unbalance, there is certain unbalance cancellation occurring all the time, especially at bus 22.

When comparing between time zones, the darker blue in Fig. 4.18 indicates that the discrepancy between the calculated value and true value gets smaller when the total loading is larger. Also, in terms of the sizes of individual loads, the cumulative results are more accurate for large loads such as loads at bus 15 and bus 23, whose discrepancies are closer to 0% than any other buses in Fig. 4.18. That phenomenon results from the large size of the denominator of the Relative Error since heavier loading leads to larger VUF (in other words, the denominator).

The discrepancies calculated using method 2 are demonstrated in Table 4.10 and Fig. 4.19.

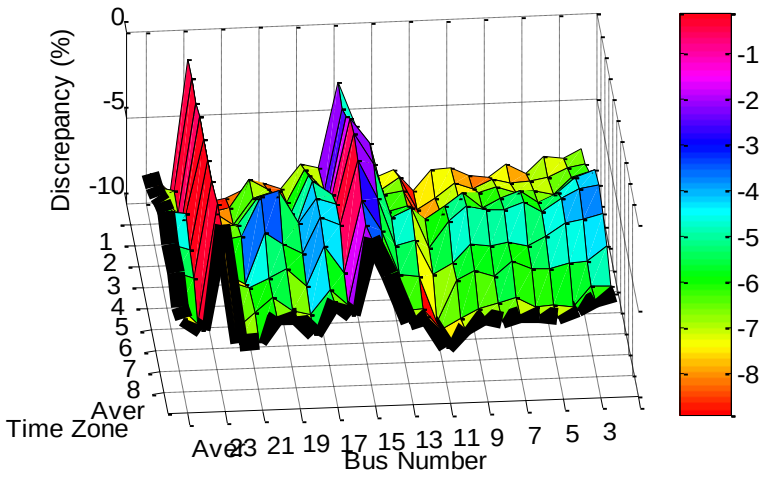

Fig. 4.19 Discrepancy between cumulative VUF and reference VUF using method 2.

The absolute values of average discrepancies are smaller than the ones in method 1. The overall difference drops to 5.68%, smaller than the previous 7.13%.

Table 4.10 Relative Errors of Two Groups According to Method 2.

Bus Number	Relative Error (%)								
	Time Zone								Average
	1	2	3	4	5	6	7	8	
2	6.57	6.19	5.44	4.11	3.71	4.24	4.87	6.01	5.14
3	7.12	6.46	5.71	4.53	3.98	4.51	5.70	5.92	5.49
4	6.91	6.98	6.66	5.36	4.49	4.67	5.80	7.08	5.99
5	7.86	7.09	6.40	5.91	5.22	5.40	6.07	6.91	6.36
6	7.28	7.14	6.52	5.19	4.64	5.88	6.01	7.02	6.21
7	8.08	6.91	6.13	5.56	4.96	5.67	5.53	6.44	6.16
8	7.83	7.47	6.46	6.06	4.93	5.81	6.41	6.70	6.46
9	7.38	7.00	6.68	5.16	4.64	5.65	6.05	7.01	6.20
10	7.48	7.85	7.54	5.91	5.55	6.78	6.50	7.50	6.89
11	8.66	8.50	8.11	6.61	7.03	7.36	8.89	8.12	7.91
12	7.33	6.60	6.15	5.79	4.73	5.33	6.18	6.90	6.12
13	7.80	7.31	6.35	6.14	5.20	5.58	6.09	7.00	6.43
14	4.76	4.96	3.87	2.04	2.03	2.83	3.47	4.84	3.60
15	2.14	2.47	1.64	0.50	0.25	0.57	1.66	1.91	1.39
16	7.09	7.22	6.51	4.93	4.25	4.26	5.83	6.54	5.83
17	6.87	5.97	5.03	4.13	3.95	3.82	4.27	5.54	4.95
18	8.26	7.79	7.19	6.96	5.34	5.84	6.57	6.93	6.86
19	7.89	6.96	6.00	4.89	3.42	5.29	5.49	6.66	5.83
20	8.15	6.32	6.19	5.05	3.64	4.52	5.97	5.87	5.71
21	8.68	8.02	7.71	6.47	5.92	7.48	6.45	6.75	7.18
22	8.80	8.15	7.00	6.58	6.18	6.86	6.13	7.69	7.17
23	0.40	0.29	0.56	0.09	0.18	0.19	0.23	0.29	0.28
24	8.17	6.87	7.01	6.03	4.54	5.36	5.86	7.31	6.39
Average	7.02	6.54	5.95	4.96	4.30	4.95	5.48	6.22	5.68

Although the relative errors in method 2 are smaller than results in method 1, method 2 requires large numbers of data sets to compare the difference, which can hardly be applied to an estimation of momentary VUF. However, for long time monitoring (such as one-week monitoring according to EN50160), method 2 provides more accurate results than method 1.

The example of a comparison between VUF_{ref} and mean VUF_{cum} for all buses according to method 2 is displayed in Fig. 4.20. In the figures, for eight time zones, blue round points denote the calculated VUF and red cross stands for the reference value. As seen in Fig. 4.20, bus 15 is the most affected bus by unbalance, with the mean VUFs exceeding 2% in six time zones. The mean VUFs of the remaining buses stay below or

around 2%, i.e., within the standard limitation. The curve of calculated VUFs overlaps the curve of reference VUFs, with small deviations.

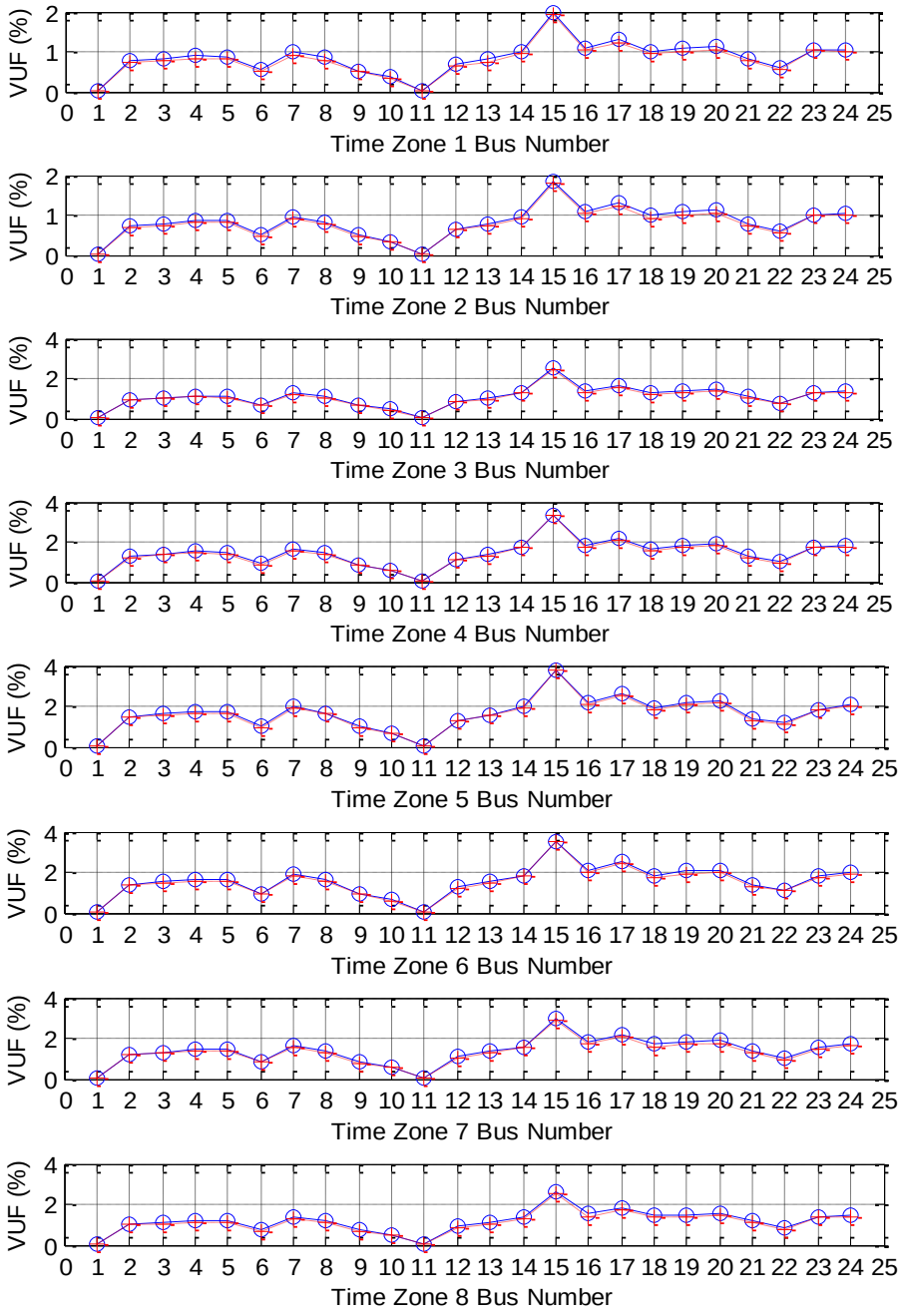

Fig. 4.20 Comparison of VUFs of eight time zones according to method 2. Blue circle: mean VUF_{cum}; red cross: VUF_{ref}.)

As required by EN50160 [48] that 95% of weekly 10-minute averages should be below 2%, the 95th percentiles of VUFs of both reference group and cumulative group are compared and shown in Fig. 4.21. As seen from the figure, the 95th percentiles usually stay at the same level, i.e., over 2% or below 2%, with only one exception. In Time

Zone 4, the 95th percentile of VUF_{cum} of bus 4 is 2.011% while the corresponding VUF_{ref} is 1.976%. Although they present different levels with respect to the conformance with the standard, the relative error between them is just -1.77%.

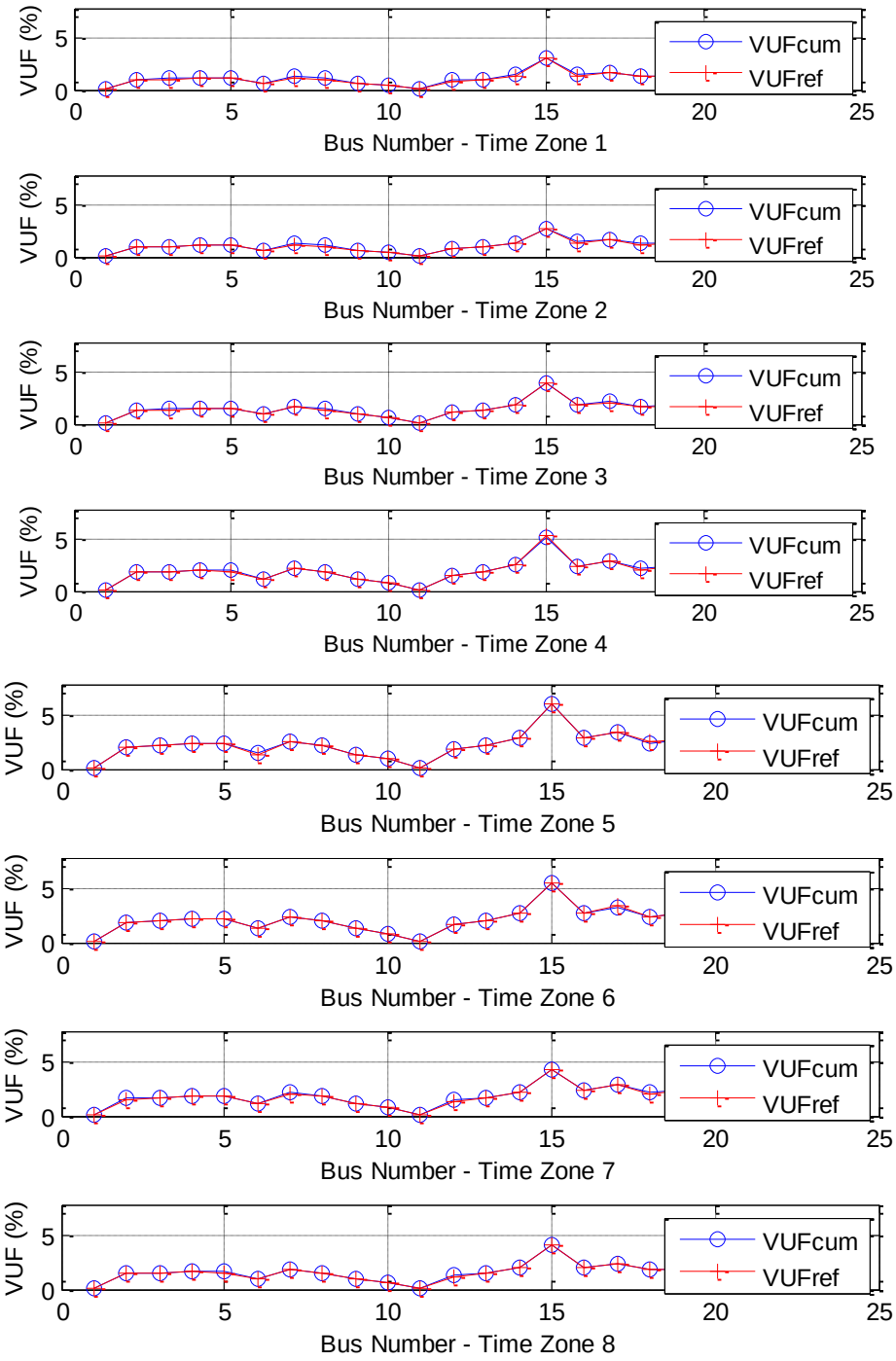

Fig. 4.21 The 95th VUF_{cum} and VUF_{ref} of 24 buses in 8 time zones.

The maximum values of both groups are compared in Fig. 4.22. When referring to the individual cases, the cumulative VUF may appear smaller than the actual VUF,

reflected by the positive values in relative errors. The centre of distribution of discrepancy in VUF is around 0% in this case. This individual case does not show any correlation between the size of load and the resultant discrepancy.

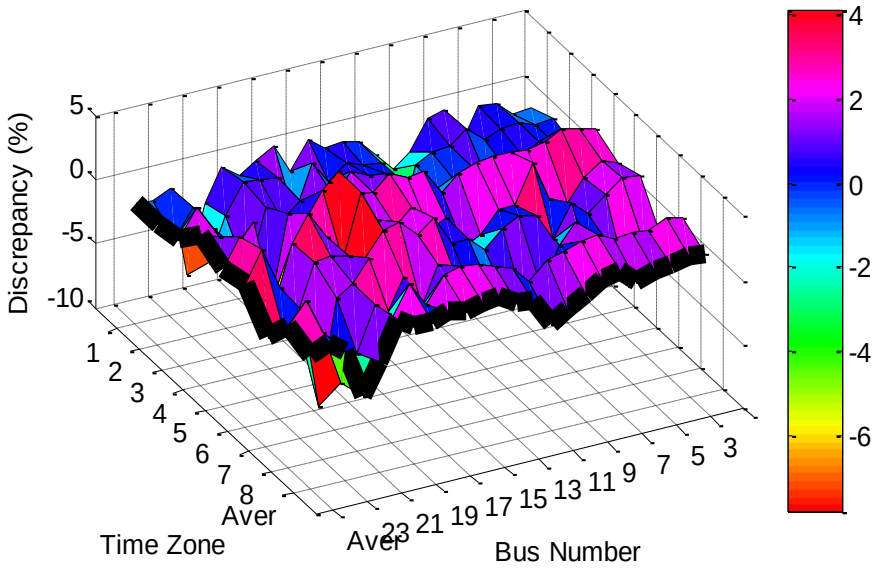

Fig. 4.22 Discrepancy between maximum cumulative VUF and maximum reference VUF using method 3.

The general pattern for the unbalanced source superposition is beneficial for estimating the VUF level in the network. After identifying the locations of unbalanced sources, according to historical monitoring data or the probabilistically simulated results (which can give the overall resultant VUF level of a single unbalanced source), the current unbalance level can be approximately computed. This is a reasonably accurate method to derive the unbalanced level of the network even when current network data are not available. It considers the number of unbalanced sources, locations of sources and the individual impacts of sources. The changing trend of unbalance can be estimated from these results as well.

4.5.3.2 Comparison of Algebraic and Vectorial Summation of VUFs

In the above discussion, VUF_{cum} at the selected bus was calculated by adding up the absolute values of VUFs calculated for individual unbalance source in the network. According to the analysis presented in Chapter 3.3.3, however, the unbalances

originating from different buses in the network may cancel each other out at the bus of interest and even result in perfectly balanced voltage. Therefore, VUF_{cum} at the selected bus should be calculated as the sum of individual VUF vectors, instead of the algebraic sum of absolute values of VUFs, to avoid misunderstanding. The comparisons of the relative errors for the algebraic sum (ALG) and vectorial sum (VEC) for 8 time zones (averages of 24 buses) and 24 buses (averages of 8 time zones) are listed in Table 4.11 and Table 4.12.

Table 4.11 Algebraic and Vectorial Relative Errors for 8 Time Zones

Time Zone	RE(ALG)	RE(VEC)
1	8.07%	2.09%
2	7.67%	2.03%
3	7.30%	2.72%
4	5.74%	3.86%
5	6.05%	3.88%
6	6.08%	4.21%
7	6.60%	3.77%
8	7.75%	3.07%
Average	6.91%	3.20%

Table 4.12 Algebraic and Vectorial Relative Errors for 24 Buses

Bus Number	RE(ALG)	RE(VEC)
1	9.31%	1.23%
2	6.76%	3.07%
3	6.77%	3.28%
4	6.75%	3.68%
5	6.98%	3.75%
6	7.74%	2.65%
7	6.96%	4.04%
8	7.18%	3.68%
9	7.73%	2.64%
10	8.46%	2.27%
11	9.25%	1.29%
12	7.06%	3.14%
13	7.11%	3.55%
14	5.61%	3.18%
15	5.99%	3.50%
16	6.44%	4.29%
17	5.54%	4.78%
18	7.08%	4.15%
19	6.68%	4.30%
20	6.88%	4.20%
21	8.53%	3.26%
22	9.86%	2.54%
23	1.66%	0.38%
24	7.46%	4.02%
Average	6.91%	3.20%

It can be seen that the absolute vectorial relative error is always smaller than the algebraic relative error, confirming that the vectorial sum is more accurate in the estimation of superposition than the algebraic sum. With all the vectorial relative error smaller than 5%, it indicates that the VUFs resulting from different individual sources can be vectorially added up to derive the overall level of unbalance for the network.

Although the algebraic sum is less accurate, the error between two groups of VUF is usually smaller than 10%. It can be inferred therefore that the cancellation of unbalance in complex networks is not significant and that, as the first approximation, the algebraic sum of individual VUFs could be used when angular information of VUF is not available.

Fig. 4.23 geographically illustrates the level of unbalance in the network using contour plots. It compares VUF_{ref}, VUF_{cum} obtained using the algebraic sum and VUF_{cum} obtained using the vectorial sum. It can be seen by inspecting areas around bus 21, 20, 16 and 19 in particular, that the vectorial sum of VUFs provides a closer match to the actual VUFs in the network.

4.5.3.3 COMPARISON OF VECTORIAL SUMMATIONS OF VOLTAGES AND VUFS

Under unbalanced conditions, the negative sequence voltages (which do not exist in balanced conditions) originating from the source of unbalance "propagate" through the network. Depending on the types of loads in the network, this propagation can be very different (and exacerbated by the presence of motors and generators which have different negative and positive sequence reactances) from the "propagation" of balanced voltages, i.e., voltage drops across the network are different. Since VUF at a selected bus is calculated using negative and positive sequence voltages at the bus, the superposition of negative sequence voltages, originating from each source of unbalance, reveals the extent of cancellation of unbalance from different sources.

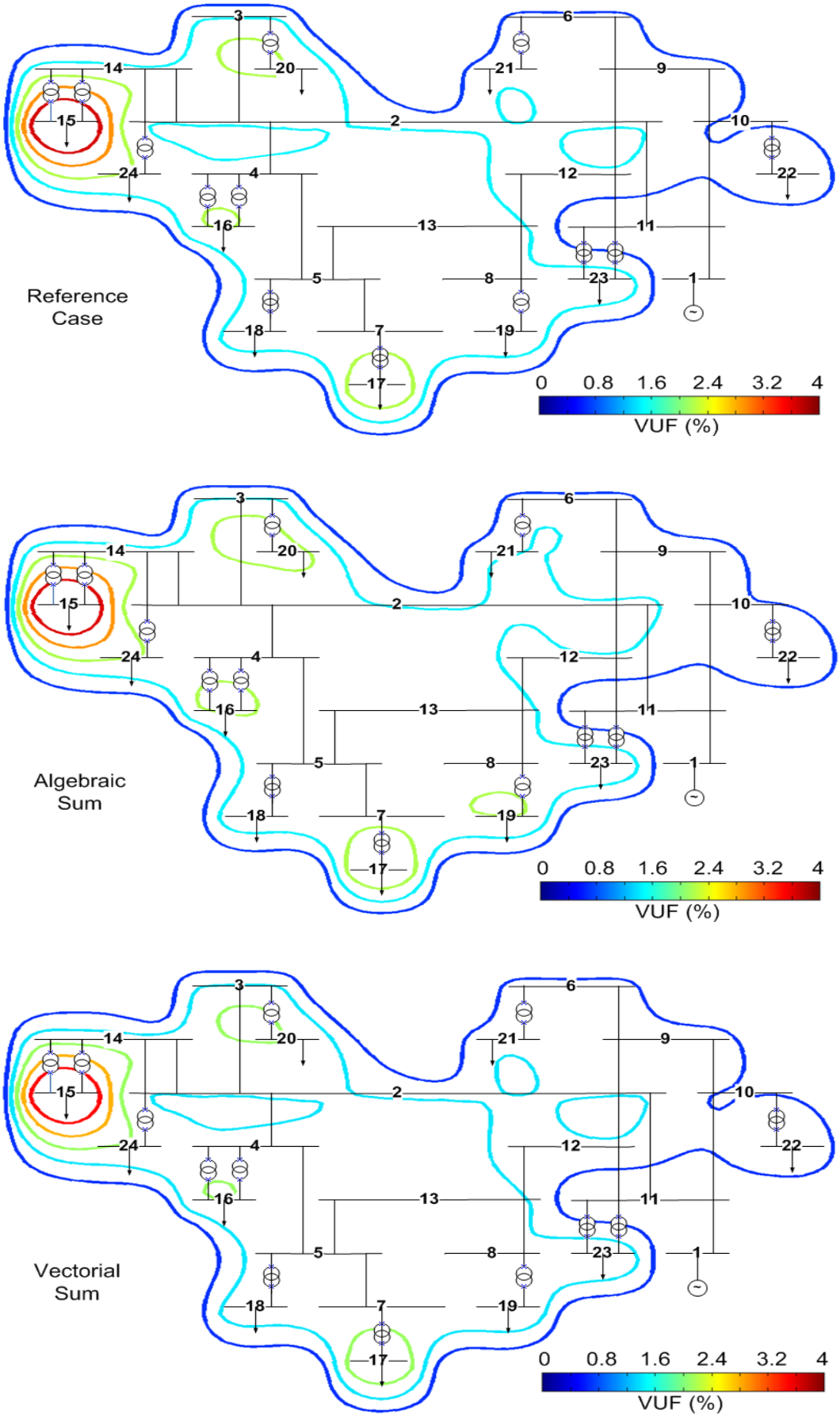

Fig. 4.23 Contour maps of reference VUF, algebraic superposition of VUF and vectorial superposition of VUF.

Fig. 4.24 shows the PDFs of VUF of bus 15 for Time zone 5 calculated using three different methods: with ten unbalanced sources in the network; calculated by superposition of the individual sequence voltages from ten sources; calculated by vectorial superposition of individual VUFs from ten sources. It can be seen that the VUF derived as the sum of sequence voltages has the smallest mean value and it is less accurate than the vectorial sum of VUFs. Since the superposed negative sequence voltage is accurately calculated, the reason for this reduced accuracy is the small deviation of the superposed positive sequence voltage (average of ten positive sequence voltages) from the actual positive sequence voltage calculated in reference case.

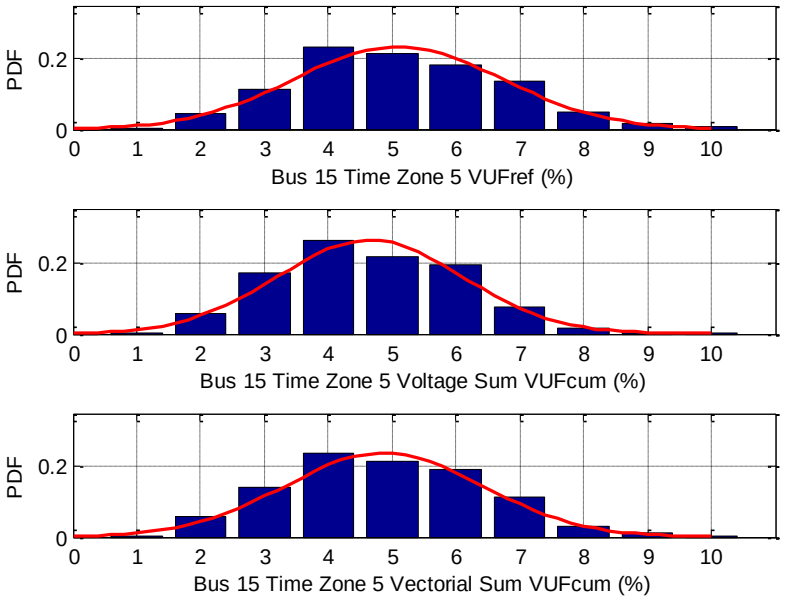

Fig. 4.24 VUFs of bus 15 with ten sources from direct simulation, sum of voltage and vectorial sum of VUF.

Generally, when recording the range of VUF of a bus, the most used values are the maximum value, minimum value and mean value. Table 4.13 shows the ranges of VUFs with ten sources in the network calculated with the three aforementioned superposition methods when only the minimum, maximum and mean value are considered. The vectorial sum of VUFs is still a more accurate way of assessing unbalance using superposition than the sum of individual sequence voltages. Despite the small error, the similarity of the three subfigures of Fig. 4.24 provides a simple way for estimating the possible degree of unbalance of a bus using either of the described methods from

limited-available historical data. This table also shows that by adding up the maximum, minimum and mean values of VUFs from individual sources, the possible range of VUF can be established, enabling the prediction of VUF at non-monitored buses during a particular time period (monitored or non-monitored period).

Table 4.13 Comparison of Calculated Values of VUFs Obtained From Direct Simulation with Ten Unbalanced Sources, Sum of Unbalanced Voltages (VOL) and Vectorial Sum (VEC) of VUFs

Bus Number	$VUF_{ref\ (\%)}$			Vol VUF_{cum} (%)			Vec VUF_{cum} (%)		
	min	mean	max	min	mean	max	min	mean	max
1	0.03	0.12	0.19	0.03	0.12	0.19	0.03	0.12	0.19
2	0.49	1.73	3.27	0.48	1.65	3.05	0.48	1.66	3.09
3	0.69	1.86	3.49	0.68	1.78	3.25	0.68	1.79	3.29
4	0.66	2.02	3.57	0.64	1.92	3.31	0.64	1.93	3.34
5	0.69	1.98	3.46	0.67	1.89	3.21	0.67	1.89	3.24
6	0.42	1.20	2.20	0.41	1.16	2.08	0.41	1.16	2.09
7	0.74	2.23	3.84	0.72	2.11	3.54	0.72	2.12	3.57
8	0.77	1.92	3.34	0.75	1.83	3.10	0.75	1.83	3.12
9	0.41	1.19	2.19	0.41	1.15	2.07	0.41	1.15	2.08
10	0.32	0.83	1.47	0.32	0.80	1.39	0.32	0.81	1.40
11	0.04	0.17	0.28	0.04	0.17	0.28	0.04	0.17	0.28
12	0.51	1.54	2.80	0.50	1.48	2.62	0.50	1.48	2.64
13	0.66	1.82	3.21	0.64	1.74	2.98	0.64	1.74	3.01
14	0.54	2.33	4.70	0.52	2.21	4.33	0.52	2.24	4.43
15	1.33	5.10	11.33	1.25	4.65	9.86	1.29	4.87	10.62
16	0.85	2.57	4.46	0.82	2.42	4.10	0.82	2.43	4.15
17	0.85	3.09	5.65	0.81	2.88	5.17	0.81	2.91	5.25
18	0.74	2.16	3.61	0.71	2.05	3.33	0.71	2.06	3.36
19	0.89	2.47	4.58	0.83	2.33	4.18	0.84	2.34	4.22
20	0.73	2.63	4.64	0.71	2.48	4.25	0.71	2.50	4.30
21	0.38	1.59	2.79	0.37	1.53	2.61	0.37	1.53	2.62
22	0.34	1.40	2.41	0.32	1.35	2.29	0.32	1.36	2.31
23	0.21	2.32	4.60	0.21	2.25	4.43	0.22	2.31	4.58
24	0.73	2.47	4.30	0.71	2.33	4.03	0.71	2.34	4.06

The contributions of individual sources of unbalance, characterised by VUF, can be calculated to obtain the total unbalance in the network. The errors, resulting from either algebraic summation of VUF, vectorial summation of VUF or voltage summation, stay below 10% of the true value, which is deemed acceptable considering other uncertainties involved.

By using this simple superposition, the contribution of individual unbalanced loads can be easily established from statistical data or results of probabilistic estimation. Similarly, by identifying the individual sources of unbalance, the VUF of the whole network can be estimated. The superposition of unbalance in the network enables DNOs to estimate the degree of unbalance in different parts of the network, thus facilitating network planning and corresponding troubleshooting.

4.6 Daily Loading Simulation with Mixed Load

4.6.1 Mixed Load Composition

As described in previous section, the three types of loads are of different loading capacities, quantities, peaks and changing trends. Instead of a single class load at every bus, in real network, the aggregated loads are usually mixtures of different types of loads. In order to simulate realistic levels of unbalance for the network, all the loads at the 24-bus network are assumed to be composed of 85% domestic load, 13% commercial load and 2% industrial load according to customer record. The loading factors of domestic, commercial and industrial loads are the same as listed in Table 4.2. As a result of the mixed types of load, the network is dominated by domestic loads and the new total loading curve is shown in Fig. 4.25. The peak loading appears in Time Zone 7 while Time Zone 2 has the lightest loading during the day. The developed daily loading curve closely models the changing demand for active power in the network.

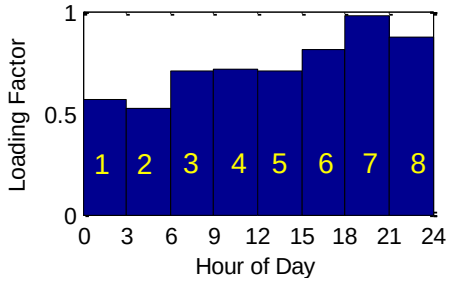

Fig. 4.25 Daily loading curve for the network with mixed types of load.

The methodology used for mixed types of load is the same as the simulations with single class loads. For a particular time zone, the active power per phase is kept constant and the load unbalance is modelled by varying only the reactive power component per phase using the probabilistic methodology developed, considering specified limitations (4.1). The power factors of domestic load are selected from the normal distribution with mean value 0.99. Because power factors of three phases are randomly and independently selected, the unbalance among three phases is guaranteed. The mean value of the normal distribution for commercial load is 0.95. Industrial load is usually three-phase and is assumed to be balanced with a fixed power factor 0.8.

The only difference in simulations between mixed type load and single class load is the first and second steps of load variation. The simulation procedure can be described as below:

- For a selected time zone, apply loading factors of the time zone according to the proportion of composition to all loads to derive the active powers for each bus in each time zone;
- Calculate *Q* by varying power factor for given *P* using 500 MC simulations. This yields 500 random groups of unbalanced loads for all ten loads such that the random variables for every load are independent and different;
- Run repeatedly (500 times) three-phase load flow with only one unbalance source in the network – bus 15, while keeping all other loads balanced. This results in 500 VUFs for each bus in the network;
- Select second unbalance source – bus 17 and repeat step 3 with two unbalance sources in the network;
- Repeat step 4 by adding one new source of unbalance every time until all 10 loads are modelled as unbalance sources. (In the tenth simulation, all ten loads are modelled as unbalanced.) The results of each simulation are stored separately;
- Repeat steps 1-5 for the remaining seven time zones.

4.6.2 PROBABILISTIC RESULTS WITH MIXED LOAD

The median values of VUFs from 500 simulations at all buses in the network for Time Zone 7 with the sequential addition of one unbalance source at a time are displayed in Fig. 4.26. Two sequences are involved: the initial sequence and ascending sequence, shown in Fig. 4.26 (a) and Fig. 4.26 (b) respectively.

The impact of a source is proportional to its size (except bus 23). The critical factor, as before, is the load at bus 15. It is clear that only when the load at bus 15 is set to unbalanced, six buses have VUF larger than 0.5%. Therefore, by ensuring the symmetry of the load at bus 15, the unbalance in the whole network can be maintained within a low level.

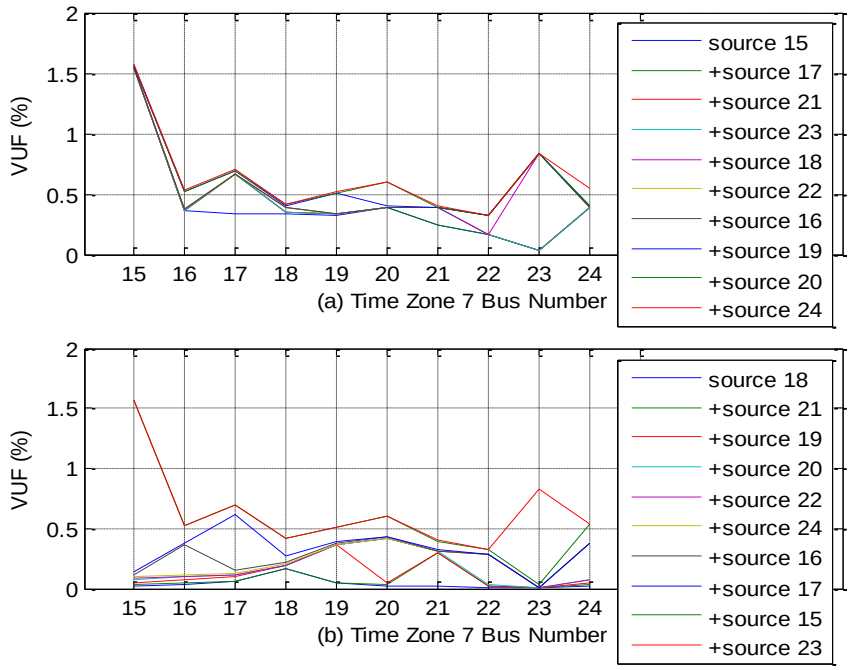

Fig. 4.26 VUFs of 24 buses of different sequences of Time Zone 7. (a)Initial order; (b) Ascending order.

As described above, Time Zone 2 has the lightest loading and Time Zone 7 has the heaviest loading. With ten unbalance sources in the network, the distributions of VUFs across the network of two time zones are illustrated in Fig. 4.27. Heat maps (Fig. 4.28) for the two time zones are plotted using the mean values of 500 VUFs of all buses.

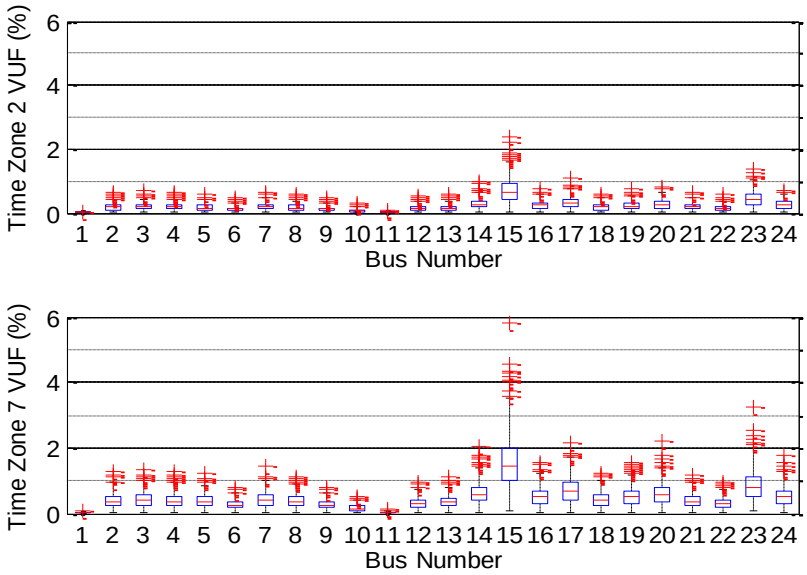

Fig. 4.27 Distributions of VUFs of Time Zone 2 and Time Zone 7.

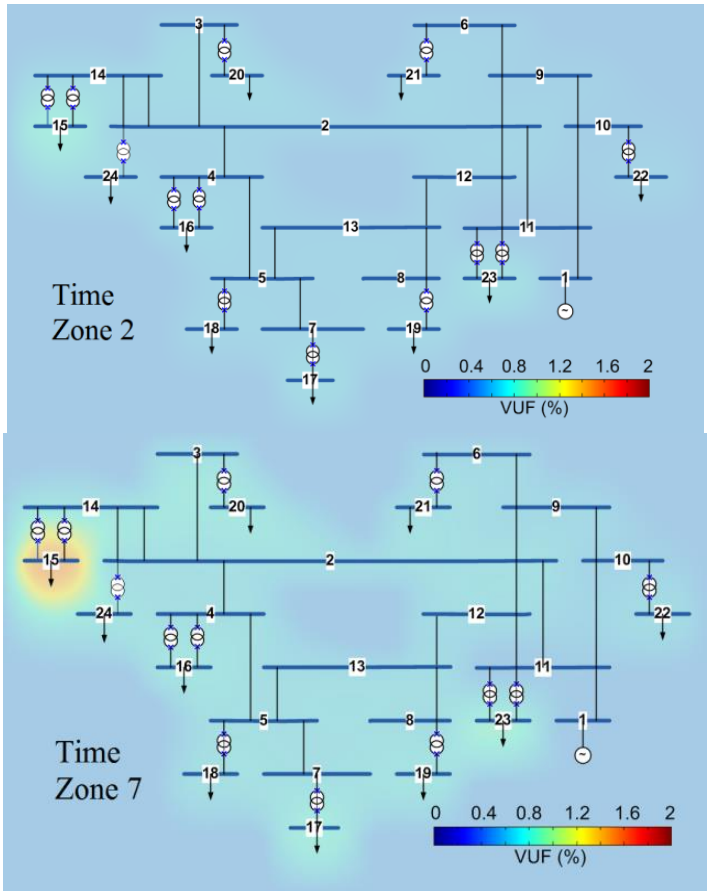

Fig. 4.28 Heat map for Time Zone 2 and 7 with mixed load.

For bus 15, the VUF of Time Zone 7 raises beyond 4% under some extreme conditions while only 2 values out of 500 of Time Zone 2 exceed 2%. Focusing on the inter-quartile ranges, in Time Zone 7, there is possibility of reaching 2% unbalance while in

Time Zone 2 there are no risks for the whole system. Therefore, during the peak loading period of the day, the network is exposed to a higher level of unbalance than at any other time. Seen from the heat maps, buses 15, 20 and 17, for example, in Time Zone 7 are more "orange" than in Time Zone 2.

The simulation results are compared to the real monitored VUF in Fig. 4.29 for bus 16 and 24 where the real readings are provided by the DNO and plotted using magenta solid lines with circles. All the real values locate within the boxes, verifying that the methodology provides correct estimation of unbalance for the network. During the peak loading period, the simulation results are overestimated because the provided loading curve is for winter days while the unbalance in the network was recorded for a summer day. The consumption of heating load increases the peak loading, and therefore unbalance in the network, during winter days.

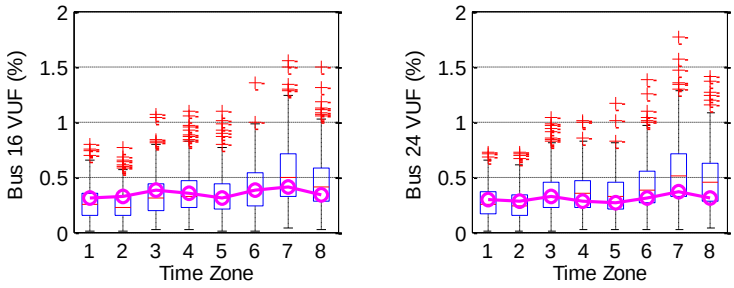

Fig. 4.29 Comparison between estimated VUF using proposed methodology and the real monitoring VUF.

Six typical buses are chosen for the study of the changing trends in different time zones with different numbers of unbalanced sources, shown in Fig. 4.30. The adding sequence of sources is the original sequence. The similarity of shapes of curves for each added source shows that the changing trend of the curves is dominated by the total loading level. With the mixed type of load, the dominant class is the domestic load so that the peak unbalance for every bus appears in Time Zone 7. It can be still observed that when a load at a bus is modelled as unbalanced, the VUF of that bus increases significantly as

well as the VUF of the pairing upstream bus. The VUF increments at inter-connecting bus such as bus 2 are almost constant.

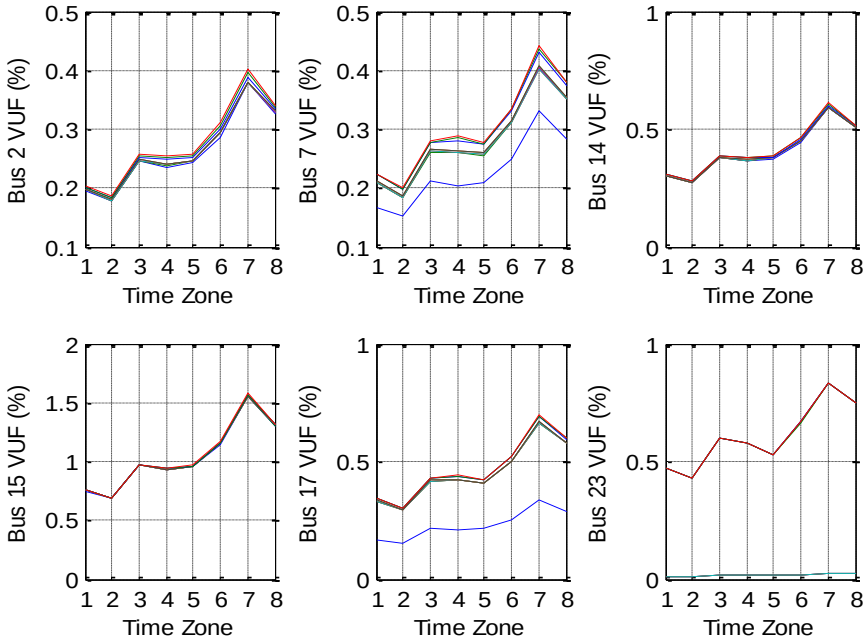

Fig. 4.30 VUF curves for all time zones with adding sources for individual buses.

The grouping of the buses (except bus 1 which stays balanced all the time) into five groups, according to the mean values of their VUFs with ten sources of unbalance in the network, is shown in Table 4.14. Still, group 1 only contains 33kV buses while Group 4 and Group 5 comprise all 11kV load buses. The interconnecting buses 2, 12 and 13, are all classified in Group 2, maintaining a relatively low level of unbalance. Group 3 contains the rest of the buses.

Table 4.14 Grouping of Buses According to the Mean Level of Unbalance

Group	VUF Range	Bus Number
1	<0.3%	6, 9, 10, 11
2	0.3% ~ 0.45%	2, 3, 4, 5, 7, 8, 12, 13, 18, 21, 22
3	0.45% ~ 0.55%	14, 16, 19, 24
4	0.55% ~ 1%	17, 20, 23
5	>1%	15

In Fig. 4.31, all the results from 500 MC simulations, instead of only the mean values, are shown for five characteristic groups. It shows the VUF variations of typical buses in eight time zones with ten unbalance sources. The scaled loading curves (magenta thick solid lines) of the buses are also shown in this figure. It can be seen that the peak VUF

values under certain conditions can be as high as triple the median values. The most reliable estimation of unbalance however, is the inter-quartile range (blue rectangles). By overlapping the scaled loading curves and the resultant mean VUFs from each time zone in the individual plots of Fig. 4.31, a close match between the two can be observed, i.e., there is close correlation between loading level and mean VUF.

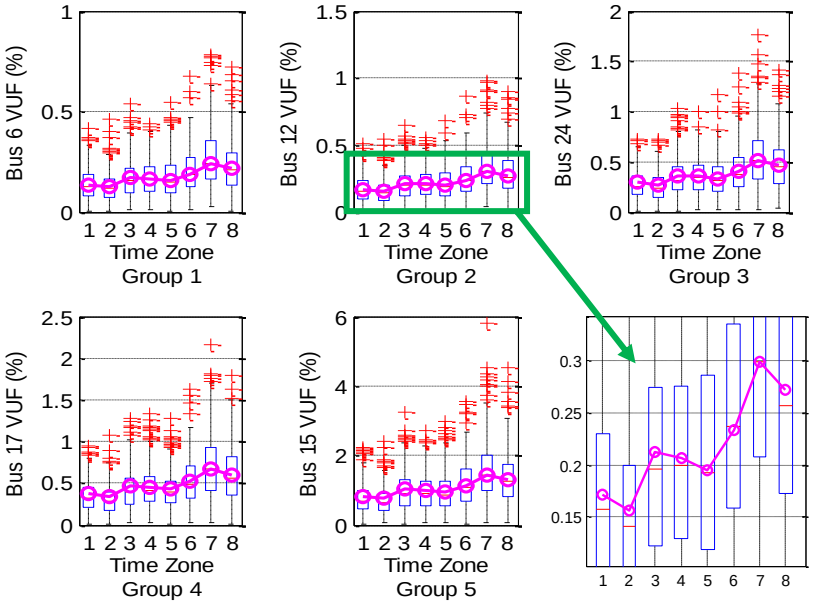

Fig. 4.31 VUF distributions for typical buses of five groups, with loading curve plotted.

Fig. 4.32 shows the probability density functions of the same five typical buses from five groups for Time Zone 7 with ten sources of unbalance in the network. The PDFs of these five buses correspond to slightly skewed normal distribution. The mean value (μ) of these PDFs moves towards higher values gradually from Group 1 to Group 5 and the standard deviations (σ) also increase, indicating bigger ranges of possible VUF and wider propagation of unbalance.

The overall accuracy of vectorial sum for 24 buses for all time zones is 1.12%. Fig. 4.33 geographically illustrates the level of unbalance in the network using contour plots for VUF_{ref} and VUF_{cum}. It can be seen that the vectorial sum of VUFs provides a close match to the actual VUFs in the network.

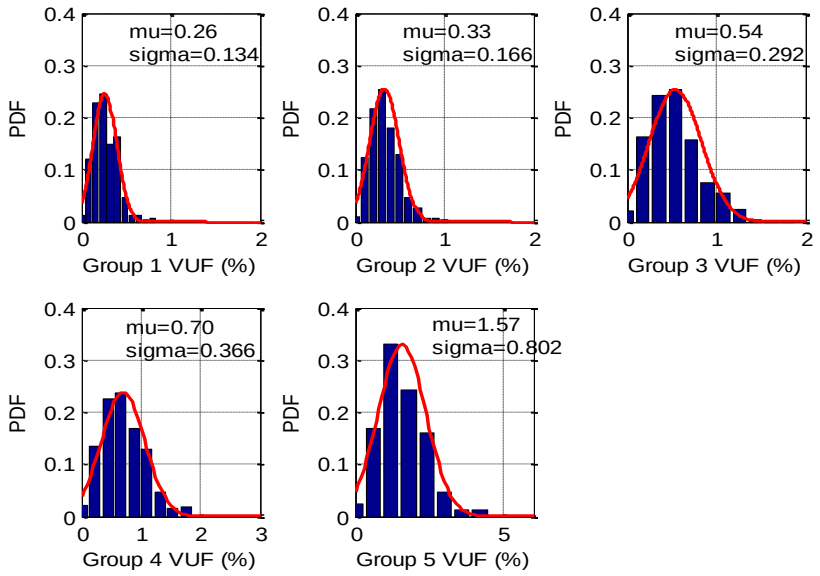

Fig. 4.32 PDFs of VUF distributions of typical buses in five groups.

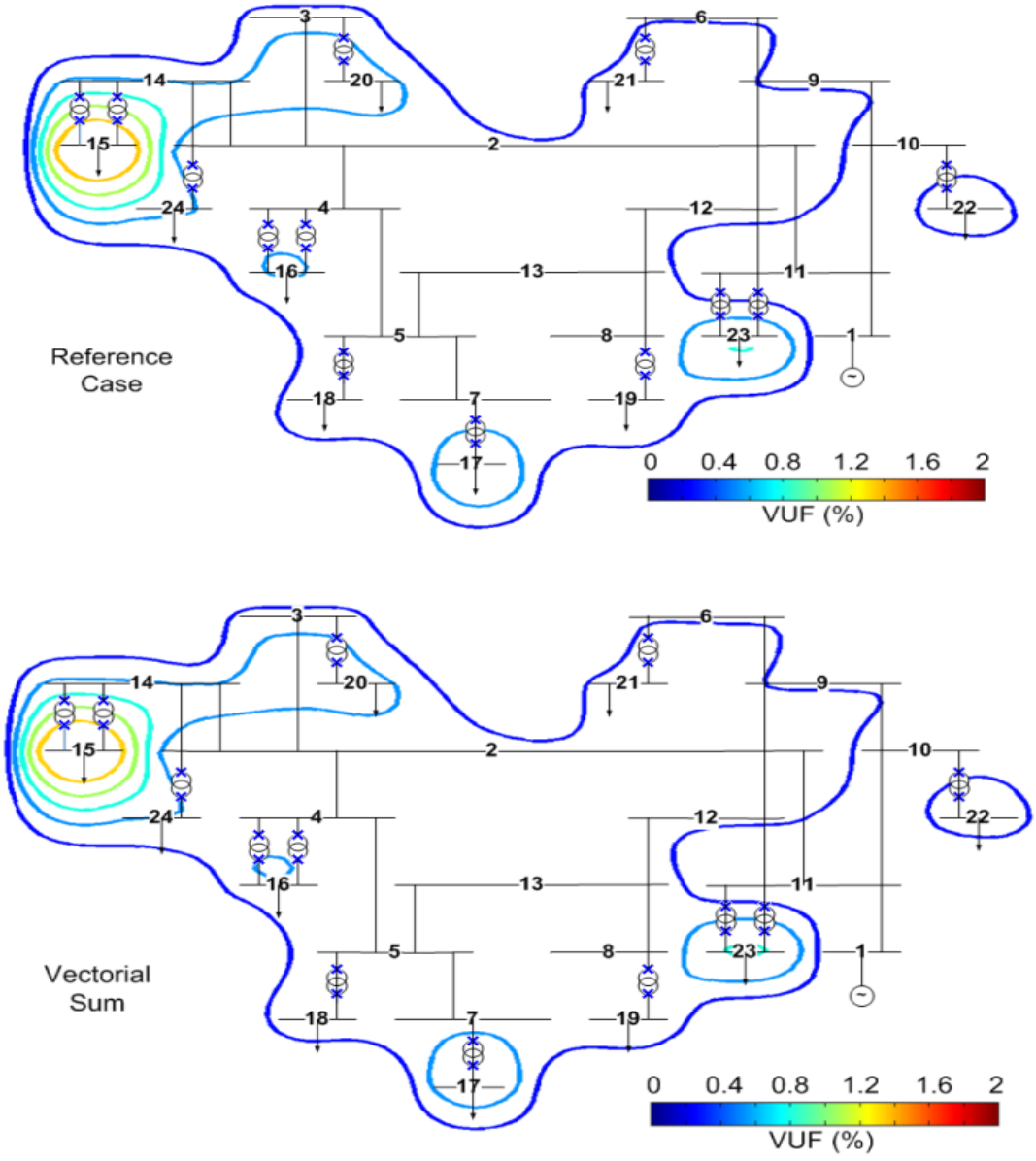

Fig. 4.33 Contour maps of reference VUF and vectorial superposition of VUF.

With mixed type of load, the overall accuracy of VUFs obtained by voltage summation for 24 buses for all time zones is 2.28%. Therefore, the degree of unbalance in the network can be assessed with very good accuracy by applying simple vectorial summation of VUFs resulting from individual unbalanced sources or by negative sequence voltage superposition.

Table 4.15 lists the relative errors (RE) calculated by (4.4) for algebraic sum (ALG), vectorial sum (VEC) and voltage superposition (VOL). It can be seen that the vectorial sum of VUFs results in the closest match to the true VUFs in the network. Despite the small error, the similarity of the three ways of superposition confirms that any of the methods can be used to estimate the possible degree of unbalance at a bus by using either described method from limited-available historical data.

Table 4.15 Accuracies of 3 Superposition Methods for 24 Buses

Bus Number	RE_{ALG}(%)	RE_{VEC}(%)	RE_{VOL}(%)
1	3.094	0.299	0.499
2	2.082	0.979	2.079
3	2.470	1.071	2.204
4	2.892	1.278	2.361
5	3.153	1.298	2.368
6	2.499	0.878	1.674
7	3.152	1.517	2.643
8	3.012	1.295	2.318
9	2.486	0.877	1.665
10	2.848	0.762	1.360
11	3.093	0.323	0.543
12	2.578	1.026	1.979
13	3.000	1.202	2.222
14	1.453	0.975	2.520
15	0.553	1.007	4.571
16	2.993	1.659	2.969
17	2.413	1.914	3.566
18	3.609	1.578	2.670
19	2.990	1.707	2.988
20	2.398	1.608	3.057
21	2.930	1.177	2.236
22	2.184	0.835	1.612
23	0.144	0.054	1.674
24	2.549	1.519	2.883
Average	2.524	1.118	2.278

4.7 Impact of Connected Power System Equipment

4.7.1 Attenuation Due to Induction Motors

The 24-bus network is dominated by the domestic loads and contains only a few industrial loads as reported. However, if the composition proportion is different, with induction motors connected, the unbalance will be attenuated as described in Fig. 4.34. The figure is produced by changing 15% of the load at bus 15 into big induction motors and another 15% into small induction motors respectively. In that way, the domestic load and commercial load together only represent 70% of the total load at the bus. Three time zones are plotted: Time Zone 2 which is the lightest loading for both the total loading and industrial loading, Time Zone 5 which is the peak loading for industrial loading, and Time Zone 7 which is the peak loading for total load. By comparing the mean values of bus 15 over all time zones with corresponding ones with previous loading condition, the presence of induction motors reduces unbalance by an average value of 41.85%. The biggest attenuation appears in Time Zone 5 where the induction motor load reaches its peak.

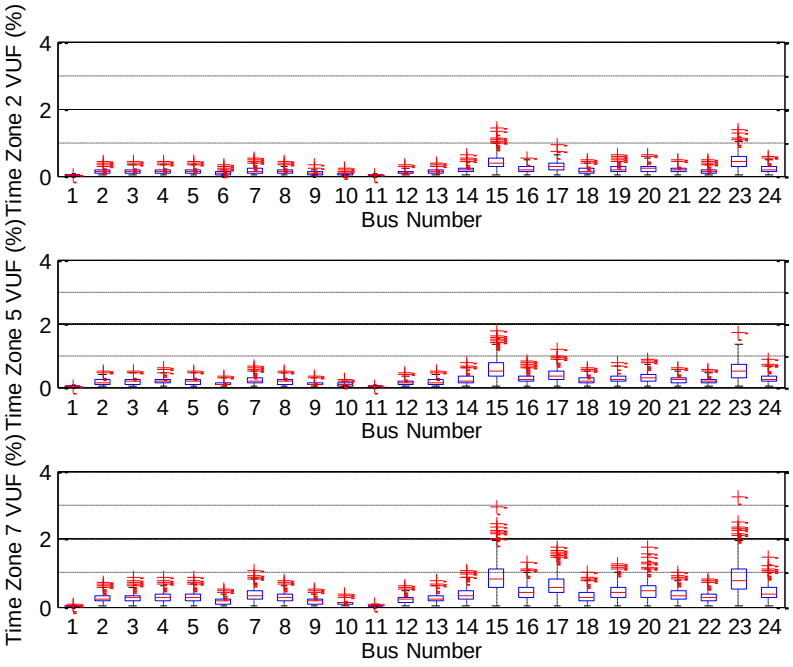

Fig. 4.34 Distributions of VUFs of Time Zone 2, 5 and 7 with 70% domestic and commercial loads and 30% induction motors.

4.7.2 Attenuation Due to Wind Turbine Generators

The power output of the wind turbine generators used in this simulation is varied according to the data created by the University of Strathclyde (see Appendix D.1). It is assumed that the average wind speed is 8m/s, with 10% turbulence. The maximum output power of the wind turbine is 1.5174MW, which equals to 6.9% of the total loading at bus 15 which is the worst served bus and where the wind turbine is connected to.

With the presence of wind turbine, the VUFs of the most severe source bus 15 are shown in Fig. 4.35 for three time zones. It can be seen that the attenuation introduced by the wind turbine is nearly the same with the attenuation of induction motors.

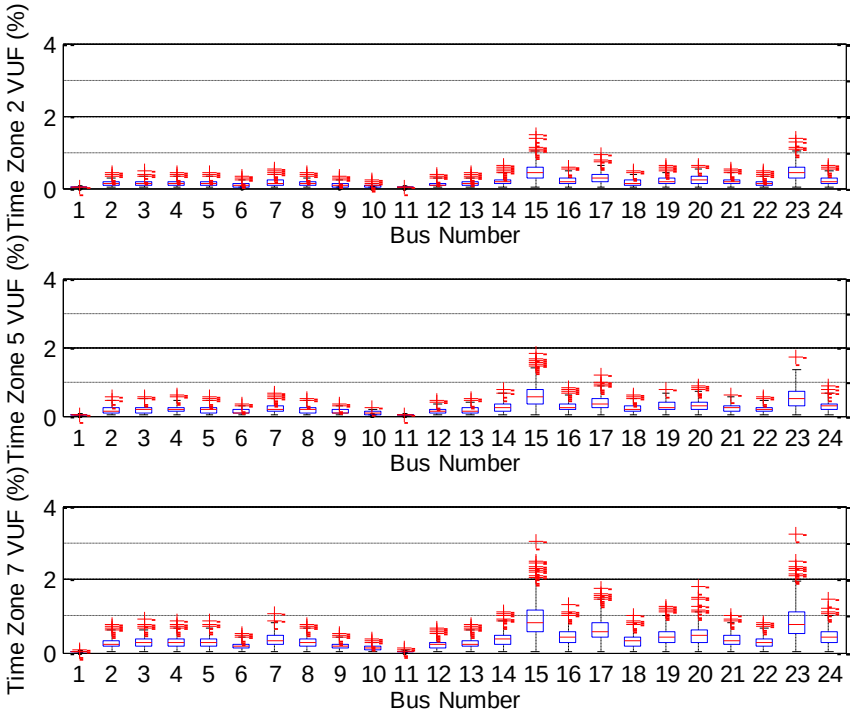

Fig. 4.35 Distributions of VUFs of Time Zone 2, 5 and 7 with connected wind turbine.

4.7.3 Attenuation Due to Photovoltaic Generators

The power output of photovoltaic generators is determined by the photocurrent and the environment temperature. In the simulation, the two parameters are set to be varying

according to the solar insolation. The curve of direct radiation for a sunny summer day 17th August at latitude 53 degree (the latitude of the UK is between 51 and 58) is shown in Fig. 4.36 [159] with detailed data listed in Appendix D.2. The PV is generating at 0.7kV voltage level and is connected to the mains grid through a transformer. The maximum photocurrent output is 142.85A.

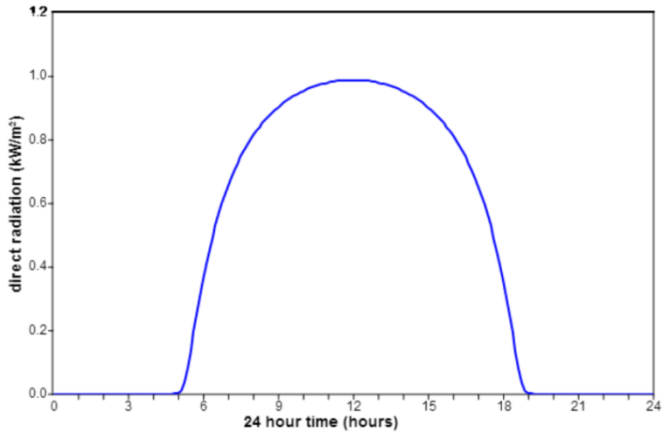

Fig. 4.36 Solar insolation of a sunny day on 17th August in latitude 53 degree [159].

For the 24-bus network, the photovoltaic generator is assumed to be connected to bus 15, as well as the induction motors and wind turbine. The results are shown in Fig. 4.37. Compared to Fig. 4.34 with no generation and Fig. 4.35 with the generation of wind turbines, the assembly of photovoltaics mitigates the unbalance during high insolation period but has little impact on the level of unbalance in the evening when the risky peak demand appears. Note that the results of the integrated photovoltaics are restricted to this case and the effect of photovoltaics can be completely different.

4.8 DNSE WITH REAL LOADING AND REAL MONITORING DATA

4.8.1 PROBABILISTIC DNSE WITH REAL LOADING DATA

The real loading data of August 2012 were provided by the DNO. Loadings at every bus were recorded once per half an hour from 1st August to 1st September. There are 1490 time points in total. Because the data were read from the transformers, once a

transformer is disconnected, the loading at the downstream bus is marked as zero, although it may be connected to other upstream buses via other transformer paths.

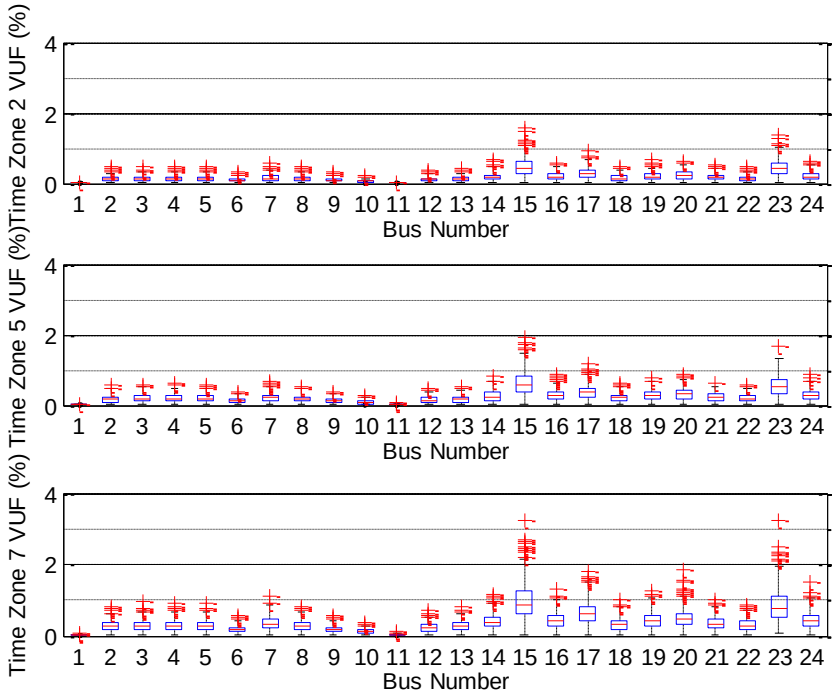

Fig. 4.37 Distributions of VUFs of Time Zone 2, 5 and 7 with connected wind turbine.

By adjusting all the loads according to Table 4.16, the VUF values for all buses for the whole month are shown in Fig. 4.38. From the figure, the peak and bottom of each day can be easily distinguished and it is clear that unbalance at weekends is lower than that of weekdays, as the overall loading decreases and people's activities change. The top three curves are plotted separately in Fig. 4.39.

Table 4.16 Unbalance Setting for All Loads

Phase	Scaling Factor to Active Power	Power Factor
A	1.1	0.97
B	0.95	0.97
C	0.95	0.97

By analysing the figure, it can be seen that the VUF at bus 15 and bus 23 exceed 1% for more than 5% of the total period and therefore mitigation may need to be carried out. The VUFs of these buses are more likely to exceed the limit even further during the peak loading period. Fig. 4.40 uses box plot to illustrate the 1490 values for every bus. It shows that bus 15 has about 50% (precisely 52.35%) values larger than 1% VUF and

bus 23 has less than a quarter (precisely 4.16%) values larger than 1%. Some buses, such as bus 20 and 24, have wider ranges of VUFs than others because of the outages of the transformers.

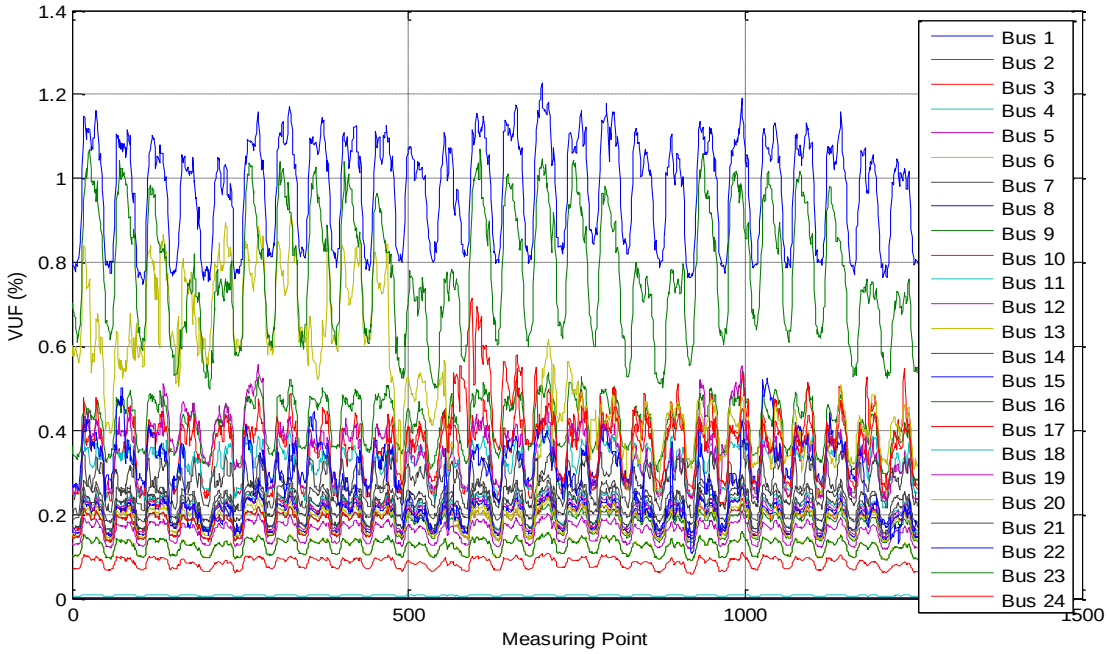

Fig. 4.38 One-month prediction of unbalance using real loading data.

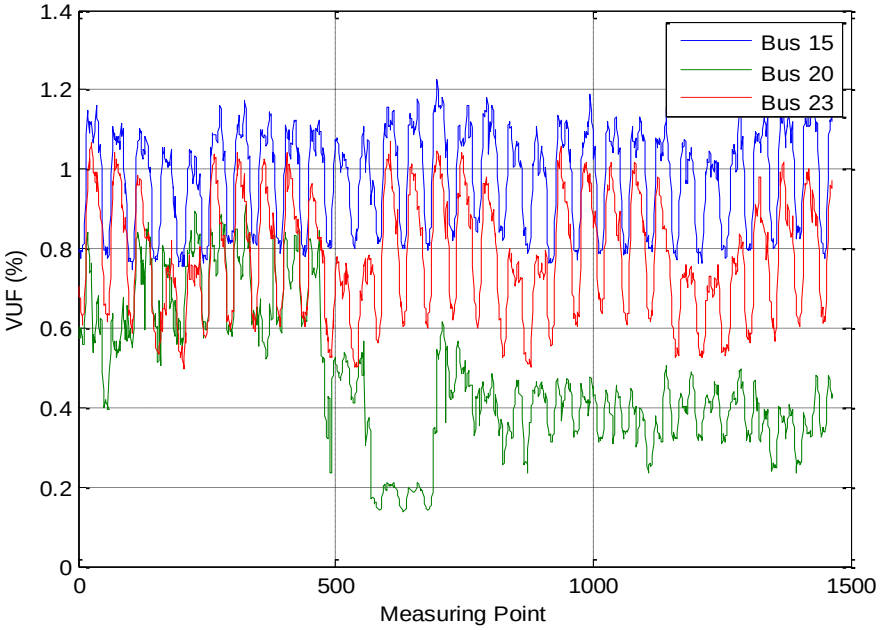

Fig. 4.39 The top three curves of one-month prediction of unbalance using real loading data.

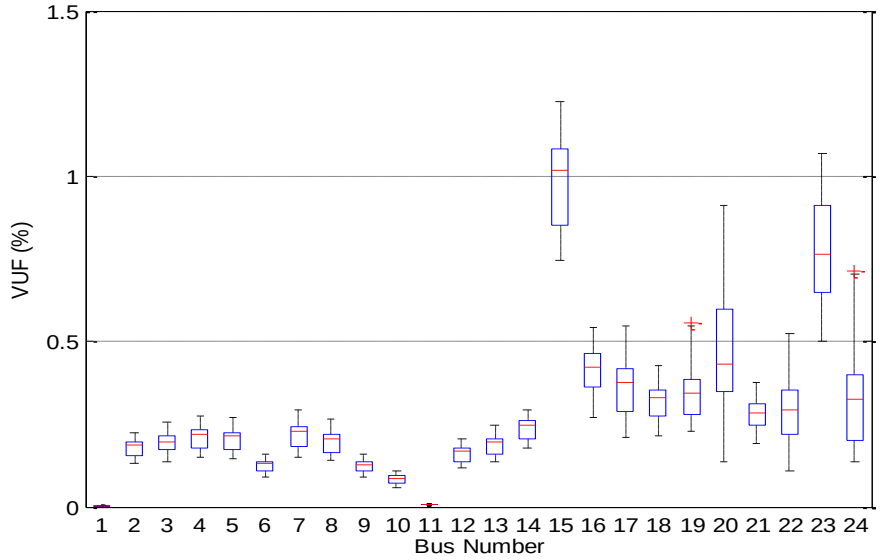

Fig. 4.40 Box plot of one-month prediction of unbalance using real loading data for all buses.

4.8.2 Comparison of DNSE Results with Real Monitoring Data

The distribution network is monitored using "EMS sub.net" monitors. This type of monitor records P, Q, $|S|$, $|V|$and$|I|$ of all three phases [160]. Because the monitor only records three-phase magnitudes of voltages and lacks angular information, the phase shifts between each two phases in the study are set to be equal. The monitors are installed at the transformers so that voltages of both the primary side and the secondary side are recorded. The voltage profile is read once every ten minutes. The VUFs of available buses are plotted in Fig. 4.41. The estimations of VUFs of the same buses using the real loading data (the simulation in previous section) are plotted in Fig. 4.42. Both groups of data are discontinuous because of the outage of the transformer or the breakdown of information delivery. The simulated results using real loading data broadly match the real monitored results without considerations of any faults or disruptions. It can be seen from Fig. 4.42 that even when bus 24 is unloaded, there are still VUF values at this bus because of the propagation of unbalance from its upstream bus.

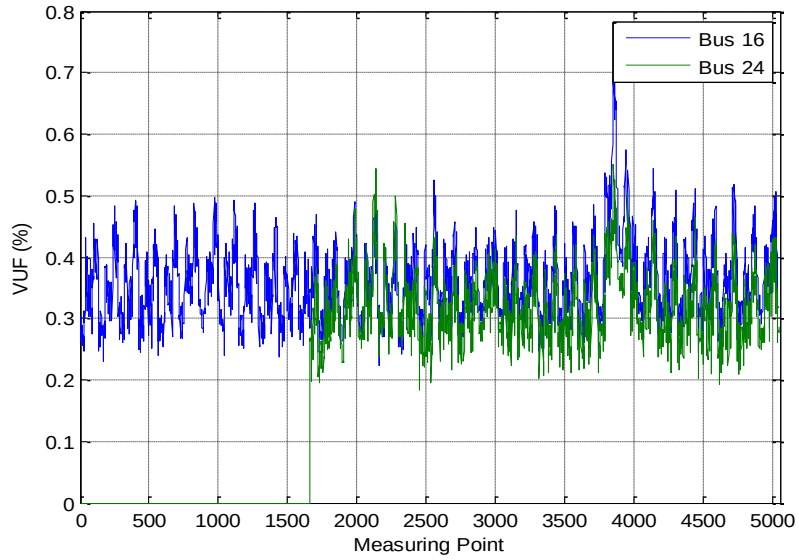

Fig. 4.41 Real one-month monitoring data for bus 16 and 24.

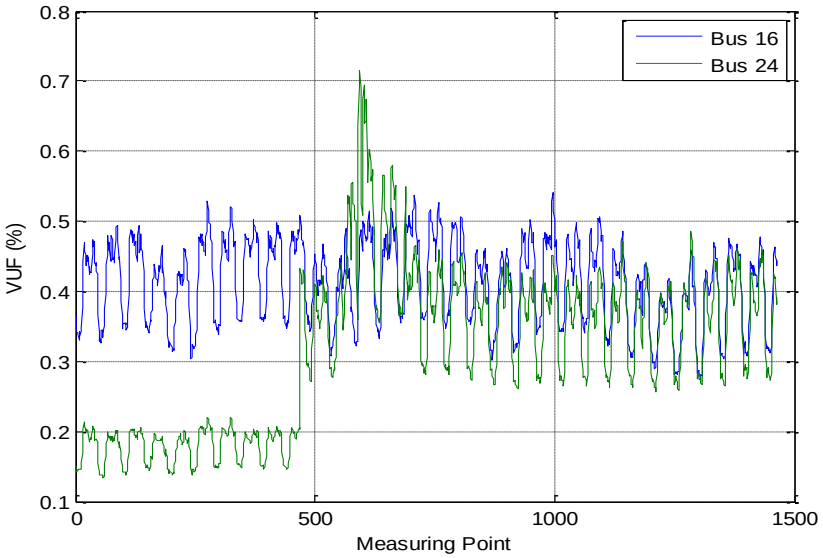

Fig. 4.42 One-month estimation using real loading data for bus 16 and 24.

Therefore, based on the results of simulation of real loading data, DNSE provides the possible ranges of unbalance for every bus. Fig. 4.43 shows a one-day simulation using the real loading data of 17th August, 2012. The two blue lines in each sub-figure indicate the estimated range building on the load flow results and the two red lines in the sub-figures of bus 16 and 24 are the actual monitoring data for the same day.

It can be seen that the actual levels of unbalance locate within the estimated range with a few exceptions at bus 16. This demonstrates that by using the developed DNSE,

(when the monitoring data are not available,) the possible level of unbalance can be estimated based on the real loading data.

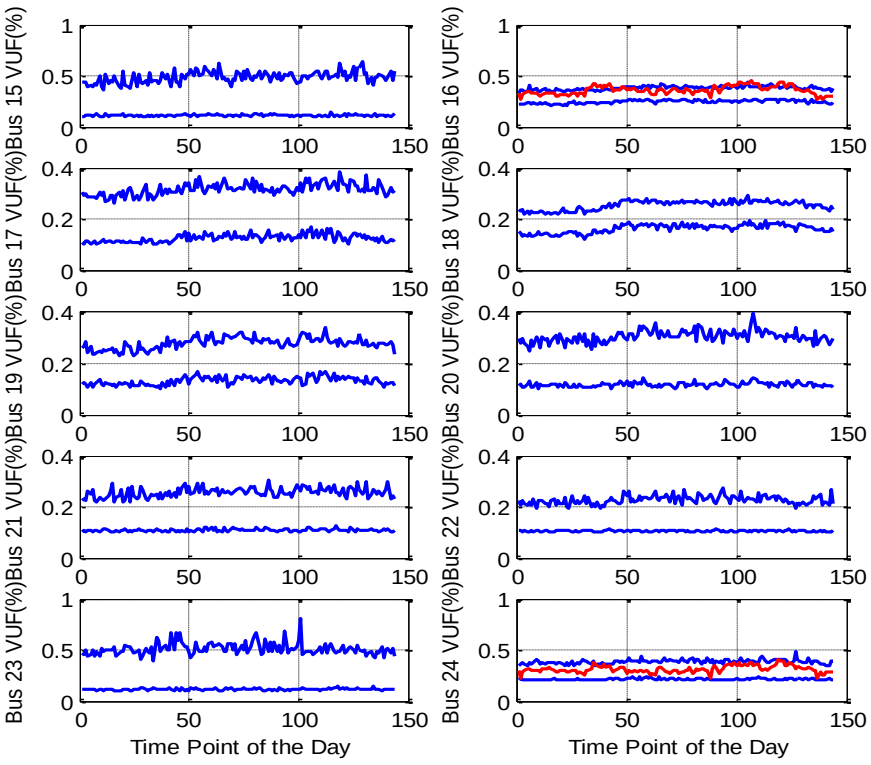

Fig. 4.43 One-day estimation of unbalance based on real loading data, with real monitoring data indicated at bus 16 and 24.

4.9 SUMMARY

Either real power or reactive power, or both of them, of a single-phase load could be varied to create variable power factor and consequently simulate required unbalance at the source. In all cases the care must be taken to avoid using unrealistic values of real power in order to generate required power factor variation. It is demonstrated that the largest VUF at the source can be simulated by varying reactive power and keeping active power constant. In real networks though, the selection of the most suitable method for simulating unbalanced source will depend on the available information about the load at the bus of interest providing that there is no software imposed restriction.

The chapter focused on illustrating application of the developed probabilistic approach to model voltage unbalance and to study unbalance propagation in real distribution network. It demonstrated that the methodology can be used to realistically assess expected level of voltage unbalance in the network by considering different loading conditions, composition of different classes of loads and uncertain sources of unbalance simultaneously. The studies carried out on the real 24-bus distribution network using single class load show that the VUFs at some buses in the network can be greater than standard defined thresholds of 2% for 95^{th} percentile or 4% for maximum value, during certain loading conditions. The highest increase of VUF (excluding the source of unbalance) was observed at the bus adjacent to the source of unbalance. The results of the study using mixed loads correspond to the real monitored VUFs.

The contributions of individual sources of unbalance can be summed up algebraically or vectorially (more accurate assessment) in order to assess the total level of unbalance at any bus in the network. The summation of sequence voltages provides similar results and can be used with available data. Once the unbalance at a bus is detected, either from statistical data or from the results of probabilistic estimation, the methodology can be used to assess the individual contribution of each load to overall unbalance at any given bus in the network.

The presence of induction motors can mitigate the unbalance by about 40%, according to specified assumption. Three-phase distributed generators such as wind turbine generators, have the similar mitigating effect as induction motors. The attenuation effect of single-phase PVs is dependent on the solar insolation.

The methodology of DNSE demonstrates a framework for performing a three-phase load flow. By identifying network parameters such as line impedance, size of load and transformer impedance, DNSE provides the possible state of the power system. The

proposed probabilistic framework enables DNOs to estimate and predict the degree of unbalance in the network at any given time, even when the monitoring data is not available, and as such facilitates network planning and preventive unbalance mitigation.

5 UNBALANCE DUE TO ASYMMETRICAL LINE

5.1 INTRODUCTION

Under the same manufacturers' instructions, inductances and capacitances of the three phases of a transmission line are identical. Therefore, the source of unbalance of a line is the mutual coupling impedances between phases [96] which depend on the physical spacing of three phases on the towers. This non-equilateral spacing causes unequal voltage drops among three phases along the line and interchanging powers between phases, which results in an unbalanced voltage at the end of the line [161]. In other words, the differences in the mutual coupling impedances between any two of the three phases are the decisive factor of stimulating unbalance, rather than the phase impedance or equal mutual coupling impedances. As seen from the network data given by DNO and by the IEEE example networks, the mutual coupling impedance is usually half of the phase impedance and results in a smaller deviation than the phase impedance when calculating the load flow.

To troubleshoot the unbalance problem due to uneven voltage drops along the line, transposition provides the solution. Transposition denotes the position exchange of phase conductors at regular intervals along the line [161]. In this way, each conductor is located in the original positions of all three phases at different sections over equal distances.

In practice, the line is transposed by dividing it into 3 equal sections, where each conductor occupies a position for one third of the total length. For example, Fig. 5.1 (adopted from [162]) shows one approach of transposition. In the first section of the line, Position #1 for phase *A* is employed. When it comes to the middle section of the line, the position of phase *A* is changed to Position #2. Then Position #3 occupies the last 1/3 section of the line.

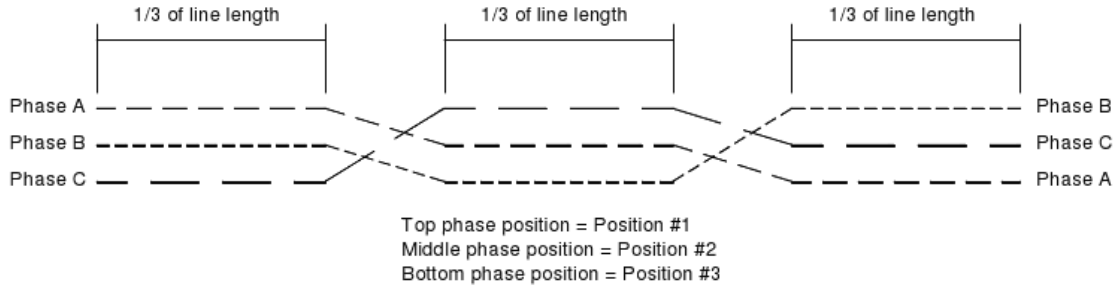

Fig. 5.1 Graphical representation of transposition (adopted from [162]).

By changing the position of the conductors of different phases, the reactances of all phases are balanced, leading to even voltage drops of three phases along the line. The mutual coupling impedances are made equal after transposition. This eliminates the unbalance at the end of the line.

In Russia, the lengths of transposition cycles for horizontal-allocated lines and triangle-allocated lines (referring to different tower designs) should be no more than 24 km and 48 km respectively [163]. In [164], the transposition is said to be on lines longer than 100 km at voltages over 110 kV. A length of not more than 300km should be covered

by a complete phase transposition cycle. The lines in distribution networks are actually shorter than the specified distances. No manufacturing requirements were found for the UK. As reported by the DNO, they do not transpose the lines.

According to the report of UK's Stakeholder Advisory Group on ELF EMFs (SAGE, organized by National Grid) [165], for 132 kV lines, between 70% and 90% of double-circuit lines (occupying between 70% and 90% of all lines) are already transposed. Within the remaining 132 kV lines, there are lines (estimated as 12% of the lines in quantity and around 2000 km in length) that are not transposed but reasonably could be [165]. The data for voltage levels below 132kV are not mentioned.

In distribution networks, the lines are short in length compared to the lines in transmission networks and are usually non-transposed or partially transposed. The impact of the lines on unbalance has not been systematically analyzed with respect to the unbalance caused by loads. If the unbalance stays below the statutory limit with asymmetrical lines in distribution networks, there may be no necessity for transposition.

5.2 Transformation of Line Admittance Matrix (Y)

5.2.1 Theoretical Line Model

The lines are computed in the load flow using the equivalent π model, as described in Chapter 2.2.2. In reality, the phase impedances and mutual coupling impedances are determined by the material and physical structure.

In transmission networks, the transmission lines are fully transposed and hence eliminate the mutual coupling impedance. In previous research on voltage unbalance in Chapters 2, 3 and 4, the asymmetry of transmission line has not been taken into account.

Without considering the asymmetry of transmission lines, the $\boldsymbol{Z_L}$ matrix is presumed to have equal off-diagonal elements.

However, in practice, due to the existence of non-transposed lines and partially transposed lines, lines are widely composed of phase impedances and unequal mutual coupling impedances and. In order to study the influence of asymmetrical lines, the values of off-diagonal elements need to be defined.

For the line impedance matrix $\boldsymbol{Z_L}$, initially, it can be assumed that all the phase impedances of single phases are identical to each other, and so are the mutual coupling impedances between any two phases. In terms of the three phases, the impedance matrix of a line is:

$$\boldsymbol{Z_L} = \begin{bmatrix} Z_s & Z_m & Z_m \\ Z_m & Z_s & Z_m \\ Z_m & Z_m & Z_s \end{bmatrix} \tag{5.1}$$

where Z_s is the phase impedance of the line and Z_m is the mutual coupling impedance between phases.

The voltage drops in both time domain and sequence domain along the line are:

$$\begin{bmatrix} \Delta V_a \\ \Delta V_b \\ \Delta V_c \end{bmatrix} = \begin{bmatrix} Z_s & Z_m & Z_m \\ Z_m & Z_s & Z_m \\ Z_m & Z_m & Z_s \end{bmatrix} \begin{bmatrix} I_a \\ I_b \\ I_c \end{bmatrix} \tag{5.2}$$

$$\begin{bmatrix} \Delta V_0 \\ \Delta V_1 \\ \Delta V_2 \end{bmatrix} = \begin{bmatrix} Z_0 & & \\ & Z_1 & \\ & & Z_2 \end{bmatrix} \begin{bmatrix} I_0 \\ I_1 \\ I_2 \end{bmatrix} \tag{5.3}$$

Because the provided line data are given in terms of the impedances in the sequence domain, the relationship between the time domain impedance and the sequence domain impedance should be studied. The transformation between the time domain components and the sequence domain components is given by (1.1) and repeated here as (5.4) to facilitate easy referencing:

$$\begin{bmatrix} V_a \\ V_b \\ V_c \end{bmatrix} = \begin{bmatrix} 1 & 1 & 1 \\ 1 & a^2 & a \\ 1 & a & a^2 \end{bmatrix} \begin{bmatrix} V_0 \\ V_1 \\ V_2 \end{bmatrix} = \boldsymbol{A} \begin{bmatrix} V_0 \\ V_1 \\ V_2 \end{bmatrix} \tag{5.4}$$

where $a=e^{j120°}$.

In (5.4), the voltage symbol "*V*" can be directly replaced by the current symbol "*I*".

By using the transformation of sequence domain elements of (5.4) to substitute the time domain components in (5.2), (5.5) to (5.7) can be derived:

$$\boldsymbol{A} \begin{bmatrix} \Delta V_0 \\ \Delta V_1 \\ \Delta V_2 \end{bmatrix} = \left\{ \begin{bmatrix} Z_s - Z_m & & \\ & Z_s - Z_m & \\ & & Z_s - Z_m \end{bmatrix} + \begin{bmatrix} Z_m & Z_m & Z_m \\ Z_m & Z_m & Z_m \\ Z_m & Z_m & Z_m \end{bmatrix} \right\} \boldsymbol{A} \begin{bmatrix} I_0 \\ I_1 \\ I_2 \end{bmatrix} \tag{5.5}$$

$$\begin{bmatrix} \Delta V_0 \\ \Delta V_1 \\ \Delta V_2 \end{bmatrix} = \boldsymbol{A^{-1}} \left\{ (Z_s - Z_m) \begin{bmatrix} 1 & & \\ & 1 & \\ & & 1 \end{bmatrix} + Z_m \begin{bmatrix} 1 & 1 & 1 \\ 1 & 1 & 1 \\ 1 & 1 & 1 \end{bmatrix} \right\} \boldsymbol{A} \begin{bmatrix} I_0 \\ I_1 \\ I_2 \end{bmatrix} \tag{5.6}$$

$$\begin{bmatrix} \Delta V_0 \\ \Delta V_1 \\ \Delta V_2 \end{bmatrix} = \begin{bmatrix} Z_s + 2Z_m & & \\ & Z_s - Z_m & \\ & & Z_s - Z_m \end{bmatrix} \begin{bmatrix} I_0 \\ I_1 \\ I_2 \end{bmatrix} \tag{5.7}$$

By comparing the impedance matrices in (5.7) and (5.3), (5.8) can be obtained:

$$\begin{cases} Z_0 = Z_s + 2Z_m \\ Z_1 = Z_s - Z_m \\ Z_2 = Z_s - Z_m \end{cases} \tag{5.8}$$

Finally, the mutual coupling impedances are derived and prepared for load flow calculations.

The data for Z_0 and Z_1 are provided by DNO, benefiting the computation of Z_s and Z_m:

$$\begin{cases} Z_s = (Z_0 + 2Z_1)/3 \\ Z_m = (Z_0 - Z_1)/3 \end{cases} \tag{5.9}$$

When running a load flow, the impedance matrix must be transformed into an admittance matrix, which is actually employed. The admittance matrix is [46]:

$$\boldsymbol{Y_L} = \boldsymbol{Z_L}^{-1} = G + \mathrm{j}B \tag{5.10}$$

5.2.2 LINE MODEL IN PROGRAMMING

The provided line data are the sequence impedances. Therefore, in programming, the line admittance matrix of the time domain should be converted from the sequence domain impedance matrix. After identifying the values of Z_0 and Z_1 for the line (Z_2 is always the same as Z_1), the sequence domain impedance matrix is derived:

$$\boldsymbol{Z_{012}} = \begin{bmatrix} Z_0 & & \\ & Z_1 & \\ & & Z_2 \end{bmatrix} \tag{5.11}$$

Using the relationship in (5.3) and (5.4) to substitute the values in (5.2), (5.12) and (5.13) can be obtained:

$$\boldsymbol{A^{-1}} \begin{bmatrix} \Delta V_a \\ \Delta V_b \\ \Delta V_c \end{bmatrix} = \begin{bmatrix} Z_0 & & \\ & Z_1 & \\ & & Z_2 \end{bmatrix} \boldsymbol{A^{-1}} \begin{bmatrix} I_a \\ I_b \\ I_c \end{bmatrix} \tag{5.12}$$

$$\begin{bmatrix} \Delta V_a \\ \Delta V_b \\ \Delta V_c \end{bmatrix} = \boldsymbol{A} \begin{bmatrix} Z_0 & & \\ & Z_1 & \\ & & Z_2 \end{bmatrix} \boldsymbol{A^{-1}} \begin{bmatrix} I_a \\ I_b \\ I_c \end{bmatrix} \tag{5.13}$$

By comparing the impedance matrices in (5.12) and (5.2), there is the transformation between the sequence domain impedance matrix and the time domain impedance matrix:

$$\boldsymbol{Z_L} = \boldsymbol{A Z_{012} A^{-1}} \tag{5.14}$$

By obtaining $\boldsymbol{Z_L}$, the time domain admittance matrix which is required in load flow programming can be computed using (5.10).

5.2.3 DIFFERENCE BETWEEN BALANCED LINE AND UNBALANCED LINE IN Y MATRIX

Acquiring the values of Z_0 and Z_1, the values of Y_0 and Y_1 can be calculated:

$$\begin{cases} Y_0 = \dfrac{1}{Z_0} = \dfrac{1}{Z_s + 2Z_m} \\ Y_1 = \dfrac{1}{Z_1} = \dfrac{1}{Z_s - Z_m} \end{cases} \tag{5.15}$$

The negative sequence impedance or admittance is always the same as the corresponding positive one.

By using the relationship $\boldsymbol{I}=\boldsymbol{YV}$ and the similar process as in Section 3.2.2, the transformation between admittance matrices is given by:

$$\boldsymbol{Y_L} = \boldsymbol{A}\boldsymbol{Y_{012}}\boldsymbol{A^{-1}} \tag{5.16}$$

$$\boldsymbol{Y_L} = \begin{bmatrix} Y_0 + Y_1 + Y_2 & Y_0 + aY_1 + a^2Y_2 & Y_0 + a^2Y_1 + aY_2 \\ Y_0 + a^2Y_1 + aY_2 & Y_0 + Y_1 + Y_2 & Y_0 + aY_1 + a^2Y_2 \\ Y_0 + aY_1 + a^2Y_2 & Y_0 + a^2Y_1 + aY_2 & Y_0 + Y_1 + Y_2 \end{bmatrix} \tag{5.17}$$

Substituting (5.17) by using the values in (5.15), the first element of $\boldsymbol{Y_L}$, which corresponds to Y_s, becomes:

$$Y_s = \frac{Z_s + Z_m}{(Z_s + 2Z_m)(Z_s - Z_m)} \tag{5.18}$$

The admittance is decided by not only the phase impedance, but also the mutual coupling impedances between phases. In distribution systems, lines, especially underground cables, are not fully transposed. In addition to the load which can be a source of unbalance, the non-transposed or partially transposed line forms another source of unbalance that creates and spreads unbalance inside the network. Hence, being the potential source of unbalance, the Z_m components should not be neglected when aiming at high accuracy of results. However, as the variation in mutual coupling impedance is rarely recorded and the involvement of asymmetrical lines increases the complexity of the methodology for the estimation of unbalance, the impact of the unbalanced lines and a tolerance range for justifying the emission of the influence of unbalanced lines must be established.

5.2.4 INFLUENCE OF LINE IMPEDANCE ON LOAD FLOW CALCULATION

As described in Chapter 2.4.1, three-phase full Newton-Raphson load flow is employed in this research, which takes both the phase impedance and mutual coupling impedance of a line into account.

Following the determination of admittance matrices for lines, the rectangular form (G+jB) of the impedances of lines is used in the three-phase load flow. In the partial differential equations for creating Jacobian matrices, G and B are unchanged. Therefore, being pure coefficients of the equations, the bigger they are, the bigger is the determinant modulus of the resultant Jacobian matrix and the smaller is the determinant modulus of the inverse Jacobian matrix. For example, if the $\boldsymbol{Y}$ matrix is half the initial line admittance matrix, the Jacobian matrix doubles the previous one obtained using an initial line admittance matrix, and the inverse Jacobian matrix is half the previous inverse Jacobian matrix. The correlation of changes between the admittance matrix and the resulting inverse Jacobian matrix is linear.

Consequently, the admittance matrix, the inverse Jacobian matrix and the deviation from the starting point are in linear relationship. The small line impedance leads to smaller discrepancies between phases, hence achieving a more balanced condition. By reducing the impedance of the line, the unbalance in the system, whatever the source of unbalance is, can be mitigated.

5.3 IMPACT OF SIZE OF LINE IMPEDANCE

The example of the impact of impedance size is illustrated using the 4-bus radial network in Fig. 5.2. The network is composed of one power supply, four buses, three identical transmission lines and three identical loads (see Fig. 2.5).

In this study, it is assumed that all the transmission lines are balanced without any unequal phase coupling. The power flow is calculated based on constant power loads. Among the three loads, only the load at bus 3 (middle one) is adjusted to an unbalanced condition, with the load (both active and reactive powers) of phase *A* multiplied by 1.5. The loads at bus 2 and bus 4 remain balanced. This means that the only unbalance source in the network is the load at bus 3. As a result, the positive sequence impedances and zero sequence impedances of all the three lines are multiplied by a weighting factor each time. The weighting factor varies from 0.1 to 1, with an increment of 0.1.

Therefore, after ten load flows with different line impedances, the VUF curves against the p.u. line impedance can be plotted as shown in Fig. 5.2.

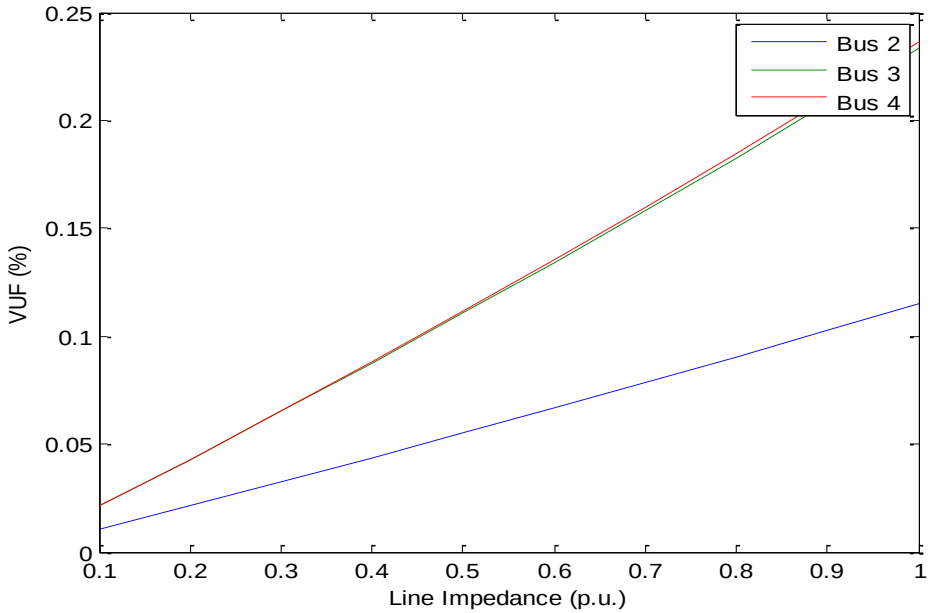

Fig. 5.2 VUF against different line impedance.

It can be seen from the figure that the relationship between VUF and the size of line impedance is nearly linear. The VUFs at bus 3 and bus 4 are almost the same values while the VUF of bus 2 is half of them. The reason is that, the line impedance between bus 1 and bus 2 is half that between bus 1 and bus 3, so the resultant VUF at bus 2 is half the VUF at bus 3.

In contrast, the line impedance between bus 1 and bus 4 is 1.5 times that between bus 1 and bus 3, which does not have significant impact on the VUFs of the two buses. This indicates the VUF is also determined by the location of the source of unbalance. The VUFs at bus 3 and bus 4 are not strictly the same. The reason can be revealed by plotting individual sequence voltage curves.

The three sequence voltages of the three loaded buses are plotted in Fig. 5.3. When investigating the sequence voltages of a balanced network, the voltage changes according to the change of line impedance. The positive sequence voltage experiences voltage drops due to the line loss which is linear to the increase of the line impedance. The magnitudes of positive sequence voltages of the three buses for any value of line impedance are in fixed proportions to each other, but not double or triple each other. This can be explained using an equivalent circuit (see Fig. 5.4).

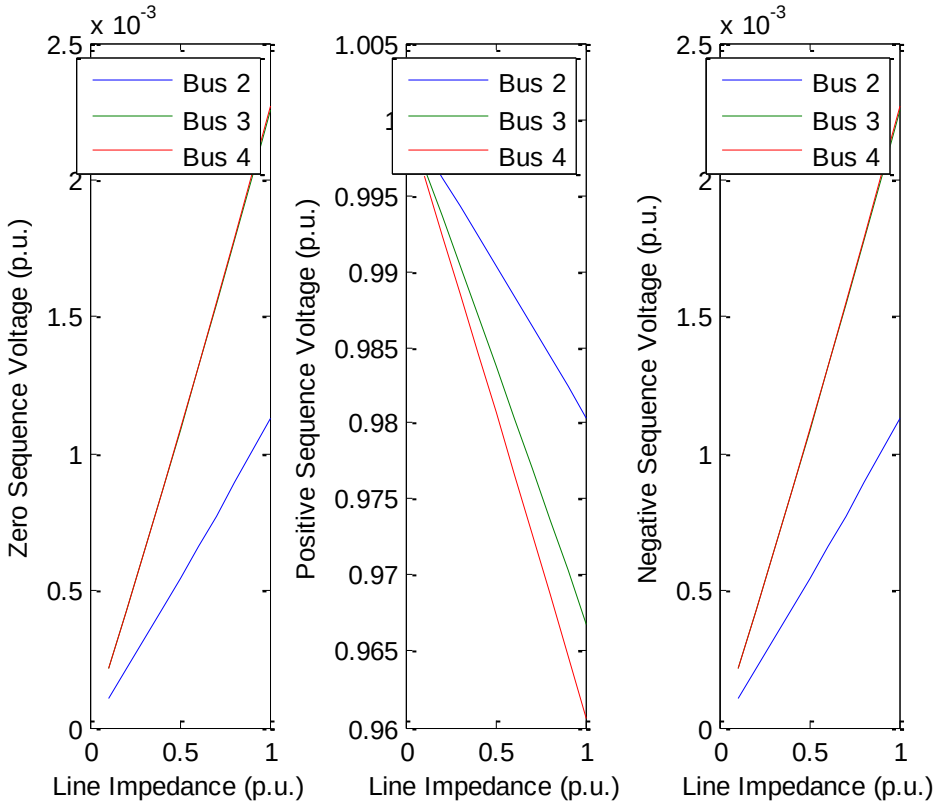

Fig. 5.3 Sequence voltages of three buses.

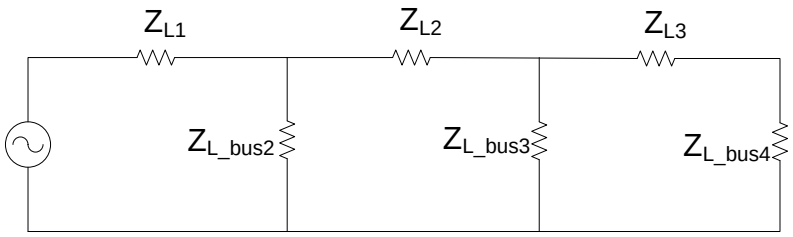

Fig. 5.4 Equivalent circuit of 4- bus network in impedance form.

In the equivalent circuit, every line or load is represented using an impedance symbol. The voltage distribution on the six equivalent impedances is fixed. Owing to the parallel impedances, the voltage distribution on the three loads does not represent integral multiple relationships. In reality, the loads are much bigger than the line impedances, resulting in over 0.9 per unit voltage consumed by the loads.

Under a balanced condition, there is no sequence coupling; hence no zero sequence voltage or negative sequence voltage exists. When the network is operating under an unbalanced condition, zero sequence power injection and negative sequence power injection appear due to the sequence coupling impedances. These two sequence voltages at bus 3 are double those at bus 2 due to the mitigation of the balanced power supply at bus 2. But the voltages at bus 4 show the same magnitude as the voltages at bus 3 without mitigation.

Regarding the propagation of unbalance, if one unbalance source exists in the network, the unbalance will spread to the whole network. Assuming the power supply remains balanced all the time, the unbalance propagating upwards is eliminated by the balanced generation. Therefore, the VUF along the line between the power supply and the unbalance source is reduced with respect to the total line impedance between the power supply and measuring point. When the unbalance propagates to downstream buses, with unchanged negative sequence voltage and dropping positive sequence voltage, the VUF will increase slightly.

It can be concluded that when the line impedance between the balanced power supply and an unbalance source decreases, the VUF of the network is diminished. Therefore, one effective method for mitigating the unbalance is to reduce the line impedance in real networks. Because the total lengths of lines in real networks are fixed, the way to reduce line impedance is to use lines with low impedance, replace the old lines, or in extreme cases add additional line in parallel to the existing one.

5.4 IMPACT OF ASYMMETRICAL LINE

The phase impedance and mutual impedance of lines are determined by the physical construction and spacing on the tower [96]. In this way, the phase impedances of three phases are considered as identical and the source of line asymmetry is the mutual coupling impedances between phases. To study the impact of line asymmetry, when the lines are unbalanced, the 24-bus network is used and the following assumptions are made:

- The power supply is always balanced.
- All the loads at all buses are evenly distributed among three phases. All the loads maintain initial values without any adjustment. The loads may be adjusted to an unbalanced condition if required.
- If there are transformers, they are delta-earthed-star, blocking the flow of zero sequence current. Transformer impedances do not have phase coupling.
- The whole system is assumed as fully observable without measurement errors.

Therefore, the only unbalance source in the network is the line. With mutual coupling impedances of the line, the induced sequence coupling impedance is believed to introduce negative sequence and zero sequence power flow which generates unbalance within the system and delivers unbalanced power to customers.

5.4.1 RESULTS OF SIMULATIONS WITH ASYMMETRICAL LINE

Three cases will be compared: unbalance due to line asymmetry, unbalance due to load asymmetry and unbalance due to both line asymmetry and load asymmetry.

In the line asymmetry case, it is assumed that the two mutual impedances out of three of all lines are increased or decreased by the same percentage with the third one staying constant. The percentage is set at 4% in this simulation (see Section 5.4.2 for justification of this assumption). Employing the 24-bus network, under this condition, the VUFs of all buses are shown in Fig. 5.5. Maximum VUF=0.22% is calculated at bus 15.

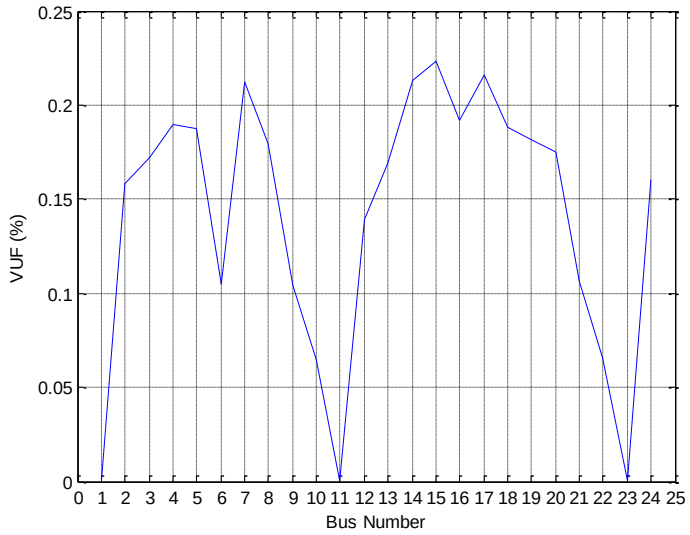

Fig. 5.5 VUFs of 24 buses when lines are unbalanced.

When the loads are all balanced, the levels of VUF are no longer related to the size of load. The buses near the balanced power supply usually do not have any unbalance. However, with increasing distance from the power supply, the unbalance significantly increases. Although bus 2 is not far from the power supply area, because it is connected to multiple lines, there is an aggregated impact of the lines on the VUF of bus 2.

Fig. 5.6 shows the results of unbalanced load and balanced lines. In this simulation, for all loads, the active power and reactive power consumed in phase *A* are assumed to be 115% of the initial loading and the powers in phase *B* and *C* are 92.5% of the initial

loading; therefore the three-phase total loading remains unchanged. As the sources of unbalance are the loads, the 11kV buses have larger VUFs than the 33kV buses and the resultant VUF is proportional to the sizes of the loads. Maximum VUF=0.9% is calculated at bus 15.

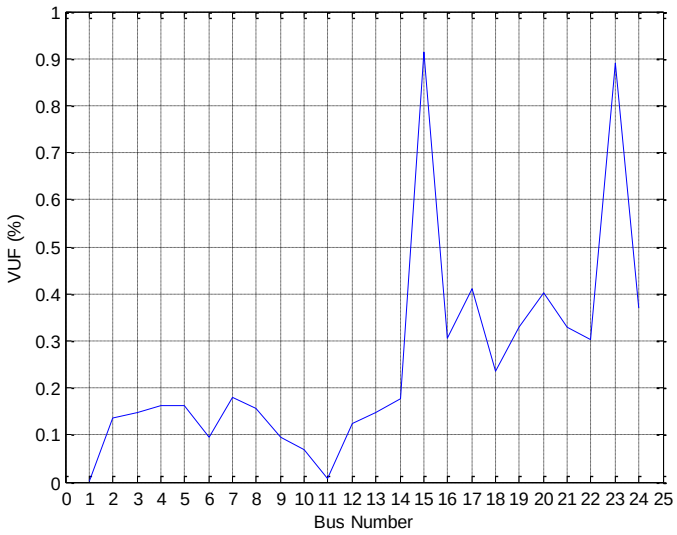

Fig. 5.6 VUFs of 24 buses when loads are unbalanced.

The third case considers the unbalanced line and unbalanced load simultaneously. The results are shown in Fig. 5.7 and the comparison of the three cases is shown in Table 5.1. The term "Difference" in Table 5.1 is calculated as (5.19).

$$Difference\ (\%) = \left| \frac{VUF_{Line\&Load} - VUF_{Line} - VUF_{Load}}{VUF_{Line\&Load}} \right| \times 100\% \tag{5.19}$$

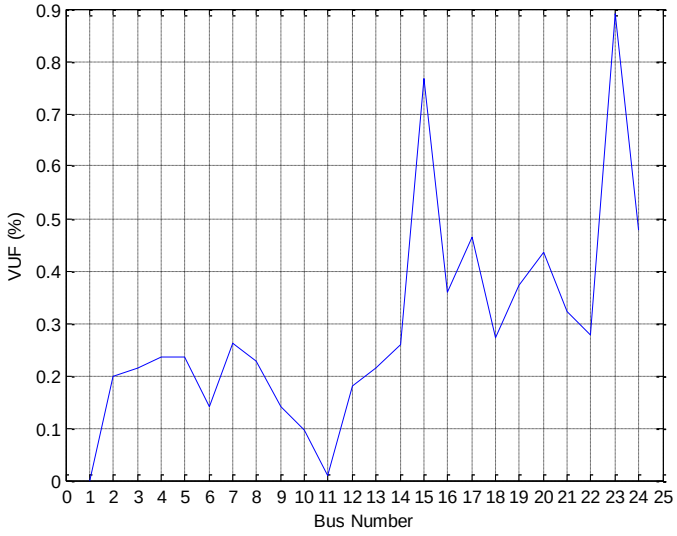

Fig. 5.7 VUFs of 24 buses when both lines and loads are unbalanced.

Table 5.1 VUFs due to Unbalanced Line, Unbalanced Load and both Unbalanced Line and Load.

Bus Number	VUF (%)				Difference
	VUF_{Line}	VUF_{Load}	$VUF_{Line\&Load}$	$VUF_{Line}+VUF_{Load}$	
1	0.0000	0.0000	0.0000	0.0000	0.00%
2	0.1585	0.1359	0.1986	0.2944	48.21%
3	0.1723	0.1477	0.2151	0.3200	48.75%
4	0.1901	0.1621	0.2356	0.3522	49.47%
5	0.1874	0.1616	0.2346	0.3490	48.76%
6	0.1051	0.0964	0.1414	0.2015	42.51%
7	0.2123	0.1808	0.2618	0.3931	50.16%
8	0.1795	0.1573	0.2273	0.3368	48.15%
9	0.1038	0.0956	0.1401	0.1994	42.36%
10	0.0648	0.0676	0.0964	0.1324	37.31%
11	0.0000	0.0087	0.0087	0.0087	0.00%
12	0.1391	0.1230	0.1811	0.2621	44.72%
13	0.1695	0.1486	0.2156	0.3181	47.56%
14	0.2132	0.1755	0.2580	0.3887	50.65%
15	0.2231	0.9149	0.7678	1.1380	48.21%
16	0.1920	0.3067	0.3581	0.4987	39.28%
17	0.2157	0.4122	0.4635	0.6279	35.46%
18	0.1884	0.2341	0.2734	0.4225	54.55%
19	0.1814	0.3281	0.3733	0.5095	36.49%
20	0.1749	0.4020	0.4362	0.5769	32.24%
21	0.1066	0.3297	0.3222	0.4363	35.41%
22	0.0656	0.3017	0.2782	0.3673	32.02%
23	0.0000	0.8907	0.8907	0.8907	0.00%
24	0.1608	0.3703	0.4770	0.5311	11.33%
Average	0.1418	0.2563	0.2939	0.3981	36.82%

It can be seen from the table that the VUF that resulted from the lines and the VUF that resulted from the loads superpose. However, regarding the superposition, whether it aggravates or mitigates the unbalance caused by the load, is not guaranteed and is related to the geographical location of the buses, which will be discussed in the following section. There is a certain extent of cancellation in the superposition, because the VUF caused by lines and loads simultaneously is always smaller than the sum of individual VUFs caused by lines or loads separately.

5.4.2 BOUNDARY OF SEQUENCE IMPEDANCES OF THE LINE

Because unbalanced lines introduce unbalance to the network together with unbalanced load, it is important to find the critical value of line impedance that starts to have a significant impact on the level of unbalance of the system.

An issue which presents difficulty in modelling the asymmetrical lines is that the asymmetry in the mutual coupling impedances in real networks is rarely recorded, so there is a lack of data in this respect. Due to the missing information, the degree of unbalance that the line asymmetry can introduce is uncertain and difficult to verify. To investigate the impact of an asymmetrical line, assumptions are made about the mutual coupling impedances.

Fig. 5.8 shows the increase in VUF with respect to the variation of the mutual impedance with fixed unbalanced load. Two mutual impedances of all the lines in the network are increased or decreased by a same percentage while the third one stays constant. The influence of the untransposed lines increases with increasing discrepancy between mutual impedances.

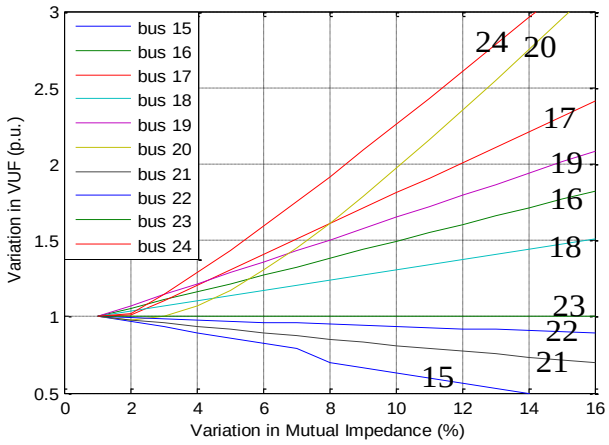

Fig. 5.8 Increase of VUF due to increasing unbalance in the mutual coupling impedances of the line.

It can be seen that the buses near the balanced power supply area (bus 1, 11 and 23) are less affected by line asymmetry. The VUFs of neighbouring buses behave similarly while the performances of the buses far away from the balanced supply point cannot be

predicted as it is consequence of combination of the influence of line asymmetry and unbalanced loads. It can be seen from the figure that as long as discrepancy in mutual impedances is <4%, the VUF will not vary more than ±15% of the initial VUF for majority of the buses (maximum observed increase/decrease is about +25% and -10%, respectively) and that the impact of unbalanced lines on VUF can be ignored to a large extent. Note that this figure is only valid with the proposed load asymmetry. If the unbalance caused by load is smaller, the impact of line asymmetry will be more severe.

The mutual impedance of a line in distribution network can be approximately calculated by (5.20) [166]:

$$Z_{pm} = 0.0953 + j0.12134 \times (\ln \frac{1}{D_{pm}} + 7.93402) \frac{\Omega}{mile} \tag{5.20}$$

where Z_{pm} and D_{pm} are the impedance and spacing distance between phase p and phase m, respectively.

According to British Standard BS162:1961 [167], the minimum clearance between phases for 33kV lines is 0.432m. Due to associated costs, the actual placing distance would not be much larger, if at all, than the minimum required clearance. Assuming that the line is untransposed and that the clearance between the phases is twice the minimum required clearance (very large and highly unlikely to be the case in reality), i.e., 0.864m, the variation in the mutual impedance with respect to the one calculated using minimum clearance is 4.29%. The relationship between the clearance and the variation in the mutual coupling impedance is listed in Table 5.2. Therefore, for standard and typically short distribution lines, the impact of the line asymmetry may be ignored as it will not affect the VUFs due to unbalanced loads at different buses by more than ±25%.

In the remaining chapters where the unbalance due to load asymmetry are investigated, the impact of lines will be neglected.

Table 5.2 Relationship between Clearance and Variation in Mutual Coupling Impedance.

Clearance (m)	Variation in Length with Respect to Initial Clearance	Variation in Mutual Coupling Impedance
0.432	0%	0%
0.518	20%	1.14%
0.605	40%	2.09%
0.691	60%	2.92%
0.778	80%	3.65%
0.864	100%	4.29%

5.5 SUMMARY

Transposition rebalances the mutual coupling impedance between phases of the lines. However, in distribution networks, the lines are not fully transposed. If the impact of transposition can be neglected in the short lines in distribution networks, there is no necessity to transpose lines.

The impedances used to calculate load flow can be obtained from the provided profiles of the lines. When unbalanced loads are the only source of unbalance, the relationship of size of line impedance and the resulting VUF is linear. A large unbalanced load and the consequent propagation through long lines are expected to cause a large unbalance in the network owing to the proportional positive sequence voltage drop. Therefore, reducing the line impedance can effectively reduce unbalance in the network.

Simulations with the 24-bus network show that the unbalance caused by the asymmetry of lines depends on the difference between three-phase mutual coupling impedances. There is no direct correlation between the unbalances caused by the line and load. However, they will add up with a certain degree of cancellation. For the lines at 33kV voltage and below, the unbalance caused by the lines is not likely to result in more than 125% of the initial VUF. Therefore, in an approximate calculation, the influence of lines can be ignored.

6 OPTIMAL MONITOR PLACEMENT FOR MONITORING UNBALANCE

6.1 INTRODUCTION

Being a long term power quality problem, monitoring unbalance requires full observability of the power system. For economic considerations, monitors are not installed at every bus in the network. Where and how many monitors should be installed to estimate the unbalance across the network with the highest degree of accuracy forms the main objective for optimal monitor placement. However, limited research has been done in this area and this chapter aims to fill this gap.

With incomplete monitoring data, DNSE provides the solution for estimating missing values of the whole network. It calculates the possible range and distribution of unbalance at all buses with random errors considering the network topology and parameters of power system equipment. Because the number of actual measurements is usually less than the number of required state estimates, a three-phase state estimator

using a pseudo measurement is employed in this study to enable the real-time detection of unbalance and the long term prediction of unbalance.

By using DNSE, the location of the source of unbalance can be detected and the health status of the network can be obtained. This is particularly relevant to DNOs as maintenance and mitigation can be carried out accordingly to avoid penalties due to breaching standard requirements or customer contract. The state estimation results also demonstrate the accuracy of different monitor sets. By statistically analysing the number and location of monitors, a method for optimal monitor placement can be suggested, aiming at determining minimum number of monitors and minimum economic cost while achieving full observability of the whole network.

6.2 Monitor Used for Monitoring Unbalance

Practical overall monitoring accuracy depends on the installation of monitors, including the accuracy of the monitor itself, the location of the monitor and the coverage of the monitor. The monitors may record some or all of the values: active and reactive power flows (P and Q) at a bus, voltage magnitude and angle ($|V|$ and θ_v) of a bus, and current magnitude and angle ($|I|$ and θ_I) flowing through a bus. The monitors are expected to have full observability of the whole network; however some buses may remain unobservable or have some data missing. The state estimators are designed to complete the dataset of the network under this condition.

6.2.1 Monitored Parameters

There are different types of monitors, covering different ranges of parameters that can be measured. For example, most monitors record single-phase parameters while three-phase monitors observe the values for three phases. Some monitors can only monitor

local data while Phasor Measurement Unit (PMU) records the local voltage and all incoming and outgoing currents to neighbouring buses. Table 6.1 (adopted from [94]) classifies the monitors working in a UK distribution network.

Table 6.1 Monitor Types and Measurements Used in A UK Distribution Network (Adopted from [94])

Point in the Network	**Pervasiveness of Measurements**	**Types of Measurements**	**Voltage Reference and Number**	**Current Measurements and Number**	**No. of Power Measurements**
Primary side of 132kV:XkV Transformer	100%	|S|, |V|, |I|, P* ,Q*	1 mostly line to line (some line to ground)	1 phase (typically yellow)	1 phase
Secondary side of XkV:33kV Transformer	100%	|S|, |V|, |I|, P* ,Q*	1mostly line to line (some line to ground)	1 phase (typically yellow)	1 phase
Secondary side of XkV:11kV Transformer	100%	|S|, |V|, |I|, P* ,Q*	1mostly line to line (some line to ground)	1 phase (typically yellow)	1 phase
Secondary side of XkV:6.6kV Transformer	100%	|S|, |V|, |I|, P* ,Q*	1 mostly line to line (some line to ground)	1 phase (typically yellow)	1 phase
33kV Feeders	100%	|S|, |V|, |I|	1 mostly line to line (some line to ground)	1 phase (typically yellow)	1 phase
11kV Feeders	100%	|S|, |V|, |I|	1mostly line to line (some line to ground)	1 phase (typically yellow)	1 phase
Monitored 33kV and 11kV Feeders	<10% (EMS Sub.net [160])	P, Q, |S|, |V|, |I|	3 line to line or 3 phase to ground	3 phases	3 phases
LV Network	No metering sent back to control centre	Maximum demand indicators are installed on the majority of the LV network transformers. These are periodically read and recorded in central databases by operators.			
Monitored LV Network and Customers Sites	<10% (Ad-hoc Schneider PM710 [168] monitors)	P, Q, |S|, |V|, |I|	3 phase to ground	3 phases	3 phases

6.2.2 ACCURACY AND CLASSES OF MONITORS

There are different types of monitors, covering different ranges of parameters that can be measured. For example, some monitors record single-phase parameters while three-phase monitors measure the values for three phases. Owing to the physical materials

and structure, all monitors have inevitable inherent errors in monitoring data. For the quality of measurements, the errors must be restricted within certain limits. Table 6.2 lists the accuracy of monitors utilized in the UK distribution network, with parameters provided by the manufacturers [149][160][169].

Table 6.2 Measurement Accuracy of Monitor (Adopted from [94])

Meter Name	**Symmetrical Voltage**		**Three-phase Current**	**Three-phase Voltage**	**Power Demand**	
	$\|V\|$	Θ_v	$\|I\|$	$\|V\|$	$\|P\|$	$\|Q\|$
Siemens 9610[149]	0.2% of full scale	0.2% of 2π (±0.004π at 50Hz)	0.1%	0.1%	±0.2%	±0.2%
EMS Sub.net[160]	0.1% of full scale	0.1% of full scale	0.1% of full scale	0.1% of full scale	0.1% of full scale	0.1% of full scale
GE EPM9650[169]	Not quoted	Not quoted	0.025% of full scale	0.01% of full scale	0.04% of full scale	0.04% of full scale

Errors are expected to be as small as possible because the objective of monitoring is to derive online data while assuring the reliability of the data at the same time. If a monitor is installed in a specific bus, the uncertainty in this bus will be reduced and the accuracy will be increased.

6.3 CURRENT MONITORING OF 24 BUS NETWORK

6.3.1 MONITOR LOCATION, MEASUREMENT AND ASSUMPTION

According to DNO, three-phase monitors (EMS Sub.net) are installed at bus 1, 4, 5, 11, 14, 15, 16, 18, 23 and 24. These include five load buses (bus 15, 16, 18, 23 and 24) and their matching upstream buses (bus 14, 4, 5 and 11 respectively) except bus 24. Bus 2 is not monitored while there is a three-phase monitor installed in bus 1. The installed monitors record P, Q, $|S|$, $|V|$ and $|I|$ of all three phases.

In simulation, it is essential to define the error rate for state estimation, which benefits the affirmation of the possible range of level of unbalance. Because all 33 kV buses are unloaded, the net real and reactive power injections in these buses are zero. Therefore the measurements of these buses are assumed to have an absolute standard deviation of 2×10^{-7} [123]. The measurement errors are also assumed to be independent from any other measurements. The off-diagonal elements of covariance matrix are considered as zero. For the non-monitored 11 kV buses (Bus 17, 19, 20, 21 and 22), the standard deviation is 0.07 and the covariance between two buses or two phases is 0.52, derived by calculating the average of correlation coefficients of loads. Detailed parameters can be found in Table 2.1.

6.3.2 Accuracy and Uncertainty of Existing Monitor Set

As long as a monitor is installed at a bus, parameters of the bus including magnitude of voltage and power will be accurately recorded, i.e., the results have very small errors. However, there are errors in non-monitored buses. To assess the accuracy of the used monitor set, two definitions are formulated.

For each load flow, 100 state estimations will be carried out to estimate the possible range of VUF variation. "Uncertainty" is defined as the difference between the true VUF (VUF_{TRUE}) derived from the load flow and the mean value of the 100 loops of state estimation ($VUF_{SE\text{-}MEAN}$). It is shown as (6.1).

$$\text{Uncertainty (\%)} = VUF_{SE\text{-}MEAN} - VUF_{TRUE} \tag{6.1}$$

"Uncertainty" is the value in VUF (%) while "Accuracy" is a value of relative error (%). "Accuracy" is defined as the difference between 1 and the relative error of VUF_{TRUE} and $VUF_{SE\text{-}MEAN}$. It is formulated in (6.2).

$$Accuracy(\%) = 1 - \left| \frac{VUF_{SE\text{-}MEAN} - VUF_{TRUE}}{VUF_{TRUE}} \right| \quad (6.2)$$

The value of uncertainty and accuracy is always ≤100% or 1% according to the respective measuring unit. Their values will be plotted using contour maps for visual representations in the following session.

All the simulations here are carried out using Matlab.

Fig. 6.1 and Fig. 6.2 show the accuracy and uncertainty respectively when there is only one monitor installed at bus 15. The location of the monitor is indicated by red letter "M". There are 3 buses where the accuracy is more than 96.7%: bus 15 (location of the monitor), 1 and 11 (the balanced power supply area). Decreased accuracy is observed at the remaining buses, especially the load buses, where it can be as low as about 20%. Regarding the uncertainty of the contour map, the highest level of uncertainty is observed at bus 23, corresponding to the lowest accuracy at bus 23 in Fig. 6.1. Except for bus 23, the uncertainties at other buses mostly stay below 0.2% in VUF. Although the difference is only around 0.2%, it can lead to misjudgments based on standard defined thresholds.

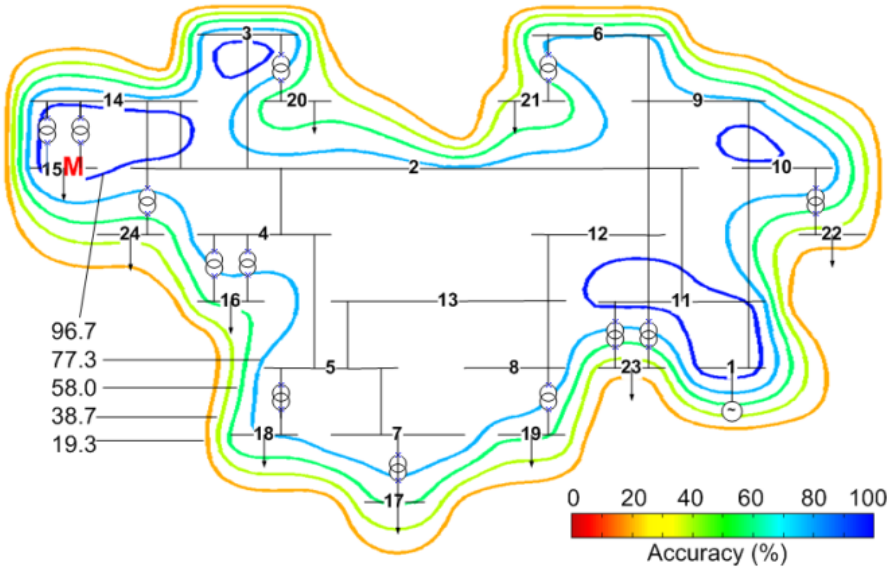

Fig. 6.1 Accuracy of monitoring for all buses with a monitor at bus 15.

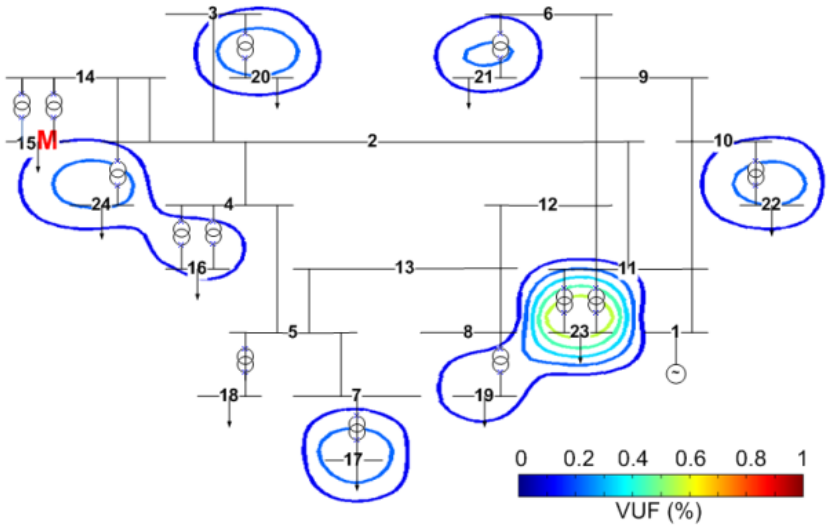

Fig. 6.2 Uncertainty of monitoring for all buses with a monitor at bus 15.

Fig. 6.3 and Fig. 6.4 show the accuracy and uncertainty respectively when there are 9 monitors in the network. All load buses are monitored except bus 19.

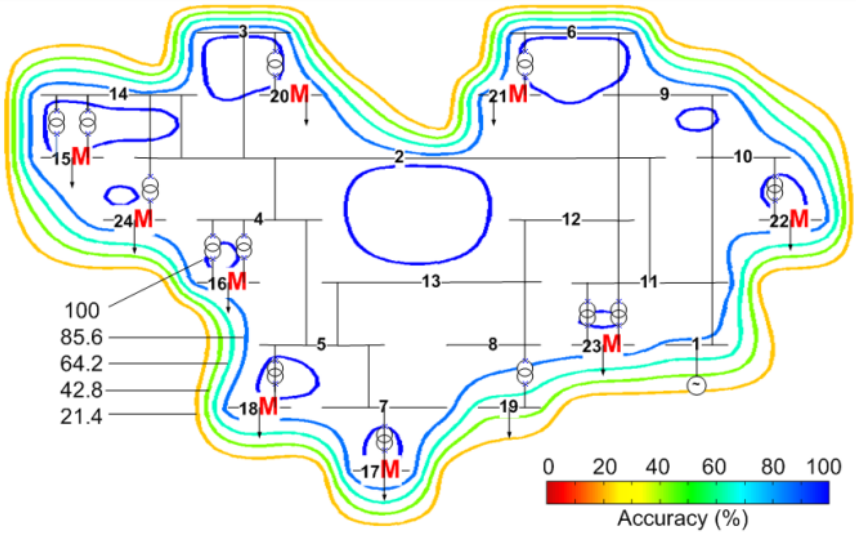

Fig. 6.3 Accuracy of monitoring for all buses with monitors installed except at bus 19.

It can be seen from the figure that the monitored accuracies of all buses are larger than 85.6% except for buses 19 and 1. The accuracy of non-monitored bus 19 is around 50% (the precise value is 50.84%). Because bus 1 is always assumed to be entirely balanced, the floating zero point in simulation leads to relatively low accuracy. Similarly, in the "uncertainty" contour map, only bus 19 shows a difference from the true value of 0.24% while for all other buses the differences are ≤0.007%. When comparing Fig. 6.3 and Fig.

6.4, the fewer number of circles and the darker colours of the circles around a bus indicate the significant reduction in the uncertainty regarding unbalance in the network.

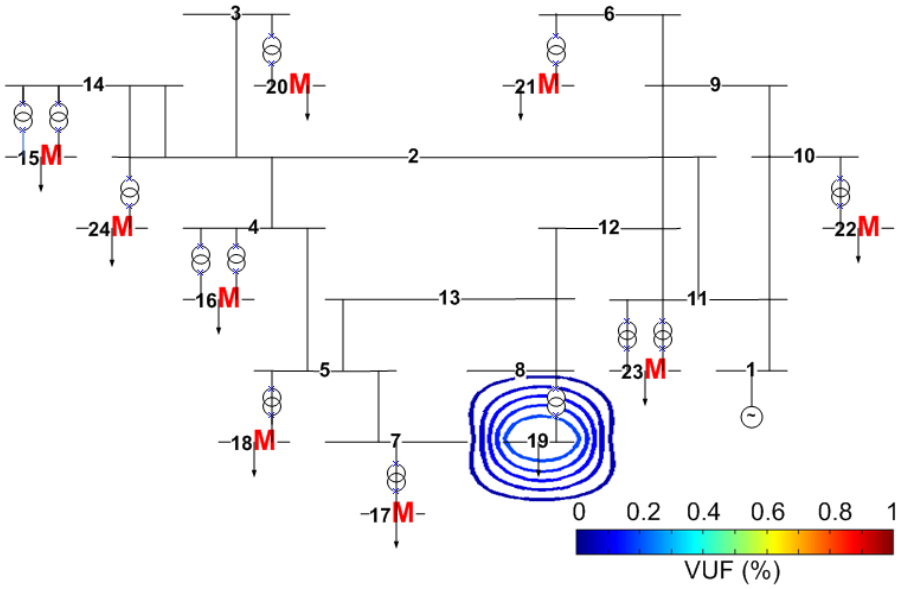

Fig. 6.4 Uncertainty of monitoring for all buses with monitors installed except at bus 19.

6.4 Optimal Monitor Placement

6.4.1 Ranking of Bus

Optimal monitor placement aims at the full observability of the network achieved using a minimum number of monitors. At the same time, the uncertainty in the result is expected to be acceptably small. When there are monitors in the network already, the optimal monitor placement should take the existing monitors into consideration in order to reduce costs.

To monitor unbalance, full observability is insufficient. Due to the different contributions of every bus to the unbalance, the various network circumstances (components and operating conditions) result in different degrees of influence on the monitored data. When monitoring the unbalance, if there are more important buses than others, then monitor installations at these highly-affected buses provide better solutions

than installation of monitors at the remaining buses, assuming the same number of meters.

To rank the buses in the network based on their influence on unbalance, a test of importance of individual buses is carried out in the test network. In this test, every load is set to be the single unbalanced source in the network, in turn. The size of active power and reactive power in one phase of the load is adjusted to generate unbalance as follows: phase *B* and phase *C* of the selected asymmetrical load remain unchanged while the active power and reactive power of phase *A* are multiplied by a same weighting factor (or scaling factor). (As long as the apparent powers of three phases are different, the voltages of three phases in the common coupling point will be unbalanced.) When the local substation (the bus to which the unbalanced load is directly connected) achieves 1% VUF, the weighting factor of phase *A* is recorded as well as the VUFs in other buses.

The weighting factors of the 10 loads in the 24-bus network are shown in Table 6.3. If the weighting factors are arranged in descending order, the ranking (from the most important to the least important) is: bus 15, 23, 17, 20, 24, 21, 22, 19, 16, and 18.

Table 6.3 Scaling Factor of Load Buses

Bus Number	Scaling Factor	Actual Load in Phase A(MW)
15	1.153	8.408
16	1.609	1.917
17	1.397	1.792
18	2.126	1.086
19	1.553	1.516
20	1.423	1.524
21	1.530	0.882
22	1.547	1.706
23	1.170	8.606
24	1.484	1.662

It can be seen from the result that the ranking of buses does not strictly follow the sequence of the size of load connected to the bus. The ranking of buses is influenced by

the sizes of the load connected to the bus, as a large load stimulates a large unbalanced current in the network, as well as by the location of buses. For example, bus 16, 17, 18 and 19 are located in the same area. So any unbalanced source inside this area will have a significant effect on this inter-connected area. Therefore, when there is a monitor in this area, it facilitates the estimation of unbalance and so the reductions of the uncertainties of all buses in the whole area.

6.4.2 RESULT OF RANKING OF BUS

For one load flow, 100 state estimations are computed. There are ten load buses in the network, i.e. ten locations for monitoring the sources of unbalance. The loads are adjusted by multiplying by 1.3 the active and reactive powers of phase *A* and by 0.85 the powers of phase *B* and *C* to achieve VUF>2% in the network. The total loading of three phases remains unchanged. When considering the number of monitors and taking the cost and accuracy of monitoring into account, the monitor set consisting of five monitors is examined as the first choice.

Fig. 6.5, Fig. 6.6 and Fig. 6.7 illustrate the results obtained with different monitor sets. Fig. 6.5 displays the monitored results with monitors in the five most important buses in the ranking except bus 15 (actually four monitors are used). The boxes in the figure denote the inter-quartile ranges of the monitored results, which stand for the possible ranges of VUFs of those buses. With a sufficiently narrow box, the uncertainty of the VUF of the bus is small. In other words, an accurate result can be inferred from metering. As seen from the figure, the results of monitored buses can be precisely read while the rest of the buses in the network still remain unidentified. Fig. 6.6 illustrates the results with the monitors at the first five buses in the ranking. Once a monitor has been installed at bus 15 (the most important bus), the overall uncertainty decreases with

a few exceptions. Fig. 6.7 shows the results with the monitors installed at the 5 least important buses in the ranking. This set of monitors observes the unbalance in local substations but results in the various fluctuations of VUFs at other buses. In addition, the monitor set used in Fig. 6.7 fails to provide correct range of VUFs for bus 15. With the same number of monitors, the average overall range of VUFs of all loaded buses is 8.28%, 6.27% and 13.19% for results illustrated in Fig. 6.5, Fig. 6.6 and Fig. 6.7, respectively.

To sum up, when the ranking of the importance of buses is applied to real monitoring, the monitors installed at the "more important" buses provide better performance than those installed at the "less important" buses. The installations of monitors at more important buses will increase not only the accuracy of monitoring locally, but also the accuracy of estimation at other non-monitored buses. The proposed ranking of buses facilitates accurate monitoring of unbalance with the same financial cost involved.

Box plots can be used to illustrate different VUF ranges of buses as results of various locations of monitors. The plots are embedded as a function in the developed user interface (more details in Appendix E) to show the results according to the monitors selected by users.

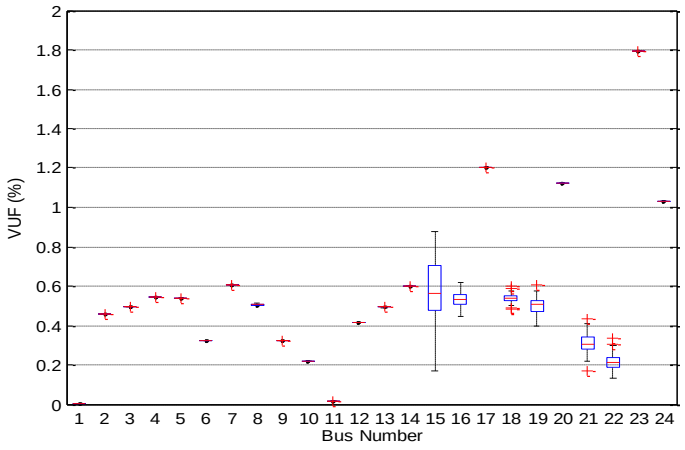

Fig. 6.5 State estimation results using the best 5 monitor locations except bus 15.

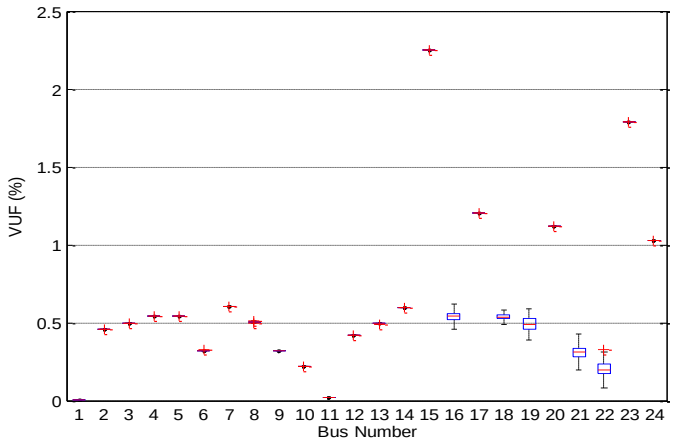

Fig. 6.6 State estimation results using the best 5 monitor locations.

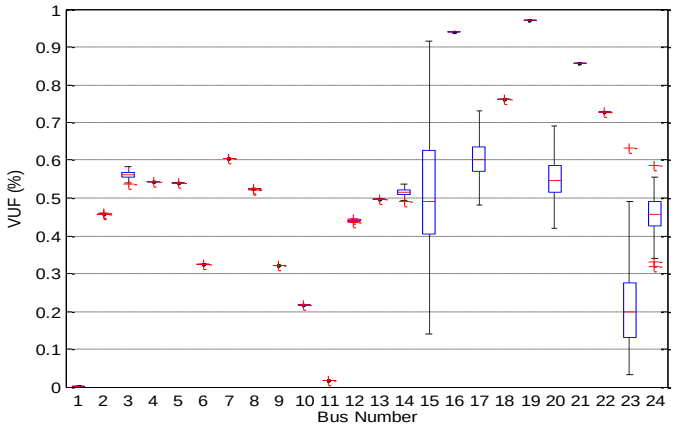

Fig. 6.7 State estimation results using the worst 5 monitor locations.

6.4.3 Optimal Monitor Placement Using Genetic Algorithm

Genetic algorithm (GA) is a sophisticated computer model of the biological evolution in natural selection. It imitates the evolution in the new generation in a fixed population. To apply GA to engineering problems, the problem has to be genetically represented using mathematical models and is arranged to have flexible set of solutions. The algorithm starts from an arbitrary set of candidate solutions to calculate its fitness to the fitness function. Based on the fitness, GA operators select appropriate candidates, though selection, crossover and mutation, from the current population to be the parent for next generation. By iterating the generation process, GA performs optimization for the designed model according to the convergence to the fitness function [170].

In GA simulation, "population" defines the range of candidates and "generation" represents a more convergent set of candidates than the previous population with respect to the fitness of the aim of optimization. The population should be neither too big nor too small to achieve reasonable efficiency for the calculation process. A small size of population will result in quick convergence and probably non-optimal solution. In contrast, a big size of population wastes computational memory and time. To have a balance between the computational time and the high fitness, the size of generation should also be restricted according to specific cases.

The iteration process is evaluated by a fitness value, calculated from the fitness function (or objective function). Therefore, the structure of the objective function determines the quality of the optimization.

The selection of the parenting candidate for the next generation depends on the fitness value calculated in the evaluation process. The higher the convergence to the objective is, the more possibility the candidate in a population can become a parent [171]. After the selection, crossover exchanges one or two current candidates of parents to evaluate the new performance. Mutation introduces random candidate to the current solution to evaluate the new performance of the set of solutions following crossover.

The termination of GA optimization is controlled by the defined sizes of population and generation. An early termination may not provide a global optimum while the long termination requires huge computational time and software memory capacity [171]. The optimization process does not stop until one of the terminating conditions is reached: 1) fixed number of generations is reached; 2) the solution fits the objective function; 3) the computational time or space is reached; 4) solutions do not significantly change; 5) manual inspection. Usually the reason of termination is 1 or 3.

For the optimal monitor placement, the aim of the placement is to derive minimum uncertainty of the network using a minimum number of monitors. Therefore, for a fixed number of monitors, the objective function is set as (6.3):

$$\min \sum_{i=1}^{n} |VUF_{SE-MEAN} - VUF_{TRUE}| \tag{6.3}$$

where i is an arbitrary bus in the network and n is the total number of buses.

The selection of the optimal number of monitors is made by considering different number of monitors to achieve the balance between the desired accuracy and financial cost.

In the simulation, the GA toolbox in Matlab is used. Because the distribution network is a small population, initial population = 10 and maximum generation = 15 are used to achieve relatively accurate result and reduce the time for optimization process. The resultant combination of monitors is expected to have the minimum uncertainty of VUF with selected number of monitors.

6.4.4 Correlation of Number of Monitors and Error

The correlation between the number of monitors and the overall uncertainty defined in (6.3) is shown in Fig. 6.8. It is obvious that there is a turning point where the gradient of the curve changes, at the point when the number of monitors is 3. With more than three monitors, the uncertainty decreases almost linearly. When there are 7 monitors, the overall uncertainty for the best location of monitors stays below 1%. However, because the scheduled number of monitors is 5, the following research on the 24-bus network will be entirely based on 5 monitors. For this network, the result of GA optimization with five monitors is: bus 15, 23, 17, 20 and 24, which is exactly the same set of buses obtained using previously discussed ranking method based on scaling factors. Therefore,

the DNSE results with the suggested set of monitors determined by GA will not be repeatedly demonstrated and further discussed in this thesis.

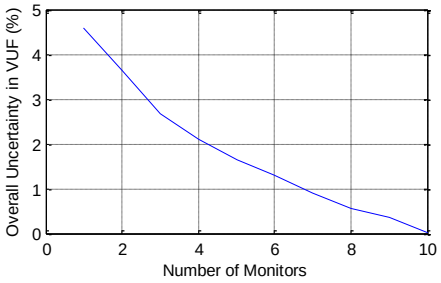

Fig. 6.8 Correlation between number of monitors and overall uncertainty for 24-bus network.

6.4.5 Optimal Monitor Placement with Existing Monitors

In real networks, it is highly likely that DNOs will have monitors installed at some buses, although the monitors may not be installed at optimal locations.

In the 24-bus test network, accessible monitors are at bus 16 and 24. The state estimation result with two monitors at bus 16 and 24 is shown in Fig. 6.9. The overall error of estimation for all buses with these two monitors is 19.83%. To ensure the accuracy of monitoring data based on the optimal monitor placement (the ranking), a new monitor is installed at bus 15. The monitoring results using a new monitor set are displayed in Fig. 6.10. The overall error after the installation of a monitor at bus 15 is 13.47%. As seen from the figure, the uncertainties at individual buses have reduced (except bus 20), providing more accurate picture of the status of the network.

To increase the accuracy of state estimation, the actual monitoring data should be included in the computation process. In reality, in addition to the monitors at bus 16 and 24, there are three more installed at bus 15, 18 and 23. However, they are not accessible due to technical problems. Considering the readings at these three sites, a new state estimation is calculated by the presence of both real monitoring data at bus 16 and 24, and the load flow results of bus 15, 18 and 24 using real loading data (varied according

to Table 4.16), shown in Fig. 6.11. The real monitored values are still shown with red curves while the load flow results that are regarded as true values of VUFs are plotted using green lines. The blue curves indicate the estimated range of VUFs at buses by DNSE. With five monitored sites, the uncertainties in VUF of the non-monitored buses are limited to about 0.2%.

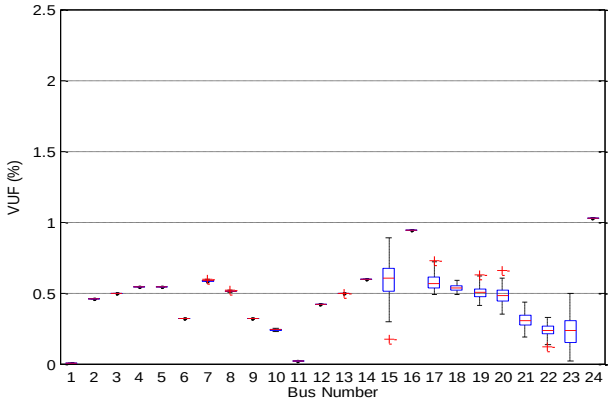

Fig. 6.9 State estimation results using existing accessible monitors (monitors at bus 16 and 24).

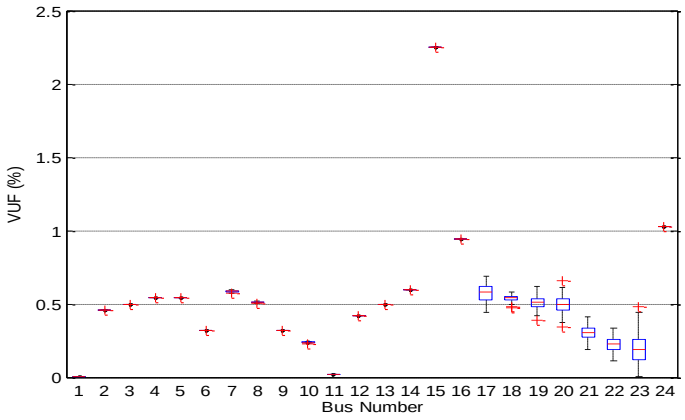

Fig. 6.10 State estimation results using existing accessible monitors and monitor at bus 15 (monitors at bus 15, 16 and 24).

The similar state estimation result with the five most important monitor locations determined using methodology developed in this chapter and discussed in Section 6.4.2 is plotted in Fig. 6.12. With real monitoring data and real loading data, the chosen set demonstrates narrower ranges than that of Fig. 6.11. The overall uncertainty (the sum of all the ranges at every bus and every measuring point, i.e., the sum of uncertainties of 1490×24 uncertainty points) in VUFs is 112.5% and it has been reduced to 97.22% if the optimal monitors are used.

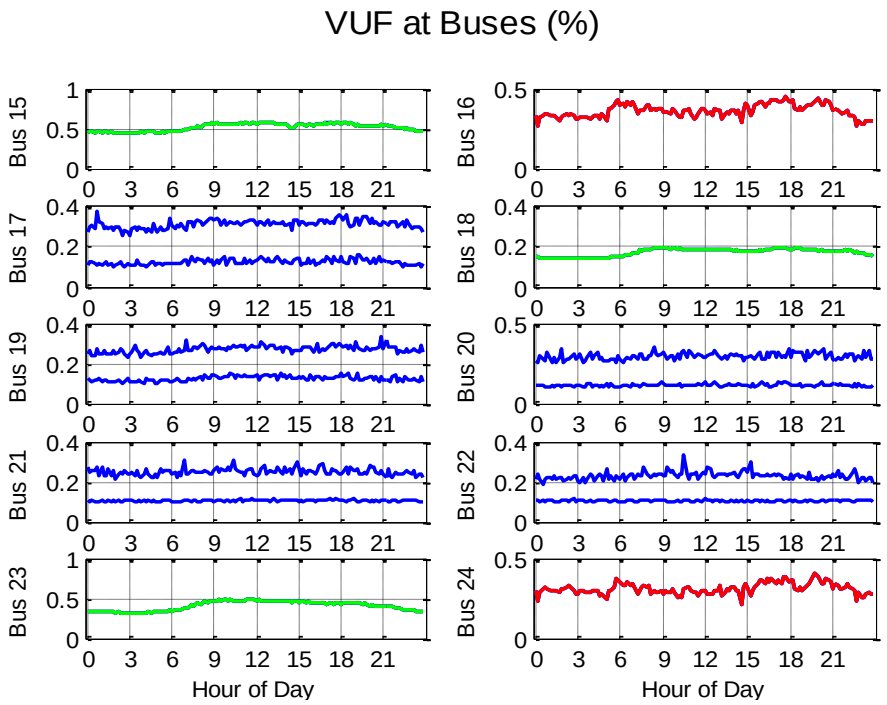

Fig. 6.11 One-day estimation of unbalance based on real loading data and real monitoring data, assuming accessible monitors are installed at bus 15, 16, 18, 23 and 24.

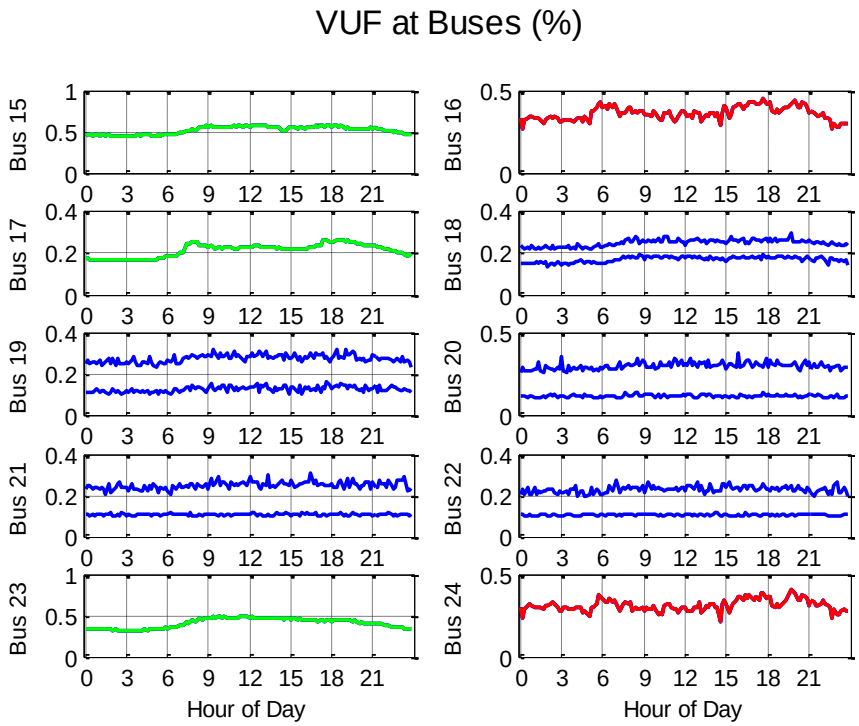

Fig. 6.12 One-day estimation of unbalance based on real loading data and real monitoring data, assuming accessible monitors are installed at bus 15, 16, 17, 23 and 24.

6.5 Methodology Validation in 295 Bus Network

Although there are 295 buses in the generic distribution network (GDS), the main concern is the 11kV buses and so simulations are only carried out on this section of radial network. The 11kV network is composed of four separate networks fed from

different 33kV feeders. From left to right in the one-line diagram as shown in Fig. 2.8, the four sections are labelled as 1 to 4 with each one containing 41, 52, 43 and 94 buses respectively.

6.5.1 CORRELATION CURVE

Because the distribution level of the 295-bus network is radial and the voltage from higher voltage level is regulated, the whole 11kV section is considered to be feed from separate 33kV feeders and can be divided into four uncorrelated sections, as indicated in Fig. 2.8. The division of the network reduces the computational capacity required for software memory and improves the computational time due to the reduced redundancy.

The correlation curve between the number of monitors and overall uncertainty for the Section 4 (94-bus section, the section with the largest number of buses) is shown in Fig. 6.13. It can be seen that the overall uncertainty decreases with the increasing number of monitors, with one exception. When there are four monitors in the network, the uncertainty is larger than with three monitors. This abnormal turning point exists because of local convergence which is the limitation of optimization methodology. Due to the huge amount of monitor combinations in this network and the balance between the simulation time and resultant accuracy, GA is limited to certain iterations and so only a part of the possible combinations of monitors is inspected. Because of the incomplete trials in reality, the solution provided by GA may not be the true optimum.

The correlation curves for Section 1, 2 and 3 are illustrated in Fig. 6.14, Fig. 6.15 and Fig. 6.16, respectively.

Fig. 6.13 Correlation between number of monitors and overall uncertainty for Section 4 of 295-bus network.

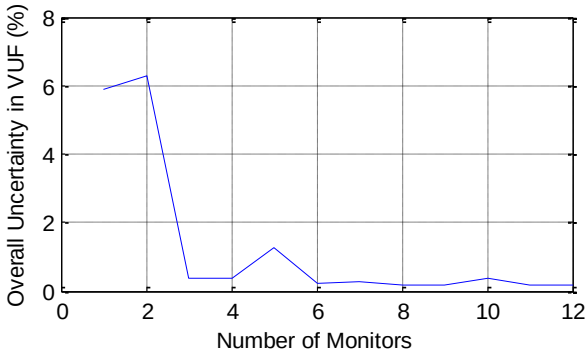

Fig. 6.14 Correlation between number of monitors and overall uncertainty for Section 1 of 295-bus network.

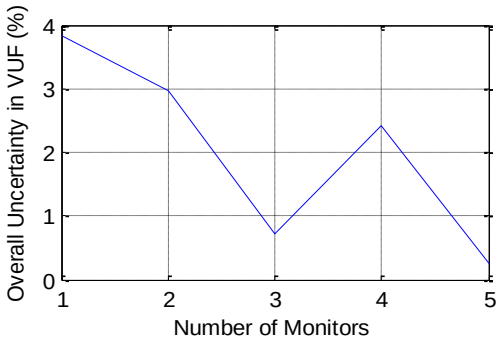

Fig. 6.15 Correlation between number of monitors and overall uncertainty for Section 2 of 295-bus network.

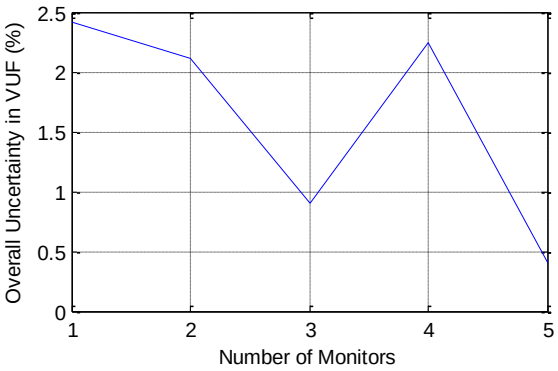

Fig. 6.16 Correlation between number of monitors and overall uncertainty for Section 3 of 295-bus network.

6.5.2 95TH OF WEEKLY VUF

From Fig. 6.13, five monitors are selected to be installed in Section 4. The same investigation is carried out for the other three sections and the results are three monitors for each of the sections respectively. In total, there are fourteen monitors in the 11kV network.

The result is evaluated according to the 95th percentile of 10-minute weekly VUF as required by the standard and it indicates where the regulation should be applied. For this purpose, the ability of the selected combination of monitors to indicate the same levels of true unbalance in the network is expected. In order to generate unbalance over 2% in the network, all the loads in the network are increased in phase A 5.5 times the initial loadings. The percentages of buses that exceed 2% during one day are shown in Fig. 6.17 using a heat map. The weak areas affected by unbalance are clearly indicated in the figure with colours different from the background colour. Sections 2 and 3 do not have VUF values over 2% and section 4 has a small area exceeding VUF threshold of 2% for 10% to 20% of the time during one week. The most vulnerable areas are in section 1, where the weekly VUFs exceed 2% threshold for about 70% of the time.

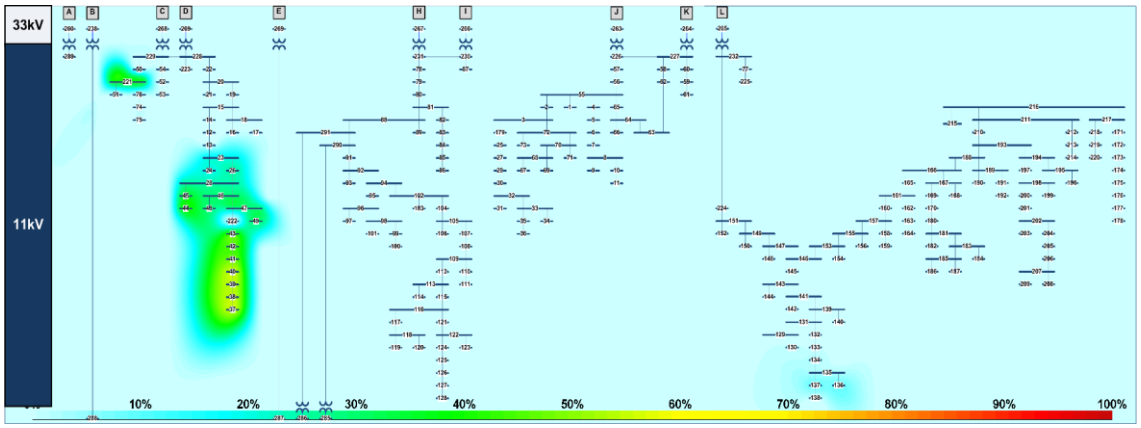

Fig. 6.17 Percentage of weekly VUFs exceeding 2% in 11kV GDS network from true values.

The estimated percentages of buses that exceed 2% during one week are shown in Fig. 6.18, with the monitor locations marked by red "M". With 14 monitors, the unbalance in section 4 is accurately estimated while the values in section 1 are significantly over-

estimated for some buses. This indicates a possible improvement of the DNSE performance by using a reasonably increased number of monitors in section 1.

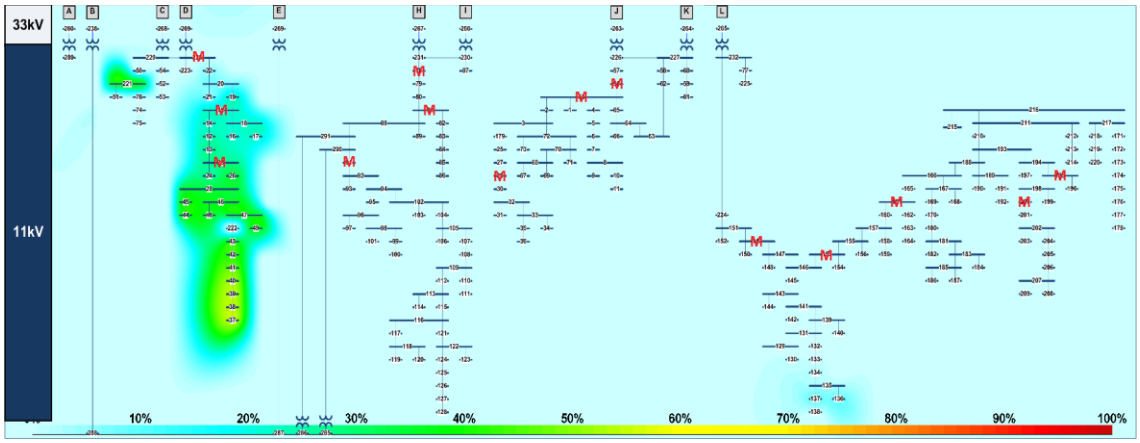

Fig. 6.18 Percentage of weekly VUFs exceeding 2% in 11kV GDS network from DNSE results with 14 monitors.

By adding three more monitors step by step in section 1, the percentages of VUFs violating the standard limitation during one day with 17, 20 and 23 monitors are shown in Fig. 6.19 to Fig. 6.21. The overall over-estimation of unbalance in section 1 is improved compared to Fig. 6.18, but a discrepancy from the true state of the network can still be observed in section 1. With the increasing number of monitors, the overall uncertainty is gradually reduced.

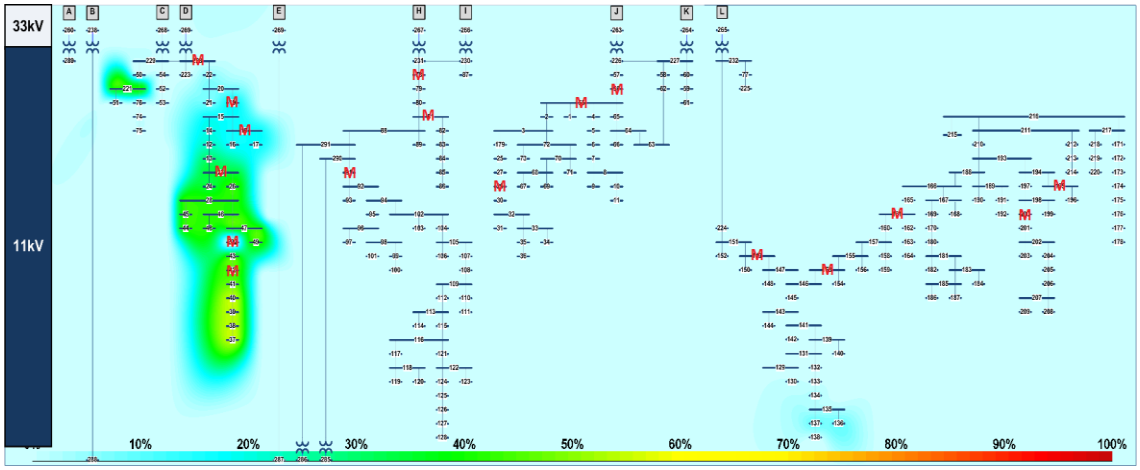

Fig. 6.19 Percentage of weekly VUFs exceeding 2% in 11kV GDS network from DNSE results with 17 monitors.

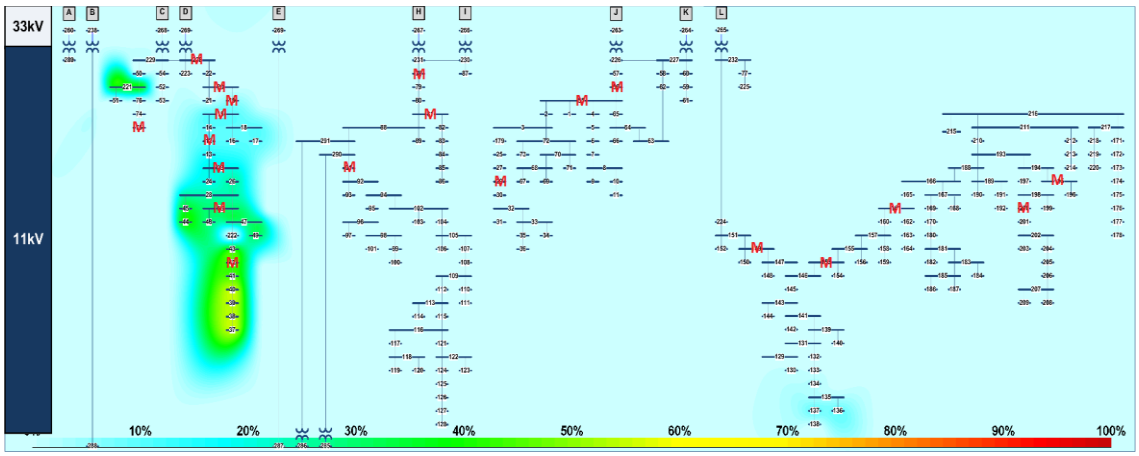

Fig. 6.20 Percentage of weekly VUFs exceeding 2% in 11kV GDS network from DNSE results with 20 monitors.

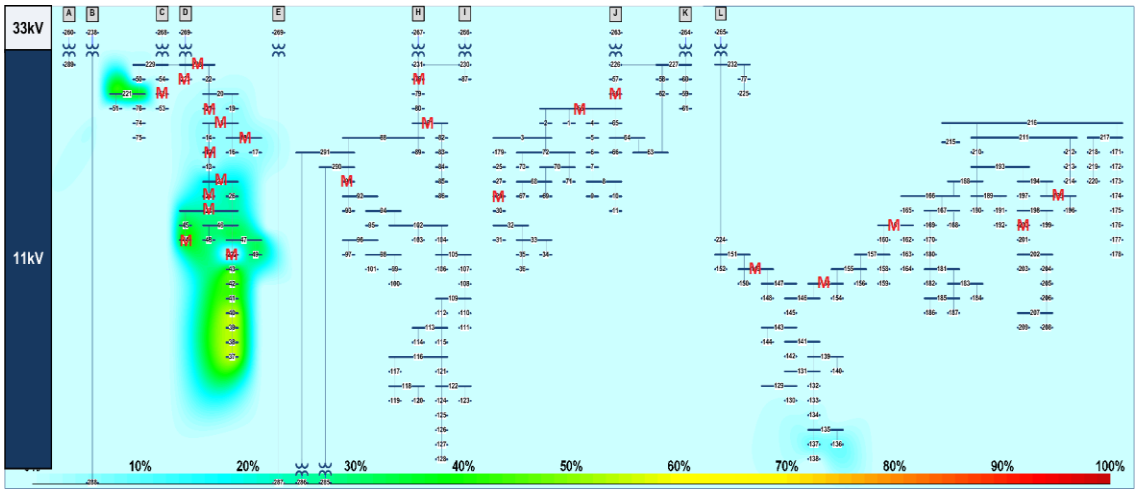

Fig. 6.21 Percentage of weekly VUFs exceeding 2% in 11kV GDS network from DNSE results with 23 monitors.

6.5.3 REAL-TIME ESTIMATION

Except for one-day estimation, DNSE is also valid for real-time estimation of unbalance. Fig. 6.22 to Fig. 6.26 show a snapshot for the peak loading period during the day for the 11kV network, with the same degree of unbalanced loads as in the previous section. Fig. 6.22 is the actual VUF in the network, assuming full observability of the network. Fig. 6.23, Fig. 6.24, Fig. 6.25 and Fig. 6.26 have 14, 17, 20 and 23 monitors in the network respectively. The locations of the monitors are correspondingly the same as those described in the previous section.

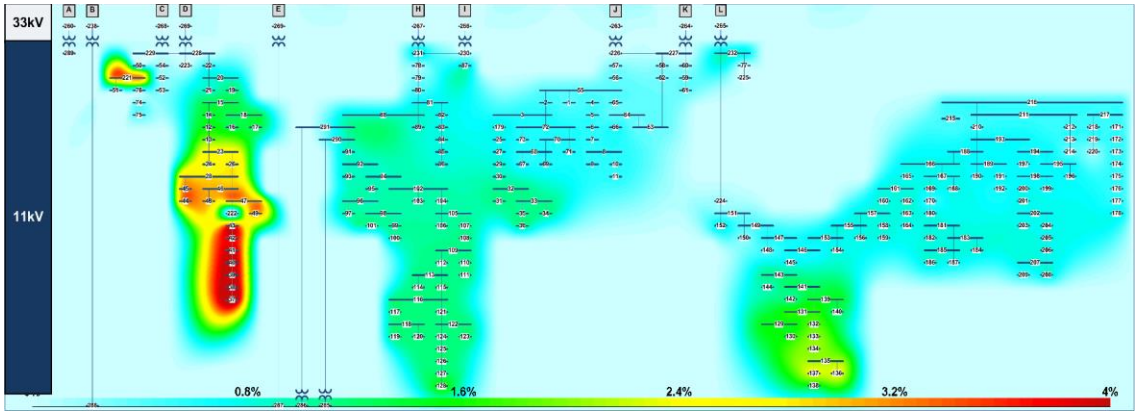

Fig. 6.22 Actual VUF in 11kV GDS network during peak loading period.

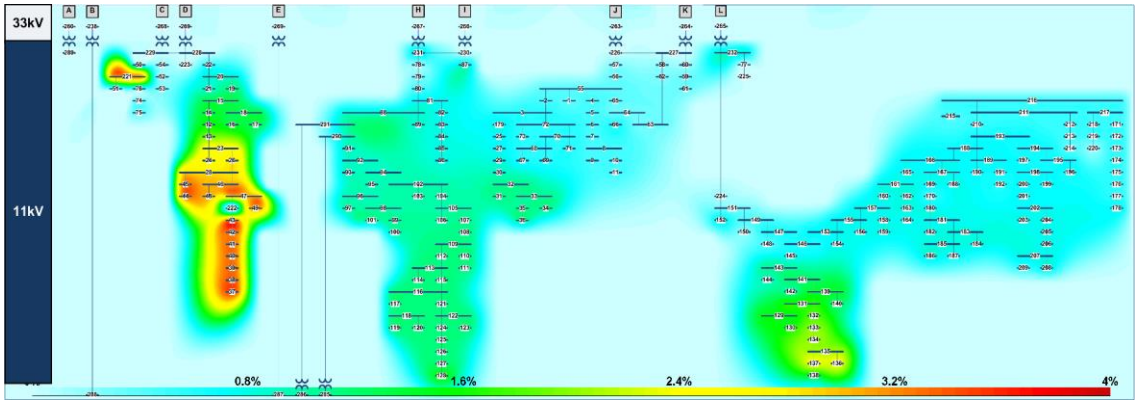

Fig. 6.23 VUF in 11kV GDS network from DNSE results with 14 monitors during peak loading period.

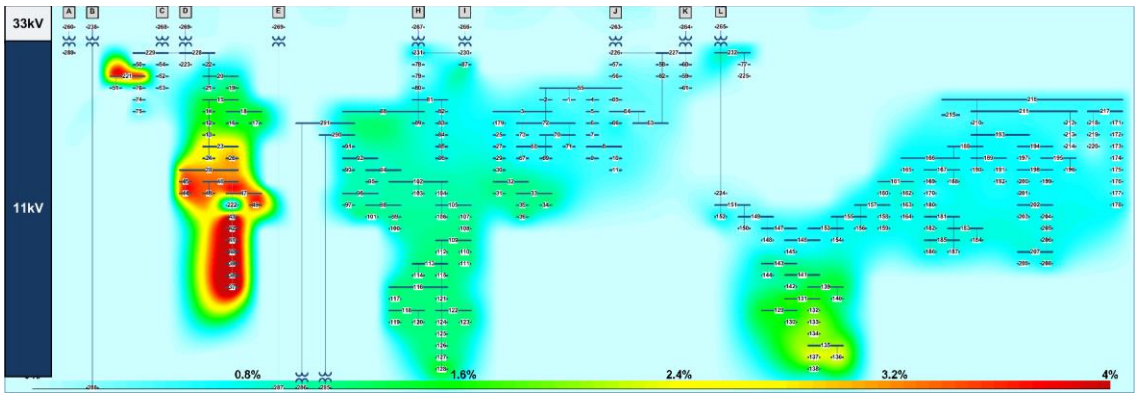

Fig. 6.24 VUF in 11kV GDS network from DNSE results with 17 monitors during peak loading period.

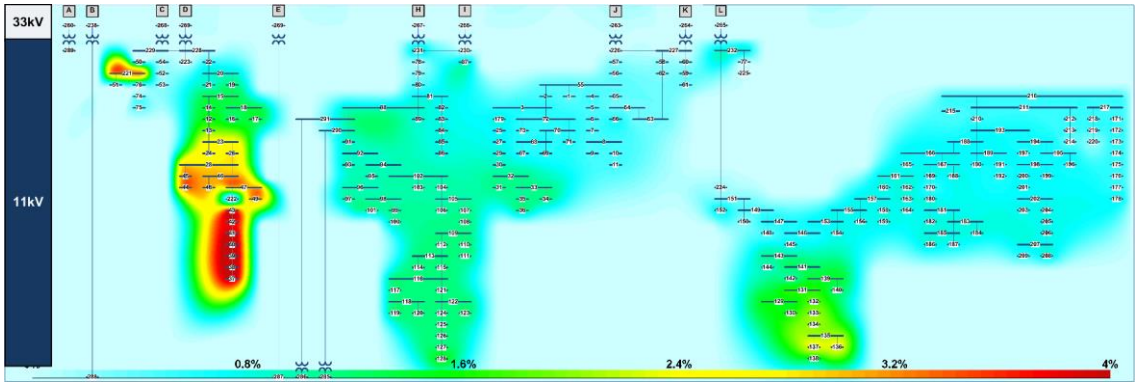

Fig. 6.25 VUF in 11kV GDS network from DNSE results with 20 monitors during peak loading period.

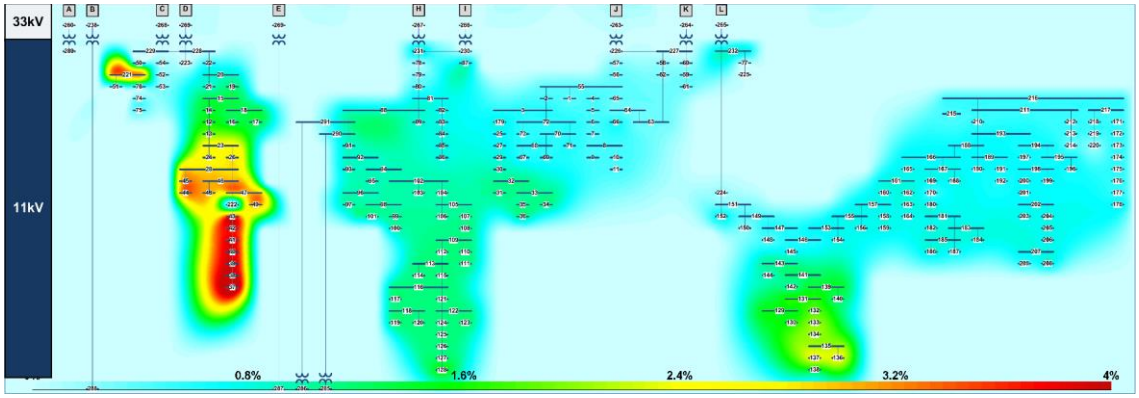

Fig. 6.26 VUF in 11kV GDS network from DNSE results with 23 monitors during peak loading period.

By comparing the estimated VUF with the actual VUF, it can be found that, Section 2, 3 and 4 are accurately assessed except Section 1. With 14 monitors in the network (3 monitors in Section 1), the overall VUF in Section 1 is significantly under-estimated due to insufficient data. With 6 monitors in Section 1, the data is probably sufficient. However, because of the possible non-convergence of state estimation, the VUF is over-estimated. With 9 monitors or 12 monitors in Section 1, the estimation of unbalance illustrates reasonable agreement with the actual VUF in the network.

Heat maps are embedded in the developed user interface (more details in Appendix E) to show the real-time level of estimated unbalance according to the monitors selected by users.

6.6 SUMMARY

The chapter presents a distribution network state estimator which enables the prediction of unbalance in a section of the UK distribution network and the fulfilment of incomplete data, as well as the correlation between monitor placement and resultant accuracy in the measurement.

With the developed DNSE, optimal monitor placement is discussed. By ranking the buses using proposed scaling factors, or by using the optimization method based on GA,

the best locations for monitor placement can be identified and better monitoring accuracy can be achieved with the same number of monitors compared to the arbitrary monitor locations. By considering the existing monitors in the network, the optimal monitor placement facilitates further planning of monitor installations. The methodology is additionally validated on a large 295-bus network.

By using DNSE and the optimal monitor set, the full observability of the network can be derived from either loading data or incomplete monitoring data. This enables not only momentary estimation of the level of unbalance in the whole network, but also a long-run prediction of unbalance even when monitoring is unavailable or incomplete.

A graphical user interface is developed to enable flexible selection of monitor locations based on the work in this chapter. The results are automatically illustrated using box plots or heat maps. More details can be found in Appendix E.

7 CONCLUSION AND FUTURE WORK

7.1 MAJOR CONCLUSION

The thesis made several original contributions, of which the two major contributions are the development of methodologies for the probabilistic estimation of unbalance resulting from the time-varying asymmetrical loading and the optimal monitor placement for estimation of unbalance in the network with a limited number of monitors.

The thesis starts by providing the fundamental background of voltage unbalance, which is one of the power quality problems growing in importance in recent year. It defines the causes, effects, quantification of unbalance and specified indices, requirements of international standards and mitigation methods for unbalance. The major consequence of this long term phenomenon is the overheating on equipment and therefore the financial losses due to unbalance render investigation into this area more important. A review of past literature indicates that, both the propagation of unbalance and the contributions of individual sources of unbalance can be deterministically quantified, providing that sufficient data is available. The overall level of unbalance in the network

is the consequence of unbalance originating from different types of sources, i.e., from unbalanced loading and unbalanced lines. Currently, most distributed generators, three-phase generators in particular, contribute to the mitigation of unbalance but this situation may change in future networks with increasing penetration of single-phase DGs (e.g., PV). With typically incomplete measurement data available, distribution state estimation should be the tool to be used for the estimation of unbalance. Furthermore, the unbalance should be studied in a probabilistic way, considering all existing and growing uncertainties in the network.

By using symmetrical components and three-phase modelling of the distribution network, three-phase load flow and three-phase state estimation jointly facilitate the studies of the propagation of voltage unbalance in power system networks. The three-phase state estimation with incomplete data is suitable for studying the behaviour of the network under limited monitoring. By investigating and comparing the commercially available software packages, DIgSILENT PowerFactory and Matlab are selected to carry out the simulations of unbalance in distribution networks. Four networks are used for the validation of different concepts and methodologies proposed in the thesis, including a section of a real UK generic distribution network and a 295-bus network.

The evaluation of unbalance starts by examining the methodologies of identification of the sources of unbalance. The results presented in this thesis indicate that the negative sequence apparent power angles are located within the third quadrant, corresponding to the existing methodology that claims the angle at the source of unbalance should be bigger than 90° and smaller than -90°. By calculating the negative sequence apparent power figure for every bus in the network, it is obvious that only the source of unbalance injects significant power into the system. The factor SUF (ratio of negative sequence apparent power to positive sequence apparent power) has significant values

for the sources of unbalance and zero values for other buses in the network, which is verified by simulating single source cases and a multiple-source case.

The study of propagation of unbalance shows that unbalance spreads to the whole network with certain levels of superposition or cancellation. Small line impedances or the vicinity to the balanced upper level power supply mitigate the propagation of unbalance. The studies on the propagation of both patterns in radial networks and meshed networks facilitate further research on bigger networks. *The study and explanation of unbalance propagation and cancellation is the first contribution of this thesis.*

To analyze the two main causes of unbalance which are the loads and the lines, research is firstly carried out on the impact of load asymmetry.

Appropriate load model is developed to present different classes of customers (industrial, commercial, domestic) with the consideration of their daily varying demands. The employment of a probabilistic approach to model uncertainty in VUF at the source of unbalance which can be any of the loads in the network, aims at realistic results about the level of unbalance. The probabilistic nature of the methodology, which uses the power factor variation in the unbalanced load, enables the modelling of frequent switching on or off of customer devices connected to the power system. The variation can be modelled in either active power, reactive power or apparent power, depending on the available network information. The studies performed on a real 24-bus network show that the VUF of the source can exceed the 2% weekly statutory limit as well as the instantaneous 4% limitation. The VUFs at other buses, however, are below this limit with a few exceptions. The highest increase of VUF was observed at buses adjacent to the source of unbalance. The results indicate the close correlation between the loading level and the resultant degree of unbalance and therefore the most risky

period of a day to breach standard defined thresholds is the peak loading period. Whatever the overall unbalance and the number of the sources is in the network, the effect of a source on VUFs of other sites is independent. By vectorially superposing the VUF or the negative sequence voltages from each source of unbalance, the VUF at every bus in the network can be calculated. When the loads in the network are represented as a mixture of industrial, domestic and commercial loads, the results of the probabilistic simulation match the unbalance level recorded in the real network. *The development of the methodology for probabilistic assessment of unbalance in networks is the second contribution of the thesis.*

The presence of three-phase loads, such as induction motors, with the assumption used in the simulation, results in reduced unbalance in the network by about 40%. Three-phase distributed generators such as wind turbine generators, have the similar mitigating effect as induction motors. The attenuation of single-phase PVs is depended on the solar insolation.

The lines in distribution networks are typically not fully transposed and can form another source of unbalance because of the existence of the unequal mutual coupling impedances between phases or sequences. The detail modelling of a three-phase line is demonstrated using impedance and admittance matrices. According to the network topology, the presence of asymmetrical lines may lead to an increase or reduction in VUF calculated based on load asymmetry only. However, for the buses near the power supply, the lines would not have significant effects on the local VUF. It is shown that with sufficiently short distances between two substations in some distribution networks, the unbalance that a line can cause is smaller than the unbalance caused by load so the effect of line asymmetry can be ignored. When the line is balanced, there is linear relationship between the size of line impedance and the resulting VUF. Therefore, an effective mitigation measure for reducing the unbalance propagation in the network is to

decrease the line impedance. *The studies of the influence of lines on unbalance and the estimation of the extent of their influence are the third contribution of this thesis.*

Both manual ranking method and automatic optimization using genetic algorithm are developed and demonstrated as the methods for optimal monitor placement. In real networks, all online operating parameters are derived from the monitors, with varying levels of accuracy. The overall accuracy of monitoring is related to the total number of monitors that exist in the network, i.e., once a monitor is installed at a bus, the flows of the local bus are recorded with high accuracy and the flows of the adjacent buses can be computed. Therefore, as the financial plan does not allow monitors to be installed at every site, optimal monitor placement aims to achieve the best accuracy of estimation with the minimum number of monitors. By ranking buses based on their importance for unbalance, monitors can be installed at these buses to improve the overall DNSE performance. The results of monitor placement based on ranking of buses give the same solution as the results obtained with developed GA optimization. The correlation curve between the number of monitors and the resultant best accuracy provide a choice for the DNO, indicating the improvement in additional installations for decision making. With enough monitors installed, the unbalance in the network can be estimated on a weekly basis or using real-time measurement to check if the standard requirements are being satisfied.

By using the proposed methodologies, either bus ranking or GA optimization, existing monitors in the network and the optimal set of additional monitors can be determined to identify the area affected by the unbalance. This is valid for the close-to-real-time estimation or the update of unbalance in the network at all network buses (monitored and non-monitored buses). *The developed optimization methodologies for optimal monitor placement represent the fourth original contribution of this thesis.*

For either methodology, heat maps can be used to graphically present the results to enable fast understanding of the current status of the network. *The development of the user-friendly visualisation of unbalance propagation through the network represents the fifth contribution of this research.*

Finally, a user-friendly graphical user interface (GUI) is developed to facilitate the use of the developed methodology by distribution network engineers. It incorporates both the automated study of unbalance propagation in given networks and the graphical representation of results using box plots and heat maps. *The development of this GUI is the sixth and final contribution of this thesis.*

7.2 FUTURE WORK

Although the objectives, aiming at the identification of the source of unbalance, tracing of unbalance propagation and optimal monitor placement for unbalance estimation have been fulfilled, there are possible further extension of this research.

The methodology is largely restricted by the available software tools in terms of computation time. For example, in order to estimate the momentary unbalance, only one set of MC simulations needs to be executed and would not take too much time. On the contrary, a daily, weekly or yearly estimation of unbalance would require a large number of simulations. The yearly estimation would take days or weeks of running time, rather than seconds. The improvement of the program, such as the coding principles, programming language and software environment, may help to save time.

In the simulations in this thesis, it is assumed that all transformers prevent the zero sequence power flow to help eliminate the unbalanced flow in the sequence domain. The impact of zero sequence power flowing through a transformer has not been

investigated. When there is a path for zero sequence flow, it is indicated in [172][173] that it can become a problem. In addition, there is a possibility that, similar with the line impedance, the size of transformer leakage impedance may have either mitigation or aggravation effects on the propagation of unbalance. In addition, other than the transformer connection type, it is indicated in [174] that the transformer winding construction (referring to step-up transformers and step-down transformers) also influences the propagation of unbalance.

The research carried out is based on probabilistic simulations instead of deterministic exploration because of the unpredictable uncertainties in real networks and also because of the complexity of the existing methodologies in identifying the transfer function or coefficient of unbalance. Due to a lack of necessary data, the calculation of transfer function according to literature review cannot be performed. This calls for a simplified definition for the transfer coefficient between buses as well as the deterministic contributions of each source of unbalance. The contribution of DGs in distribution networks would still be a relevant path to follow in order to come up with fast assessment tool.

The impact of the integration of DG is briefly reviewed in the thesis though they will play important role in future networks. Detailed models for different types of DG should be developed and incorporated in the model to study their impact on unbalance in future grids.

The thesis employs genetic algorithm as the optimization tool for monitor placement for the assessment of unbalance. However, it has been found that GA has sometimes come across premature local convergence in some cases which did not provide a practical solution. The improvement therefore could be made to the objective function used and to the algorithm itself.

As a framework for the economic cost for power quality has been developed and the calculation for harmonics is illustrated in [3], the methodology presented in this thesis can be extended to calculate the financial loss due to the presence of unbalance.

Finally, the research only focuses on unbalance, disregarding all other power quality problems. By taking other power quality phenomena into account, a universal power quality state estimator for comprehensive power quality estimation is theoretically achievable. The new state estimator could also suggest monitor placement for different aims, such as the detection of unbalance, identification of fault location, harmonics, voltage sags, etc. By combining all the above, optimal placement of monitors for global assessment of power quality can be proposed.

8 REFERENCES

[1] M. H. J. Bollen, *Understanding power quality problems: voltage sags and interruptions*, New York: IEEE Press, 1999.

[2] R. C. Dugan, M. F. McGranaghan, S. Santoso, H. W. Beaty, *Electrical power systems quality*, 2nd ed., McGraw-Hill, 2003.

[3] *CIGRE/CIRED Joint Working Group C4.107: Economic framework for power quality*. International Council on Large Electric Systems, 2010.

[4] J. Y. Chan, "Framework for assessment of economic feasibility of voltage sag mitigation solutions", PhD thesis: University of Manchester, 2010.

[5] T. Chandler, "The smart grid and power quality", [Online]. Available: http://powerqualityinc.com.my/PQSynergy2010/SmartgridvsPQsept09.pptx

[6] B. W. Kennedy, *Power quality primer*. New York; London: McGraw-Hill, 2000.

[7] J. Schlabbach, D. Blume, T. Stephanblome, *Voltage quality in electrical power systems*. London: Institution of Electrical Engineers, 2001.

[8] J. Arrillaga, S. Chen, N. R. Watson, *Power system quality assessment*. Chichester: John Wiley & Sons, 2000.

[9] R. Targosz and J. Manson, "Pan european LPQI power quality survey," in *19th International Conference on Electricity Distribution (CIRED)*, Vienna, 2007.

[10] K. K. Kariuki and R. N. Allan, "Evaluation of reliability worth and value of lost load", *IEE Proceedings Generation Transmission Distribution*, vol. 143, No. 2, 1996.

[11] E. T. B. Gross, S. W. Nelson, “Electromagnetic unbalance of untransposed transmission lines”. *AIEE Transactions on Power Apparatus and Systems*, vol. 74, No. 3, pp.887-893, 1955.

[12] R. H. Brierley, A. S. Morched, T. E. Grainger, “Compact right-of-ways with multi-voltage towers”. *IEEE Transactions on Power Delivery*, vol. 6, No. 4, pp.1682-1689, 1991.

[13] Z. Emin, D. S. Crisford, "Negative phase-sequence voltages on E&W transmission system". *IEEE Transactions on Power Delivery*, vol. 21, No.3, pp.1607-1612, 2006.

[14] A. Ametani, D. Van Dommelen, I. Utsumi, "Included in your digital subscription study of super-bundle and low-reactance phasings on untransposed twin-circuit lines", *IEE Proc. of Generation, Transmission and Distribution*, vol. 137, pp. 245-254, 1990.

[15] J. Driesen, T. Van Craenenbroeck, *Voltage disturbances*, Copper Development Association, May 2002.

[16] "Electricity distribution system losses - Non-Technical Overview," Sohn Associates, 2009, [Online]. Available: http://bit.ly/w2N82d.

[17] "Electricity distribution loss percentages by distribution network operator (DNO) Area," Ofgem, 2010.

[18] "Distribution price control review 5", Ofgem, 2010, [Online]. Available: https://www.ofgem.gov.uk/electricity/distribution-networks/network-price-controls/distribution-price-control-review-5.

[19] A. von Jouanne and B. Banerjee, "Assessment of voltage unbalance," *IEEE Transactions on Power Delivery*, vol. 16, pp. 782-790, 2001.

[20] M. Moghbel, M.A.S. Masoum, F. Shahnia, P. Moses, “Distribution transformer loading in unbalanced three-phase residential networks with random charging of plug-in electric vehicles”, *in Proc. 22nd Australasian Universities Power Engineering Conference (AUPEC)*, 2012.

[21] "Small wind systems UK market report 2011", Renewable UK, London, UK, Annual report, April, 2011.

[22] M. H. J. Bollen, I. Gu, *Signal processing of power quality disturbances*. John Wiley and Sons, 2006.

[23] T.-H. Chen, "Criteria to estimate the voltage unbalances due to high-speed railway demands", IEEE Transactions on Power Systems, vol. 9, pp. 1672-1678, 1994.

[24] W. R. Bullard, H. L. Lowe, H. W. Wahlquist, "Calculation of unbalanced voltage drops in distribution circuits with particular reference to multigrounded neutrals", *AIEE Trans. on Electrical Engineering*, vol. 63, pp. 145-148, 1944.

[25] P. V. S. Valois, C. M. V. Than, N. Kagan, H. Arango, "Voltage unbalance in low voltage distribution networks", *in Proc. International Conference on Electricity Distribution (CIRED 2001)*, 2001.

[26] E. T. B. Gross, M. H. Hesse, "Electromagnetic unbalance of untransposed transmission lines". *AIEE Transactions on Power Apparatus and Systems*, vol. 72, No. 2, pp. 1323-1336, 1953.

[27] E. H. Badawy, M. M. Said, H. I. Nour, "Electromagnetic unbalance in power systems with untransposed transmission lines", *Electric Power System Research*, vol. 5, pp. 253-258, 1982.

[28] E. H. Badawy, M. M. Said, H. I. Nour, "Inductive unbalance in power systems with untransposed transmission lines", *Electric Power System Research*, vol. 5, pp. 199-206, 1982.

[29] T. Chandler, "Smart grid overview". [Online]. Available: http://powerqualityinc.com.my/PQSynergy2010/Smart%20Grid%20Overview.ppt

[30] *NEMA Standards Publication No. MG 1-1993, Motors and generators*. National Electricity Manufacturer's Association, 1993.

[31] G. W. C. Duesterhoeft, C. C. Mosher, "Heating of induction motors on unbalanced voltages". *AIEE Trans. on Power Apparatus and Systems*, vol.78, pp.282-297, June 1959.

[32] C. Y. Lee, "Effects of unbalanced voltage on the operation performance of a three-phase induction motor". *IEEE Trans. on Energy Conversion*, vol. 14, No. 2, pp.202-208, June 1999.

[33] A. Baggini, *Handbook of power quality*. John Wiley and Sons, 2008.

[34] *IEC TS 60034-26: Effects of unbalanced voltages on the presence of three-phase induction motors*. International Electrotechnical Commission, 2002.

[35] J. W. Williams, "Operation of 3 phase induction motors on unbalanced voltages". *AIEE Trans. on Power Apparatus and Systems*, vol. 73, pp.125-133, April 1954.

[36] V. O. Zambrano, E. B. Makram, R. G. Harley, "Stability of a synchronous machine due to an unsymmetrical fault in unbalanced power system". *In Proc. of 20th Southeastern Symposium on System Theory*, pp. 231-235, 1988.

[37] E. B. Makram, V. O. Zambrano, R. G. Harley, "Stability of a synchronous machine due to multiple faults in unbalanced power system". *In Proc. of 20th Southeastern Symposium on System Theory*, pp. 226-230, 1988.

[38] R. Salustiano, E. Neto, M. Martine, "The unbalanced load cost on transformer losses at a distribution system", in *22th International Conference on Electricity Distribution (CIRED),* Stockholm, 2013.

[39] D. P. Manjure and E. B. Makrram, "Impact of unbalance on power system harmonics". *In Proc. 10th International Conference on Harmonics and Quality of Power (ICHQP 2002)*, vol. 1, pp. 328-333, 2002.

[40] L. Moran, P. Ziogas, G. Joos, "Design aspects of synchronous PWM rectifier-inverter systems under unbalanced input voltage conditions", *IEEE Transactions on Industry Applications*, vol. 28, pp. 1286-1293, 1992.

[41] K. Lee, G. Venkataramanan, T. M. Jahns, "Modeling effects of voltage unbalances in industrial distribution systems with adjustable-speed drives", *IEEE Transactions on Industry Applications*, vol. 44, pp. 1322-1332, 2008.

[42] T. H. Chen, "Evaluation of line loss under load unbalance using the complex unbalance factor". *In IEE proc. Generation, transmission and distribution*, vol. 142, No. 2, pp. 173-178, 1995.

[43] J. Kuang, S. A. Boggs, "Pipe-type cable losses for balanced and unbalanced currents". *IEEE Transactions on Power Delivery*, vol. 17, No.2, pp.313-317, 2002.

[44] L. S. Czarnecki, "Power related phenomena in three-phase unbalanced systems". *IEEE transactions on power delivery*, vol. 10, No.3, pp.1168-1176, 1995.

[45] C. A. Reineri, J. C. Gomez, E. Belenguer B., M. Felici, "Revision of concepts and approaches for unbalance problems in distribution", *In Proc. Of Transmission & Distribution Conference and Exposition*, Aug 2006.

[46] J. J. Grainger, W. D. Stevenson, *Power system analysis*, McGraw-Hill, Inc., 1994.

[47] C. L. Fortescue, "Method of symetrical co-ordinates to the solution of polyphase networks", *in 34th Annual Convention of the AIEE (American Institute of Electrical Engineers)*, Atlantic City, New Jersey, 1918.

[48] *EN 50160: Voltage characteristics in public distribution systems*. European Committee For Electrotechnical Standardization (CENELEC), Nov 1994.

[49] J. E. Parton, Y. K. Chant, "The three-limbed phase transformer with controlled zero sequence effect", *IEEE Transactions on Power Apparatus and Systems*, vol. 90, pp. 2019-2029, 1971.

[50] *NRS 048-2: Electricity Supply - Quality of Supply, Part2 - Voltage characteristics, compatibility levels, limits and assessment methods,* Standards South Africa, 2007.

[51] *National Electricity Code Australia, Version 1.0 - Amendment 9.0*. National Electricity Code Administrator Limited, Australia, 2004.

[52] *CIGRE/CIRED Joint Working Group C4.07 (formerly CIGRE WG 36.07): Power quality indices and objectives*. International Council on Large Electric Systems, January 2004.

[53] *CIGRE/CIRED Joint Working Group C4.103 (formerly C4.06). Assessment of emission limits for the connection of disturbing installations to power systems, final report*. International Council on Large Electric Systems, June 2007.

[54] *CIGRE/CIRED Joint Working Group C4.103. Assessment of emission limits for the connection of unbalanced installations to MV, HV and EHV power systems (proposed future IEC 61000-3-13)*. International Council on Large Electric Systems, April 2006.

[55] *UIE Guide to Quality of Electrical Supply for Industrial Installations - Part 1: General introduction to electromagnetic compatibility (EMC) types of disturbances and relevant standards, Ed. 1*. Union for Electricity Applications, 1994.

[56] *UIE Guide to Quality of Electrical Supply for Industrial Installations - Part 4: Voltage unbalance, Ed. 1*. Union for Electricity Applications, 1998.

[57] *IEEE 100: Standard dictionary of electrical and electronics terms*. Institute of Electrical and Electronics Engineers, 1996.

[58] *IEEE 112: Standard test procedures for polyphase induction motors and generators*. Institute of Electrical and Electronics Engineers, 1991.

[59] "Tutorial on voltage imbalance assessment". [Online]. Available: http://grouper.ieee.org/groups/1159/1/VUFAss.html.

[60] M. H. J. Bollen. "Definitions of voltage unbalance". *IEEE Power Engineering Review*, vol. 22, No. 11, pp.49-50, November 2002.

[61] *IEEE 1159: IEEE recommended practive for monitoring electric power quality*. Institute of Electrical and Electronics Engineers, 1995.

[62] *IEC/TR 61000-3-13: Limits - Assessment of emission limits for the connection of unbalanced installations to MV, HV and EHV power systems*, International Electrotechnical Commission, Feb 2008.

[63] *IEC 61000-4-30: Electromagnetic Compatibility (EMC) - Part 4-30 Environment - testing and measurement techniques – power quality measurement methods*. International Eletrotechnical Commission, 2003.

[64] D. C. Garcia, A. L. Filho, M. A. Oliveira, O. A. Fernandes, and F. A. do Nascimento, "Voltage unbalance numerical evaluation and minimization", Electric Power Systems Research, no EPSR-2874, 2009. [Online]. Available: www.elsecier.com/locate/epsr.

[65] G. Burchi, C. Lazaroiu, N. Golovanov, and M. Roscia, "Estimation of voltage unbalance in power systems supplying high speed railway", *Electrical Power Quality and Utilisation*, vol. XI, no. 2, pp. 113-119, 2005.

[66] A. K. Singh, G. K. Singh, R. Mitra, "Some observations on definitions of voltage unbalance", *in Proc. 39th North American Power Symposium(NAPS '07)*, 2007.

[67] P. Pillay, M. Manyage, "Definitions of voltage unbalance", *IEEE Power Engineering Review*, vol. 21, pp.49-51, 2001.

[68] J. S. Wu, K. L. Tomsovic, C. S. Chen, "A heuristic search approach to feeder switching operations for overload, faults, unbalanced flow and maintenance", *IEEE Transactions on Power Delivery*, vol. 6, pp. 1579-1586, 1991.

[69] M. W. Siti, D. V. Nicolae, A. A. Jimoh, A. Ukil, "Reconfiguration and load balancing in the LV and MV distribution networks for optimal performance", *IEEE Transactions on Power Delivery*, vol. 22, pp. 2534-2540, 2007.

[70] T.-H. Chen, J. -T. Cherng, "Optimal phase arrangement of distribution transformers connected to a primary feeder for system unbalance improvement and loss reduction using a genetic algorithm", *IEEE Transactions on Power Systems*, vol. 15, pp. 994-1000, 2000.

[71] P. Paranavithana, "Contributions towards the development of the Technical report IEC/TR 61000-3-13 on voltage unbalance emission allocation". PhD dissertation, University of Wollongong, 2009.

[72] F. Shahnia, P. J. Wolfs, A. Ghosh, "Voltage unbalance reduction in low voltage feeders by dynamic switching of residential customers among three phases", *IEEE Transactions on Smart Grid*, vol. 5, pp. 1318-1327, 2014.

[73] P. M. Anderson, *Analysis of faulted power systems*. John Wiley and Sons, 1995.

[74] G. V. Moodley, D. Dama, and R. Vajeth, "Consideration of electromagnetic induction during transposition studies". *In proc. 7th AFRICON conference (AFRICON 2004)*, vol. 2, pp. 1065-1070, Africa, 2004.

[75] J. -H. Chen, W. -J. Lee, M. -S. Chen, "Using a static VAR compensator to balance a distribution system", *IEEE Transactions on Industry Applications*, vol. 35, pp. 298-304, 1999.

[76] A. Campos, G. Joos, P. D. Ziogas, J. F. Lindsay, "Analysis and design of a series voltage compensator for three-phase unbalanced sources", *IEEE Transactions on Industrial Electronics*, vol. 39, pp. 159-167, 1992.

[77] K. Li, J. Liu, B. Wei, Z. Wang, "Comparison of two control approaches of static VAR generators for compensating source voltage unbalance in three-phase three-

wire systems", *in the 4th International Power Electronics and Motion Control Conference (IPEMC 2004),* 2004.

[78] T. J. E. Miller, *Reactive power control in electric systems*. New York: Wiley, 1982.

[79] X. Tong, K. Xi, M. Shen, X. Ma, "Reactive power and unbalance compensation with DSTATCOM", *in Proc. of the Eighth International Conference on Electrical Machines and Systems (ICEMS 2005),* 2005.

[80] A. Campos, G. Joos, P. D. Ziogas, J. F. Lindsay, "Analysis and design of a series voltage unbalance compensator based on a three-phase VSI operating with unbalanced switching functions", *IEEE Transactions on Power Electronics*, vol. 9, pp. 269-274, 1994.

[81] A. Campos, G. Joos, J. F. Lindsay, "Dynamic analysis and design of static series compensators for unbalanced AC voltage supplies", *in 1994 IEEE Industry Applications Society Annual Meeting,* 1994.

[82] V. B. Bhavaraju, P. N. Enjeti, "An active line conditioner to balance voltages in a three-phase system", *IEEE Transactions on Industry Applications*, vol. 32, pp. 287-292, 1996.

[83] H. -J. Jung, I. -Y. Suh, B. -S. Kim, R. -Y. Kim, S. -Y. Choi, J. -H. Song, "A study on DVR control for unbalanced voltage compensation", *in 17th Annual IEEE Applied Power Electronics Conference and Exposition (APEC 2002),* 2002.

[84] S. Barsali, E. Giglioli, F. Monachesi, D. Poli, "Compensation of voltage unbalances in LV networks due to single-phase generators", in *4th IEEE/PES Innovative Smart Grid Technologies Europe (ISGT EUROPE),* 2013.

[85] J. G. Pinto, R. Pregitzer, L. F. C. Monteiro, C. Couto, J. L. Afonso, "A combined series active filter and passive filters for harmonics, unbalances and flicker compensation", *in International Conference on Power Engineering, Energy and Electrical Drives (POWERENG 2007),* 2007.

[86] V. B. Bhavaraju, P. N. Enjeti, "Analysis and design of an active power filter for balancing unbalanced loads", *IEEE Transactions on Power Electronics*, vol. 8, pp. 640-647, 1993.

[87] M. Gong, H. Liu, H. Gu, D. Xu, "Active voltage regulator based on novel synchronization method for unbalance and fluctuation compensation ", *in 28th Annual Conference of the Industrial Electronics Society (IEEE IECON 02),* 2002.

[88] D. Graovac, V. Katic, A. Rufer, "Power quality problems compensation with universal power quality conditioning system", *in IEEE Transactions on Power Delivery*, vol. 22, pp. 968-976, 2007.

[89] K. H. Chua, Yun Seng Lim, P. Taylor, S. Morris, J. Wong, "Energy storage system for mitigating voltage unbalance on low-voltage networks with photovoltaic systems", *IEEE Transactions on Power Delivery*, vol. 27, pp. 1783-1790, 2012.

[90] *IEC 61000-2-2: Electromagnetic compatibility (EMC) - part 2.2 - environment - compatibility levels for low-frequency conducted disturbances and signalling in public low-voltage powe supply systems*. Institute of Electrical and Electronics Engineers, 2002.

[91] *IEC 61000-2-12: Electromagnetic compatibility (EMC) - part 2.2 - environment - compatibility levels for low-frequency conducted idturbances and signalling in public mediun-voltage power supply systems*. Institute of Electrical and Electronics Engineers, 2003.

[92] A. Robert and J. Marquet (on behalf of Working Group 36.05), "Assessing voltage quality with relation to harmonics, flicker and unbalance". *In Proc. CIGRE conference*, pp. 36-203, Paris, August-September, 1992.

[93] *Engineering Recommendation P29: Planning limits for voltage unbalance in the United Kingdom*, Energy Networks Association, 1990.

[94] N. C. Woolley, "Identification of weak areas and worst served customers for power quality issues using limited monitoring and non-deterministic data processing techniques", PhD thesis: University of Manchester, 2012.

[95] T. E. Seiphetlho, A. P. J. Rens, "On the assessment of voltage unbalance". *In 14th International Conference on Harmonics and Quality of Power (ICHQP 2010)*, 2010.

[96] R. Yan, T.K. Saha, "Investigation of voltage imbalance due to distribution network unbalanced line configurations and load levels", *IEEE Trans. on Power Delivery*, vol.28, no.2, pp.1829-1838, 2013.

[97] A. F. T. Neto, G. P. L. Cunha, M. V. B. Mendonca, A. L. F. Filho, "A comparative evaluation of methods for analysis of propagation of unbalance in electric systems", *2012 Sixth IEEE/PES Transmission and Distribution: Latin America Conference and Exposition (T&D-LA)*, 2012.

[98] N. C. Woolley, J. V. Milanovic, "Statistical estimation of the source and level of voltage unbalance in distribution networks", *IEEE Transactions on Power Delivery*, vol. 27, pp. 1450-1460, 2012.

[99] P. Paranavithana, S. Perera, R. Koch, Z. Emin, "Global voltage unbalance in MV networks due to line asymmetries", *IEEE Transactions on Power Delivery*, vol. 24, pp. 2353-2360, 2009.

[100] U. Jayatunga, S. Perera and P. Ciufo, "Voltage unbalance emission assessment in radial power systems", *IEEE Trans. on Power Delivery*, vol.27, no.3, pp.1653-1661, 2012.

[101] U. Jayatunga, S. Perera, P. Ciufo, A.P. Agalgaonkar, "Voltage unbalance emission assessment in interconnected power systems", *IEEE Trans. on Power Delivery*, vol.28, no.4, pp.2383-2393, 2013.

[102] S. Khushalani, J. M. Solanki, N. N. Schulz, "Development of three-phase unbalanced power flow using PV and PQ models for distributed generation and study of the impact of DG models", *IEEE Transactions on Power Systems*, vol. 22, pp.1019-1025, 2007.

[103] L. Degroote, B. Renders, B. Meersman, L. Vandevelde, "Neutral-point shifting and voltage unbalance due to single-phase DG units in low voltage distribution networks", *in PowerTech*, 2009.

[104] E. Zraik, Sung Yeul Park, "Influence of voltage unbalance due to single-phase distributed generators in the power distribution systems", in *North American Power Symposium (NAPS)*, 2013.

[105] C. Long, M. E. A. Farrag, D. M. Hepburn, C. Zhou, "Statistical evaluation of voltage unbalance in residential distribution networks with a high penetration level of small wind turbines", in *2nd IET Renewable Power Generation Conference (RPG 2013)*, 2013.

[106] F. Shahnia, R. Majumder, A. Ghosh, G. Ledwich, F. Zare, "Voltage imbalance analysis in residential low voltage distribution networks with rooftop PVs", *Electric Power Systems Research*, vol. 81, pp. 1805-1814, 2011.

[107] M. H. Bollen, F. Hassan, *Integration of distributed generation in the power system*, Wiley, 2011.

[108] M. H. Ashourian, A. A. M. Zin, A. S. B. Mokhtar, Z. bt Muda, "Steady-state behavior of distributed energy resources in unbalance radial active distribution networks" *IEEE International Conference on Power and Energy (PECon 2010)*, 2010.

[109] A. Cziker, M. Chindris, A. Miron, "Voltage unbalance mitigation using a distributed generator", *11th International Conference on Optimization of Electrical and Electronic Equipment (OPTIM 2008)*, 2008.

[110] P. Paranavithana, S. Perera, R. Koch, "An improved methodology for determining MV to LV voltage unbalance transfer coefficient", *13th Conference on International Harmonics and Quality of Power (ICHQP 2008)*, 2008.

[111] P. Paranavithana, S. Perera, R. Koch, "Propagation of voltage unbalance from HV to MV power systems", *20th International Conference and Exhibition on Electricity Distribution (CIRED 2009)*, 2009.

[112] M. Chindris, A. Cziker, A. Miron, H. Balan, A. Iacob, A. Sudria, " Propagation of unbalance in electric power systems", *9th International Conference on Electrical Power Quality and Utilisation (EPQU 2007)*, 2007.

[113] A. Abur and A. G. Exposito, *Power system state estimation*, Marcel Dekker, 2004.

[114] C. N. Lu, J. H. Teng, and W. H. E. Liu, "Distribution system state estimation," *IEEE Transactions on Power Systems*, vol. 10, No. 1, pp. 229-240, 1995.

[115] K. Li, "State estimation for power distribution systems and measurement impacts," *IEEE Transactions on Power Systems*, vol. 11, No. 2, pp. 911-916, 1996.

[116] C. W. Hansen, "Power system state estimation using three-phase models," *IEEE Transactions on Power Systems*, vol. 10, No. 2, pp. 818-824, 1995.

[117] B. Gou and A. Abur, "A direct numerical method for observability analysis," *IEEE Transactions on Power Systems*, vol. 15, No. 2, pp. 625-630, 2000.

[118] B. Xu and A. Abur, "Observability analysis and measurement placement for systems with PMUs," in *Power Systems Conference and Exposition*, 2004.

[119] M. E. Baran and A. W. Kelley, "State estimation for real-time monitoring of distribution systems," *IEEE Transactions on Power Systems*, vol. 9, No. 3, 1994.

[120] E. Manitsas, R. Singh, B. Pal, G. Strbac, "Modelling of pseudo-measurements for distribution system state estimation", *in seminar of International Conference on Electricity Distribution (CIRED)*, Frankfurt, 2008.

[121] R. Singh, B. C. Pal, and R. A. Jabr, "Distribution system state estimation through gaussian mixture model of the load as pseudo-measurement," *IET Generation, Transmission and Distribution*, vol. 4, No. 1, pp. 50-59, 2009.

[122] A. K. Ghosh, D. L. Lubkeman, M. J. Downey, and R. H. Jones, "Distribution circuit state estimation using a probabilistic approach," *IEEE Transactions on Power Systems*, vol. 12, No. 1, pp. 45-51, 1997.

[123] R. Singh, B. C. Pal, and R. B. Vinter, "Measurement placement in distribution system state estimation," *IEEE Transactions on Power Systems*, vol. 24, No. 2, 2009.

[124] V. Thornley, N. Jenkins, and S. White, "State estimation applied to active distribution networks with minimal measurements," in *15th Power Systems Computational Conference*, 2005.

[125] Y. Moon, Y. H. Moon, J. B. Choo, and T. W. Kwon, "Design of reliable measurement system for state estimation," *IEEE Transactions on Power Systems*, vol. 3, No. 3, pp. 830-836, 1988.

[126] J. Coser, A. S. Costa, and J. G. Rolim, "Metering scheme optimization with emphasis on ensuring bad-data processing capability," *IEEE Trans. on Power Systems*, vol. 21, pp. 1903-1911, 2006.

[127] B. Gou, "Optimal placement of PMUs by integer linear programming," *IEEE transactions on Power Systems*, vol. 23, No. 3, pp. 1525-1526, 2008.

[128] N. H. Abbasy and H. M. Ismail, "A unified approach for the optimal PMU location for power system state estimation," *IEEE Trans. on Power Systems*, vol. 24, pp. 806-813, 2009.

[129] L. Haijun, D. Yu, and C. Hsiao-Dong, "A heuristic meter placement method for load estimation," *IEEE Trans. on Power Systems*, vol. 17, pp. 913-917, 2002.

[130] I. Kamwa and R. Grondin, "PMU configuration for system dynamic performance measurement in large, multiarea power systems," *IEEE Trans. on Power Systems*, vol. 17, pp. 385-394, 2002.

[131] G. Olguin, F. Vuinovich, M.H.J. Bollen, "An optimal monitoring program for obtaining voltage sag system indexes", *IEEE Transactions on Power Delivery*, vol. 21, pp. 378-384, 2006.

[132] C. Madtharad, S. Premrudeepreechacharn, N. R. Watson, and R. S. Udom, "An optimal measurement placement method for power system harmonic state estimation," *IEEE Transactions on Power Systems*, vol. 20, No. 2, 2005.

[133] J. M. A. Mora, "Monitor placement for estimation of voltage sags in power systems", PhD thesis: University of Manchester, 2012.

[134] M. Avendano-Mora and J. V. Milanović, "Monitor placement for reliable estimation of voltage sags in power networks," *IEEE Trans. on Power Delivery*, vol. 27, pp. 936-944, 2012.

[135] R. K. Hartana and G. G. Richards, "Harmonic source monitoring and identification using neural networks," *IEEE Trans. on Power Systems*, vol. 5, pp. 1098-1104, 1990.

[136] Y. Liao, "Fault location observability analysis and optimal meter placement based on voltage measurements", *Electric Power Systems Research*, vol. 79, pp. 1062-1068, 2009.

[137] A. A. Bei Xu, "Optimal placement of phasor measurement units for state estimation," Texas A&M University 2005.

[138] B. Milosevic and M. Begovic, "Nondominated sorting genetic algorithm for optimal phasor measurement placement," *IEEE Transactions on Power Systems*, vol. 18, No. 1, pp. 69-75, 2003.

[139] J. C. S. De Souza, M. Brown Do Coutto Filho, M. T. Schilling, and C. de Capdeville, "Optimal metering systems for monitoring power networks under multiple topological scenarios," *IEEE Trans. on Power Systems*, vol. 20, pp. 1700-1708, 2005.

[140] M. R. Haghifam and O. P. Malik, "Genetic algorithm-based approach for fixed and switchable capacitors placement in distribution systems with uncertainty and time varying loads," *IET Generation, Transmission & Distribution*, vol. 1, pp. 244-252, 2007.

[141] Y. H. Song, *Modern optimisation techniques in power systems*. Dordrecht, Netherlands: Kluwer Academic Publishers, 1999.

[142] J. Arrillaga, N. R. Watson, *Computer modelling of power systems*: John Wiley & Sons, 2001.

[143] J. Machowski, J. W. Bialek, and J. R. Bumby, *Power system dynamics: stability and control*, 2nd ed.: John Wiley & Sons Ltd, 2008.

[144] S. M. Zali, "Equivalent dynamic model of distribution network with distributed generation", PhD thesis: University of Manchester, 2012.

[145] C. M. Kuan, "Generalized least squares theory," in Introduction to Econometric Theory: Institute of Economics, Academia Sinica, Taipei 115, Taiwan, 2004.

[146] Y. J. Wang, "Modelling of random variation of three-phase voltage unbalance in electric distribution systems using the trivariate Gaussian distribution," IEE Proceedings of Generation, Transmission and Distribution, vol. 148, pp. 279-284, 2001.

[147] P. Caramia, G. Carpinelli, V. Di Vito, and P. Varilone, "Probabilistic techniques for three-phase load flow analysis," in *Power Tech Conference*, 2003.

[148] P. Caramia, G. Carpinelli, M. Pagano, and P. Varilone, "Probabilistic three-phase load flow for unbalanced electrical distribution systems with wind farms," *in IET Renewable Power Generation*, vol. 1, pp. 115-122, 2007.

[149] Siemens, "9610 Power quality meter," 2011, [Online] available: http://bit.ly/xnC1nG.

[150] Y. Zhang, "Techno-economic assessment of voltage sag performance and mitigation", PhD thesis: University of Manchester, 2008.

[151] EPRI Power Electronics applications Center, *Input performance of ASDs during supply voltage unbalance*, Power Quality Testing Network PQTN Brief 28, 1996.

[152] A. J. Collin, I. Hernando-Gil, J. L. Acosta, S. Z. Djokic, "An 11 kV steady state residential aggregate load model. Part 1: aggregation methodology", *in 9th PowerTech*, 2011.

[153] S. Djokic, "Steady-state models of low energy consumption light sources", *in 16th Power System Computation Conference (PSCC)*, 2008.

[154] C. Cresswell, S.Djokic, "Representation of directly connected and drive-controlled induction motors. Part 1: single-phase load models", *in 18th International Conference on Electrical Machines*. 2008.

[155] C. Cresswell, S.Djokic, "Representation of directly connected and drive-controlled induction motors. Part 2: three-phase load models", *in 18th International Conference on Electrical Machines*. 2008.

[156] *CIGRE Working Group C4.605: Modelling and aggregation of loads in flexible power networks*, International Council on Large Electric Systems, 2012.

[157] L. M. Korunovic, D. P. Stojanovic, J. V. Milanovic, "Identification of static load characteristics based on measurements in medium-voltage distribution network," *in IET Generation, Transmission & Distribution*, vol. 2, pp. 227-234, 2008.

[158] L. M. Korunovic, D. P. Stojanovic, "Dynamic load modelling of some low voltage devices", *in Electronics and Energetics*, vol. 22, pp. 61-70, 2009.

[159] PV Education, "Calculation of solar insolation", [Online], available: http://www.pveducation.org/pvcdrom/properties-of-sunlight/calculation-of-solar-insolation

[160] EMS, "Embedded monitoring systems - sub.net," 2011, [Online], available: http://www.emsni.com/.

[161] S. Sivanagaraju, *Electric power transmission and distribution*: Pearson Education India, 2008.

[162] R. E. Fehr, "Sequence impedances of transmission lines," 2004. [Online], available: http://helios.acomp.usf.edu/~fehr/carson.pdf.

[163] N. N. Mirolyubov, "On transmission line electrical asymmetry," *Proceedings of LPI*, 1948.

[164] M. n. N. A, *Elektricheskie seti i sistemy*. Moscow, 1975.

[165] SAGoE. EMFs, "SAGE recommendations on phasing of overhead lines," 2001.

[166] W. H. Kersting, *Distribution system modelling and analysis*. Boca Raton, FL: CRC, 2007.

[167] *BS162:1961: Specification for electric power switchgear and associated apparatus*. British Standard, 1961.

[168] "PowerLogic PM700 series," Schneider Electric, Ed., 2011, [Online], available: http://www.powerlogic.com/literature/3020HO0701.pdf.

[169] GE, "EPM 9650 power quality meter," 2011, [Online], available: http://www.gedigitalenergy.com/multilin/catalog/epm9650.htm.

[170] D. E. Goldberg, *Genetic algorithms in search, optimization, and machine learning*: Addison Wesley Longman, Inc., 1953.

[171] M. Zbigniew, *Genetic algorithms + data structures = evolution programs*: Springer, 1992.

[172] M. B. Hughes, "Revenue metering error caused by induced voltage from adjacent transmission lines", *IEEE Transactions on Power Delivery*, Vol.7, pp. 741-745, 1992.

[173] M. T. Bina, E. P. Javid, "A critical overview on zero sequence component compensation in distorted and unbalanced three-phase four-wire systems", *in Proc. International Power Engineering Conference (IPEC 2007)*, pp. 1167-1172, 2007.

[174] A. D. Kolagar, P. Hamedani, A. Shoulaie, "The effects of transformer connection type on voltage and current unbalance propagation", *in 3rd Power Electronics and Drive Systems Technology (PEDSTC)*, 2012.

9 APPENDIX

Appendix A: COMPARISON OF RESULTS FROM DIGSILENT AND MATLAB

The VUFs of an arbitrary general case are listed in Table 9.1 to show the difference between the results from DIgSILENT PowerFactory and Matlab by using the 24-bus network. In this case, the average difference is 4.4% in VUF. The difference usually varies between 2% and 7%, and has an average of about 4.5%.

Table 9.1 Comparison of Results from DIgSILENT and Matlab

Bus Number	DIgSILENT VUF	Matlab VUF	Relative Error
1	0	0	0.00%
2	0.009475	0.009051	4.48%
3	0.009148	0.009114	0.37%
4	0.010329	0.009809	5.04%
5	0.010857	0.010307	5.07%
6	0.006055	0.005705	5.77%
7	0.013696	0.013017	4.95%
8	0.009692	0.009232	4.74%
9	0.006055	0.005704	5.80%
10	0.003903	0.003544	9.19%
11	0.000620	0.000597	3.78%
12	0.008135	0.007842	3.60%
13	0.009619	0.009184	4.53%
14	0.013887	0.013586	2.17%
15	0.015399	0.014998	2.60%

16	0.010225	0.009910	3.09%
17	0.014643	0.014390	1.73%
18	0.010853	0.010342	4.70%
19	0.009864	0.009332	5.39%
20	0.009551	0.009253	3.12%
21	0.006192	0.005758	7.02%
22	0.003830	0.003591	6.26%
23	0.000889	0.000803	9.63%
24	0.009428	0.009185	2.58%
Average			4.40%

Appendix B: MATLAB PROGRAMMING CODE FOR DNSE

```
% Example of DNSE Process

% Network Configuration: read network data
[baseMVA, bus, gen, branch] = CaseEONMeafordWithTransformers;

% Load Variation: to make three-phase unbalanced loads. This may vary
from case to case, depending on the aim of the simulation.
factorIncreaseP = 1.3;
factorIncreaseQ = 1.3;
unbalancedBuses = 15:24;
bus(unbalancedBuses,3) = bus(unbalancedBuses,3)*factorIncreaseP;
bus(unbalancedBuses,6) = bus(unbalancedBuses,6)*factorIncreaseQ;
factorDecrease = (3-factorIncreaseP)/2;
bus(unbalancedBuses,[4 5]) = bus(unbalancedBuses,[4 5])*factorDecrease;
bus(unbalancedBuses,[7 8]) = bus(unbalancedBuses,[7 8])*factorDecrease;

% Configuration for Load Flow
numberMCs = 1;
metersPF = Meters(branch);
metersPF.BusMeters = [bus(2:size(bus,1),1) 1e-15*ones(size(bus,1)-
1,2)];
bus = repmat(bus,[1 1 numberMCs]);
branch = repmat(branch,[1 1 numberMCs]);

% Three-phase load flow
[busPF branchPF ExPF xPF G B AllBranchFlowsPF convergenceIssuesPF
AllCurrentFlowsPF transformersPF] = SE3PHASEMC(bus, branch, metersPF,
'CaseEONMeaford1PhaseWithTransformers');

% Read data from load flow results
network = NetworkAnalyser(branchPF, busPF, AllCurrentFlowsPF);
negSeqPowers = network.SequencePowers(:,3,:)*100;
posSeqPowers = network.SequencePowers(:,2,:)*100;
percentRatio = abs(negSeqPowers)./abs(posSeqPowers)*100;
BASECASENegSeq =
(abs(negSeqPowers(15:24,:))./abs(posSeqPowers(15:24,:)))'*100;
BASECASEVUF = busPF(:,17)';

% Configuration for state estimation including confirmation of monitor
location. The monitor location may change due to different aims of the
simulations.
numberMCs = 100;
metersSE = Meters(branchPF, busPF);
meters = [1 2 4 14 15 16 24];
metersSE.addRealMeter(meters);
phaseAMeters = setdiff([15 16 17 18 19 20 21 22 23 24], meters);
metersSE.addPhaseAMeter(phaseAMeters);
virtualMeters = [2 3 4 5 6 7 8 9 10 11 12 13 14];
for j=1:length(virtualMeters),
metersSE.addVirtualMeter(virtualMeters(j), [1 2 3]); end
[busSE branchSE] = metersSE.generateMCPowers(busPF,numberMCs,branchPF);
busSE = metersSE.generateMCPowersFromPhaseA(phaseAMeters, busPF,
busSE);
```

```
% Three-phase state estimation: the results of monitored buses will be
automatically read from load flow results.
[busSE branchSE ExSE xSE G B AllBranchFlowsSE convergenceIssuesSE
AllCurrentFlowsSE transformersSE] = SE3PHASEMC(busSE, branchSE,
metersSE, 'CaseEONMeaford1PhaseWithTransformers',100, transformersPF,
1);

% Read data from state estimation results
network = NetworkAnalyser(branchSE, busSE, AllCurrentFlowsSE);
negSeqPowers = collapse(network.SequencePowers(:,3,:)*100);
posSeqPowers = collapse(network.SequencePowers(:,2,:)*100);
VUF = collapse(busSE(:,17,:));
sequenceFlows = network.SequenceFlows;
negSequenceFlowsFrom = collapse(sequenceFlows(:,3,:));

% Plot result
figure,boxplot(VUF');
grid on
ylabel('VUF (%)');
xlabel('Bus Number');
```

Appendix C: NETWORK DATA

C.1 24-BUS NETWORK DATA

This network receives power from bus 1 which is an ideal power supply. The loading data of the network are shown in Table 9.2. The line data (including transformers) are shown in Table 9.3.

Table 9.2 24-Bus Network Loading Data

Bus Number	15	16	17	18	19	20	21	22	23	24
P (MW)	21.876	3.574	3.848	1.532	2.929	3.212	1.73	3.308	22.067	3.36
Q (MVar)	5.484	0.896	0.964	0.384	0.734	0.805	0.433	0.829	5.531	0.842

Table 9.3 24-Bus Network Line Data

From Bus	To Bus	R_1	X_1	B_1	R_0	X_0	Transformer Type
1	11	0.0010	0.0050	0.0000	0.0000	0.0000	-
11	10	0.1025	0.2022	0.0005	0.2429	0.5697	-
10	9	0.0607	0.1260	0.0014	0.2392	0.5115	-
9	6	0.0147	0.0338	0.0002	0.0400	0.1514	-
9	2	0.0816	0.1921	0.0007	0.1793	0.8943	-
2	3	0.1419	0.1813	0.0011	0.2577	0.6873	-
2	14	0.0796	0.2186	0.0038	0.2125	1.0687	-
2	14	0.0796	0.2186	0.0038	0.2125	1.0687	-
2	4	0.2905	0.3930	0.0007	0.4578	1.7081	-
4	5	0.2494	0.3115	0.0008	0.4043	1.4150	-
5	7	0.2067	0.2436	0.0003	0.3081	1.0770	-
5	13	0.0927	0.1261	0.0003	0.1543	0.5409	-
13	8	0.1235	0.1331	0.0001	0.1710	0.5039	-
13	12	0.1294	0.1394	0.0001	0.1792	0.5280	-
12	2	0.1518	0.1635	0.0003	0.2166	0.6162	-
12	11	0.2321	0.5912	0.0005	0.5209	1.6368	-
11	2	0.2371	0.4811	0.0017	0.4923	2.3123	-
14	15	0.0442	0.9950	-	0.0191	-0.0393	DY11
14	15	0.0449	0.9917	-	0.0191	-0.0393	DY11
4	16	0.1558	1.6400	-	0.0000	0.0000	DY11
4	16	0.1588	1.6120	-	0.0000	0.0000	DY11
7	17	0.0998	1.1134	-	0.0000	-0.0877	DY11
5	18	0.0935	1.0667	-	0.0000	0.0000	DY11
8	19	0.0719	1.0821	-	0.0000	0.0000	DY11
3	20	0.0800	1.3240	-	0.0604	-0.0044	DY11
6	21	0.2778	2.1967	-	0.0000	-0.5059	DY11
10	22	0.0900	1.0667	-	0.0475	-0.0021	DY11
11	23	0.0443	1.0912	-	0.0000	0.0000	DY11

11	23	0.0407	1.1039	-	0.0000	0.0000	DY11
2	24	0.1001	1.2110	-	0.0000	0.0000	DY11

C.2 295-BUS NETWORK DATA

This network receives power from bus 300 (the bus number is not continuous) which is an ideal power supply. The bus data of the network are shown in Table 9.4. The line data (including transformers) are shown in Table 9.5.

Table 9.4 295-Bus Network Bus Data

Bus Number	P	Q	V	angle
1	0.2407	0.0392	0.9659	-5.49
2	0.1033	0.0149	0.9645	-5.52
3	0	0	0.9622	-5.55
4	0.8932	0.013	0.9646	-5.51
5	0.1699	0.0279	0.9637	-5.52
6	0.0473	0.0121	0.9632	-5.53
7	0.1474	0.0213	0.963	-5.53
8	0	0	0.9629	-5.53
9	0.0111	0.0019	0.9629	-5.53
10	0	0	0.9628	-5.53
11	0.1066	0.0185	0.9628	-5.53
12	0.102	0.0159	0.9953	-8.58
13	0.0872	0.0127	0.9896	-8.63
14	0.1731	0.0298	0.9975	-8.56
15	0	0	0.9991	-8.55
16	0.0299	0.008	0.9988	-8.55
17	0.016	0.005	0.9989	-8.55
18	0	0	0.999	-8.55
19	0.0361	0.005	1.0018	-8.52
20	0	0	1.0063	-8.48
21	0.0152	0.002	1.0062	-8.49
22	0.4105	0.0819	1.0118	-8.43
23	0	0	0.9804	-8.7
24	0.7024	0.1576	0.9803	-8.7
25	0	0	0.9597	-5.57
26	0	0	0.9757	-8.76
27	0	0	0.9594	-5.58
28	0	0	0.975	-8.77
29	0.5936	0.1395	0.9579	-5.58
30	0.0786	0.0256	0.9559	-5.58
31	0.4062	0.0881	0.9532	-5.57
32	0	0	0.9534	-5.57
33	0	0	0.9534	-5.57
34	0.6605	0.149	0.9531	-5.57

35	0.1326	0.0327	0.9531	-5.57
36	0.0391	0.0127	0.9531	-5.57
37	0.3897	0.0974	0.9542	-9.2
38	0.1095	0.0219	0.9554	-9.21
39	0.673	0.2149	0.9563	-9.21
40	0.7774	0.25	0.9569	-9.18
41	0.2059	0.0506	0.9588	-9.18
42	0.1184	0.0268	0.9617	-9.19
43	0.3977	0.0957	0.9639	-9.19
44	0.3127	0.0576	0.9719	-8.77
45	0.4198	0.0946	0.9724	-8.77
46	0	0	0.971	-8.82
47	0	0	0.971	-8.82
48	0.2733	0.0603	0.9708	-8.82
49	0.4437	0.1055	0.9706	-8.82
50	0.2681	0.0424	1.0175	-8.39
51	0.4793	0.0878	1.0164	-8.42
52	0	0	1.0171	-8.43
53	0.4992	0.0806	1.0167	-8.44
54	0.6236	0.1264	1.0178	-8.34
55	0.3901	0.0812	0.966	-5.49
56	0.1188	0.0187	0.9674	-5.47
57	0.1646	0.0273	0.9698	-5.42
58	0.5276	0.1371	0.9724	-5.38
59	0.6552	0.1307	0.973	-5.48
60	0.7942	0.1471	0.9741	-5.33
61	0.283	0.0492	0.9729	-5.48
62	0.1565	0.0245	0.9711	-5.4
63	0.4096	0.0733	0.9693	-5.43
64	0.2411	0.0413	0.9686	-5.44
65	0.44	0.0758	0.9676	-5.44
66	0.8287	0.1574	0.965	-5.43
67	0	0	0.9619	-5.56
68	0	0	0.9619	-5.56
69	0.0167	0.0028	0.9618	-5.56
70	0	0	0.9619	-5.56
71	0.1628	0.0314	0.9617	-5.56
72	0	0	0.9619	-5.56
73	0.0231	0.0037	0.9619	-5.56
74	0	0	1.0148	-8.46
75	0.4166	0.0669	1.0142	-8.47
76	0.7046	0.1391	1.015	-8.45
77	0	0	1.013	-6.64
78	0.1007	0.0147	1.0244	-7.6
79	0.4065	0.0721	1.0222	-7.64
80	0.789	0.254	1.0203	-7.67
81	0	0	1.0139	-7.61
82	0	0	1.0138	-7.62
83	0.037	0.0051	1.0134	-7.63
84	0.0308	0.0041	1.0132	-7.63
85	0	0	1.0129	-7.64

86	0.1251	0.0236	1.0126	-7.65
87	0.9032	0.163	1.0254	-7.66
88	0	0	1.013	-7.62
89	1.1915	0.3914	1.0122	-7.63
91	0	0	1.0123	-7.64
92	0	0	1.0116	-7.68
93	0.044	0.0072	1.0115	-7.68
94	0	0	1.0114	-7.7
95	0.0082	0.001	1.011	-7.7
96	0	0	1.0103	-7.71
97	0.0367	0.0061	1.0103	-7.72
98	0	0	1.0099	-7.72
99	0.0163	0.002	1.0097	-7.72
100	0.0825	0.0163	1.0094	-7.73
101	0.0734	0.0143	1.0097	-7.73
102	0	0	1.0106	-7.74
103	0.0663	0.0112	1.0103	-7.74
104	0.0092	0.001	1.0103	-7.75
105	0	0	1.0099	-7.77
106	0.0235	0.0031	1.0099	-7.77
107	0.0387	0.0061	1.0095	-7.78
108	0.0183	0.0031	1.009	-7.8
109	0	0	1.0087	-7.81
110	0	0	1.0086	-7.81
111	0.1291	0.0315	1.0083	-7.81
112	0.0203	0.0031	1.0085	-7.82
113	0	0	1.0084	-7.82
114	0.0061	0.0009	1.0083	-7.82
115	0.0102	0.001	1.0083	-7.83
116	0	0	1.0079	-7.84
117	0.0061	0.0009	1.0078	-7.84
118	0	0	1.0078	-7.84
119	0.0051	0.0007	1.0078	-7.84
120	0.0081	0.001	1.0078	-7.84
121	0	0	1.0078	-7.84
122	0	0	1.0078	-7.84
123	0	0	1.0078	-7.84
124	0	0	1.0078	-7.84
125	0.0091	0.001	1.0076	-7.84
126	0.0233	0.0071	1.0074	-7.84
127	0.0071	0.001	1.0073	-7.84
128	0.0203	0.003	1.0073	-7.85
129	0	0	0.9791	-7.67
130	0.0431	0.0077	0.9791	-7.67
131	0	0	0.9792	-7.67
132	0.0353	0.0048	0.9767	-7.71
133	0.018	0.0028	0.9744	-7.75
134	0.017	0.0028	0.971	-7.81
135	0	0	0.9699	-7.84
136	0.0094	0.0009	0.9699	-7.84
137	0.8682	0.2853	0.9657	-7.96

138	0	0	0.9657	-7.96
139	0	0	0.9808	-7.64
140	0.0096	0.0019	0.9808	-7.64
141	0	0	0.9841	-7.58
142	0.0213	0.0068	0.984	-7.58
143	0	0	0.9871	-7.53
144	0.0029	0.0004	0.9871	-7.53
145	0.0029	0.0004	0.9896	-7.48
146	0	0	0.9935	-7.42
147	0	0	0.9966	-7.35
148	0.0189	0.003	0.9965	-7.35
149	0	0	1.0029	-7.21
150	0.0201	0.003	1.0028	-7.21
151	0	0	1.0083	-7.03
152	0.0091	0.001	1.0083	-7.03
153	0	0	0.9903	-7.48
154	0.0206	0.0039	0.9902	-7.48
155	0	0	0.9865	-7.55
156	0.0127	0.0019	0.9865	-7.55
157	0	0	0.9837	-7.59
158	0.0348	0.0058	0.9835	-7.59
159	0.0203	0.0029	0.9834	-7.59
160	0.0183	0.0029	0.9825	-7.62
161	0	0	0.9791	-7.7
162	0.0345	0.0048	0.9788	-7.71
163	0.1312	0.0316	0.9785	-7.71
164	0.0048	0.0007	0.9785	-7.71
165	0.0076	0.001	0.9764	-7.78
166	0	0	0.9754	-7.81
167	0	0	0.9752	-7.81
168	0.02	0.0029	0.9752	-7.81
169	0.039	0.0076	0.9749	-7.81
170	0	0	0.9747	-7.81
171	0	0	0.9691	-8.01
172	0	0	0.9689	-8.01
173	0.1116	0.0225	0.9684	-8.02
174	0	0	0.9683	-8.02
175	0.0347	0.0047	0.9683	-8.02
176	0	0	0.9682	-8.02
177	0.0356	0.0066	0.9681	-8.03
178	0	0	0.9681	-8.03
179	0	0	0.9597	-5.57
180	0	0	0.9746	-7.81
181	0	0	0.9745	-7.82
182	0.0085	0.0009	0.9744	-7.82
183	0	0	0.9742	-7.82
184	0.0114	0.0209	0.9741	-7.81
185	0	0	0.974	-7.82
186	0.019	0.0028	0.9739	-7.82
187	0.0398	0.0085	0.9737	-7.82
188	0	0	0.9743	-7.84

189	0	0	0.9743	-7.84
190	0.0047	0.0065	0.9743	-7.84
191	0.0047	0.0007	0.9743	-7.84
192	0.0047	0.0007	0.9743	-7.84
193	0.018	0.0028	0.9726	-7.9
194	0	0	0.9719	-7.91
195	0.0085	0.0009	0.9719	-7.91
196	0.0085	0.0009	0.9718	-7.91
197	0.0151	0.0028	0.9717	-7.91
198	0	0	0.9713	-7.92
199	0.016	0.0019	0.9713	-7.92
200	0.017	0.0028	0.9711	-7.93
201	0.0226	0.0047	0.9708	-7.93
202	0	0	0.9706	-7.94
203	0.0198	0.0028	0.9705	-7.94
204	0.0075	0.0009	0.9703	-7.94
205	0	0	0.9702	-7.95
206	0	0	0.9701	-7.95
207	0	0	0.97	-7.95
208	0.0075	0.0009	0.97	-7.95
209	0.0442	0.0094	0.9698	-7.95
210	0	0	0.9715	-7.93
211	0	0	0.971	-7.95
212	0	0	0.971	-7.95
213	0	0	0.9709	-7.95
214	0.032	0.0047	0.9707	-7.95
215	0	0	0.9703	-7.97
216	0	0	0.9703	-7.97
217	0	0	0.9696	-7.99
218	0.0789	0.0197	0.9691	-8
219	0	0	0.9688	-8.01
220	0.0619	0.0094	0.9687	-8.01
221	0	0	1.0166	-8.41
222	0	0	0.9678	-9.19
223	0.9151	0.1797	1.0192	-8.36
224	0	0	1.0121	-6.66
225	0.6706	0.1313	1.0126	-6.68
226	17.0941	3.069	0.9761	-5.3
227	0	0	0.9761	-5.3
228	2.4472	0.4207	1.0205	-8.32
229	0	0	1.0205	-8.32
230	0	0	1.0273	-7.53
231	1.8787	0.3504	1.0273	-7.53
232	0.9612	0.1756	1.0134	-6.62
233	68.8649	14.4206	0.988	-2.12
234	0	0	0.988	-2.12
235	0	0	1.0343	23.78
236	0	0	1.0343	23.78
237	0	0	1.0112	24.49
238	0	0	1.0343	23.78
239	0	0	1.0343	23.78

240	3.4953	0.7065	0.9751	25.45
241	0	0	1.0125	25.17
242	31.783	8.8286	1.0323	23.69
243	28.0839	5.4088	1.0088	24.62
244	0	0	1.0088	24.62
245	14.6242	2.3698	1.0144	24.72
246	0	0	1.0144	24.72
247	40.7015	8.7496	0.9719	24.23
248	0	0	0.9719	24.23
249	26.1959	5.3742	1.0358	23.82
250	0	0	1.0358	23.82
251	0	0	1.0157	24.73
252	0	0	1.0191	24.35
253	0	0	0.9906	-1.92
254	68.3597	12.1889	0.9874	-2.3
255	0	0	0.9874	-2.3
256	0	0	0.991	-1.86
257	0	0	0.991	-1.86
258	42.9038	9.161	0.986	-2.1
259	0	0	0.986	-2.1
260	0	0	1.0173	24.54
261	0	0	1.0173	24.54
262	0	0	0.9872	-2.25
263	0	0	0.9901	-1.89
264	0	0	0.9901	-1.89
265	0	0	0.9727	25.2
266	0	0	1.0341	23.78
267	0	0	1.0341	23.78
268	0	0	1.0294	23.68
269	0	0	1.0294	23.68
270	0	0	0.9814	-2.16
271	0	0	0.9865	-2.18
272	0	0	0.9812	-2.16
273	0	0	0.985	-2.18
274	0	0	0.9907	-1.9
275	0	0	0.9909	-2.03
276	0	0	0.9864	-2.18
277	0	0	0.9892	-2.15
278	0	0	0.9892	-2.15
279	0	0	0.99	-2.04
280	0	0	0.99	-2.04
285	0	0	1.0126	22.37
286	0	0	1.0126	22.37
287	0	0	0.9826	53.78
288	0	0	0.9826	53.78
289	0	0	1.0173	54.54
290	0	0	1.0126	-7.63
291	0	0	1.0126	-7.63
292	0	0	0.9987	-0.19
293	0	0	0.9987	-0.19
294	0	0	0.9987	-0.5

295	0	0	0.9996	-0.08
296	0	0	0.9993	-0.12
297	0	0	0.9993	-0.12
298	0	0	0.9992	-0.13
299	0	0	0.9992	-0.13
300	0	0	1	0

Table 9.5 295-Bus Network Line Data

From Bus	To Bus	R_1	X_1	B	Transformer
233	234	0.0000	0.0000	0.0000	0
233	279	0.0084	0.0060	0.0014	0
279	257	0.0010	0.0074	0.0017	0
234	280	0.0084	0.0060	0.0014	0
280	256	0.0010	0.0074	0.0017	0
257	256	0.0000	0.0000	0.0000	0
280	277	0.0014	0.0099	0.0023	0
279	278	0.0014	0.0099	0.0023	0
248	247	0.0000	0.0000	0.0000	0
254	255	0.0000	0.0000	0.0000	0
234	254	0.0039	0.0276	0.0063	0
233	255	0.0039	0.0276	0.0063	0
257	264	0.0059	0.0044	0.0339	0
256	263	0.0059	0.0044	0.0339	0
227	226	0.0000	0.0000	0.0000	0
227	58	0.1249	0.0740	0.0003	0
58	62	0.0564	0.0216	0.0001	0
62	63	0.0847	0.0412	0.0001	0
62	61	0.0940	0.0360	0.0001	0
61	59	0.0294	0.0198	0.0001	0
59	60	0.0600	0.2760	0.0001	0
60	227	0.1050	0.0483	0.0001	0
63	64	0.0424	0.0206	0.0001	0
64	60	0.3542	0.0522	0.0001	0
226	57	0.1271	0.0618	0.0002	0
57	56	0.0494	0.0240	0.0001	0
56	55	0.0283	0.0137	0.0000	0
64	65	0.2180	0.0321	0.0001	0
61	55	0.0940	0.0360	0.0001	0
65	55	0.1350	0.0621	0.0002	0
64	66	0.4087	0.0602	0.0001	0
66	67	0.0470	0.0180	0.0001	0
67	68	0.0917	0.1626	0.0000	0
68	69	0.0752	0.0288	0.0001	0
68	70	0.0765	0.1355	0.0000	0
70	71	0.1128	0.0431	0.0001	0
70	72	0.0343	0.0231	0.0001	0
72	73	0.0841	0.1491	0.0000	0
72	3	0.1200	0.0552	0.0002	0

3	2	0.0975	0.0449	0.0001	0
2	55	0.0600	0.0276	0.0001	0
55	1	0.0545	0.0080	0.0000	0
3	74	0.0188	0.0072	0.0000	0
74	75	0.1316	0.0503	0.0013	0
74	76	0.0565	0.0275	0.0001	0
3	179	0.1128	0.0431	0.0001	0
179	25	0.0000	0.0000	0.0000	0
25	26	0.0000	0.0000	0.0000	0
27	28	0.0000	0.0000	0.0000	0
179	26	0.0000	0.0000	0.0000	0
25	27	0.0147	0.0099	0.0000	0
26	28	0.0147	0.0099	0.0000	0
55	4	0.1025	0.0264	0.0001	0
4	5	0.1757	0.0453	0.0001	0
5	6	0.1464	0.0377	0.0001	0
6	7	0.0752	0.0288	0.0001	0
7	8	0.0564	0.0216	0.0001	0
8	9	0.0752	0.0288	0.0001	0
8	10	0.0470	0.0180	0.0001	0
10	11	0.0188	0.0079	0.0000	0
10	12	0.3269	0.0482	0.0001	0
12	14	0.0376	0.0144	0.0000	0
12	13	0.1034	0.0396	0.0010	0
13	23	0.1692	0.0647	0.0002	0
24	23	0.0188	0.0072	0.0000	0
23	26	0.0989	0.0481	0.0002	0
27	29	0.0732	0.0189	0.0000	0
29	30	0.1362	0.0201	0.0000	0
30	32	0.1907	0.0281	0.0000	0
32	31	0.0282	0.0108	0.0000	0
32	33	0.0000	0.0000	0.0000	0
33	34	0.0282	0.0108	0.0000	0
33	35	0.1171	0.0302	0.0001	0
35	36	0.1090	0.0161	0.0000	0
36	37	0.3269	0.0482	0.0001	0
37	38	0.2724	0.0401	0.0001	0
38	39	0.1635	0.0241	0.0000	0
28	46	0.0989	0.0481	0.0002	0
46	48	0.0817	0.0120	0.0000	0
47	46	0.0000	0.0000	0.0000	0
47	49	0.0817	0.0120	0.0000	0
28	45	0.3269	0.0482	0.0001	0
45	44	0.1464	0.0377	0.0001	0
44	222	0.0732	0.0189	0.0000	0
222	47	0.0494	0.2401	0.0001	0
222	43	0.1318	0.0340	0.0001	0
43	42	0.0875	0.0226	0.0001	0
42	41	0.1171	0.0302	0.0001	0
41	40	0.0878	0.0226	0.0001	0
40	39	0.0381	0.0562	0.0001	0

228	229	0.0000	0.0000	0.0000	0
76	221	0.1412	0.0687	0.0002	0
221	50	0.0565	0.0275	0.0001	0
50	229	0.1554	0.0756	0.0002	0
221	51	0.0441	0.0298	0.0001	0
51	52	0.0294	0.0198	0.0001	0
52	53	0.0752	0.0288	0.0001	0
52	54	0.0940	0.3595	0.0001	0
54	229	0.2343	0.0604	0.0001	0
14	15	0.0282	0.0108	0.0000	0
15	18	0.2787	0.0911	0.0000	0
18	16	0.5543	0.2428	0.0000	0
18	17	0.4850	0.2125	0.0000	0
15	19	0.0470	0.0180	0.0001	0
19	20	0.0752	0.0288	0.0000	0
20	21	0.1316	0.0503	0.0001	0
20	22	0.0940	0.0360	0.0001	0
22	228	0.1350	0.0621	0.0002	0
256	274	0.0028	0.0030	0.0293	0
257	253	0.0028	0.0030	0.0293	0
244	243	0.0000	0.0000	0.0000	0
244	237	0.0127	0.0163	0.0029	0
237	252	0.0095	0.0505	0.0001	0
252	260	0.0050	0.0267	0.0000	0
251	261	0.0059	0.0270	0.0000	0
252	242	0.0178	0.0624	0.0001	0
241	251	0.0118	0.0624	0.0001	0
251	245	0.0241	0.0862	0.0001	0
245	246	0.0000	0.0000	0.0000	0
275	253	0.0035	0.0161	0.0035	0
259	258	0.0000	0.0000	0.0000	0
256	258	0.0040	0.0262	0.0060	0
257	259	0.0040	0.0262	0.0596	0
260	261	0.0000	0.0000	0.0000	0
276	258	0.0028	0.0127	0.0028	0
271	259	0.0020	0.0110	0.0025	0
270	258	0.0020	0.0110	0.0025	0
258	262	0.0014	0.0090	0.0020	0
259	272	0.0014	0.0090	0.0020	0
249	250	0.0000	0.0000	0.0000	0
249	242	0.0232	0.0862	0.0001	0
249	235	0.0232	0.0137	0.0015	0
235	268	0.0747	0.0441	0.0049	0
250	236	0.0232	0.0137	0.0015	0
236	269	0.0747	0.0441	0.0049	0
262	254	0.0031	0.0200	0.0046	0
249	267	0.0531	0.0314	0.0035	0
250	266	0.0531	0.0314	0.0035	0
230	231	0.0000	0.0000	0.0000	0
75	231	0.4685	0.1207	0.0025	0
231	78	0.0784	0.0529	0.0019	0

78	79	0.0588	0.0397	0.0001	0
79	223	0.0784	0.0529	0.0002	0
223	228	0.1274	0.0860	0.0003	0
79	80	0.0605	0.0339	0.0001	0
80	81	0.3060	0.0276	0.0001	0
81	88	0.0450	0.0207	0.0001	0
88	89	0.0600	0.0281	0.0001	0
88	291	0.0600	0.0281	0.0001	0
290	291	0.0000	0.0000	0.0000	0
290	91	0.0450	0.0207	0.0001	0
91	92	0.0765	0.1355	0.0000	0
92	93	0.1475	0.0750	0.0000	0
92	94	0.0306	0.0542	0.0000	0
94	102	0.1643	0.1979	0.0000	0
102	103	0.3835	0.1950	0.0000	0
102	104	0.0587	0.0707	0.0000	0
104	105	0.1056	0.1272	0.0000	0
105	106	0.1475	0.0750	0.0000	0
105	107	0.1050	0.1015	0.0000	0
107	108	0.1800	0.1740	0.0000	0
108	109	0.0900	0.0870	0.0000	0
109	110	0.1180	0.0600	0.0000	0
110	111	0.2121	0.0260	0.0000	0
109	112	0.1509	0.1309	0.0000	0
112	113	0.1724	0.1178	0.0000	0
113	114	0.1475	0.0812	0.0000	0
113	115	0.0862	0.0589	0.0000	0
115	116	0.3879	0.2651	0.0000	0
116	117	0.4720	0.2400	0.0000	0
117	118	0.2360	0.1200	0.0000	0
118	119	0.2360	0.1200	0.0000	0
118	120	0.1770	0.0900	0.0000	0
116	121	0.1724	0.1178	0.0000	0
121	122	0.0545	0.0080	0.0000	0
122	123	0.0545	0.0080	0.0000	0
122	124	0.0545	0.0080	0.0000	0
124	125	0.2065	0.1050	0.0000	0
125	126	0.4130	0.2100	0.0000	0
126	127	0.1770	0.0900	0.0000	0
127	128	0.2068	0.1050	0.0000	0
81	82	0.0376	0.0144	0.0000	0
82	83	0.2155	0.1473	0.0000	0
83	84	0.1293	0.0884	0.0000	0
84	85	0.2155	0.1473	0.0000	0
85	86	0.1724	0.1178	0.0000	0
85	87	0.1643	0.1979	0.0000	0
87	230	0.1682	0.2982	0.0000	0
94	95	0.1475	0.0750	0.0000	0
95	96	0.2950	0.1500	0.0000	0
96	97	0.1180	0.0600	0.0000	0
96	98	0.2360	0.1200	0.0000	0

98	101	0.2655	0.1350	0.0000	0
98	99	0.1770	0.0900	0.0000	0
99	100	0.2950	0.1500	0.0000	0
259	273	0.0088	0.0218	0.0046	0
240	265	0.0418	0.1178	0.0012	0
232	224	0.0488	0.0506	0.0002	0
224	151	0.0976	0.3328	0.0000	0
151	152	0.1732	0.0759	0.0000	0
151	149	0.2100	0.2030	0.0000	0
149	150	0.2451	0.1062	0.0000	0
149	147	0.2586	0.1767	0.0000	0
147	148	0.3465	0.1518	0.0000	0
147	146	0.1293	0.0884	0.0000	0
146	153	0.2950	0.1500	0.0000	0
146	145	0.3017	0.2062	0.0000	0
145	143	0.1940	0.1326	0.0000	0
143	144	0.1732	0.0759	0.0000	0
143	141	0.2371	0.1620	0.0000	0
141	142	0.2079	0.0911	0.0000	0
141	139	0.2586	0.1767	0.0000	0
139	140	0.1386	0.0607	0.0000	0
139	131	0.1293	0.0884	0.0000	0
131	132	0.2155	0.1473	0.0000	0
131	129	0.1724	0.1178	0.0000	0
129	130	0.1078	0.0736	0.0000	0
129	123	0.3663	0.2504	0.0002	0
232	77	0.0549	0.0569	0.0027	0
77	225	0.0388	0.1040	0.0000	0
225	215	0.5112	0.2134	0.0000	0
215	216	0.1293	0.0884	0.0000	0
216	217	0.1940	0.1326	0.0000	0
217	171	0.2586	0.1767	0.0000	0
171	172	0.0647	0.0442	0.0000	0
172	173	0.2724	0.0401	0.0001	0
173	174	0.1635	0.0241	0.0000	0
174	175	0.0862	0.0589	0.0000	0
175	176	0.1509	0.1031	0.0000	0
176	177	0.2724	0.0401	0.0001	0
217	218	0.2772	0.1214	0.0000	0
218	219	0.4850	0.2125	0.0000	0
219	220	0.2262	0.0469	0.0001	0
153	154	0.2079	0.0911	0.0000	0
153	155	0.3540	0.1800	0.0000	0
155	156	0.2425	0.1062	0.0000	0
155	157	0.2772	0.1214	0.0000	0
157	158	0.2586	0.1767	0.0000	0
158	159	0.3118	0.1366	0.0000	0
157	160	0.1115	0.0738	0.0000	0
160	161	0.3461	0.2065	0.0000	0
161	162	0.1561	0.1033	0.0000	0
162	163	0.2230	0.1475	0.0000	0

163	164	0.2135	0.0913	0.0000	0
161	165	0.3448	0.2356	0.0000	0
165	166	0.1293	0.0884	0.0000	0
166	167	0.1180	0.0600	0.0000	0
167	168	0.2079	0.0911	0.0000	0
167	169	0.2360	0.1200	0.0000	0
169	170	0.1770	0.0900	0.0000	0
170	180	0.0940	0.0360	0.0001	0
180	181	0.1770	0.0900	0.0000	0
181	182	0.2360	0.1200	0.0000	0
181	183	0.3540	0.1800	0.0000	0
183	184	0.3540	0.1800	0.0000	0
183	185	0.2772	0.1214	0.0000	0
185	186	0.2135	0.0913	0.0000	0
185	187	0.5337	0.2282	0.0000	0
132	133	0.1940	0.1326	0.0000	0
133	134	0.3017	0.2062	0.0000	0
134	135	0.0900	0.0870	0.0000	0
135	136	0.1316	0.0503	0.0000	0
135	137	0.3600	0.3480	0.0000	0
137	138	0.1200	0.1160	0.0000	0
166	188	0.1724	0.1178	0.0000	0
188	189	0.2079	0.0911	0.0000	0
189	190	0.2772	0.1214	0.0000	0
189	191	0.4157	0.1821	0.0000	0
191	192	0.2772	0.1214	0.0000	0
188	193	0.3017	0.2062	0.0000	0
193	210	0.2586	0.1767	0.0000	0
210	211	0.1293	0.0884	0.0000	0
211	216	0.2155	0.1473	0.0000	0
211	212	0.1826	0.0762	0.0000	0
212	213	0.2921	0.1220	0.0000	0
213	214	0.4382	0.1767	0.0000	0
193	194	0.3652	0.1524	0.0000	0
194	197	0.1461	0.0610	0.0000	0
194	195	0.1732	0.0759	0.0000	0
195	196	0.3118	0.1366	0.0000	0
197	198	0.2556	0.1067	0.0000	0
198	199	0.2079	0.0911	0.0000	0
198	200	0.1826	0.0762	0.0000	0
202	203	0.0940	0.0360	0.0001	0
202	204	0.4382	0.1829	0.0000	0
204	205	0.2191	0.0915	0.0000	0
205	206	0.0752	0.0288	0.0001	0
206	207	0.1461	0.0610	0.0000	0
207	208	0.2921	0.1220	0.0000	0
207	209	0.4017	0.1677	0.0000	0
246	250	0.0436	0.2010	0.0002	0
200	201	0.2921	0.1220	0.0000	0
201	202	0.2556	0.1067	0.0000	0
235	238	0.0360	0.3851	0.0000	0

236	239	0.3630	0.0385	0.0000	0
177	178	0.4904	0.0722	0.0001	0
299	300	0.0001	0.0100	0.0000	1
233	299	0.0033	0.1466	0.0000	1
298	300	0.0001	0.0100	0.0000	1
234	298	0.0033	0.1467	0.0000	1
247	277	0.0083	0.3000	0.0000	1
248	278	0.0083	0.3000	0.0000	1
254	297	0.0042	0.1833	0.0000	1
297	300	0.0001	0.0100	0.0000	1
255	296	0.0042	0.1833	0.0000	1
296	300	0.0001	0.0100	0.0000	1
256	295	0.0056	0.2222	0.0000	1
295	300	0.0001	0.0100	0.0000	1
257	294	0.0028	0.0138	0.0000	1
294	300	0.0001	0.0050	0.0000	1
227	264	0.0159	0.4444	0.0000	1
226	263	0.0159	0.4444	0.0000	1
244	253	0.0125	0.4000	0.0000	1
243	274	0.0125	0.4000	0.0000	1
242	270	0.0125	0.4000	0.0000	1
241	271	0.0125	0.4000	0.0000	1
245	275	0.0250	0.5500	0.0000	1
246	276	0.0250	0.5500	0.0000	1
293	300	0.0001	0.0100	0.0000	1
258	293	0.0021	0.1000	0.0000	1
292	300	0.0001	0.0050	0.0000	1
259	292	0.0010	0.0500	0.0000	1
249	272	0.0083	0.3000	0.0000	1
250	262	0.0083	0.3000	0.0000	1
228	268	0.0333	0.6000	0.0000	1
229	269	0.0333	0.6000	0.0000	1
231	267	0.0667	0.8000	0.0000	1
230	266	0.0667	0.8000	0.0000	1
240	273	0.0250	0.5500	0.0000	1
232	265	0.0667	0.8000	0.0000	1
289	260	0.0179	0.2857	0.0000	1
288	238	0.0214	0.1714	0.0000	1
287	239	0.0214	0.1714	0.0000	1
286	291	0.0230	0.1442	0.0000	1
285	290	0.0230	0.1442	0.0000	1

Appendix D: DISTRIBUTED GENERATION DATA

D.1 WIND TURBINE GENERATOR DATA

The average wind speed is assumed to be 8m/s, with 10% turbulence. By calculating the output of the generator using (2.2), the generation of the wind turbine generator is listed in Table 9.6. The data is repeatedly used if the simulating period of time is more than 800 points.

Table 9.6 Wind Turbine Generator Output

Time Point	P (MW)	Time Point	P (MW)	Time Point	P (MW)	Time Point	P (MW)
1	0.7282	201	0.9405	401	1.1101	601	0.6652
2	0.7282	202	0.9400	402	1.1023	602	0.6741
3	0.7261	203	0.9322	403	1.0939	603	0.6707
4	0.7166	204	0.9333	404	1.0821	604	0.6719
5	0.7096	205	0.9151	405	1.0628	605	0.6680
6	0.6969	206	0.9180	406	1.0547	606	0.6706
7	0.6891	207	0.9054	407	1.0344	607	0.6733
8	0.6753	208	0.9048	408	1.0281	608	0.6728
9	0.6674	209	0.8960	409	1.0086	609	0.6741
10	0.6569	210	0.8965	410	1.0020	610	0.6725
11	0.6474	211	0.8954	411	0.9885	611	0.6703
12	0.6395	212	0.9059	412	0.9856	612	0.6752
13	0.6274	213	0.9129	413	0.9793	613	0.6756
14	0.6234	214	0.9300	414	0.9707	614	0.6812
15	0.6169	215	0.9445	415	0.9686	615	0.6819
16	0.6148	216	0.9740	416	0.9652	616	0.6869
17	0.6099	217	0.9857	417	0.9637	617	0.6901
18	0.6066	218	1.0176	418	0.9654	618	0.6974
19	0.6059	219	1.0355	419	0.9662	619	0.7060
20	0.6027	220	1.0595	420	0.9723	620	0.7149
21	0.5978	221	1.0812	421	0.9786	621	0.7240
22	0.5990	222	1.0993	422	0.9790	622	0.7373
23	0.5979	223	1.1142	423	0.9862	623	0.7509
24	0.5990	224	1.1309	424	0.9916	624	0.7617
25	0.5991	225	1.1428	425	0.9965	625	0.7708
26	0.6007	226	1.1569	426	1.0018	626	0.7878
27	0.6000	227	1.1690	427	1.0079	627	0.7987
28	0.5994	228	1.1743	428	1.0136	628	0.8102
29	0.6045	229	1.1727	429	1.0251	629	0.8203
30	0.6054	230	1.1858	430	1.0223	630	0.8256
31	0.6066	231	1.1870	431	1.0295	631	0.8394

32	0.6089	232	1.1932	432	1.0230	632	0.8484
33	0.6120	233	1.2017	433	1.0244	633	0.8640
34	0.6128	234	1.2041	434	1.0186	634	0.8698
35	0.6154	235	1.2134	435	1.0138	635	0.8814
36	0.6174	236	1.2266	436	1.0048	636	0.8956
37	0.6240	237	1.2413	437	0.9928	637	0.9079
38	0.6284	238	1.2539	438	0.9862	638	0.9176
39	0.6366	239	1.2624	439	0.9729	639	0.9315
40	0.6480	240	1.2738	440	0.9669	640	0.9438
41	0.6533	241	1.2793	441	0.9584	641	0.9516
42	0.6633	242	1.2900	442	0.9485	642	0.9572
43	0.6727	243	1.2949	443	0.9405	643	0.9574
44	0.6831	244	1.2985	444	0.9362	644	0.9625
45	0.6943	245	1.2950	445	0.9246	645	0.9650
46	0.7014	246	1.2961	446	0.9285	646	0.9587
47	0.7104	247	1.2871	447	0.9206	647	0.9597
48	0.7243	248	1.2920	448	0.9311	648	0.9576
49	0.7321	249	1.2909	449	0.9269	649	0.9576
50	0.7441	250	1.2848	450	0.9268	650	0.9596
51	0.7471	251	1.2901	451	0.9310	651	0.9637
52	0.7593	252	1.2885	452	0.9324	652	0.9652
53	0.7585	253	1.2902	453	0.9412	653	0.9710
54	0.7707	254	1.3029	454	0.9399	654	0.9738
55	0.7632	255	1.3011	455	0.9511	655	0.9735
56	0.7751	256	1.3048	456	0.9469	656	0.9807
57	0.7712	257	1.3122	457	0.9558	657	0.9754
58	0.7789	258	1.3052	458	0.9544	658	0.9760
59	0.7767	259	1.3087	459	0.9603	659	0.9682
60	0.7800	260	1.3011	460	0.9581	660	0.9645
61	0.7832	261	1.2931	461	0.9629	661	0.9472
62	0.7868	262	1.2794	462	0.9633	662	0.9477
63	0.7926	263	1.2654	463	0.9616	663	0.9302
64	0.7958	264	1.2532	464	0.9625	664	0.9311
65	0.8025	265	1.2396	465	0.9595	665	0.9162
66	0.8078	266	1.2265	466	0.9611	666	0.9158
67	0.8144	267	1.2130	467	0.9536	667	0.9040
68	0.8144	268	1.1890	468	0.9483	668	0.9008
69	0.8279	269	1.1800	469	0.9351	669	0.9007
70	0.8249	270	1.1597	470	0.9293	670	0.9050
71	0.8345	271	1.1478	471	0.9121	671	0.9081
72	0.8366	272	1.1310	472	0.9079	672	0.9171
73	0.8445	273	1.1223	473	0.8957	673	0.9257
74	0.8459	274	1.1056	474	0.8849	674	0.9388
75	0.8512	275	1.0952	475	0.8788	675	0.9584
76	0.8647	276	1.0832	476	0.8724	676	0.9678
77	0.8660	277	1.0757	477	0.8697	677	0.9980
78	0.8865	278	1.0565	478	0.8709	678	1.0027
79	0.8873	279	1.0571	479	0.8781	679	1.0313
80	0.9068	280	1.0507	480	0.8843	680	1.0409
81	0.9124	281	1.0677	481	0.8942	681	1.0719
82	0.9320	282	1.0683	482	0.8997	682	1.0861

83	0.9379	283	1.0875	483	0.9123	683	1.1117
84	0.9499	284	1.0967	484	0.9215	684	1.1203
85	0.9560	285	1.1129	485	0.9324	685	1.1413
86	0.9589	286	1.1311	486	0.9480	686	1.1532
87	0.9626	287	1.1481	487	0.9528	687	1.1749
88	0.9588	288	1.1730	488	0.9698	688	1.1872
89	0.9584	289	1.1915	489	0.9775	689	1.1983
90	0.9492	290	1.2142	490	0.9927	690	1.2109
91	0.9384	291	1.2295	491	0.9950	691	1.2241
92	0.9298	292	1.2509	492	1.0118	692	1.2366
93	0.9180	293	1.2751	493	1.0135	693	1.2483
94	0.9152	294	1.2887	494	1.0252	694	1.2637
95	0.9025	295	1.3181	495	1.0300	695	1.2719
96	0.9025	296	1.3304	496	1.0391	696	1.2742
97	0.8880	297	1.3524	497	1.0420	697	1.2934
98	0.8885	298	1.3716	498	1.0490	698	1.2921
99	0.8803	299	1.3811	499	1.0511	699	1.3043
100	0.8843	300	1.3987	500	1.0583	700	1.3092
101	0.8777	301	1.4113	501	1.0637	701	1.3192
102	0.8807	302	1.4255	502	1.0643	702	1.3104
103	0.8784	303	1.4411	503	1.0685	703	1.3111
104	0.8804	304	1.4576	504	1.0652	704	1.3015
105	0.8831	305	1.4682	505	1.0628	705	1.3009
106	0.8834	306	1.4776	506	1.0582	706	1.2772
107	0.8861	307	1.4867	507	1.0588	707	1.2623
108	0.8877	308	1.5019	508	1.0593	708	1.2435
109	0.8878	309	1.5001	509	1.0556	709	1.2265
110	0.8857	310	1.5128	510	1.0541	710	1.2061
111	0.8816	311	1.5174	511	1.0508	711	1.1815
112	0.8829	312	1.5093	512	1.0504	712	1.1642
113	0.8725	313	1.5079	513	1.0483	713	1.1440
114	0.8732	314	1.4989	514	1.0521	714	1.1344
115	0.8641	315	1.4962	515	1.0539	715	1.1260
116	0.8605	316	1.4755	516	1.0572	716	1.1187
117	0.8487	317	1.4496	517	1.0597	717	1.1164
118	0.8422	318	1.4182	518	1.0656	718	1.1188
119	0.8346	319	1.3972	519	1.0685	719	1.1237
120	0.8202	320	1.3660	520	1.0677	720	1.1303
121	0.8121	321	1.3318	521	1.0755	721	1.1403
122	0.7948	322	1.3032	522	1.0706	722	1.1427
123	0.7871	323	1.2735	523	1.0751	723	1.1526
124	0.7693	324	1.2502	524	1.0684	724	1.1577
125	0.7628	325	1.2153	525	1.0751	725	1.1650
126	0.7488	326	1.1904	526	1.0659	726	1.1641
127	0.7375	327	1.1581	527	1.0622	727	1.1710
128	0.7281	328	1.1261	528	1.0560	728	1.1677
129	0.7147	329	1.1005	529	1.0443	729	1.1719
130	0.7104	330	1.0665	530	1.0411	730	1.1593
131	0.6992	331	1.0411	531	1.0308	731	1.1597
132	0.7007	332	1.0042	532	1.0267	732	1.1527
133	0.6954	333	0.9790	533	1.0187	733	1.1487

134	0.6915	334	0.9462	534	1.0102	734	1.1471
135	0.6908	335	0.9321	535	0.9942	735	1.1407
136	0.6899	336	0.9070	536	0.9884	736	1.1347
137	0.6910	337	0.8985	537	0.9717	737	1.1263
138	0.6945	338	0.8784	538	0.9683	738	1.1175
139	0.7035	339	0.8760	539	0.9555	739	1.1090
140	0.7066	340	0.8650	540	0.9526	740	1.0960
141	0.7218	341	0.8622	541	0.9431	741	1.0919
142	0.7207	342	0.8536	542	0.9474	742	1.0761
143	0.7420	343	0.8548	543	0.9442	743	1.0778
144	0.7444	344	0.8471	544	0.9514	744	1.0566
145	0.7657	345	0.8521	545	0.9457	745	1.0626
146	0.7745	346	0.8486	546	0.9529	746	1.0406
147	0.7872	347	0.8608	547	0.9451	747	1.0412
148	0.7958	348	0.8642	548	0.9448	748	1.0197
149	0.8031	349	0.8813	549	0.9376	749	1.0230
150	0.8160	350	0.8919	550	0.9332	750	1.0084
151	0.8222	351	0.9092	551	0.9270	751	1.0056
152	0.8324	352	0.9242	552	0.9142	752	0.9854
153	0.8395	353	0.9495	553	0.9061	753	0.9799
154	0.8422	354	0.9667	554	0.8952	754	0.9626
155	0.8542	355	0.9946	555	0.8934	755	0.9587
156	0.8486	356	1.0175	556	0.8889	756	0.9500
157	0.8629	357	1.0412	557	0.8836	757	0.9417
158	0.8621	358	1.0611	558	0.8814	758	0.9357
159	0.8708	359	1.0877	559	0.8797	759	0.9301
160	0.8665	360	1.1024	560	0.8847	760	0.9285
161	0.8687	361	1.1160	561	0.8831	761	0.9287
162	0.8616	362	1.1162	562	0.8872	762	0.9306
163	0.8630	363	1.1184	563	0.8893	763	0.9286
164	0.8546	364	1.1145	564	0.8902	764	0.9309
165	0.8510	365	1.1146	565	0.8919	765	0.9274
166	0.8425	366	1.1135	566	0.8957	766	0.9296
167	0.8317	367	1.1150	567	0.8970	767	0.9282
168	0.8249	368	1.1015	568	0.8993	768	0.9275
169	0.8151	369	1.1071	569	0.9000	769	0.9280
170	0.8108	370	1.1002	570	0.8989	770	0.9273
171	0.8037	371	1.1042	571	0.8880	771	0.9265
172	0.8045	372	1.0963	572	0.8872	772	0.9267
173	0.7958	373	1.0962	573	0.8767	773	0.9278
174	0.7960	374	1.0888	574	0.8720	774	0.9302
175	0.7890	375	1.0813	575	0.8631	775	0.9265
176	0.7962	376	1.0727	576	0.8494	776	0.9269
177	0.7867	377	1.0593	577	0.8405	777	0.9240
178	0.7963	378	1.0496	578	0.8232	778	0.9222
179	0.7905	379	1.0417	579	0.8154	779	0.9168
180	0.8016	380	1.0245	580	0.7974	780	0.9170
181	0.7997	381	1.0236	581	0.7887	781	0.9090
182	0.8147	382	1.0119	582	0.7756	782	0.9075
183	0.8246	383	1.0092	583	0.7649	783	0.8989
184	0.8392	384	1.0103	584	0.7529	784	0.8962

185	0.8561	385	1.0134	585	0.7431	785	0.8910
186	0.8694	386	1.0152	586	0.7298	786	0.8863
187	0.8868	387	1.0208	587	0.7269	787	0.8816
188	0.9021	388	1.0255	588	0.7152	788	0.8749
189	0.9204	389	1.0341	589	0.7095	789	0.8644
190	0.9360	390	1.0409	590	0.7008	790	0.8609
191	0.9470	391	1.0496	591	0.6942	791	0.8508
192	0.9576	392	1.0552	592	0.6877	792	0.8418
193	0.9604	393	1.0615	593	0.6853	793	0.8294
194	0.9683	394	1.0731	594	0.6795	794	0.8213
195	0.9651	395	1.0827	595	0.6776	795	0.8093
196	0.9707	396	1.0884	596	0.6722	796	0.7950
197	0.9627	397	1.1000	597	0.6702	797	0.7913
198	0.9616	398	1.1019	598	0.6683	798	0.7815
199	0.9548	399	1.1088	599	0.6670	799	0.7824
200	0.9503	400	1.1079	600	0.6737	800	0.7699

D.2 PHOTOVOLTAIC DATA

The solar insolation data for 17th August at latitude 53 degree is shown in Table 9.7. The data are calculated every 7.5 minutes. According to the data, the average output photocurrents for the PV for all time zones are listed in Table 9.8.

Table 9.7 Solar Insolation during A Day

Time Point	Direct Radiation (kW/m^2)	Time Point	Direct Radiation (kW/m^2)	Time Point	Direct Radiation (kW/m^2)	Time Point	Direct Radiation (kW/m^2)
1	0.0000	49	0.3568	97	0.9873	145	0.3568
2	0.0000	50	0.4053	98	0.9872	146	0.3048
3	0.0000	51	0.4502	99	0.9868	147	0.2496
4	0.0000	52	0.4916	100	0.9862	148	0.1924
5	0.0000	53	0.5298	101	0.9853	149	0.1350
6	0.0000	54	0.5649	102	0.9841	150	0.0811
7	0.0000	55	0.5973	103	0.9827	151	0.0368
8	0.0000	56	0.6271	104	0.9810	152	0.0091
9	0.0000	57	0.6547	105	0.9791	153	0.0004
10	0.0000	58	0.6801	106	0.9768	154	0.0000
11	0.0000	59	0.7036	107	0.9743	155	0.0000
12	0.0000	60	0.7253	108	0.9714	156	0.0000
13	0.0000	61	0.7455	109	0.9683	157	0.0000
14	0.0000	62	0.7642	110	0.9649	158	0.0000
15	0.0000	63	0.7815	111	0.9611	159	0.0000
16	0.0000	64	0.7977	112	0.9570	160	0.0000
17	0.0000	65	0.8127	113	0.9525	161	0.0000
18	0.0000	66	0.8267	114	0.9477	162	0.0000

19	0.0000	67	0.8398	115	0.9424	163	0.0000
20	0.0000	68	0.8519	116	0.9368	164	0.0000
21	0.0000	69	0.8633	117	0.9307	165	0.0000
22	0.0000	70	0.8739	118	0.9242	166	0.0000
23	0.0000	71	0.8838	119	0.9172	167	0.0000
24	0.0000	72	0.8930	120	0.9097	168	0.0000
25	0.0000	73	0.9017	121	0.9017	169	0.0000
26	0.0000	74	0.9097	122	0.8930	170	0.0000
27	0.0000	75	0.9172	123	0.8838	171	0.0000
28	0.0000	76	0.9242	124	0.8739	172	0.0000
29	0.0000	77	0.9307	125	0.8633	173	0.0000
30	0.0000	78	0.9368	126	0.8519	174	0.0000
31	0.0000	79	0.9424	127	0.8398	175	0.0000
32	0.0000	80	0.9477	128	0.8267	176	0.0000
33	0.0000	81	0.9525	129	0.8127	177	0.0000
34	0.0000	82	0.9570	130	0.7977	178	0.0000
35	0.0000	83	0.9611	131	0.7815	179	0.0000
36	0.0000	84	0.9649	132	0.7642	180	0.0000
37	0.0000	85	0.9683	133	0.7455	181	0.0000
38	0.0000	86	0.9714	134	0.7253	182	0.0000
39	0.0000	87	0.9743	135	0.7036	183	0.0000
40	0.0000	88	0.9768	136	0.6801	184	0.0000
41	0.0004	89	0.9791	137	0.6547	185	0.0000
42	0.0091	90	0.9810	138	0.6271	186	0.0000
43	0.0368	91	0.9827	139	0.5973	187	0.0000
44	0.0811	92	0.9841	140	0.5649	188	0.0000
45	0.1350	93	0.9853	141	0.5298	189	0.0000
46	0.1924	94	0.9862	142	0.4916	190	0.0000
47	0.2496	95	0.9868	143	0.4502	191	0.0000
48	0.3048	96	0.9872	144	0.4053	192	0.0000

Table 9.8 Photocurrent Generated by PVs during A Day

Time Zone	1	2	3	4	5	6	7	8
Photocurrent (A)	0	6.0066	99.5279	136.959	137.469	102.771	8.1303	0

Appendix E: MANUAL FOR DEVELOPED SOFTWARE AND GRAPHICAL USER INTERFACE

E.1 INTRODUCTION

A probabilistic framework for assessing the unbalance in the distribution network is presented using probabilistically varying loads and designed measurement errors for the monitors. By incorporating these two main features in an integrated program, a methodology for the Distribution Network State Estimator (DNSE) is developed. Various graphical plots can be used to illustrate the probabilistic results.

In order to facilitate easy-using, DNSE is integrated into a graphical interface using Matlab, enabling flexible selection of sources of unbalance, degree of unbalance and location of monitors. If daily loading is embedded, one-day estimation can be performed as well. The structure of the program and instruction for using this program are introduced in the following sections.

E.2 SOFTWARE DESIGN

The designed program is written in Matlab and accelerated by built-in Java integration. It is composed of two main parts: the calculating program using MatPower, developed three-phase Newton-Raphson load flow and three-phase state estimation; the user friendly interface using Matlab Graphic User Interface (GUI). The calculating program operates as a backstage supporter and cannot be seen from the interface. All operations should be defined in the user interface unless the user wants to change the embedded

power system for the program. A 24-bus network is embedded as the example power system and the default display on the interface.

The program is developed to facilitate robustness and customization at higher level than the interface. The built-in calculation blocks are able to include user defined values in the calculation and can be flexibly combined for different aims. The replaceable power system enables wider application of the program to be used for general distribution networks.

E.2.1 ENVIRONMENT SETUP

The Distribution Network State Estimator (DNSE) is developed in Matlab 2012a environment. It has been tested and it can be used in Matlab 2013 environment, as well.

All the programs are packed in the "DNSE" folder. To initiate the program, firstly, the folder (including all subfolders) needs to be added to the Matlab default path. Secondly, set the current working pathway to the DNSE folder, for example, shown as Fig. 9.1. When the root path is correct, the Java configuration will be performed automatically once the program is running. Lastly, use "*DNSE()*" in the command window to activate interface.

Fig. 9.1 Set current working path for DNSE in Matlab.

E.2.2 USER INTERFACE

The user interface for DNSE is shown in Fig. 9.2. The interface comprises three panels: option panel, one-line diagram display and output buttons, as indicated in Fig. 9.2.

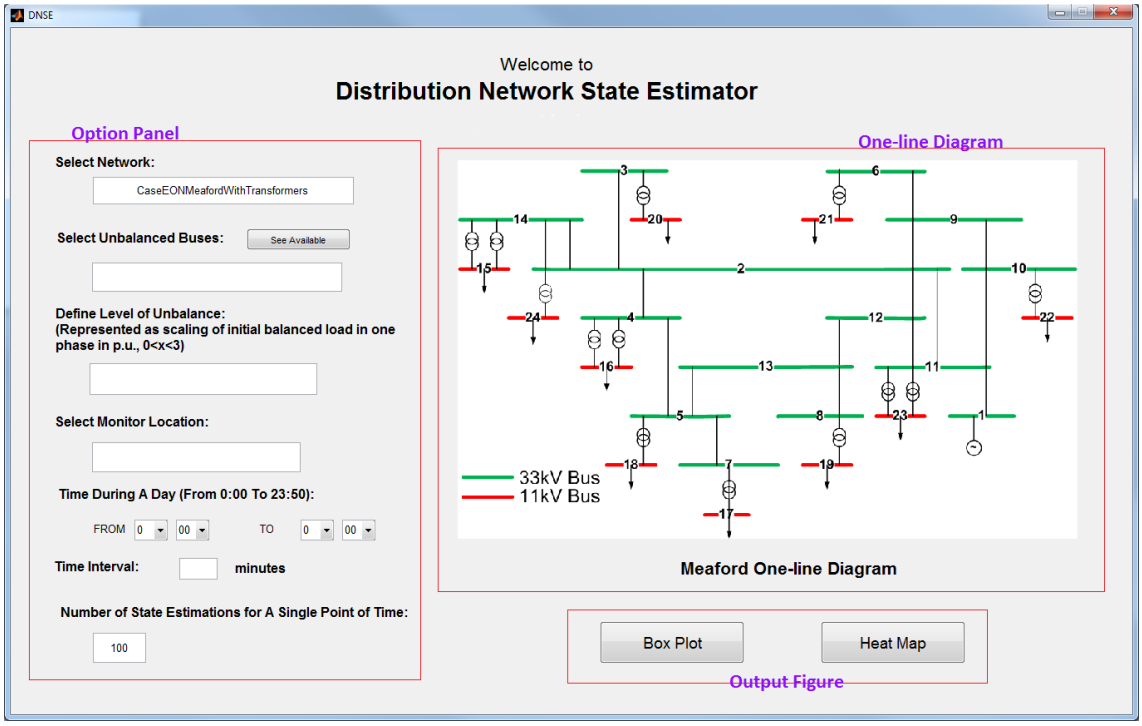

Fig. 9.2 User interface for DNSE.

The option panel is the main control panel for DNSE and indicates the necessary factors for DNSE. It consists of seven easy-to-use options which are related to operational functions. The users have flexible input options in terms of their available data and the assumptions they would like to make. All the options are compulsory although they can have different ranges of values. The values for the options will be discussed in the following section.

One-line diagram is used to indicate the location of buses and such helps the selection of relevant factors. The one-line diagram also corresponds to the heat map. In DNSE, the default display of the one-line diagram is the 24-bus network. If the user wants to replace the embedded network, the one-line diagram needs to be drawn by the user, both for one-line diagram display and for the configuration of heat maps.

The program produces automatic on-screen display of results using box plots or heat maps. This visual representation enables the user to identify the status of the network and the possible weak areas in the network. The figures will automatically update

according to the varying time and all the figures are automatically saved to the current working folder of Matlab (i.e., DNSE folder).

E.3 MAIN FUNCTION

E.3.1 OPTIONS IN THE GUI

The major options in the interface are illustrated and numbered in Fig. 9.3.

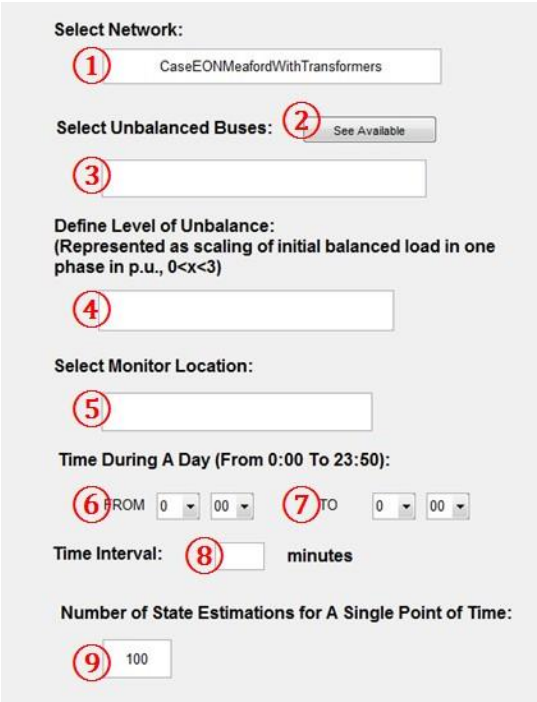

Fig. 9.3 Interface – numbered option panel.

① **Select Network**: this text box defines which network is used for the DNSE calculation.

As the program can be used to calculate results for various networks, this step selects the network data to be read for the calculation. The name of the test network entered in the text box must be exactly the same with the *m file* where the network data are stored. The structure of the network data file is discussed in the following section where the replacement of embedded network is discussed.

② **Show Available Unbalanced Buses**: in this program, the unbalance is generated from loads and all loads can be chosen to be the source of unbalance. This button provides a list of load buses that can be set as the source of unbalance. A full list of load buses will be shown in the text box ③ when button ② is selected.

③ **Select Unbalanced Buses**: this text box defines the unbalanced buses in the simulation. Buses are selected by entering their numbers (the number must correspond to the one-line diagram) in the text box. If more than one bus number is entered, the numbers should be separated by a space or a comma.

④ **Define Level of Unbalance**: this text box defines the degree of unbalance in the three-phase loads so that the level of overall unbalance is defined.

The entered number in this text box is represented as a scaling factor for phase *A* of the unbalanced load. In simulation, the total load for three phases is 3 (1.0 p.u. per phase). Therefore, $0 \leq \text{factor} \leq 3$. Then phases *B* and *C* will be varied to (3-factor)/2. To represent a relatively reasonable source of unbalance, the recommended value for the "factor" is $0.5 < \text{factor} < 1.5$.

Each number entered in text box ④ corresponds to the sequence of the selected bus numbers in text box ③. If more than one bus number is entered, the numbers should be separated by a space or a comma. For different unbalanced buses, different factors can be used. The defined degrees of unbalance for different unbalanced buses are independent from each other.

⑤ **Select Monitor Location**: this text box defines the location of the monitors in the simulation. Once a monitor is installed, it means the parameters of the local bus are available for the state estimation.

Monitors can be installed at any bus in the network. The slack bus is usually assumed to have a monitor installed. The selection of monitors is input as bus numbers which are correspondingly the same as the numbers in the one-line diagram. If more than one bus number is entered, the numbers should be separated by a space or a comma.

⑥&⑦ **Time of Interest**: this dropdown menu defines the sampling time point for DNSE.

Because the daily loading is varying, at different time period of a day, the input unbalance has different level of unbalance. The daily simulation enables the user to observe the behaviour of the power system for a whole day. One-day loading for the default network is embedded in the program. If a new network is selected, the new one-day loading needs to be specified before running DNSE.

Values are inspected every ten minutes. If more than one time point are selected, the output figure will automatically update.

⑧ **Time Interval**: this text box defines the time interval for the daily simulation.

The minimum time interval is 10 minutes and so the time interval entered in text box ⑧ should be a multiple of 10 minutes. For example, for time period from 1:00 to 3:00, if time interval = 60 minutes, one value is estimated per hour, i.e., 1:00, 2:00 and 3:00; if time interval = 40 minutes, four values are estimated in total, i.e., 1:00, 1:40, 2:20 and 3:00.

⑨ **Number of State Estimation**: this text box defines the number of iterations of state estimation for a single point of time.

The number of iterations defines the accuracy of resultant estimation. Considering that every state estimation varies with random measuring error, more samples provide more

accurate cumulative results. To achieve a balance between simulation time and accuracy, the number should range from 10 to 200. The recommended value is 100.

E.3.2 SIMULATION PROCEDURE

Fig. 9.4 shows the simulation procedure of the DNSE program. In the flow chart, the grey boxes denote the user-defined values read from the interface. The green boxes are the main program for calculating DNSE in the backstage.

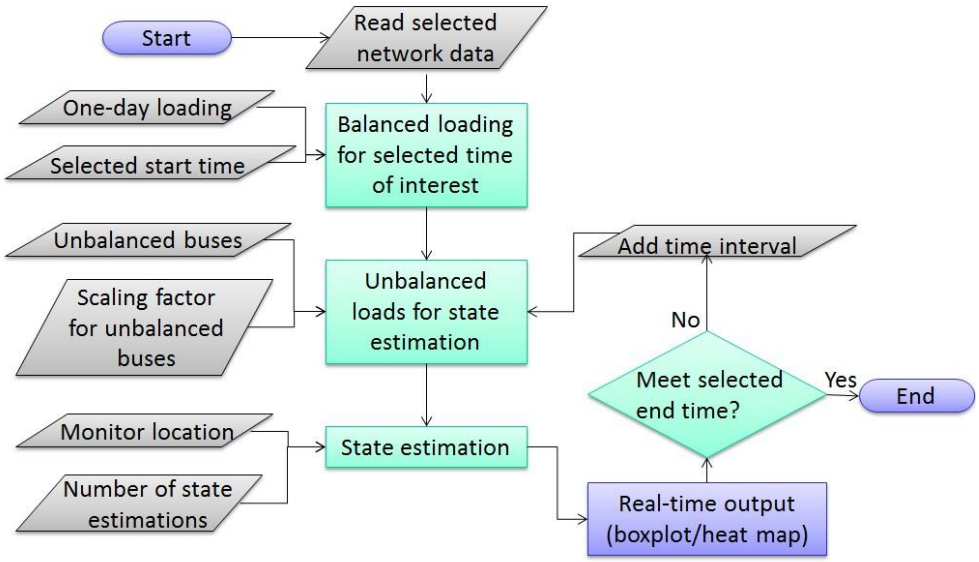

Fig. 9.4 Flow chart of simulation procedure of DNSE program.

E.3.3 OUTPUT FIGURE

For the real-time output, the program uses box plots and heat maps to represent the simulation results, shown as Fig. 9.5 and Fig. 9.6. The figures will be automatically saved in *png* format by the program and can be found in the current working folder. The name of the figures is: *Boxplot000.png* or *Heatmap000.png*. "000" in the file name denotes the simulated time point that is saved and may be different from 000.

The two figures can be time-varying plot if more than one time point is inspected. If the user would like to have a fixed plot, it can be achieved in two ways. One way is to put

only one time point for simulation and therefore only one figure is produced. The other one is to search for the figure from the automatically saved figures.

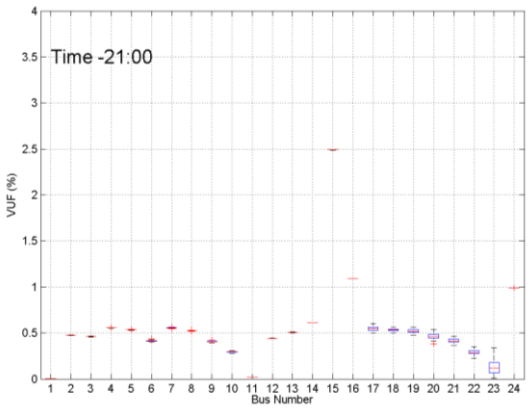

Fig. 9.5 Box plot – output of DNSE program.

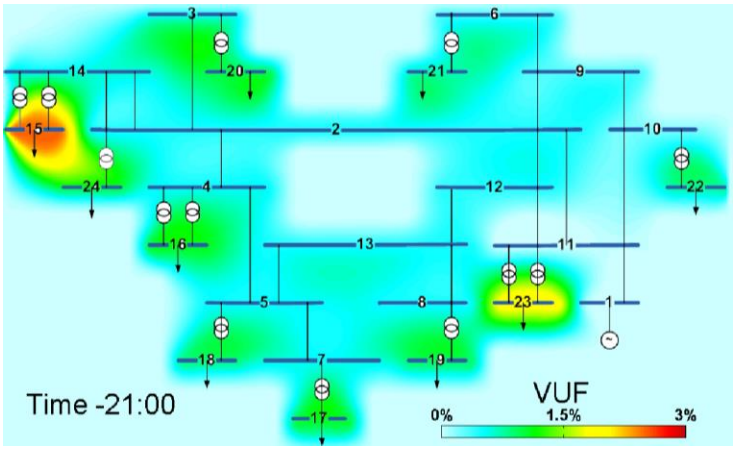

Fig. 9.6 Heat map – output of DNSE program

For **box plots**, by ordering the data for each bus in ascending sequence, the 25th percentile (1st quartile) and 75th percentile (3rd quartile) form the blue box in the box plot. The red horizontal line inside the box denotes the mean value (50th percentile) of the data. The black vertical lines at both ends of the blue box indicate the full scales of data distribution. The maximum length of the black lines is 1.5 times the height of the box. If there are any extreme values locating outside the maximum range, they will be shown as red crosses.

For **heat maps**, they are colourful indication of network status. The hazardous area is indicated by red and can be easily identified.

E.4 REPLACEMENT OF EMBEDDED POWER SYSTEM

In order to use a new network in the DNSE program, the replacement of the network data, loading data and configuration for heat maps are discussed in this section.

E.4.1 CONFIGURATION OF NETWORK DATA

The network data of the new power system should include the following information: *system power base (in MVA), all bus data, line data, and generator data*. The information should be arranged in an *m file* to be called as a function and a unique name should be assigned to this *m file*. The format of data should be the same as the format used for MatPower. An example file can be found in the MatPower folder (under the DNSE folder): *case2.m*.

Format of bus data:

Bus number, Type, Real power demand (MW), Reactive power demand (Mvar), Shunt conductance, Shunt susceptance, Area, Voltage magnitude (p.u.), Voltage angle (degree), Base voltage (kV), Zone, Maximum voltage magnitude (p.u.), Minimum voltage magnitude (p.u.).

In the "Type", PQ bus = 1, PV bus = 2, and slack bus = 3. "Area" and "Zone" are randomly defined by the user from 1 to 100 (not influential in DNSE study).

Example:

```
%  bus_i  type  P    Q   G  B  area  Vm  Va  baseKV  zone  Vmax Vmin

bus = [
      1     3    0    0   0  0   1     1  0    230      1    1.1  0.9;
      2     1   170   40  0  0   1     1  0    230      1    1.1  0.9;
];
```

Format of line data:

From bus (bus number), To bus (bus number), Resistance (p.u.), Reactance (p.u.), Susceptance (p.u.), Long term MVA rating, Short term MVA rating, Emergency MVA

rating, transformer turns ratio, transformer phase shift angle, status, zero sequence resistance (p.u.), zero sequence reactance (p.u.).

In the "Transformer turns ratio", a value = 0 means that is a line. In the "Status", a value = 1 means "in service" and a value = 0 means "out of service".

Example:

```
%  fbus  tbus    r       x         b    rateA  rateB  rateC  ratio  angle
status
branch = [
     1     2  0.01008  0.0504  0.1025  250    250     250    0       0
1;
];
```

Format of generator data:

Bus number, Real power output (MW), Reactive power output (MVar), Maximum reactive power output (MVar), Minimum reactive power output (MVar), Voltage magnitude (p.u.), MVA base, Status, Maximum real power output (MW), Minimum real power output (MW).

In the "Status", a value = 1 means "in service" and a value = 0 means "out of service".

Example:

```
%   bus Pg   Qg   Qmax    Qmin     Vg    mBase   status   Pmax    Pmin
gen = [
     1  0    0    100     -100    1.05    100      1        0       0;
];
```

After the network data arrangement is completed, use the function "*ConvertToThreePhaseCase*" to convert the network to three phases to be called in the DNSE program based on three-phase calculation.

One-day loading should contain 144 time points. For each time point, the three-phase total active power demand for every bus is required. The sequence of the loading data should be arranged according to the sequence of bus numbering.

E.4.2 CONFIGURATION OF HEAT MAP

A one-line diagram should be drawn for the preparation of a heat map. Then it can be called by "*imshow(Figure Name)*" function in Matlab. On the pop-up figure, use the data cursor to get the edge, location of buses and define the location of zero points.

Configuration of every bus location:

```
bus_loc(i,:) = [x_start, x_end, y];
```

Configuration of every zero point:

```
for i = y_start:y_end
    zeropoints(length(zeropoints(:,1))+1,:) = [x_start, i, x_end, i];
end
```

An example file of the configuration for the default 24-bus network can be found in the DNSE folder: *Heat_Location_Meaford.m*.

E.5 SUMMARY

The developed DNSE program enables the user to define the varying degree of three-phase loading and therefore the resultant level of unbalance in the network. A user friendly interface is also developed to facilitate easy usage of the program. By flexibly selecting the source of unbalance, the severity of the source and the monitor location, the users can have probabilistically estimated value from the program. The integration

of daily loading models the changing demand during a day for selected network and so the simulated results are more accurate for different time period of a day. The time of interest can also be selected from the program and the time points are inspected according to the user defined time intervals. The results of simulation are automatically plotted and presented using box plots or heat maps. The figures are automatically updated and saved.

All the example files, program, electronic version of the user manual and the example videos of time-varying results used in this description are provided in a CD.

Appendix F: AUTHOR'S THESIS BASED PUBLICATION

Journal Paper:

[F1] Z. Liu and J.V. Milanović, "Probabilistic Estimation of Voltage Unbalance in MV Distribution Networks with Unbalanced Load", *accepted for publication in the IEEE Transactions on Power Delivery*, TPWRD-01283-2013 (5/5/14).

Submitted Journal Paper:

[F2] H. Liao, Z. Liu, J.V. Milanović, and N.C. Woolley, "Monitor Placement for Estimation of Voltage Unbalance in Distribution Networks Using Dedicated Power System Optimisation Framework", *submitted to IEEE Transactions on Smart Grids, Special issue on "Monitoring, Visualization, and State Estimation for Distribution Systems"*, TSG-00392-2014 (08/05/14).

International Conference Paper:

[F3] Z. Liu and J.V. Milanović, "Probabilistic Estimation of Propagation of Unbalance in Distribution Network with Asymmetrical Loads", *CD Rom of the 8th Mediterranean Conference on Power Generation, Transmission Distribution and Energy Conversion (MedPower 2012)*, Cagliari, Italy, October 1 - 3, 2012.

[F4] Z. Liu and J.V. Milanović, "Probabilistic estimation of voltage unbalance in distribution networks with asymmetrical loads", *22nd International Conference on Electricity Distribution (CIRED 2013)*, Stockholm, Sweden, June 10-13, 2013.

[F5] Z. Liu and J.V. Milanović, "Adequacy of Superpostition Method for Probabilistic Assessment of Unbalance in Distribution Network", *IEEE PowerTech 2013*, Grenoble, France, June 16-20, 2013.